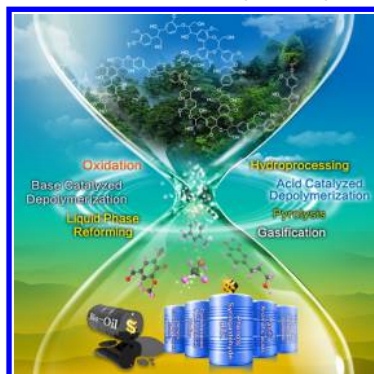


## Catalytic Transformation of Lignin for the Production of Chemicals and Fuels

Changzhi Li,<sup>†</sup> Xiaochen Zhao,<sup>†</sup> Aiqin Wang,<sup>†</sup> George W. Huber,<sup>†,‡</sup> and Tao Zhang<sup>\*,†</sup><sup>†</sup>State Key Laboratory of Catalysis, iChEM (Collaborative Innovation Center of Chemistry for Energy Materials), Dalian Institute of Chemical Physics, Chinese Academy of Sciences, Dalian 116023, China<sup>‡</sup>Department of Chemical and Biological Engineering, University of Wisconsin—Madison, Madison, Wisconsin 53706, United States

## CONTENTS

1. Introduction	A
2. Lignin: structure, property, and isolation	C
2.1. Structure: building blocks and linkage types	C
2.1.1. Building blocks	C
2.1.2. Linkage types	D
2.2. Lignin isolation, type, and property	F
3. Base-catalyzed depolymerization	I
4. Acid-catalyzed depolymerization	K
4.1. Mineral acid	K
4.2. Lewis acid	M
4.3. Ionic liquid mediated acid catalysis	M
5. Pyrolysis of lignin	Q
5.1. Kinetics of lignin pyrolysis	Q
5.2. Thermal pyrolysis	R
5.3. Catalytic pyrolysis	R
6. Hydroprocessing	T
6.1. Hydrogenolysis	T
6.2. Hydrodeoxygenation	X
6.2.1. Monometallic catalysts	X
6.2.2. Bimetallic catalysts	Z
6.2.3. Bifunctional catalysts	AA
6.3. Hydrogenation	AB
6.4. Integrated hydrogen-processing	AB
7. Oxidation	AE
7.1. Organometallic catalysis	AF
7.1.1. Catalysis by methyltrioxo rhenium	AF
7.1.2. Catalysis by salen complexes	AG
7.1.3. Catalysis by other metal complexes	AI
7.1.4. Biomimetic metal complex catalysts	AJ
7.2. Metal-free organocatalytic system	AN
7.3. Base and acid catalysis	AP
7.3.1. Base catalysis	AP
7.3.2. Acid catalysis	AQ
7.4. Metal salt catalysis	AR

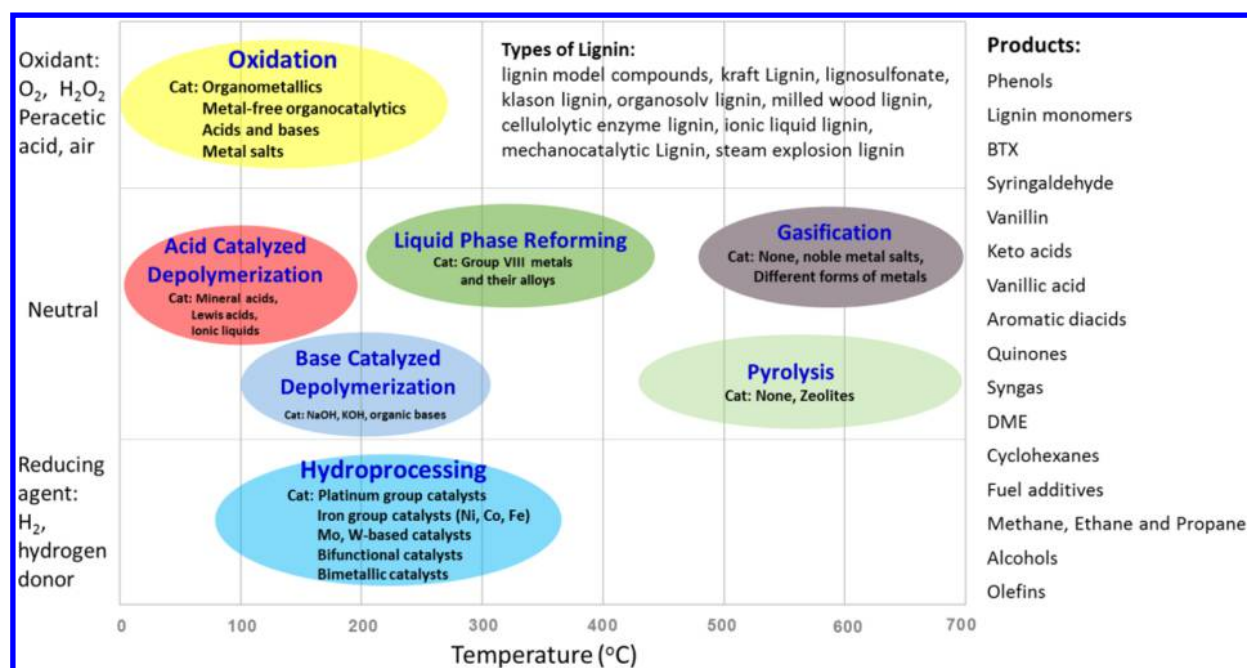
7.4.1. Polyoxometalates	AR
7.4.2. Other transition metal salts	AR
7.5. Photocatalytic oxidation	AU
7.6. Electrocatalytic oxidation	AV
8. Other depolymerization process	AW
8.1. Gasification	AW
8.2. Liquid-phase or steam reforming	AX
9. Concluding remarks	AY
Associated Content	AZ
Special Issue Paper	AZ
Author Information	AZ
Corresponding Author	AZ
Notes	AZ
Biographies	AZ
Acknowledgments	BA
References	BA

## 1. INTRODUCTION

Biomass is any organic matter that is renewable over time. In the context of energy, this is often used to mean plant-based materials, such as agricultural residues, forestry wastes, and energy crops. Among various renewable resources (e.g., solar energy and wind, etc.), biomass is the only renewable organic carbon resource in nature, which endows it with unique advantage in producing value-added products.<sup>1–4</sup> The worldwide energy crisis and related environmental impact have provoked extensive research and development programs on biomass conversion.<sup>5–7</sup> In the context of the 2012 “International Year for Sustainable Energy for All” (SE4ALL), the International Renewable Energy Agency has launched a global roadmap “REMAP 2030” in a bid to help double the share of renewable energy by 2030.<sup>8</sup> The Chinese National Energy Administration has carried out a “National Twelfth Five-Year Plan” on biomass energy.<sup>9</sup> In this project, the consumption of biofuel (mainly ethanol and biodiesel) will reach 12 million metric tons by 2020. The U.S. Department of Energy also set an ambitious goal to generate 20% of the transportation fuel from biomass by 2030.<sup>10</sup> Nowadays, about 10% of the world’s primary energy is biomass. Biomass is primarily used to generate heat and power, and it is the fourth largest source of energy in the world (following oil, coal, and natural gas).<sup>11</sup>

Lignocellulose is the most abundant form of biomass, with an annual production of around 170 billion metric tons.<sup>12</sup> Unlike corn and starch, lignocellulose is inedible for human beings, and

Received: March 19, 2015



**Figure 1.** Summary of processes for conversion of lignin (Note: the abscissa represents the typical temperature range of the lignin conversion processes).

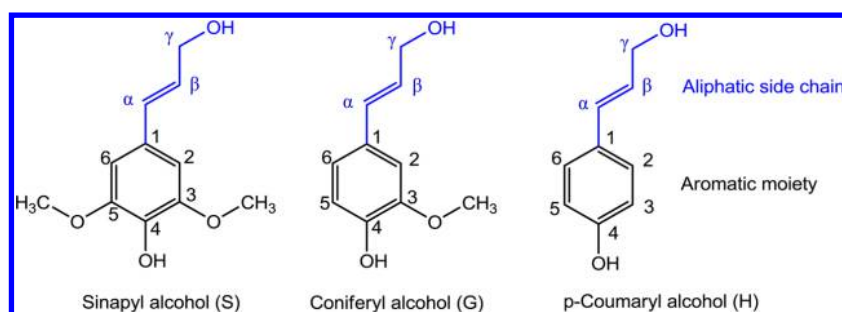
its use will not impose a direct negative impact on food supplies, even though in some cases, competition for arable land use occurs between lignocellulosic biomass and edible biomass. Therefore, it has long been recognized as a promising alternative for fossil-based fuels and chemicals.

There are mainly three components in lignocellulosic materials: hemicellulose, cellulose, and lignin. Among them, hemicellulose (20–30%) and cellulose (40–50%) are the polymers of C5 and C6 sugars.<sup>13</sup> They have been studied for long time, and some well-rounded utilization technologies have been industrially applied for the production of biofuels and important chemicals.<sup>14–16</sup> In comparison with the above two components, lignin is a complex three-dimensional amorphous polymer consisting of methoxylated phenylpropanoid units of various types.<sup>17</sup> The structure and composition of lignin depend strongly on the type of biomass and even on the part of the plant, and they are relatively intractable.<sup>18</sup> Due to the carbon-based inactive property, lignin is typically a waste stream in most current biorefinery processes that is combusted to produce heat and power for the biorefinery. Only 5% of lignin is used in low-value commercial applications, as a low-grade fuel for heat and power applications,<sup>18</sup> or as concrete additive (lignosulfonate).<sup>19</sup> Several researchers have suggested that the effective utilization of lignin could play a major role in biorefinery conception: (1) Lignin accounts for 10–35% by weight, up to 40% by energy in biomass,<sup>20</sup> the production chemicals and/or fuels from lignin will greatly improve the economics of the overall biorefinery process. (2) Lignin is by far the most abundant renewable source composed of aromatic units in nature; the chemical structure of lignin renders it a sustainable candidate feedstock for aromatic chemicals.<sup>21</sup> (3) In raw lignocellulosic biomass, lignin protects hemicellulose and cellulose from chemical and biological attack to a large extent. Conversion of lignin will release carbohydrate fractions so that they are more accessible to chemical and biological digestion.<sup>13</sup> And (4) approximately 7 tonnes of black liquor are produced in order to obtain one tonne of pulp;<sup>22</sup> therefore, utilization of

lignin byproducts will address the problem of environmental impacts associated with the paper-making process and other delignification processes.

Over the past few decades, research on the production of value-added chemicals, alternative fuels, and platform compounds from lignin has grown rapidly on account of the importance of lignin in the biorefinery. Several reviews<sup>23,24</sup> have summarized the applications of lignin either directly or chemically modified as renewable materials, such as bio-dispersant, wood panel products, emulsifier, polyurethane foams, automotive brakes, and epoxy resins for printed circuit boards, as well as the principal component of thermoplastic materials, in industry. Besides the above applications, the depolymerization of lignin to aromatics as an alternative to the petrochemical industry is probably the most promising way to sustainable utilization of lignin.<sup>21,25</sup> Development of technical- and cost-effective depolymerization strategies with new catalysts has now attracted ever-increasing attention. The state-of-the-art strategies can be broadly classified into acid/base catalyzed depolymerization/hydrolysis, pyrolysis (thermolysis), hydrotreating (hydrodeoxygenation, hydrogenation, hydrogenolysis, and hybrid processes therein), chemical oxidation, liquid-phase reforming, and gasification, as well as biodegradation.

A simplified summary of processes for lignin chemical conversion is given in Figure 1. The developed processes occur in an oxidating environment (with O<sub>2</sub>, H<sub>2</sub>O<sub>2</sub>, peracetic acid, or air as an oxidant), in a reducing environment (with H<sub>2</sub> or a hydrogen donor solvent as a reductant), or in a neutral environment. Hydroprocessing involves thermal reduction in the presence of a hydrogen source at temperatures typically ranging from 100 to 350 °C, which has the potential to produce simple bulk aromatic compounds such as phenols, benzene, toluene, and xylene, and even alkane fuels via hydrogen participated upgrading. Oxidation reaction occurs at lower temperatures of 0–250 °C. It favors the production of aromatic alcohols, aldehydes, and acids that are target fine chemicals or



**Figure 2.** Structures of monolignols, the primary building blocks of lignin.

platform chemicals. In most of the oxidative treatment of lignin, a radical chemistry mechanism plays an important role in the production of functionalized aromatics, which will be discussed in section 7. A radical mechanism is also found in other lignin technologies, such as pyrolysis of lignin (typically at 450–700 °C) to produce a liquid product known as “bio-oil”. Depolymerization reactions catalyzed by both acid (typically at 0–200 °C) and base (100–300 °C) break the C–O or C–C linkages between lignin units to offer small segments including monomeric phenols. Integration of this strategy with hydro-processing or oxidation is frequently attempted for lignin conversion. Liquid-phase reforming (typically at 250–400 °C) has been attempted for lignin conversion where authors have produced hydrogen and light gases from the lignin. Gasification is the process that produces synthesis gas (CO and H<sub>2</sub>) from a range of real lignin feedstocks and model compounds.

Biocatalysis has also been used to try and degrade lignin in an environmentally friendly way. The three main lignin degrading enzymes are manganese peroxidase, lignin peroxidase, and laccase.<sup>26</sup> As this review focuses on the chemocatalytic transformation of lignin, biocatalysis is out of the scope of this review. For the history, microbiology, chemistry, and potential applications of biocatalysis on lignin degradation, one can read other literature.<sup>27</sup>

In the last ten years, a large number of advanced analysis techniques have been developed to understand the structure of lignin at the molecular level. These developments in lignin structure chemistry, accompanied by modern reactors such as high pressure visual vessels, and advanced catalysis technologies, as well as characterization techniques, have promoted a vast number of improvements in almost every topic of lignin conversion technologies. These improvements are especially embodied in hydrodepolymerization, oxidation, pyrolysis, hydrolysis, and one-pot multistep depolymerization<sup>25</sup> to produce aromatic chemicals and liquid fuels. Recently, Weckhuysen<sup>28</sup> and co-workers provided an elegant review regarding the valorization of lignin via the approaches of (hydro)cracking, lignin reduction and oxidation reactions. Ragauskas,<sup>29</sup> Luque<sup>30</sup> and their co-workers also nicely reviewed the biosynthesis, characterization and recovery and briefly summarized valorization of lignin as a whole. These reviews are valuable for the development of lignin utilization technology. Notwithstanding, comprehensive summary and analysis of the latest advances in the chemical reactions of lignin and model compounds, particularly those in recent five years, has not been made. The present review gives a summary of the advances in the production of chemicals, fuels, and materials from lignin.

## 2. LIGNIN: STRUCTURE, PROPERTY, AND ISOLATION

### 2.1. Structure: building blocks and linkage types

**2.1.1. Building blocks.** In raw lignocellulosic biomass, lignin is primarily a complex cross-linked macromolecule that adds strength and rigidity to cell walls. It is widely accepted that lignin composition and its content in biomass differ between the types of plants and also between the botanical species and even between trees and morphological parts of the tree.<sup>31</sup> For example, lignin accounts for 30% by weight in softwood, while this share falls to 20%–25% in hardwood.<sup>23</sup> Grass lignin only shares 10–15% of the total plant mass.<sup>32</sup>

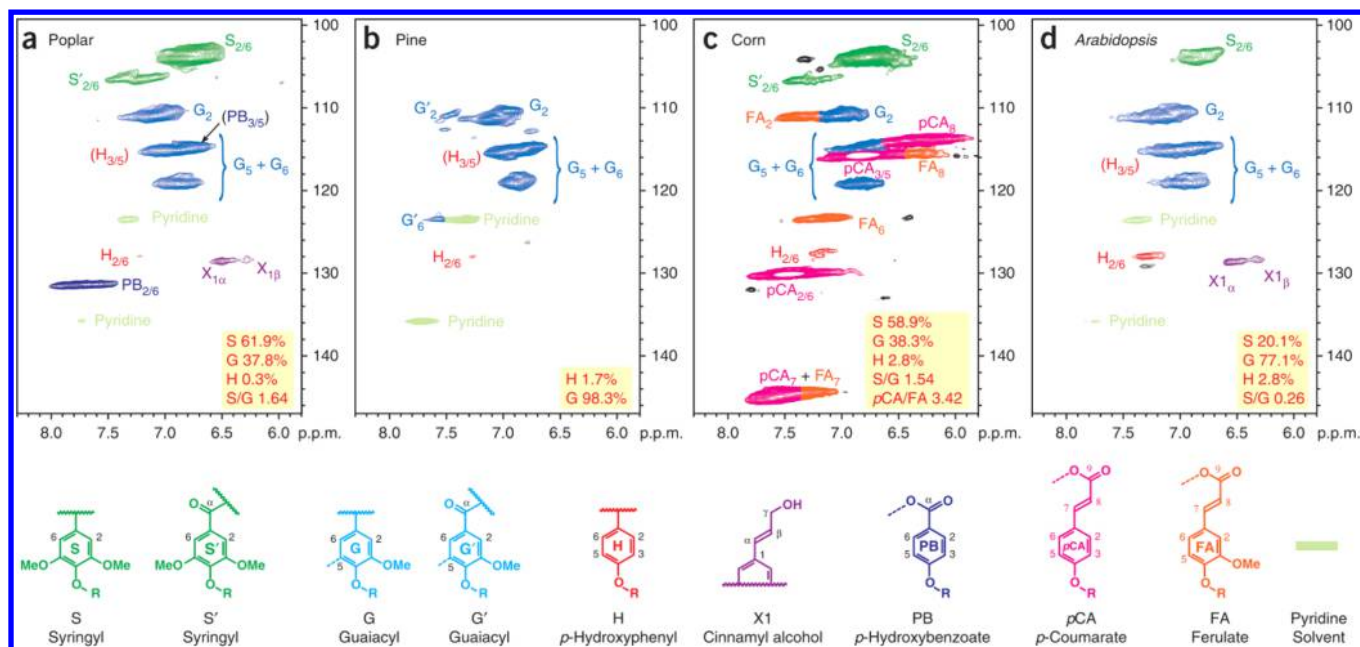
Lignin is mainly an amorphous tridimensional polymer of three primary units: sinapyl (3,5-dimethoxy 4-hydroxycinnamyl), coniferyl (3-methoxy 4-hydroxycinnamyl), and *p*-coumaryl (4-hydroxycinnamyl) alcohols, joined by ether and C–C linkages. These three monolignols are also known as syringyl (S), guaiacyl (G), and *p*-hydroxyphenyl (H) units (Figure 2), respectively. All these monomeric units contain a phenyl group and a propyl side chain; therefore, the typical aromatic unit in lignin is generally called a phenylpropane unit (ppu). These monolignols differ in the number of methoxy groups that are attached to the aromatic moiety; that is, sinapyl alcohol has two methoxy groups, coniferyl alcohol has one methoxy group, and *p*-coumaryl alcohol has none. The content of each monolignol in lignin is related to plant taxonomy. For example, softwood (gymnosperm) lignin contains more guaiacyl units, hardwood (angiosperm) lignin has a mixture of guaiacyl and syringyl units, and grass lignin presents a mixture of all three aromatic units.<sup>23</sup> Based on the abundance of the three basic units in lignin, these polymers can be classified as type-G (softwood lignin), type-G-S (hardwood lignin), type-H-G-S (grass lignin), and type-H-G (compression wood lignin).<sup>31</sup> Table 1 shows the typical content of the three primary lignin units in different types of plant.<sup>33</sup>

**Table 1.** Abundance of the Primary Lignin Units in Different Types of Plants<sup>33</sup>

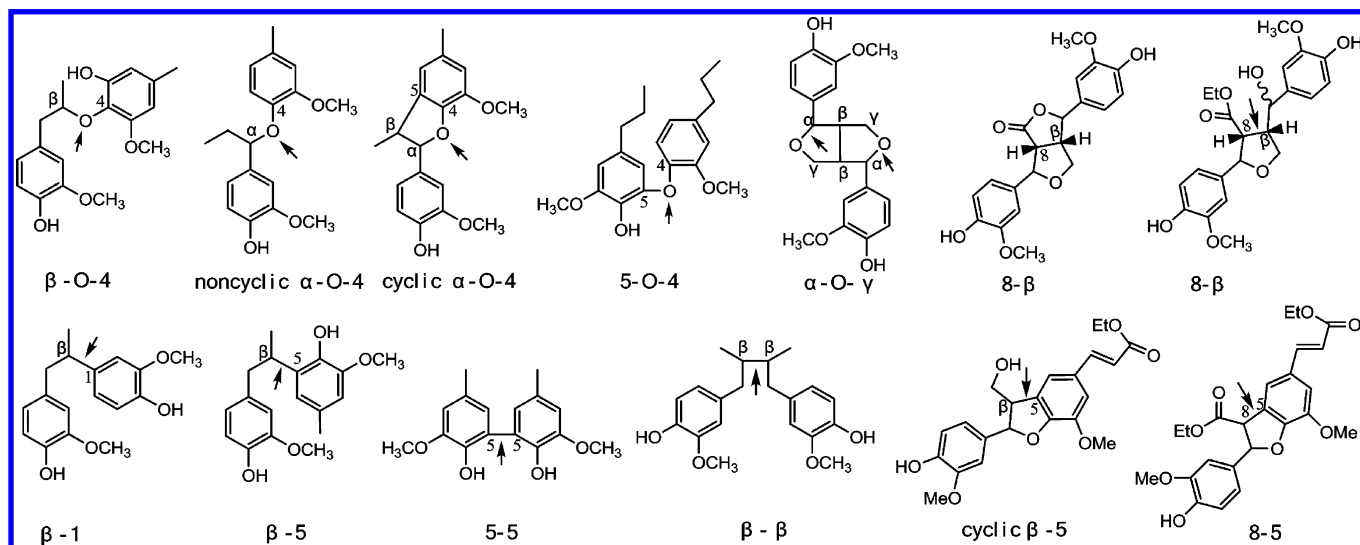
Monolignol	Grass	Conifer wood	Broadleaf wood
Sinapyl alcohol (S)	25–50%	0–1%	50–75%
Coniferyl alcohol (G)	25–50%	90–95%	25–50%
<i>p</i> -Coumaryl alcohol (H)	10–25%	0.5–3.4%	Trace

It should be noted that, besides the three primary building blocks of H, G, and S units, some other molecular species can also participate in the formation of the lignin polymer.<sup>34,35</sup> It is accepted that no plant contains lignin that is only derived from the three primary precursors. Noncanonical subunits that have been identified include ferulic acid, ferulates (which form





**Figure 3.** 2D NMR spectra revealing lignin unit compositions. Partial short-range  $^{13}\text{C}$ - $^1\text{H}$  (HSQC) correlation spectra (aromatic regions only) of cell wall gels in 4:1 (v/v)  $\text{DMSO-}d_6$ /pyridine- $d_5$  from (a) 2-year-old greenhouse-grown poplar wood, (b) mature pine wood, (c) senesced corn stalks, and (d) senesced *Arabidopsis* inflorescence stems. Adapted with permission from ref 38. Copyright 2012 Nature Publishing Group.



**Figure 4.** Typical linkages between the primary units of lignin.

linkages between hemicellulose and lignin), coniferaldehyde, sinapaldehyde, 5-hydroxyconiferyl alcohol, and acylated monolignols containing acetate, *p*-hydroxybenzoate, or *p*-coumarate moieties.<sup>36,37</sup> Figure 3 shows the aromatic region of high-resolution solution-state 2D  $^{13}\text{C}$ - $^1\text{H}$ -correlated (HSQC) NMR spectra from four whole cell wall materials, namely, poplar, pine, corn, and *Arabidopsis*. It is evident that *p*-hydroxybenzoate, *p*-coumarates, as well as ferulate, etc. were detected in the structures.<sup>38</sup> It should be noted that the amount of ferulate linkages is dramatically higher in corn stover.

**2.1.2. Linkage types.** Lignin monolignols are predominantly linked either by ether or by C-C bonds. In native lignin, two-thirds or more of the total linkages are ether bonds, while the other linkages are C-C bonds. In order to categorize the various types of linkages between two monolignols, the carbon atoms in the aliphatic side chains of the monolignols are

labeled as  $\alpha$ ,  $\beta$ , and  $\gamma$  and those in the aromatic moieties are numbered 1–6. For instance, a  $\beta$ -O-4 linkage represents a bond formed between the  $\beta$  carbon of the aliphatic side chain and the oxygen atom attached to the C4 position of the aromatic moiety (Figure 4, the first structure model). The major linkages between the structural units of lignin are  $\beta$ -O-4 ( $\beta$ -aryl ether),  $\beta$ - $\beta$  (resinol), and  $\beta$ -5 (phenylcoumaran).<sup>35</sup> Other linkages include  $\alpha$ -O-4 ( $\alpha$ -aryl ether), 4-O-5 (diaryl ether), 5-5,  $\alpha$ -O- $\gamma$  (aliphatic ether), and  $\beta$ -1 (spirodienone), etc. Representative structures of these linkages are shown in Figure 4, and typical proportion values of these linkages and the functional groups in lignin are listed in Table 2. It should be noted that these data vary considerably even for the same plant species due to some factors such as growing environment, area, and even analysis methods.<sup>39</sup>

**Table 2. Linkages and Functional Groups in Different Lignins (Linkage/Functional Groups per 100 ppu)**<sup>40,41</sup>

Linkage	Number/100 ppu		Functional group	Number/100 ppu	
	Softwood	Hardwood		Softwood	Hardwood
$\beta$ -O-4	43–50	50–65	Methoxyl	92–96	132–146
$\beta$ -5	9–12	4–6	Phenolic hydroxyl	20–28	9–20
$\alpha$ -O-4	6–8	4–8	Benzyl hydroxyl	16	
$\beta$ - $\beta$	2–4	3–7	Aliphatic hydroxyl	120	
5–5	10–25	4–10	Carbonyl	20	3–17
4-O-5	4	6–7	Carboxyl		11–13
$\beta$ -1	3–7	5–7			
Others	16	7–8			

The proportion of each linkage is determined by the contribution of a particular monomer to the polymerization process. As indicated in Table 2,  $\beta$ -O-4 ( $\beta$ -aryl ether) is, by far, the most frequent linkage in lignin, the frequency of which is reported to vary from *ca.* 43% (softwood) to *ca.* 65% (hardwood). G-type lignin (softwood lignin)<sup>28</sup> contains more resistant linkages ( $\beta$ -5, 5–5) than SG lignin (hardwood lignin)<sup>41</sup> because the C<sub>5</sub> positions of G-type monolignols are available for coupling whereas those in S units are sterically inhibited (see the structures in Figure 2). These features result in the fact that softwood possesses higher condensation degree than hardwood lignin. Additionally, the steric effect of the methoxy groups on the aromatic rings of S units causes more linear structural forms in the hardwood lignin polymer compared with softwood. In grass plants, more noncanonical subunits such as ferulates/diferulates and acylated monolignols are involved in the lignin biosynthesis process, which makes grass lignin special in structure.<sup>42</sup> A representative lignin structure showing typical linkages is illustrated in Figure 5. This model is not the accurate structural formula for lignin in the usual sense, but is a model for illustrating the types of monolignols. The model also describes the linkages between

adjacent monolignol units, as well as the proportions in which they are believed to exist in lignin.

The linkages between monolignols basically determine the reactivity of lignin. As  $\beta$ -O-4 ( $\beta$ -aryl ether) is the most frequent linkage in lignin, its chemical reactivity dictates considerably the resistance of lignin to chemical digestion. Another important factor that affects the reactivity is the functional groups, including methoxyl, benzyl alcohol, phenolic and aliphatic hydroxyl, noncyclic benzyl ether, carboxyl and carbonyl groups, etc. Table 3 shows the hydroxyl group content in the lignins from hardwoods, softwoods, and grasses. The aliphatic hydroxyl signal is typically dominant among various hydroxyl groups in lignin, while the amount of carboxylic OH groups is usually the smallest (i.e., 0.02–0.29 mmol·g<sup>-1</sup>). In softwood lignin, the order of hydroxyl contents is as follows: aliphatic OH > phenolic OH > carboxylic OH. The major phenolic hydroxyls in softwood lignin (i.e., pine, spruce, fir, redwood, etc.; see Table 3, entries 1–17) are guaiacyl phenolics with a minor amount of phydroxyphenyl, while syringyl phenolics are usually not detected, which is in agreement with the overall G/H/S composition of softwood lignin. In hardwood lignin, the general order of the hydroxyl group content (Table 3, entries 18–29) is somewhat different from that in softwood lignin: aliphatic > guaiacyl phenolic  $\sim$  syringyl phenolic > *p*-hydroxyphenyl  $\sim$  carboxylic OH. In comparison with the wood lignin, grass lignin has much higher *p*-hydroxyphenyl content (Table 3, entries 30–41).

Previously, a variety of degradative methods are traditionally used for cell wall compositional analysis, which usually cause changes in structure and are actually not precise to some extent. It is important to point out that recent advances in NMR technology such as HSQC<sup>38</sup> have made it possible to rapidly screen plant material and discern whole cell wall information without the need to deconstruct and fractionate the plant cell wall. This technology is efficient in elucidating lignin subunit composition and lignin interunit linkage distribution, and it should play a crucial role in analysis of the detailed lignin chemistry that occurs during lignin conversion technologies.

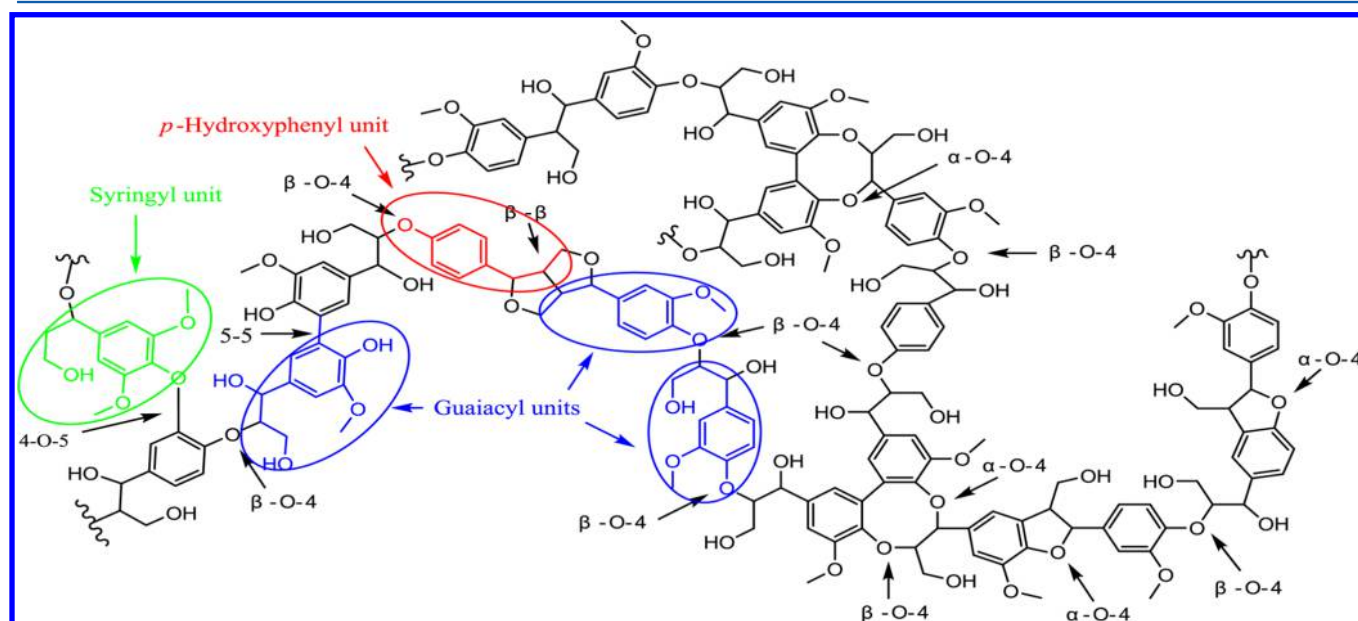
**Figure 5.** Representative structure models of lignin. Adapted from Weckhuysen et al.<sup>28</sup> and Rodrigues et al.<sup>41</sup>

Table 3. Hydroxyl Group in Lignin as Determined by  $^{31}\text{P}$  NMR Characterization<sup>a</sup>

Entry	Lignin sample	Aliphatic OH (mmol·g <sup>-1</sup> )	Phenolic OH, (mmol·g <sup>-1</sup> )				COOH (mmol·g <sup>-1</sup> )
			C <sub>5</sub> substituted	Syringyl	Guaiacyl	<i>p</i> -Hydroxy-phenyl	
1	Loblolly pine, MWL <sup>43</sup>	4.16	0.08		0.57	0.12	0.02
2	Loblolly pine, AP <sup>43</sup>	3.42	0.34		1.82	0.06	
3	Loblolly pine, EOL <sup>44</sup>	4.70	1.80		1.20	0.10	
4	Southern pine, CEL <sup>45</sup>		0.46				0.11
5	Southern pine, MWL <sup>45</sup>		0.5				0.16
6	Southern pine, EMAL <sup>45</sup>		0.43		0.79	0.12	0.11
7	Blackspruce, MWL <sup>45</sup>	4.27	0.36		0.77		0.21
8	Blackspruce, MWL <sup>46</sup>	4.21	0.50		0.76	0.08	0.15
9	Blackspruce, MWL <sup>47</sup>	4.13	0.44		0.67	0.09	0.11
10	Blackspruce, EAL <sup>47</sup>	4.92	0.30		0.72	0.06	0.09
11	Norway spruce, MWL <sup>48</sup>	1.03	0.06		0.14	0.01	0.02
12	Norway spruce, MWL <sup>49</sup>	4.57			1.18	0.03	0.22
13	Norway spruce, EMAL <sup>48</sup>	1.25	0.08		0.17	0.01	0.03
14	Norway spruce, CEL <sup>48</sup>	0.92	0.08		0.12	0.02	0.02
15	Douglas fir, EMAL <sup>46</sup>		0.41		0.84	0.10	0.13
16	White fir, EMAL <sup>46</sup>		0.56		0.93	0.11	0.19
17	Redwood, EMAL <sup>46</sup>		0.63		1.06	0.16	0.16
18	<i>P. tremuloides</i> , MWL <sup>47</sup>	4.53	0.29	0.23	0.37	0.17	0.14
19	<i>P. tremuloides</i> , EAL <sup>47</sup>	3.91	0.22	0.24	0.33	0.14	0.11
20	<i>P. tremuloides</i> , MWL <sup>50</sup>	5.72	0.13	0.16	0.25	0.20	0.06
21	<i>E. globules</i> , EMAL <sup>46</sup>			0.62	0.35	0.02	0.15
22	<i>E. globules</i> , Dioxane acidolysis <sup>40</sup>	88 <sup>b</sup>	Total phenolic OH groups: 29 <sup>b</sup>				4 <sup>b</sup>
23	<i>E. ulmoides</i> oliv, MWL <sup>51</sup>	4.05		0.19	0.19	0.03	
24	<i>B. davidii</i> , MWL <sup>52</sup>	4.51	0.27		0.43		0.03
25	<i>B. davidii</i> , EOL <sup>53</sup>	2.51	0.98		1.53		0.17
26	Poplar, WL <sup>50</sup>	5.72	0.13	0.16	0.25	0.20	0.06
27	Poplar, SE <sup>54</sup>	0.53		0.34	0.18		0.08
28	Aspen, SE <sup>54</sup>	0.67 <sup>c</sup>		0.23 <sup>c</sup>	0.13 <sup>c</sup>		0.06 <sup>c</sup>
29	Aspen, SE <sup>49</sup>	1.14	0.80 <sup>d</sup>		0.36	0.10	0.25
30	Wheat straw, MWL <sup>55</sup>	3.49	0.18	0.09	0.51	0.68	0.12
31	Wheat straw, Dioxane acidolysis <sup>55</sup>	3.80	0.13	0.10	0.51	0.50	0.18
32	Wheat straw, EOL <sup>56</sup>	1.38	0.23	0.77	1.12	0.38	0.15
33	Wheat straw, EMAL <sup>57</sup>	1.26	0.18	0.21	0.57	0.30	ND
34	Triticale straw, EOL <sup>56</sup>	1.50	0.12	0.69	0.79	0.42	0.17
35	Corn residue <sup>56</sup>	1.39	0.11	0.78	0.88	0.94	0.23
36	Flax shives <sup>56</sup>	2.95	0.19	0.56	1.20	0.02	0.02
37	Hemp hurds <sup>56</sup>	1.19	0.49	1.53	1.20	0.17	0.01
38	<i>Micanthus × giganteus</i> , MWL <sup>49</sup>	5.54		0.14	0.38	0.32	0.18
39	<i>Micanthus × giganteus</i> , MWL <sup>58</sup>	4.00		0.22	0.67	0.64	0.13
40	Switchgrass, MWL <sup>59</sup>	3.88	0.20		0.48	0.32	0.29
41	AP Switchgrass, MWL <sup>59</sup>	2.83	0.35		0.57	0.33	0.33

<sup>a</sup>MWL: milled wood lignin; EMAL: enzymatic mild acidolysis lignin; CEL: cellulolytic enzymatic lignin; EAL: enzymatic/acidolysis lignin; AP: acid pretreatment; EOL: ethanol organosolv lignin; SE: steam explosion. <sup>b</sup>Phenolic hydroxyls were analyzed by aminolysis, and total hydroxyl groups were analyzed by acetylation, and carboxyl groups were determined by a chemisorption method with calcium acetate. Amounts of functional groups were calculated per 100 ppu. <sup>c</sup>Expressed as mol/ppu. <sup>d</sup>The data is the total amount of C5 substituted and syringyl phenolic -OH groups.

## 2.2. Lignin isolation, type, and property

Due to the complicated physical and chemical linkages between lignin and other components in plants, isolation of lignin from lignocellulosic feedstocks is one of the most challenging, but crucial, processes in a biorefinery cycle. The impurities (minerals, organic acids) in natural biomass might also be solubilized with the lignin streams. These impurities can deactivate the catalysts and accumulate in continuous processes. Therefore, the advanced fraction technologies for lignin depolymerization must also analyze the impurities that would be in these streams. A number of lignin fractionation technologies have been developed during the last century, as listed in Table 4. Cellulose, hemicelluloses, and lignin have a

wide range of solubilities in different solvents, Kim<sup>60</sup> and co-worker sorted the fractionation technologies into two major groups by solubility. The first group includes methods in which carbohydrate fraction is removed by solubilization, leaving lignin as an insoluble residue. The enzyme process, enzymatic mild acidolysis process, and Klason method belong to this group. The second group is the methods involving dissolution and removal of lignin, leaving the carbohydrate fraction as insoluble residues, followed by the recovery of lignin from the solution. The Björkman process, the organosolv process, some ionic liquid (IL) selective pretreatments, and the alkaline wet oxidation pretreatment, as well as two major industrial processes of the kraft and lignosulfonate processes are in the

Table 4. Comparison of Various Lignin Isolation Methods

Isolation method	Lignin name	Typical process	Characteristics	Nature of the disruption	Sort
Klason method <sup>62</sup>	Klason lignin	72% sulfuric acid	Extensive structure change, hardwood lignin is partly dissolved.	Chemical pretreatment	(Hemi-) cellulose
Kraft process, kraft pulping or sulfate process <sup>63</sup>	Kraft lignin	Na <sub>2</sub> S/NaOH	Highly modified, partially fragmented.	Chemical pretreatment	Lignin
Sulfite pulping process, Lignosulfonate process	Lignosulfonate	Extract lignin from waste liquor of the sulfate pulping process of soft wood.	Highly modified, high average molecular weights, cleavage of ether linkages, loss of methoxyl groups and formation of new C–C bonds.	Chemical pretreatment	Lignin
Björkman process <sup>45,64</sup>	Milled wood lignin (MWL)	Ball milling, then extracted by aqueous dioxane.	Most similar to the native structure, possible depolymerization due to extensive milling.	Physical pretreatment	Lignin
Organosolv process <sup>65,66</sup>	Organosolv lignin	Using organic solvents to extract lignin.	Mild conditions, results in more unaltered lignin, solvent could be recovered by distillation.	Solvent fraction	Lignin
Enzyme process <sup>67,68</sup>	Cellulolytic enzyme lignin (CEL)	Hydrolysis of cellulose, leave lignin as a residue.	Low structure change, bears less phenolic hydroxyl groups than MWL.	Biological process	(Hemi-) cellulose
Enzymatic mild acidolysis process <sup>45,57</sup>	Enzymatic mild acidolysis lignin (EMAL)	Two steps of enzymatic hydrolysis, and mild acidolysis.	Higher yield and purity than those of MWL and CEL.	Biological-Chemical process	(Hemi-) cellulose
Ionic liquid pretreatment <sup>69</sup>	Ionic liquid lignin	Stepwise precipitation or selective extraction.	Tunable strategy, low structure change, more uniform molar mass distribution compared to those of Kraft lignin.	Solvent fraction	Lignin
Steam explosion process <sup>49</sup>	Steam explosion lignin	High temperature steam explosion of the fibers.	Require little or no chemical input, short treatment time, low energy requirement, changes of certain functional groups.	Physical pretreatment	Lignin
Mechano- catalytic process <sup>70</sup>	Mechano- catalytic Lignin	Mechano- catalytic depolymerization	Sulfur-free lignin	Physical-Chemical pretreatment	(Hemi-) cellulose
Alkaline wet oxidation <sup>71</sup>	Alkaline wet oxidation lignin	Oxidative pretreatment under alkaline conditions.	Partial degradation via $\beta$ -O-4 breaking.	Chemical pretreatment	Lignin



range of this category. Based on the nature of the cell wall disruption, da Costa Sousa<sup>61</sup> and co-workers categorized the approaches into four groups, namely, solvent fraction (organosolv process, ILs pretreatment, etc.), biological process (enzymatic), physical pretreatment (i.e., ball milling), and chemical pretreatment (acidic, alkaline, and oxidative). As these isolation strategies have been well described by Zakzeski,<sup>28</sup> Lu,<sup>36</sup> da Costa Sousa<sup>61</sup> and co-workers in recent literature, herein we just compare and discuss their advantages and disadvantages in a biorefinery manner instead of individually, considering the detailed procedures of all methods for lignin isolation and purification, with the aim to give an evaluation for choosing the ideal isolation method for lignin study and utilization.

Lignin preparation techniques such as the Klason method<sup>62</sup> use strong mineral acids to reach a high lignin yield. The Kraft Lignin Process<sup>63</sup> uses strong alkalis to cleave the ester bonds between hemicelluloses and lignin macromolecules. These two strategies can be manipulated in large scale and have been applied in industrial processes. However, they usually proceed under drastic conditions and, thus, cause irreversible reactions that severely change the structure of the isolated lignin. The Klason method is more suitable for extraction of softwood lignin, since hardwood lignin can be partly dissolved during the acid hydrolysis. Generally, kraft lignin is highly modified and hydrophobic, and it possesses lower molecular weight than the original lignin and has low sulfur content. Another commonly used treatment process in the pulp and paper industry is sulfite pulping process. Most sulfite pulping delignification processes involve acidic cleavage of ether bonds, accompanied by loss of methoxyl groups and formation of new carbon–carbon bonds. The electrophilic carbocations produced during ether cleavage react with bisulfite ions to give lignosulfonates ( $R-O-R' + H^+ \rightarrow R^+ + R'OH$ ;  $R^+ + HSO_3^- \rightarrow R-SO_3H$ ), also known as sulfonated lignin, which can be recovered from the spent pulping liquids by addition of excess calcium hydroxide. Lignosulfonates have higher average molecular weights than kraft lignin. They can be used as an additive in oil-well drilling mud, as plasticizers in concrete and leather tanning, and as a source of vanillin. These lignin feedstocks (lignosulfonates, kraft lignin, and Klason lignin) are, however, not the ideal lignin source in future biorefinery operation because of the complicated processes and large amount of wastewater generated from these processes.

One technique that is used to isolate lignin with little structure change is the extraction of ball-milled wood by neutral solvents (usually with dioxane/water, 9/1 of volume ratio).<sup>45</sup> This so-called Björkman process was developed in 1954 by Björkman.<sup>64</sup> The lignin obtained in this way is called milled wood lignin (MWL), although MWL does not represent the whole lignin because of possible depolymerization during extensive milling and the low extraction yield (25–50% of theoretical).<sup>72</sup> The structure of MWL is considered most similar to the unaltered lignin because of the mild extraction condition and neutral solvent used. MWL has been proven to be the best model for the elucidation of native lignin structure. It should be noted, however, that new free-phenolic hydroxyl groups may be generated through cleavage of  $\beta$ -aryl ether linkages during the ball-milling process. This increases the amount of  $\alpha$ -carbonyl groups as a result of side-chain oxidation.<sup>47</sup>

Another isolation technique that is suitable for lignin structure research is organosolv fractionation.<sup>58,73</sup> Like the

Björkman process, it extracts lignin from biomass feedstock by using organic solvents such as primary alcohols under mild conditions in a green manner. Methanol- and ethanol-based fractionation processes are used extensively, owing to their high solubility for lignin and easy recovery by distillation.<sup>74</sup> Formic acid and acetic acid fractionations<sup>49</sup> have also proved to be promising processes to achieve relatively complete isolation of lignin in lignocellulosic materials without an impact on the environment.<sup>75</sup>

In cellulosic ethanol biorefinery processes, cellulolytic enzymes are commonly used to hydrolyze the carbohydrate fraction, leaving behind a solid cellulolytic enzyme lignin (CEL) residue. The enzyme process occurs at mild conditions, producing some slight structural changes in the lignin. These structural changes include decreasing the phenolic hydroxyl group content, increasing the  $\beta$ -O-4 linkages, and increasing the molecular weight compared to that of MWL.<sup>68</sup> The major drawback of cellulolytic enzyme lignin is the presence of protein and carbohydrate impurities.<sup>76</sup> In addition, it requires long residence time (from several hours to few days) to obtain a high yield of isolated lignin. To avoid these disadvantages, Argyropoulos's group<sup>47,48</sup> integrated enzymatic and mild acidolysis methods to isolate lignin (EMAL, enzymatic mild acidolysis lignin) from milled wood. Molecular weight distribution analysis and comparison of the chemical structures revealed that EMAL, MWL, and CEL showed only subtle differences in structure.

Since Ragauskas<sup>77</sup> and co-workers reported in 2007 that some ILs could serve as superior solvents for lignin, the use of ILs in separation of lignin has been studied intensively.<sup>73,78–85</sup> A recent review by Hossain and Aldous<sup>86</sup> provided a comprehensive summary of the multifunctional use of ILs in lignin processing. Two major processes have been developed for isolation of lignin using ILs. The first process was developed by Rogers and co-workers.<sup>69</sup> In this process, IL dissolves all major components of the biomass, and then the polysaccharides and lignin are stepwise precipitated by addition of an antisolvent. However, this process is relatively time-, solvent-, and energy-intensive. To improve the efficiency, selective dissolving, and extraction of lignin, specialized ILs, such as dialkylimidazolium cations in combination with acetates<sup>80</sup> and alkylbenzenesulfonates,<sup>87</sup> have been developed. Overall, the IL process is a tunable strategy that could be conducted under mild conditions. The obtained lignin has little structural change, larger average molar mass, and more uniform molar mass distribution compared to those of Kraft lignin. The precise circumstances surrounding lignin dissolution in ILs have not yet been fully understood. Many parameters, including extraction conditions (temperature, time, etc.), purity of IL, wood species, wood particle size, wood load, and both IL anion and cation species, influence the extraction efficiency.<sup>80</sup> Although pretreatment of lignin with ILs has shown promise in biorefinery processes, the problem of high IL cost and recyclability issues hampers the use at a commercial scale.

Very recently, chemical treatment for the isolation of lignin has received increased attention. Schüth and Rinaldi<sup>70</sup> reported a novel fractionation process via a mechanocatalytic depolymerization of lignocellulose. The carbohydrate fraction (cellulose and hemicellulose) was converted to water-soluble products, and lignin was precipitated as a sulfur-free material. Further, Rinaldi<sup>88</sup> and co-workers developed a catalytic hydrogen transfer method that is able to isolate depolymerized lignin as a nonpyrolytic bio-oil and producing pulp, which is susceptible



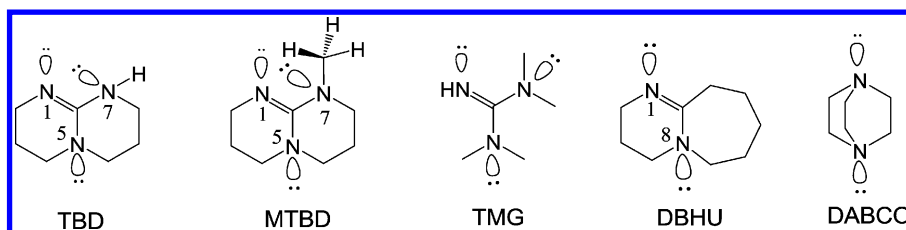
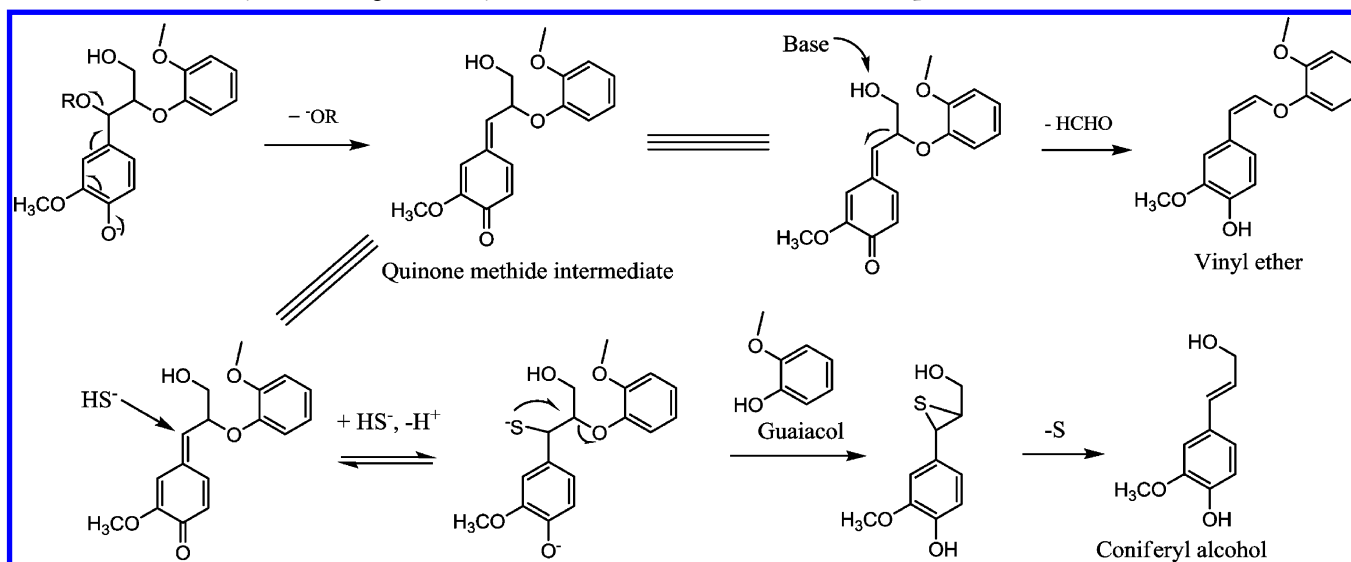


Figure 6. Structures of organic N-bases developed for lignin depolymerization. Adapted from Ekerdt et al.<sup>111</sup>

Scheme 1. Base-Catalyzed Cleavage of  $\alpha$ -Aryl Ether Bonds in Phenolic Model Compounds<sup>a</sup>



<sup>a</sup>Adapted from Ekerdt,<sup>111</sup> Ragauskas,<sup>113</sup> and their co-workers.

to enzymatic hydrolysis, as a byproduct. Another promising method to obtain lignin with high purity is one-step fractionation of lignocellulose components by the selective organic acid-catalyzed depolymerization of hemicellulose in a biphasic water/2-methyltetrahydrofuran system.<sup>89</sup>

Other pretreatment strategies for lignin extraction include pyrolysis,<sup>90</sup> steam explosion,<sup>49,91</sup> alkaline wet oxidation,<sup>71,72</sup> etc. The typical properties of lignin produced in these processes are reported in Table 4.

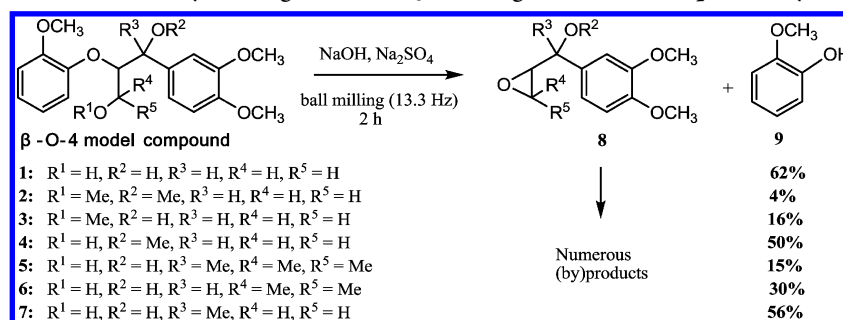
The ideal isolation approach should consider not only technological factors, but also the economic and environmental impacts. On the one hand, each process possesses its unique advantages and shortages; on the other hand, different lignocellulosic feedstocks, ranging from hardwoods, softwoods, and grasses have different physical and chemical properties. Hence, the fraction technologies, in most cases, are not used solely in an isolation process.<sup>92</sup> There is interdependence between pretreatment, assistant technologies, the type of substrate, and the way it is eventually processed. For instance, CEL usually contains a certain amount of carbohydrates (*ca.* 13 wt %), while if this technology is in combination with alkaline organosolv treatment, the purity of the lignin fraction could be significantly improved, and the original structure of the lignin macromolecule is basically kept.<sup>93</sup> If microwave irradiation was used to replace oil-based heating during the mild acidolysis step of the enzymatic mild acidolysis method, greater yield and purity of EMAL could be obtained.<sup>94</sup> Combining percolation-mode ammonia pretreatment of poplar sawdust with mild organosolv purification of the extracted lignin could also

produce lignin with high purity in up to 31% yield and 50% recovery.<sup>95</sup>

### 3. BASE-CATALYZED DEPOLYMERIZATION

Most lignin depolymerization processes are conducted at temperatures of 250–650 °C, with or without catalysts. As a result, a complex phenolic mixture of alkylated and polyhydroxylated phenol compounds as well as volatile components and char are formed, which presents challenges for downstream processing to separate phenolic-like compounds or upgrading to more homogeneous mixtures. Base-catalyzed hydrolysis of lignin is one exceptional route for the production of simple aromatic chemicals under mild conditions. The catalytic reagents are cheap and commercially available bases such as LiOH, NaOH, and KOH. As aryl-alkyl ether bonds, including  $\beta$ -O-4 bonds, are the weakest bonds in lignin structure,<sup>96</sup> cleavage of ether linkages is a dominant reaction in alkaline delignification processes.<sup>97,98</sup>

An ideal base-catalyzed depolymerization would be a reaction affording high yields of monomers aromatics while also allowing their easy separation from the reaction mixture. In the base-catalyzed lignin hydrolysis reaction, the selectivity and yield of the products are particularly dependent on pressure, temperature, time, concentration of the base, and lignin/solvent ratio.<sup>97,99,100</sup> Equally important, the oil yield and products composition vary strongly depending on the nature of the base. Usually, stronger base gives higher conversion since the polarization of the base governs the kinetics and the mechanism of the depolymerization reaction.<sup>101,102</sup> The kinetics of reactions is faster in phenols<sup>97</sup> or alcohols<sup>102</sup> than in water

Scheme 2. Mechanochemical Base Catalyzed Degradation of  $\beta$ -O-4 Lignin Model Compounds by Solvent-Free Grinding<sup>a</sup>

<sup>a</sup>Adapted from Bolm and co-workers.<sup>112</sup>

due to the ether linkages solvolysis effect. A higher temperature and longer reaction time favor monomers generation. The formation of a solid residue increases due to the condensation/repolymerization reactions of the degradation intermediates/products. Indeed, repolymerization reactions are believed to be one of the main problems in the production of monomers. Therefore, decreasing the rate of repolymerization and oligomerization reactions during base-catalyzed lignin depolymerization is the key issue to enhance the yields of the products.

One strategy that has been proposed to solve this problem involves using a capping agent to capture the reactive species. Lercher,<sup>99</sup> Adschiri,<sup>103</sup> Labidi,<sup>104</sup> Li,<sup>105</sup> and their co-workers have attempted this approach and added boric acid, phenol, 2-naphthol, and *p*-cresol in water to entrap reactive fragments, such as phenolic compounds and formaldehyde, and mask active sites, such as C <sub>$\alpha$</sub>  in the lignin structure. In these approaches, complete conversion of lignin without char formation was realized. The use of H-donating solvents, such as formic acid,<sup>106</sup> and other stabilizing compounds, such as alcohols,<sup>107,108</sup> has also been shown to suppress char formation. Other approaches that should be considered to tune the reaction selectivity for base-catalyzed lignin depolymerization include the development of more active catalysts that allow for more milder conditions (e.g., synergetic catalysis of organic acid and base,<sup>109</sup> sequential combination of base-catalyzed depolymerization, and hydrogenolysis<sup>110</sup>) and the design of multi-phase reactors (e.g., in situ reaction–extraction system) that extract monomers before undesired reactions occur. It should be noted that, in base-catalyzed reactions, acidic molecules are produced during depolymerization reactions, which, over time, can induce the deactivation of the catalyst via acid/base neutralization.

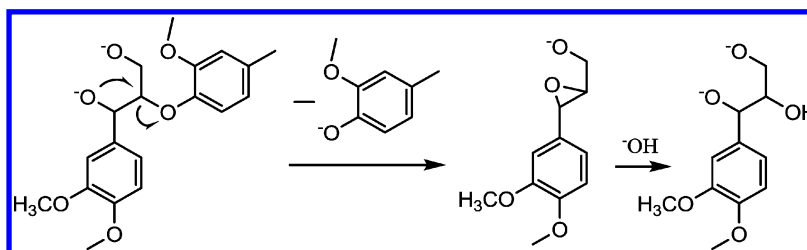
Organic bases have recently been used for lignin depolymerization. Ekerdt<sup>111</sup> and co-workers explored the combination of an IL 1-butyl-2,3-dimethylimidazolium chloride ([BDMI][Cl]) and nonaqueous organic N-bases (Figure 6) in cleaving the  $\beta$ -O-4 bonds. 1,5,7-Triazabicyclo[4.4.0]dec-5-ene (TBD) showed the highest activity, leading to more than 40%  $\beta$ -O-4 ether bond cleavage. It was proposed that two exposed nitrogen atoms (N<sub>1</sub> and N<sub>7</sub>) in TBD enable it to work as a dibasic nucleophile, both attacking the  $\alpha$ - and  $\beta$ -carbon of quinone methide in a manner similar to hydrosulfide anion (HS<sup>-</sup>, see in Scheme 1) and thereby assisting the cleavage reaction. In the same year, Song<sup>109</sup> and co-workers developed a novel hydrolysis strategy based on synergetic catalysis of organic acid and base in a batch reactor to convert lignocellulosic biomass. In their reaction system, oxalic acid acted as a proton

donor to cleave the glycosidic bond of polysaccharides, and tetramethylammonium hydroxide catalyzed the depolymerization of lignin. This strong synergetic effect afforded significantly higher conversion of the biomass compared with the reactions with either of them.

Mechanochemical strategies are commonly used for particle size reduction as a pretreatment for a chemical depolymerization processes. Bolm<sup>112</sup> and co-workers first applied solvent-free ball milling in the presence of a (solid) base for the degradation of lignin (Scheme 2). It was found that 3.5 equiv of sodium hydroxide or sodium *tert*-butoxide could effectively degrade various lignin model compounds (compounds 1–7). Importantly, 55–76% of the  $\beta$ -O-4 binding motifs present in the untreated organosolv lignin or even naturally dried beech wood were cleaved during the process. The reaction mechanism was in agreement with the classical kraft pulp process.<sup>113</sup> The initial deprotonation at the primary hydroxyl group followed by intramolecular cleavage of the  $\beta$ -ether bond generates two products: an unstable epoxide 8 and guaiacol 9.

Although solvent-free mechanochemical transformation is proposed as a sustainable alternative to conventional solution-based and solvothermal chemical processes, its energy-efficiency should be improved; in addition, the base quantity is too large to be applied in large scale.

As has been discussed above, in most alkaline delignification processes, cleavage of ether linkages is a dominant reaction. Gierer<sup>113–116</sup> et al. summarized these ether bonds into two groups: (i) *a*-Aryl ether bonds if they contain a free alcoholic OH group on the *p*-carbon atom or a free phenolic OH group ion in the *para*-position of the *a*-aryl ether group. They are readily cleaved by the conversion of the phenolate unit into the corresponding quinone methide intermediate (Scheme 1). This intermediate can be further transformed to guaiacol and coniferyl alcohol in alkaline aqueous solution with a nucleophile such as hydrogen sulfide. Alternatively, quinone methide can generate reactive formaldehyde and alkali-stable vinyl ether via base-catalyzed dealkylation reaction.<sup>117</sup> This mechanism is also in agreement with Ekerdt's<sup>111</sup> study about organic N-bases catalyzed decomposition of phenolic lignin model compounds. (ii)  $\beta$ -Aryl ethers as long as the  $\alpha$ -position of the propane side chain possesses a free alcoholic OH group and if the phenolic OH group in the *para*-position to the  $\beta$ -aryl ether side chain is etherified. The cleavage of  $\beta$ -aryl ether linkages in nonphenolic units involves deprotonated hydroxyl groups in  $\alpha$ - or  $\gamma$ -carbon, which serve as nucleophiles in replacing the neighboring aroxy substituent by forming an oxirane ring, which is then opened by addition of a hydroxide ion to form a glycol group, as summarized in Scheme 3.

Scheme 3. Base-Catalyzed Cleavage of  $\beta$ -Aryl Ether Bonds in Nonphenolic Model Compounds<sup>a</sup>

<sup>a</sup>Adapted from Chakar and Ragauskas.<sup>113</sup>

During the base catalyzed degradation process (see Table 5), it is suggested that the repolymerization (condensation) reaction takes place simultaneously and that both reaction pathways share the same intermediate state. Scheme 4 illustrates alkali-promoted condensation reactions in phenolic units.<sup>113</sup> In Route A, the condensation reaction of quinone methide proceeds via Michael addition, while the same intermediate generated in Scheme 1 degrades to guaiacol and coniferyl alcohol with nucleophile. In the condensation reactions, quinone methides are not the only acceptors. Route B in Scheme 4 illustrates the reaction between formaldehyde (generated from the dealkylation reaction, as illustrated in Scheme 1) and two phenolate units.<sup>118</sup> A hydroxybenzyl alcohol, which was obtained from the addition of the phenolic ion and formaldehyde, is first converted to an *o*-quinone methide; this intermediate reacts with another phenolic ion and generates the final diarylmethane structure.

#### 4. ACID-CATALYZED DEPOLYMERIZATION

Historically, acid pulping was mainly used for isolation of lignin fractions from the lignocellulose matrix, rather than in designing the depolymerization of lignin into valuable aromatic monomers.<sup>126</sup> The first acid-catalyzed lignin hydrolysis reaction was reported in 1924, when Hägglund and Björkman<sup>127</sup> distilled lignin with 12% hydrochloric acid to obtain thiobarbituric acid, phloroglucinol, and barbituric acid. Recently, different types of mineral acids,<sup>128–131</sup> Lewis acids,<sup>132–135</sup> zeolites,<sup>136–138</sup> acidic ILs,<sup>139–141</sup> as well as organic acids<sup>109,126</sup> have been tested for hydrolysis of lignin and the related model compounds.

Like the behavior of the base-catalyzed lignin hydrolysis reaction, in acid-catalyzed delignification of wood and lignocellulosic biomass, the hydrolytic cleavages of  $\alpha$ - and  $\beta$ -aryl ether linkages also play a dominant role<sup>129</sup> because aryl-aryl ether bonds, the phenolic C–O bond, and C–C bonds between aromatic lignin units are more stable.<sup>96,142</sup>

##### 4.1. Mineral acid

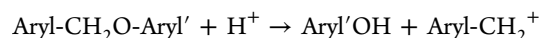
Adler et al. first tried mineral acid promoted hydrolysis of Björkman lignin.<sup>143</sup> Johansson and Miksche<sup>144</sup> demonstrated that the rate of hydrolysis of  $\alpha$ -aryl ether was 102 times faster than that of  $\beta$ -aryl ether. Furthermore, phenolic  $\alpha$ -ethers hydrolyze faster than nonphenolic ones. Meshgini and Sarkanen<sup>129</sup> synthesized a series of  $\alpha$ -aryl and  $\beta$ -aryl ether compounds with different substitution groups (Figure 7, compounds 1–10), and their hydrolysis rates promoted by acid decreased in the order: 4-methoxy- > 3,4-dimethoxy- >> 3,4,5-trimethoxybenzyl. On the other hand, varying structures of the aryl ether moiety caused the following rate effects: 2,6-dimethoxy- >> 2-methoxy-4-methyl- > 2-methoxyphenyl. It was<sup>129,145</sup> also found that the hydrolysis rates of these linkages

are first-order with respect to both catalyst and substrate concentrations. The range of activation energies for the hydrolysis of the  $\alpha$ -aryl ether bonds (80–118 kJ/mol) is much lower than for the  $\beta$ -aryl ether hydrolysis (148–151 kJ/mol).<sup>102b,109</sup> Thus, when lignin is subjected to acidic degradation, the  $\alpha$ -ether linkages depolymerize before the  $\beta$ -aryl ether linkages (see Table 6).

Recently, Ekerdt<sup>139</sup> et al. carried out the hydrolysis of the phenolic  $\beta$ -O-4 bonds of guaiacylglycerol- $\beta$ -guaiacyl ether (GG, Figure 7, compound 9) and nonphenolic veratrylglycerol- $\beta$ -guaiacyl ether (VG, Figure 7, compound 10) in dimethyl sulfoxide (DMSO) with a catalytic amount of hydrochloric acid. A moderate guaiacol yield of 55.2% was obtained from GG with 100% conversion. The activity of VG was lower than that of GG. Higher HCl concentration appears to impose a minor effect on the hydrolysis efficiency. Similar to base-catalyzed hydrolysis reaction, most acid-catalyzed lignin hydrolysis processes involve extensive condensation reactions.<sup>128,134</sup> Barta and co-workers<sup>126</sup> provided a good example that markedly suppresses such an undesired pathway by capturing the unstable compounds with diols and by in situ conversion of the reactive intermediates. In order to maximize the amount of monomeric products, future research could focus on in-depth mechanistic understanding of lignin conversion pathways and the precise role of reaction intermediates.

In order to clarify the acid-catalyzed depolymerization mechanism, several studies have been carried out on both phenolic and nonphenolic model compounds. As previously shown in Scheme 1, the phenolate unit is first converted into the corresponding quinone methide intermediate in base-catalyzed hydrolysis reaction of  $\beta$ -aryl ether linkages, whereas in acid-catalyzed degradation (Scheme 5), the primary step is a dehydration reaction, yielding enol aryl ether (EE). This dehydration step is the rate-determining step for  $\beta$ -phenyl ether hydrolysis. EE intermediate can be rapidly hydrolyzed to guaiacol and  $\alpha$ -ketocarbinol. The latter is gradually converted to a mixture of four compounds called “Hibbert’s ketones” via allylic rearrangement.<sup>145</sup> This mechanism was later proved by Ekerdt,<sup>134</sup> Beckham,<sup>147</sup> and their co-workers using GG, VG (Figure 7, compounds 9–10), and four other dimers as model compounds.

For  $\alpha$ -aryl ether linkages, acid-catalyzed hydrolysis reactions follow predominantly a SN1-type mechanism with first-order kinetics as outlined in the following two equations:<sup>129</sup>



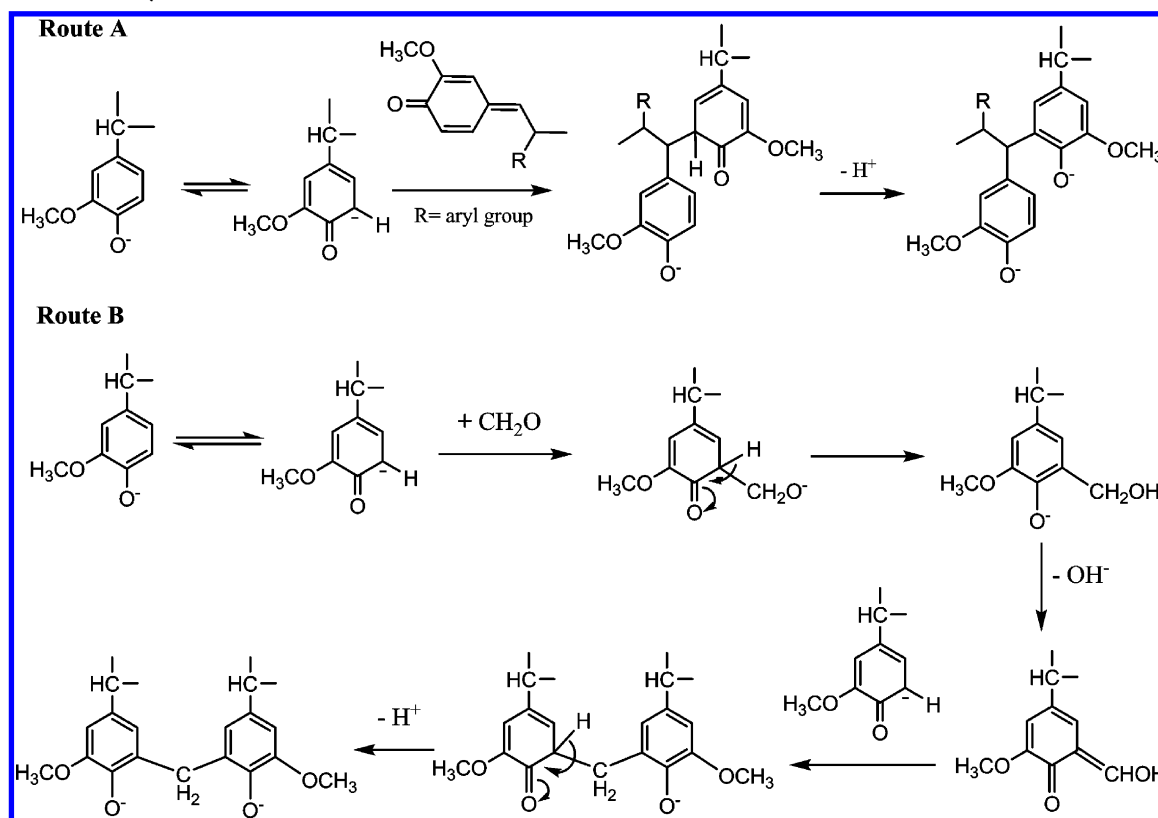
(ROH is water or low molecular alcohol)

Table 5. Base Catalyzed Degradation (BCD) of Lignin and Model Compounds

Catalyst	Reaction conditions	Substrate	Product	Note	ref
NaOH	Anaerobic BCD	$\beta$ -O-4 bond dimers	Monomeric phenols	Up to 80% yield	119
NaO $t$ -Bu	<i>m</i> -xylene, 100 °C, 2 h.	Veratrylglycerol- $\beta$ -guaiaicyl ether	Guaiaacol	89% yield	120
TBD <sup>a</sup>	Equal molar amount of GG and cat. in [BDMfm]Cl, 150 °C, 2 h.	Guaiaacylglycerol- $\beta$ -guaiaicyl ether	Guaiaacol, Coniferyl alcohol, Enol ether	GG conv. 94.3%	111
Solid NaOH	Solvent-free ball milling, 12 h	$\beta$ -O-4 model compounds	Monomeric phenols	57–91% yield	112
TBD <sup>a</sup>	Equal molar amount of GG and cat. in [BDMfm]Cl at 130 °C for 2 h.	Guaiaacylglycerol- $\beta$ -guaiaicyl ether	Guaiaacol, Coniferyl alcohol, Guaiaacol, Coniferyl alcohol, Enol ether	GG conv. 66.9%	111
MTBD <sup>a</sup>				GG conv. 36.6%	111
TMG <sup>a</sup>				GG conv. 11.1%	111
DBHU <sup>a</sup>				GG conv. 31.2%	111
NaOH	BCD at 300 °C for 80 min.	Organosolv lignin from olive tree	Oil yields 13.0%–18.5%	Coke: 8.3%–16.7%; Gas: 1.0%	121
Various inorganic bases	BCD at 300 °C	Organosolv lignin	Monomeric phenols	Base nature strongly affects oil yield (5–20%) and oil composition.	101
NaOH	300–330 °C, 1300–1900 psi	Steam explosion lignin	Monomers, dimers and trimmers, char	70% monomers, dimers and trimmers.	98
NaOH	BCD at 315 °C in a continuous flow reactor.	Kraft lignin from soft wood	Gas, small organic compounds, aromatic monomers and modified lignin	Yield of aromatic monomers: 19.1%	122
Alkaline	BCD at 250 °C	HCl lignin	Monomeric phenols	16–18 wt % yield	123
Various inorganic bases	290 °C, supercritical alcohol	Alcell lignin	Monomeric phenols	Dominant route is the solvolysis of ether linkages.	102
Black liquor	BCD at 250 °C	Chinese date, Pine wood, Wheat straw, etc.	35% aromatics and 65% organic acids	Oxygen transfer between lignin and carbohydrates is the mechanism.	124
Oxalic acid and tetramethylammonium hydroxide	Sequential combination of organic acid and base	White spruce	Monomeric phenols	Synergetic effect of organic acid and base. Twice conversion than the reaction with base alone.	109
NaOH	NaOH solution, 180 °C, 6 h	Poplar wood sawdust	Low-molecular phenol compounds	21.8%–53.2% yields	125

<sup>a</sup>Structures of these organic bases are shown in Figure 6.



Scheme 4. Base-Catalyzed Condensation Reactions in Phenolic Units<sup>a</sup>

<sup>a</sup>Adapted from Chakar and Ragauskas.<sup>113</sup>

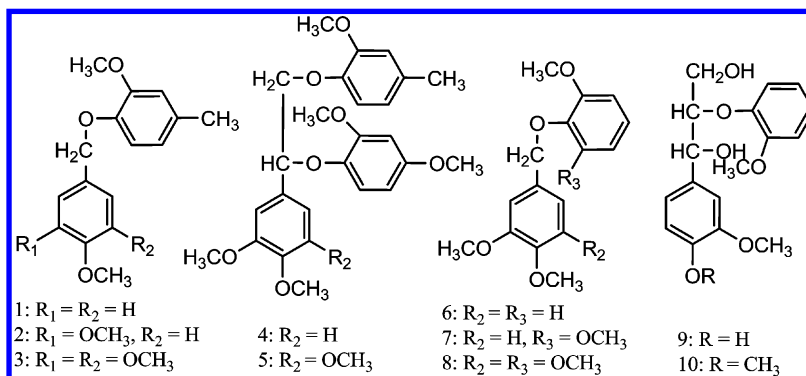


Figure 7. Model compounds synthesized for acid-catalyzed hydrolysis kinetics. Adapted from Papadopoulos et al.<sup>128</sup> and Meshgini et al.<sup>129</sup>

The kinetics of reactions is usually faster in phenols<sup>97</sup> or alcohols<sup>102</sup> than in water due to solvent effects. However, phenol solvents should be carefully selected, as they are active species that can initiate nucleophilic substitution reaction with cations to form the corresponding phenolated byproducts.<sup>148,149</sup>

#### 4.2. Lewis acid

Lewis acid catalysts such as FeCl<sub>3</sub>, ZnCl<sub>2</sub>, BF<sub>3</sub>, and AlCl<sub>3</sub> have been used to depolymerize lignin, with the result that low yields of phenols were produced.<sup>132,135</sup> This was proposed to be a thermodynamically favorable process, since the performance highly depends on the reaction temperature.<sup>150</sup>

Studies by Ekerdt,<sup>134</sup> Vuori,<sup>151</sup> Thring,<sup>132</sup> and their co-workers have demonstrated that Lewis acids became active for lignin depolymerization when they were converted to their Brønsted acid form. It was also found that the reactivity was not

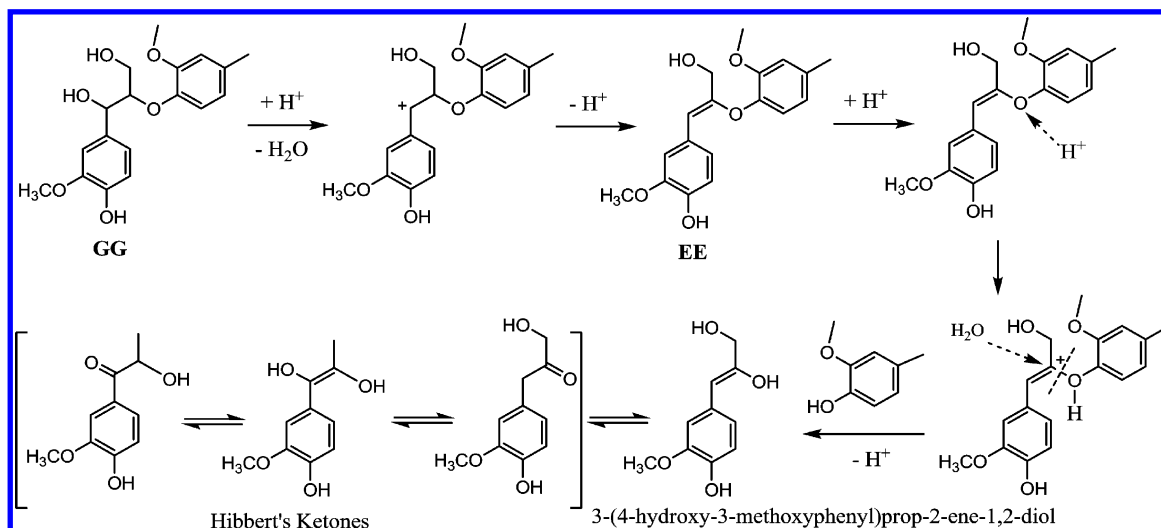
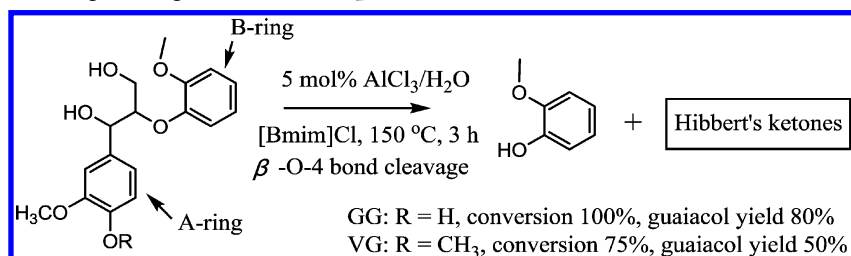
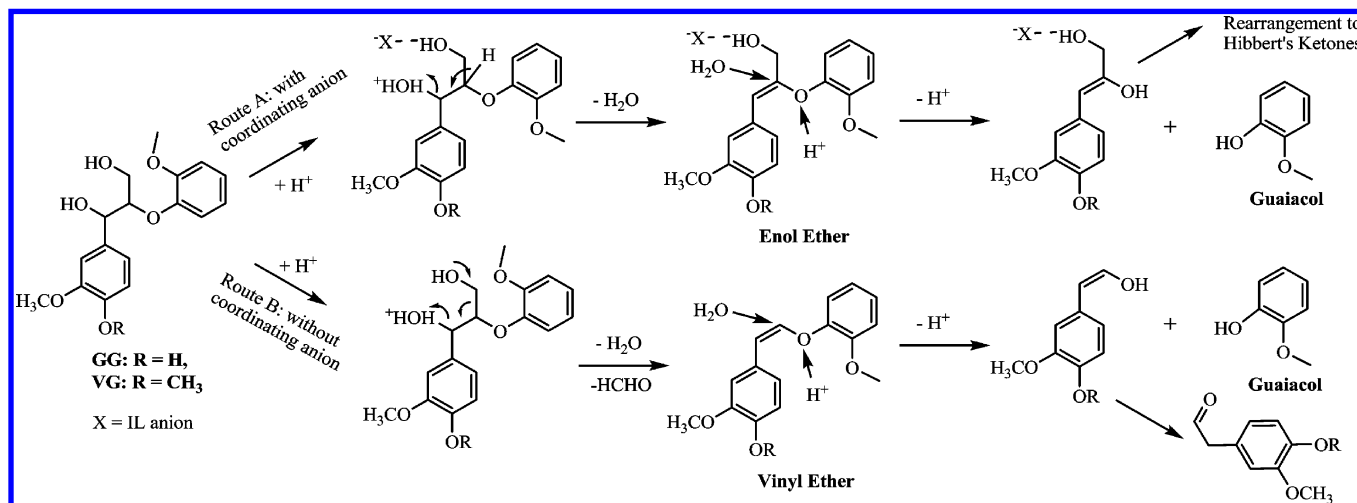
an accurate match for the acidity sequence for the hydrolytic cleavage of C–O linkages in lignin model compounds.<sup>152</sup> Nevertheless, the catalytic activity of the Lewis acid form itself is unclear. The formation of Brønsted acid is thought to occur via a reaction of the Lewis acid with water, or alcohol. Hence, Lewis acids are normally used in combination with water or low molecular alcohol for lignin depolymerization.

#### 4.3. Ionic liquid mediated acid catalysis

Ionic liquid (IL) solvents are advantageous for lignin conversion because they readily dissolve lignin<sup>69,77,81,82,84</sup> and favor carbocation-forming reactions.<sup>153,154</sup> When Lewis acid catalysts such as metal chlorides are applied in ILs, they are more effective in cleaving the β-O-4 bond of lignin and model compounds (Scheme 6).<sup>134</sup> In this process, the real catalytic species is the hydrochloric acid, which is formed *in situ* by the hydrolysis of the metal chlorides. GG gave higher conversion

Table 6. Acid-Catalyzed Degradation of Lignin and Model Compounds

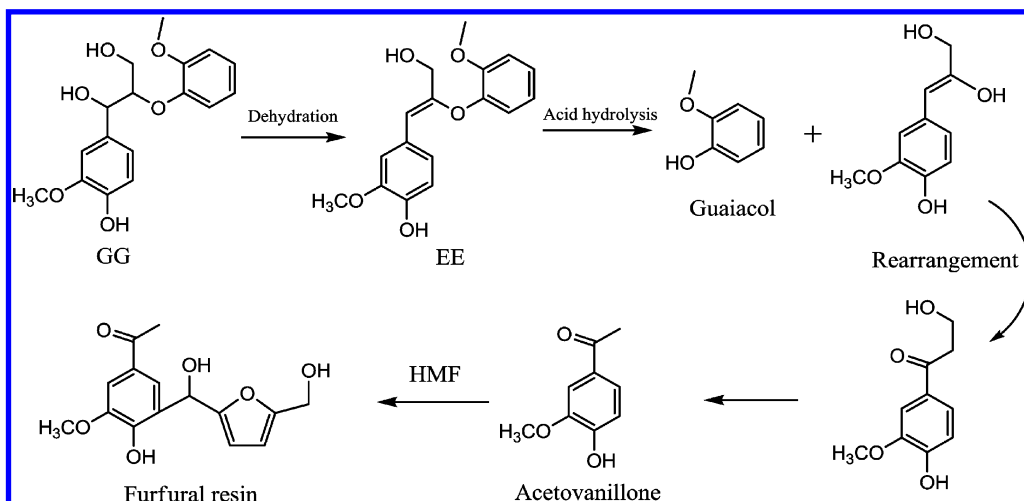
Catalyst	Reaction conditions	Substrate	Product	Note	ref
Metal chloride and water	H <sub>2</sub> O (4:1 to the substrate), 150 °C, 120–240 min, [Bmim]Cl as solvent.	GG and VG	Guaiaicol	Yield: 70%–80%	134
Acidic imidazolium-based ILs	170 $\mu$ L IL, 6.0 mg substrate, 2.0 $\mu$ L water, 150 °C for 1 h	GG and VG	Guaiaicol	Yield: 25%–82%	140
CrCl <sub>3</sub> ·6H <sub>2</sub> O	CrCl <sub>3</sub> ·6H <sub>2</sub> O, GG and glucose, [Bmim]Cl solvent, 170 °C, 2 h.	GG and glucose	Furfural resin	Quantitatively converted.	133
[Hmim]Cl	Hydrolysis in [Hmim]Cl, 110–150 °C, 1 h.	GG and VG	Guaiaicol	Yield of 70% and 65% from GG and VG.	139
Hydrochloric acid	Hydrolysis in [Hmim]Cl, 150 °C, 1 h.	GG	Guaiaicol	100% conv., 55.2% yield.	139
Hydrochloric acid	Hydrolysis in DMSO, 150 °C, 2 h.	VG	Guaiaicol	98.3% conv., 39.1% yield.	139
NiCl <sub>2</sub> ·FeCl <sub>3</sub>	10 wt % catalyst, water solvent, 305 °C, 1 h.	Organosolv lignin	Ether-soluble products	Conversion: 26–30%	132
HZSM-5	Bronsted acidic zeolite catalysts, 500 °C	Alcell lignin	Gasoline range hydrocarbons	85% combined yield	136
HUSY, HZSM-5, HMOR, Clay K10, etc.	Hydrolysis in H <sub>2</sub> O/CH <sub>3</sub> OH (1:5 v/v), 250 °C, 30 min, 500 rpm, 0.7 MPa N <sub>2</sub> .	Dealkaline lignin	Aromatic monomers	40%–60% yields	137
Mineral acid	Refluxing lignin in dioxane-water (9 to 1) containing 0.2 N HCl.	Björkman lignin	Ether-soluble products	Yield: 55%	143
CF <sub>3</sub> SO <sub>3</sub> H	Lignin was destructed in CF <sub>3</sub> SO <sub>3</sub> H at 0 °C for 2 h.	Björkman lignin	Destructed lignin	Molecule mass decreased from 600 to 4400 Da to 150–1800 Da	146
Ga(OTf) <sub>3</sub>	160 °C, 2 h, aqueous ethanol (EtOH 65%, H <sub>2</sub> O 35%) as solvent	Wheat straw	Ethanol-soluble products	Yield: 47 ± 2%	135
Hydrochloric acid	Hydrolysis in [Amim]Cl, 120 °C, 5 h.	Woody biomass	Aromatic molecules	Significant degradation.	130

Scheme 5. Mechanism of Acid-Catalyzed Hydrolysis of  $\beta$ -Phenyl Ether Linkages of Lignin<sup>a</sup><sup>a</sup>Adapted from Ekerdt et al.<sup>139</sup>Scheme 6.  $\beta$ -O-4 Bond Cleavage of Lignin Model Compounds GG and VG<sup>a</sup><sup>a</sup>For the structures of Hibbert's ketones, please refer to Scheme 5. Adapted from Ekerdt and co-workers.<sup>134</sup>Scheme 7. GG and VG Degradation Pathways in Acidic ILs<sup>a</sup><sup>a</sup>Adapted from Ekerdt and co-workers.<sup>140</sup>

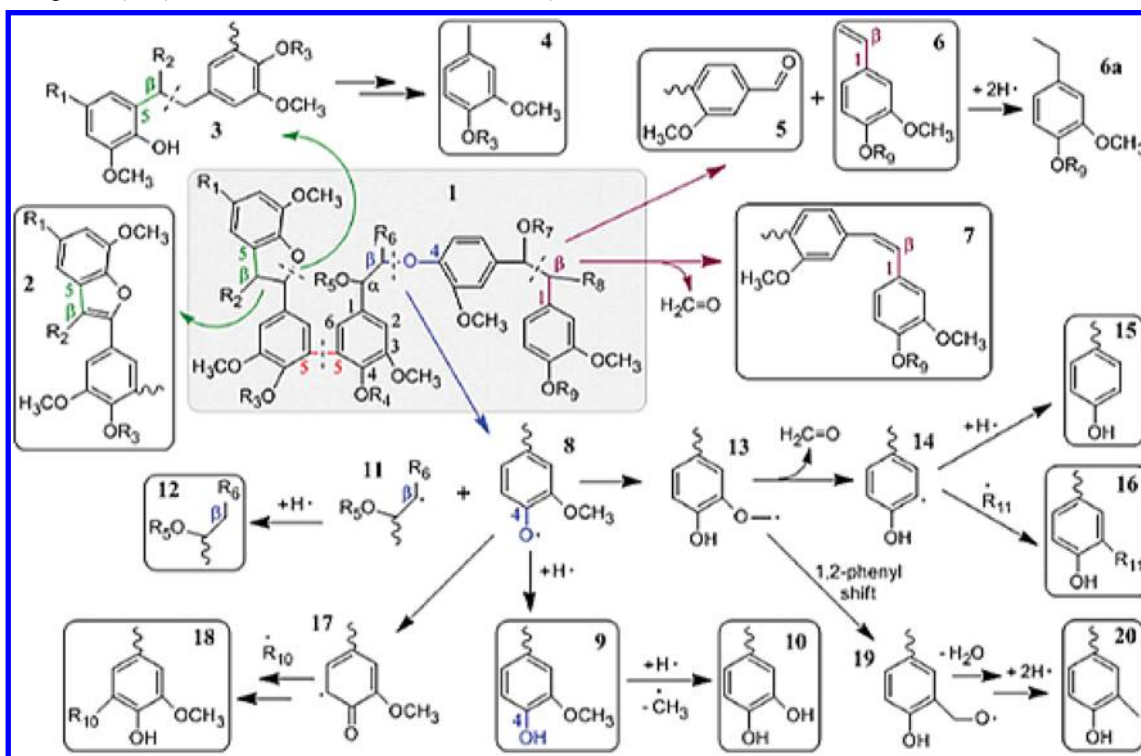
and guaiacol yield than VG, suggesting that the phenolic hydroxide group in the “A-ring” of GG (Scheme 6) may also serve as a proton donor to provide HCl *in situ* by the interaction with metal chlorides.

Using acidic IL as both catalyst and solvent for the hydrolysis of lignin model compounds has also been tested. Ekerdt<sup>139</sup> and co-workers employed 1-H-3-methylimidazolium chloride ([Hmim]Cl) for the treatment of GG and VG. These two

model compounds underwent catalytic hydrolysis to produce guaiacol as the main product with yields higher than 70% at 150 °C. The reactivity and mechanism of the model compounds in the IL depend not only on the acidity, but also on the nature of cations and anions, and their interaction with the substrate.<sup>140</sup> For ILs with bromide, chloride, and hydrogen sulfate as the anions, these ILs could stabilize the hydroxyl group and prevent deprotonation through coordination. The hydrolysis follows a

Scheme 8. Synthesis of Furfural Resin Based on Hydrolysis of GG and Dehydration of Glucose in IL<sup>a</sup>

<sup>a</sup>Adapted from Chang et al.<sup>133</sup>

Scheme 9. Lignin Pyrolysis Reaction Routes as Predicted by NMR Results<sup>a</sup>

<sup>a</sup>1, hypothetical lignin source representing the most common bonds in acid precipitated black liquor; 2, relatively stable  $\beta$ -5 product in the primary decomposition step; 3,  $\alpha$ -O cleavage product; 4, methyl guaiacols; 5, aldehydes; 6, styrenes; 6a ("reduced vinyl-") ethyl-phenols; 7, stilbenes; 8, phenoxy radicals; 9, guaiacols; 10, catechols; 11, 13, 14, 17, 19, transient radicals; 12, aliphatics; 15, phenols; 16, 18, condensation products (e.g. 4-O-5 dimers); 20, cresols. Question mark shows possible 5-5 bond breakage, detailed in the <sup>31</sup>P NMR section. R<sub>1</sub>, cinnamyl group (propanoid unit); R<sub>2</sub>, R<sub>6</sub>, R<sub>8</sub>  $\gamma$  carbons in cinnamyl groups; R<sub>3-5</sub>, R<sub>7</sub>, R<sub>9-11</sub> H, CH<sub>3</sub> or whole phenylpropanoid units/macromolecules. Reprinted with permission from ref 160. Copyright 2011 Royal Society of Chemistry.

typical Brønsted acid catalyzed reaction mechanism (Scheme 7, Route A). Using IL as a solvent with a less coordinating anion such as BF<sub>4</sub><sup>-</sup>, a significant amount of vinyl ether (VE) and formaldehyde were formed through deprotonation of the  $\gamma$ -hydroxyl group following break-off of the  $\gamma$ -carbon (Scheme 7, Route B). It should be noted, however, that repolymerization of lignin fragments via alky-aryl radical coupling reaction occurred

concomitantly in the IL reaction mixture<sup>141</sup> and that the result of real lignin conversion is not given in this catalytic system.

The ability of ILs to swell or dissolve lignocellulose makes it possible to obtain the direct conversion of raw biomass under mild conditions without pretreatment.<sup>155</sup> Argyropoulos<sup>130</sup> and co-workers showed that the acidic pretreatment of the raw wood species in IL [Amim]Cl resulted in not only the complete hydrolysis of cellulose and hemicellulose but also lignin



depolymerization to obtain phenols. In the one-pot hydrolysis of GG and dehydration of glucose in IL with the Lewis acid  $\text{CrCl}_3$ , furfural resin was obtained via the reaction of the dehydration product HMF and the lignin hydrolysis product acetovanillone (Scheme 8).<sup>133</sup> As has been pointed out in section 2.2, there are several challenges with using ILs for biomass conversion, including their high cost, downstream separation issues, and high viscosity.

## 5. PYROLYSIS OF LIGNIN

Pyrolysis is one of the primary thermochemical methods for producing bio-oil directly from lignocellulosic biomass.<sup>156</sup> It is the rapid heating of biomass at temperatures between 450 and 600 °C often in the absence of oxygen to generate a mixture of noncondensable gases, liquid oil, and solid, with or without any catalyst.<sup>157</sup> It represents a straightforward strategy to break down lignin into smaller fragments.

Fast pyrolysis,<sup>158</sup> or pyrolysis with rapid heating of the biomass (above 100 °C/s), has received particular attention because it has been shown to be the thermochemical process that produces the highest yield of a liquid product called a pyrolysis oil or bio-oil.<sup>159</sup> Lignin pyrolysis produces CO and CO<sub>2</sub> (by reformation of C=O and COOH functional groups), and H<sub>2</sub>O, gaseous hydrocarbons (CH<sub>4</sub>, C<sub>2</sub>H<sub>4</sub>, C<sub>2</sub>H<sub>2</sub>, C<sub>3</sub>H<sub>6</sub>, etc.), volatile liquids (benzene and alkyl substituted derivatives, methanol, acetone, and acetaldehyde), monolignols, monophenols (such as phenol, syringol, guaiacol, and catechol), and other polysubstituted phenols,<sup>60</sup> as well as the thermally stable products char and coke. The composition of each fraction and the yield of individual compounds are strongly dependent on the lignin source and the isolation methods.<sup>160–162</sup> For instance, klason lignin produces fewer liquid products compared with steam explosion lignin.<sup>163</sup>

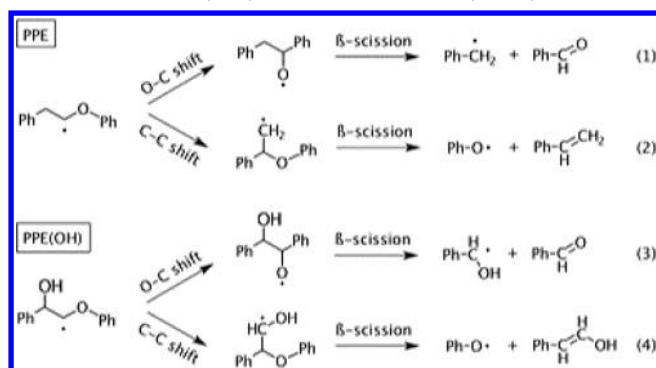
The proportion of each pyrolysis product is dependent on the process variables, particularly the temperature and heating rate.<sup>164</sup> At low temperatures, ether bonds and hydroxyl groups attached to  $\beta$  or  $\gamma$  carbons are readily cleaved to form condensable volatile products and water. A large fraction of methoxyl phenols, such as syringol and guaiacol, are contained in the condensable volatile products due to the fact that the methoxyl groups are more resistant than the ether linkages against thermal degradation. C–C is the most stubborn bond in all chemical transformations; its breaking only occurs at very high temperatures.<sup>165</sup>

The reaction chemistry of lignin pyrolysis is very complicated and occurs over a very broad temperature range. Klein proposed that lignin pyrolysis occurs by free radical chemistry.<sup>166</sup> Whereafter, Britt and co-workers further confirmed that the thermal degradation of lignin principally follows a multiple, parallel radical, and rearrangement pathway.<sup>167</sup> Similar pathways were also reported by Chu,<sup>168</sup> Mullen,<sup>169</sup> Evans,<sup>170</sup> Kotake,<sup>171</sup> Custodis,<sup>172</sup> and Huang<sup>172,173</sup> et al. in their study on lignin pyrolysis with or without catalyst. The main lignin pyrolysis reaction routes were summarized by Ragauskas and co-workers<sup>160</sup> (Scheme 9).

Beste and Buchanan<sup>174</sup> disclosed the role of carbon–carbon phenyl migration in the pyrolysis of  $\beta$ -O-4 lignin model compounds using density functional theory. The activation energy for products produced by  $\beta$ -scission of the oxygen–carbon bond was 15 kcal/mol lower than that produced by carbon–carbon bonds. Therefore, the oxygen–carbon shift reaction was an inert part in the pyrolysis mechanism of phenethyl phenyl ether (PPE) and its derivatives, while the

carbon–carbon shift only accounted for ca. 15% of  $\beta$ -radical conversion at 618 K (Scheme 10).

**Scheme 10.** Shift Reactions and the Subsequent  $\beta$ -Scission Reaction in the Pyrolysis of PPE and  $\alpha$ -Hydroxy PPE<sup>a</sup>



<sup>a</sup>Reprinted from ref 174 with permission. Copyright 2012 American Chemical Society.

### 5.1. Kinetics of lignin pyrolysis

Knowledge of lignin pyrolysis kinetics is critical for predicting the pyrolysis behavior and optimizing the pyrolysis parameters in order to obtain the target products. A number of studies have estimated the lumped kinetic parameters of lignin pyrolysis as summarized in Table 7. In most cases, the apparent activation energies ( $E$ ) of lignin pyrolysis are between 50 and 150  $\text{kJ}\cdot\text{mol}^{-1}$ , with the majority of the kinetic models being first order, single step reactions (Table 7, entries 1–16). However, these publications investigated different types of lignins and used different approaches to measure the kinetics, making it hard to compare the various studies. In a comprehensive study, Cai et al. used a distribution activation energy model to fit pyrolysis data of 7 different biomass feedstocks.<sup>175</sup> The distributed activation energy model assumes that the pyrolysis has a range of activation energies that are centered on an average value. In this model both the average activation energy and the standard deviation of the pyrolysis values are obtained. The lignin pyrolysis could be fit to a model that had an activation energy ranging from 234 to 270  $\text{kJ}/\text{mol}$  for all 7 biomass samples. The cellulose and hemicellulose portions of the biomass samples had a very narrow standard deviation (less than 6  $\text{kJ}/\text{mol}$ ) while the lignin samples had a very broad standard deviation (30–40  $\text{kJ}/\text{mol}$ ), demonstrating that lignin pyrolysis occurs over a broader temperature range than cellulose and hemicellulose pyrolysis. Jiang et al.<sup>176</sup> conducted a systematic investigation on the pyrolysis kinetics of various types of lignins using a dynamic TGA technique. The results (Table 7, entry 17) showed that the estimated apparent activation energies (134–172  $\text{kJ}\cdot\text{mol}^{-1}$ ) depended on both separation methods and the plant species, and were higher than most of reported values, while the frequency factor ( $A$ ) was independent of either separation methods or plant species. Importantly, while the pyrolysis of organosolv lignin, alkali lignin, and hydrolytic lignin were proved to be the first order reactions via unimolecular decomposition, Klason lignin had a reaction order of 1.5 because its condensed structure underwent a bimolecular decomposition mechanism.

Wang<sup>177</sup> and Cho<sup>164</sup> et al. used more complicated kinetic models for lignin pyrolysis. These two research groups proposed a two-step pyrolysis mechanism relying on the

Table 7. Reported Kinetic Parameters for Lignin Pyrolysis<sup>a</sup>

Entry	Lignin type	Method	Temp range (°C)	E(kJ/mol)	Reaction order (n)	A (min <sup>-1</sup> )	ref
1	Klason (Douglas fir)	TGA	25–600	79.8	1		179
2	Periodate (spruce)	TGA	20–600	54.6	1		179
3	Kraft (pine)	Microwave reactor	160–680	25.2	1	4.7 × 10 <sup>2</sup>	180
4	Milled wood (sweetgum hardwood)	Microwave reactor	500–1000	82.0	1	2.0 × 10 <sup>7</sup>	181
5	Kraft (unknown species)	TGA	25–800	129–361	1	3.3 × 10 <sup>7</sup> to 1.8 × 10 <sup>9</sup>	182
6	Alcell (unknown species)	TGA	25–800	80–158	1	6.2 × 10 <sup>11</sup> to 9.3 × 10 <sup>22</sup>	182
7	Steam exploded (aspen)	TGA	25–800	58.6–291.6	1.09	2.7 × 10 <sup>8</sup>	183
8	Klason (hardwood)	TGA	226–435	12.5, 39.4, 42.6	0.5		184
9	Unknown type and species	TGA	390–500	70.7	1	1.26 × 10 <sup>7</sup>	185
10	Organosolv (Eucalyptus)	TGA	30–900	19.1–42.5	0.3–0.74		186
11	Unknown type, birch	Microwave reactor	300–600	75	1	1.2 × 10 <sup>6</sup>	187
12	Alkali (bamboo + hardwood)	TGA	25–900	47.9–54.5	1	6.8 × 10 <sup>2</sup> to 6.6 × 10 <sup>4</sup>	188
13	Alcell (hardwood)	TGA	25–300	8.5–67.9	1		189
14	Unknown type and species	TGA	25–600	120.7–197.3	1	1.0 × 10 <sup>8</sup> to 5.5 × 10 <sup>12</sup>	190
15	Alcell (hardwood)	TGA	25–700	83–195	1		191
16	Enzymatic (Douglas-fir)	TGA	300–650	213	1	2.2 × 10 <sup>24</sup>	192
17	Various types and species	TGA	105–900	134–172	1.5 (Klason), 1 (others)	2.4 × 10 <sup>10</sup> to 9.4 × 10 <sup>12</sup>	176
18	Klason (hardwood)	TGA-FTIR	154–527	87.2 (E1), 141.7 (E2)	Two-step reactions	1.3 × 10 <sup>10</sup> to 7.9 × 10 <sup>13</sup>	177
19	Klason (soft wood)	TGA-FTIR	149–492	72.9 (E1), 136.9 (E2)	Two-step reactions	6.8 × 10 <sup>8</sup> to 5.2 × 10 <sup>9</sup>	177
20	Enzymatic (Maplewood)	TGA-MS	250–400	74 (E1), 110 (E2)	Two-step reactions	8.3 × 10 <sup>5</sup> 2.3 × 10 <sup>6</sup>	164

<sup>a</sup>TGA is the abbreviation of “thermogravimetric analyzer”.

reaction temperature (Table 7, entries 18–20). In the first pyrolysis step, lignin undergoes fast decomposition to solid polyaromatics and volatile products at a low temperature. These primary products are then converted to gases, volatiles, tar, and coke by a variety of reactions, including thermal decomposition, radicals recombination, water gas shift reactions, reforming, and dehydrations.<sup>164,178</sup> In these models, the first step in lignin pyrolysis occurs at *ca.* 450–700 K with an activation energy of 72.9–87.2 kJ·mol<sup>-1</sup>. The second step has a higher activation energy (110–141.7 kJ·mol<sup>-1</sup>) at a temperature above 700 K which produces polyaromatics. This model is able to predict lignin pyrolysis behavior in a temperature range of 250–400 °C.<sup>164</sup> Despite the above progresses, a comprehensive reaction-transport lignin pyrolysis model is currently not available because of the complexity of reactions that occur during lignin pyrolysis. Therefore, we recommend that a future area of research is to try and develop a detailed comprehensive reaction-transport lignin pyrolysis model that accurately models the reaction chemistry in all three phases: solid, liquid, and gas.<sup>171</sup>

## 5.2. Thermal pyrolysis

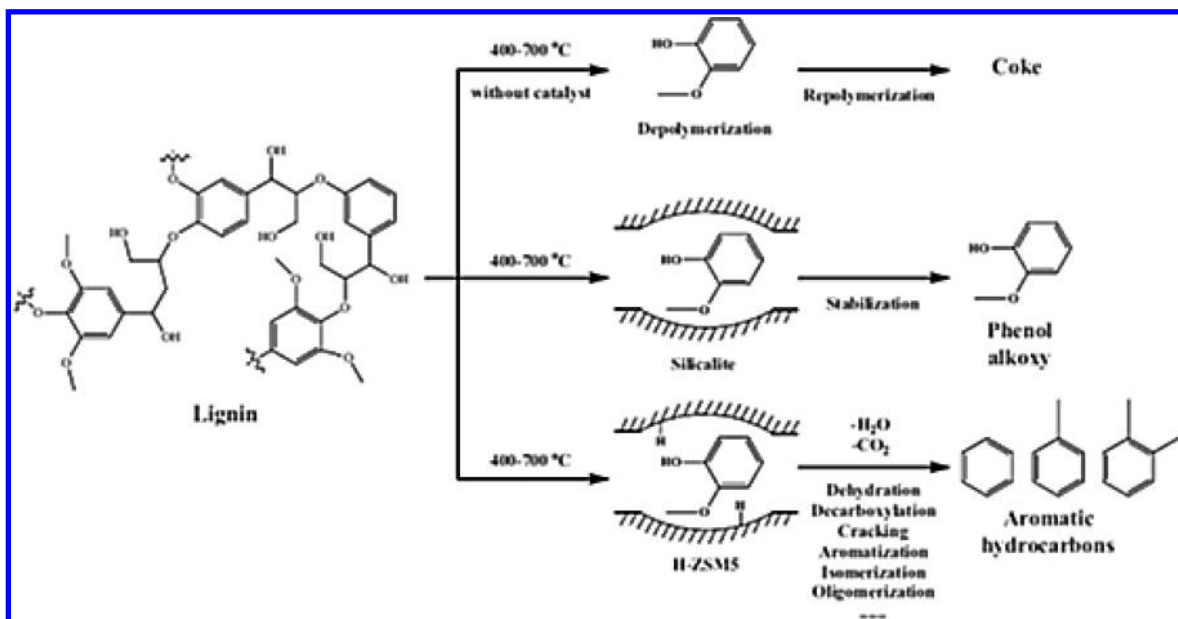
The gases used during pyrolysis can change the reaction chemistry that occurs. Dellinger<sup>193</sup> et al. compared pyrolysis of lignin in N<sub>2</sub> and in 4% O<sub>2</sub> in N<sub>2</sub>. The majority of products from conventional pyrolysis peaked between 400 and 500 °C, while oxidative pyrolysis peaked between 200 and 400 °C. It is interesting to note that the presence of oxygen could not clearly change the type and distribution of the products. In both cases, the phenolic compounds contributed over 40% of the total products detected, and the principal products were guaiacol (2-methoxy phenol), syringol (2,6-dimethoxy phenol), phenol,

and catechol. EPR (electron paramagnetic resonance) results suggested that methoxyl, phenoxy, and substituted phenoxy radicals were the precursors of the major products.

A good solvent could enhance the pyrolysis efficiency. Thring et al.<sup>194</sup> proposed that the presence of ethanol could increase the solubility of lignin and thus increase the amount of ether-soluble phenols. Using ethanol–water binary solvent, Chang et al.<sup>195</sup> developed a process for the hydrothermal depolymerization of cornstalk lignin, and phenolics with the yield of *ca.* 70 wt % were obtained. With an appropriate reagent that absorbs microwave radiation, rapid heating throughout the entire reactor can be achieved. For example, liquefaction of lignocellulosic materials in methanol under microwave irradiation at 180 °C for the short time of 15 min afforded the conversion of 75%. The lignin conversion increased to 88% when a glycerol–methanol mixture was used as solvent.<sup>196</sup>

## 5.3. Catalytic pyrolysis

The addition of a catalyst to the pyrolysis reactor is in favor of controlling the product distribution to valuable hydrocarbon compounds.<sup>169,197–199</sup> Zeolites are one type of catalyst that have often been used in the literature for catalytic pyrolysis of lignin to gasoline range hydrocarbons.<sup>200–202</sup> It has been proposed that zeolite plays two roles in the lignin pyrolysis process.<sup>201</sup> The acid zeolite sites catalyze the depolymerization of lignin into desirable and more stable products. The small volume inside the pores could prevent repolymerization and coke formation reactions. By tuning of the acidity and pore size of zeolites, the selectivity to desired products and the yield of liquid can be controlled. However, low yields (less than 30 wt %) of liquid hydrocarbon products are obtained during catalytic pyrolysis of lignin. Another challenge is that coke/char

Scheme 11. Proposed Lignin Fast Pyrolysis Pathway with or without Catalyst<sup>a</sup>

<sup>a</sup>Reprinted with permission from ref 201. Copyright 2012 Elsevier.

forms on the zeolites, which will cause deactivation of the catalyst upon both pore blockage and active site poisoning.<sup>198,202</sup> The coke/char can be removed by a cation treatment of the zeolite.<sup>202–204</sup> Nevertheless, a gradual decrease in the regenerated catalyst activity was observed due to some irreversible poisoning effect.

Incorporation of cerium into hierarchical HZSM-5 could reduce acidity and thereby slightly decrease coke formation and shift the pyrolysis products from typical HZSM-5 products (benzene, toluene, and xylenes) to valuable oxygenated chemicals (furans, aldehydes, ketones).<sup>198</sup> The addition of cerium to a Pd/TiO<sub>2</sub> catalyst was also helpful in the fast pyrolysis of lignin in poplar wood into monomeric phenols.<sup>197</sup>

Another challenge with zeolites is their low hydrothermal stability in steam and especially in hot liquid water.<sup>205</sup> It has been reported that ZSM-5 is stable in liquid water between 150 and 200 °C for 6 h regardless of the SiO<sub>2</sub>/Al<sub>2</sub>O<sub>3</sub> ratio, while zeolite Y degraded through the hydrolysis of Si–O–Si bonds under the same conditions.<sup>206</sup> Therefore, when considering aqueous-phase processing for lignin conversion, further study and optimization of the stability of zeolites in the presence of water or steam is an arduous task.

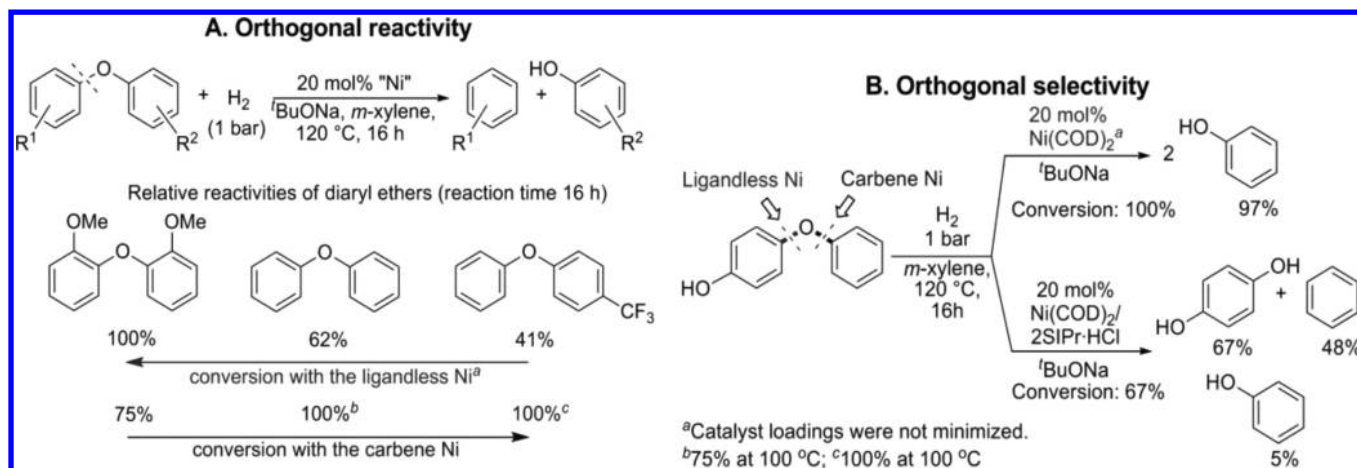
Scheme 11 illustrates the dual roles of zeolite in the lignin pyrolysis reaction, namely, the role of porosity to stabilize intermediates and of acid sites to cleave C–O and C–C bonds.<sup>201</sup> Thermal pyrolysis without catalyst first generates depolymerization intermediates via a radical mechanism.<sup>207</sup> These active primary products are readily repolymerized to produce solid, or stabilized to form low molecular weight aromatics.<sup>202</sup> In the presence of porous materials without acidic sites, such as Na-ZSM-5 and silicalite, the intermediates are stabilized by adsorption in the porous materials; thus, the yield of solid is decreased with the increasing of the liquid yield. Addition of acid functionality results in the cleavage of C–O and C–C bonds. The strong acid sites in zeolites can even induce decarboxylation, dehydration, dealkylation, isomerization, cracking, and oligomerization reactions. In all the above processes, the gases mainly consist of CO<sub>2</sub>, CO, and

CH<sub>4</sub>, which are probably generated from cracking of different side-chain structures and the methoxy groups on aromatic ring, via a direct hydrogen-transfer mechanism, via a radical coupling mechanism,<sup>178,208</sup> or from pyrogallol via an *o*-quinone intermediate.<sup>178</sup> Guo and co-workers<sup>209</sup> reported that, under pyrolysis conditions, the pyrolytic lignins generate 40% aromatics based on carbon yield at 600 °C and more than 90% of which are phenols.

Zaror and co-workers<sup>210</sup> showed that the addition of Na<sub>2</sub>CO<sub>3</sub>, K<sub>2</sub>CO<sub>3</sub>, KCl, and NaCl could accelerate dehydration and promote recombination reactions among the volatile species to yield more char than untreated wood, while Shanks and co-workers<sup>211</sup> observed no significant difference in the char yield when inorganic salts were added to corn stover organosolv lignin. A recent study by Yin and co-workers<sup>212</sup> showed that both inorganic and organic Na salts could reduce the pyrolysis temperature of alkali lignin. Furthermore, organic Na could increase the yields of phenol and guaiacol by the elimination of alkyl substituents, while inorganic Na promotes the formation of ethers by the elimination of phenolic hydroxyl groups. The basic additives such as KOH were also reported to improve the depolymerization efficiency.<sup>213</sup> When a Lewis acid ZnCl<sub>2</sub> was used in the pyrolysis of different types of lignins (steam-explosion, kraft, and ball-milled lignins), an increased amount of guaiacol and methylguaiacol, accompany with carbonyl-containing compounds such as homovanillin, acetovanillone, and coniferaldehyde appeared in the liquid products (compared to the results with no catalyst).<sup>170</sup>

In summary, thermal depolymerization of lignin follows a series of random and complicated reactions that produce low yields of a complex product mixture. Wet lignin from an aqueous-based biorefinery or from most pulping processes must be dried before entering a pyrolysis process decreasing the viability of this process because the evaporation of a large amount of water present in lignin feedstock requires a lot of energy. Jones and Zhu conclude that lignin pyrolysis at present is not economically attractive.<sup>214</sup> Fast pyrolysis oil, or bio-oil, is a potential feedstock to make liquid transportation fuels. The





**Figure 8.** Differences in reactivity and selectivity between the ligandless and carbene-ligated nickel catalysts. Reprinted with permission from ref 228. Copyright 2012 American Chemical Society.

pyrolysis oil consists of up to 50 wt % of pyrolytic lignin, which is thought to derive from pyrolysis of the lignin structure of biomass.<sup>215</sup> This suggests that the hemicellulose and cellulose somehow play a role in stabilizing the lignin pyrolysis intermediates during pyrolysis of the entire biomass species. The bio-oil is a low quality liquid fuel, that is an emulsion of several phases that has many undesired characteristics, including low pH, high viscosity, low energy density (high oxygen content), and stability problems, and it cannot be blended with conventional petroleum fuels.<sup>216–218</sup> Several companies, including KiOR,<sup>219</sup> are developing technology to produce liquid transportation fuels from biomass by pyrolysis and hydrotreating. The obtained oil must be upgraded (see in section 6.2) to meet the requirements of a desired transportation fuel before use.

DeSisto<sup>220</sup> and Kleinert<sup>221,222</sup> et al. recently described a novel integrated lignin liquefaction process based on pyrolysis at a temperature above 350 °C with the participant of formic acid or formate. In the inert atmosphere, the formic acid and formate serve as hydrogen donors that facilitate the HDO of the bio-oil *in situ* to produce liquid oil with very low oxygen content that is suitable as a blending component for motor fuel applications. This method provides significant improvements over conventional pyrolysis technologies through decreasing the oxygen/carbon ratio and increasing the carbon yield in the liquid product.

## 6. HYDROPROCESSING

Hydroprocessing involves thermal reduction of the feed by hydrogen. It is one of the most popular and efficient strategies applied in deconstruction of lignin into components such as low depolymerized lignin, phenols, and other valuable chemicals, and upgrading of the small compounds to hydrocarbon fuels. This section is organized according to the reaction types of hydroprocessing, in the order of hydrogenolysis, hydroalkylation, hydrodeoxygenation, hydrogenation, and integrated hydrogen-related reactions. The iron-group-based catalysts, the group VI metal-based catalysts, the platinum-group-based catalysts, and the bimetallic catalysts, as well as the bifunctional catalysts systems will be reviewed for the aforementioned reactions. In this regard, we focus on the updated results since 2010, while earlier results are only briefly mentioned.

### 6.1. Hydrogenolysis

Hydrogenolysis describes a chemical reaction whereby carbon–carbon or carbon–heteroatom bonds are cleaved by hydrogen according to eq 1:<sup>223</sup>



Generally, the X represents an alkyl chain or other functional group containing heteroatoms (OH, SH, NH<sub>2</sub>, OR, NR, etc.). Hydrogenolysis is an important reaction for lignin upgrading, particularly in cleaving of C–O bonds. Hydrodeoxygenation (HDO), removing oxygen from the phenolic molecules to produce hydrocarbons, is also included in the scope of hydrogenolysis. HDO is a paramount important process in bio-oil up-grading and thus will be discussed thoroughly in section 6.2. In this section we discuss cleavage of etheric C–O bonds. This reaction usually takes place under basic conditions with supported metal catalysts such as Pt, Ru, Ni, Pd, and Cu.<sup>224,225</sup> In the generation of fuels and chemicals, selective hydrogenolysis of aliphatic C–O bonds is preferred, while the aryl C–O bonds are far less active, and require high temperatures and/or high hydrogen pressures. The harsh hydrogenolysis condition, in turn, leads to undesired concurrent cleavage of aliphatic C–O bonds and hydrogenation of aromatic rings.

Nickel-based catalysts used for lignin hydrogenation/hydrogenolysis can be dated back to the 1940s.<sup>226</sup> In 1979, Ni-complexes were reported as a potential hydrogenolysis catalyst toward aryl C–O bonds with Grignard reagents by Wenkert.<sup>227</sup>

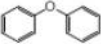
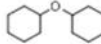
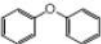
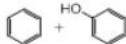
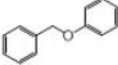

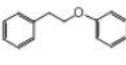
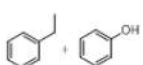
Sergeev and Hartwig<sup>120</sup> recently made great progress on soluble nickel complex catalyzed hydrogenolysis of diaryl ethers. Their catalytic system is composed of Ni(COD)<sub>2</sub> and SiPr-HCl (20 mol %) as a catalyst (where COD is 1,5-cyclooctadiene, and SiPr-HCl is a N-heterocyclic carbene ligand precursor) and NaOtBu (2.5 equiv) as an additive. The reactions were conducted under only 0.1 MPa H<sub>2</sub> at around 100 °C to afford high yields (54–99%) of the corresponding phenols and arenes. This catalytic system is suitable for fairly broad substrates including both electron-rich and electron-poor diaryl ethers, and the activity to cleave aromatic C–O bonds is in the order of Ar-OAr ≫ Ar-OMe > ArCH<sub>2</sub>-OMe. A heterogeneous Ni catalyst was developed subsequently by the same group via *in situ* decomposition of the Ni(COD)<sub>2</sub> or Ni(CH<sub>2</sub>TMS)<sub>2</sub>(TMEDA) precursor.<sup>228</sup> Even at loadings down



Table 8. Hydrogenolysis of Lignin and Lignin Model Compounds over Ni-Based Catalysts

Catalyst	Support	Reaction conditions			Lignin (model) compound	Major products	Conv. (%)	Note	Ref
		T (°C)	P (MPa)	solvent					
Ni(COD) <sub>2</sub> , SIPr·HCl	None	120	0.1	<i>m</i> -Xylene			> 85%	R=H, Me, <i>m</i> -OMe, CF <sub>3</sub>	120
Ni(COD) <sub>2</sub> , SIPr·HCl	None	120	0.1	<i>m</i> -Xylene			100	Alk=Hexyl, Me	120
Ni(COD) <sub>2</sub> , SIPr·HCl	None	120	0.1	<i>m</i> -Xylene			85	Alk=Hexyl	120
Ni(COD) <sub>2</sub> , SIPr·HCl	None	120	0.1	<i>m</i> -Xylene			> 85%	R <sup>1</sup> = <sup>t</sup> Bu, H; R <sup>2</sup> = Ph, Me; R <sup>3</sup> = H, Et	120
Heterogeneous Ni	None	120	0.1	<i>m</i> -Xylene			72		228
Heterogeneous Ni	None	120	0.1	<i>m</i> -Xylene			19	BuONa, (0.2 equiv)	228
Heterogeneous Ni	None	120	0.1	<i>m</i> -Xylene			84	BuONa, (1.0 equiv)	228
Heterogeneous Ni	None	120	0.1	<i>m</i> -Xylene			100	BuONa (2.5 equiv)	228
Heterogeneous Ni	None	120	0.1	<i>m</i> -Xylene			>90	BuONa (2.5 equiv)	228
Heterogeneous Ni	None	120	0.1	<i>m</i> -Xylene			80~99	BuONa (2.5 equiv)	228
Heterogeneous Ni	None	120	0.1	<i>m</i> -Xylene			75~97	BuONa (2.5 equiv)	228
Heterogeneous Ni	None	120	0.1	<i>m</i> -Xylene			98	BuONa (2.5 equiv)	228
Heterogeneous Ni	None	120	0.1	<i>m</i> -Xylene			80~93	BuONa (2.5 equiv)	228
Ni	SiO <sub>2</sub>	120	0.6	H <sub>2</sub> O			6~21		229
Raney Ni	None	90	5	MeOH			12.4		242
Raney Ni	None	90	5	EtOH			33		242
Raney Ni	None	90	5	2-Propanol			72.7		242

Table 8. continued

Catalyst	Support	Reaction conditions			Lignin (model) compound	Major products	Conv. (%)	Note	Ref
		T (°C)	P (MPa)	solvent					
Raney Ni	None	90	5	Decaline or methylcyclohexane			99~100		242
Ni-TiN	None	150	1.2	EtOH			99		239
Ni-TiN	None	125	1.2	EtOH			>99		239
Ni-TiN	None	150	1.2	EtOH			>99		239
Ni	AC	200	5	EG	Lignosulfonate	Monophenols	68		231
Ni	AC	200	5	H <sub>2</sub> O	Lignosulfonate	Monophenols	0		231
Ni	AC	200	5	Cyclohexane	Lignosulfonate	Monophenols	0		231
Ni	C	200	0.1 (Ar)	MeOH, EtOH, EG	Birch sawdust	Monophenols	48–54		233
Ni-W <sub>2</sub> C	AC	235	6	H <sub>2</sub> O	Raw woody biomass	Monophenols	46.5		238
Ni <sub>85</sub> Ru <sub>15</sub>	None	130	1	H <sub>2</sub> O	Organosolv lignin	Monophenols	42		241
Ni <sub>85</sub> Rh <sub>15</sub>	None	130	1	H <sub>2</sub> O	Organosolv lignin	Monophenols	50		241
Ni <sub>85</sub> Pd <sub>15</sub>	None	130	1	H <sub>2</sub> O	Organosolv lignin	Monophenols	56		241
Ni <sub>7</sub> Au <sub>3</sub>	None	170	1	H <sub>2</sub> O	Organosolv lignin	Monophenols	14		240

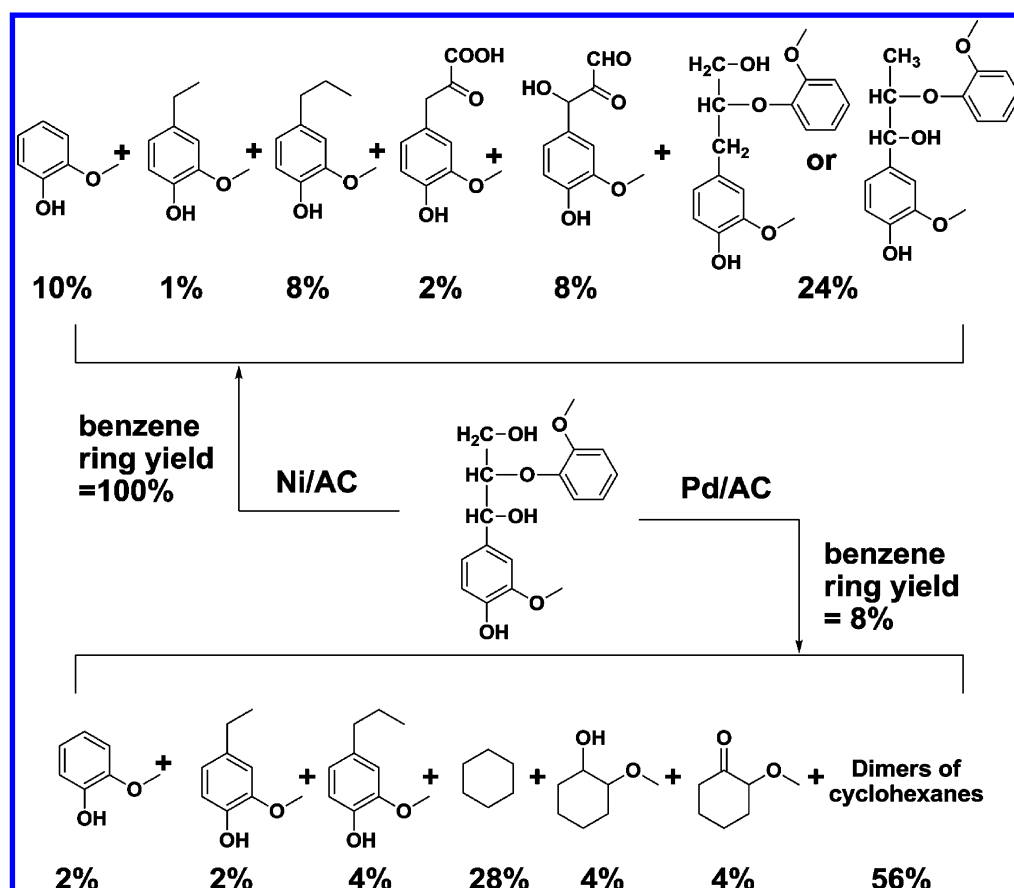
to 0.25 mol %, the catalyst can selectively cleave the aryl C–O bonds of aryl ethers without hydrogenation of aromatic rings in the presence of BuONa. It should be noted that strong bases are favorable in these hydrogenolysis reactions, though the effects are still in debate. More interestingly, the selectivities of the homogeneous and the heterogeneous catalysts are quite different for electronically varied aryl ethers (shown in Figure 8), implying that the mechanisms of these two catalysts are quite different.

Zhao and Lercher<sup>229</sup> reported a novel SiO<sub>2</sub> supported Ni catalyst to selectively cleave aromatic C–O bonds of aryl ethers in the aqueous phase. This catalyst is not water sensitive, unlike the homogeneous catalysts. The C–O bonds of  $\alpha$ -O-4 and  $\beta$ -O-4 are cleaved by hydrogenolysis, while the 4-O-5 linkage is cleaved through parallel hydrogenolysis and hydrolysis, due to the employment of aqueous solvent. In their report, however, hydrogenation of phenol proceeded over Ni catalysts along with the hydrogenolysis under the investigated conditions; thus, cyclohexanol was also observed in the products.

Ni catalysts, supported on carbon and magnesium oxide, not only are active for C–O bond cleavage of model compounds, but also are promising catalysts to selectively hydrogenolyse the aryl ether C–O bonds of  $\beta$ -O-4 without disturbing the arenes,

even when using lignosulfonate as the feedstock in methanol solvent.<sup>230,231</sup> Inspired by Agapie's work on model compounds,<sup>232</sup> Wang and Xu<sup>233</sup> showed that the hydrogenolysis of real lignin could also be conducted in alcohol solvent, including methanol, ethanol, and ethylene glycol. In this reaction the alcohol solvents can also be used as a hydrogen donor. Rinaldi<sup>88</sup> and co-workers also found similar hydrogen transfer reactions for the depolymerization of lignin with poplar wood as the feed using Ni-based catalysts.

It was well documented that the introduction of a second metal to a monometallic catalyst can enhance the catalytic performance in many reactions.<sup>234</sup> Zhang and co-workers disclosed that carbon supported Ni–W<sub>2</sub>C catalyzes not only the direct conversion of cellulose into ethylene glycol,<sup>235–237</sup> but also the hydrogenolysis of the lignin component in various woody biomass into monophenols with the yield of 46.5%.<sup>238</sup> Interestingly, neither Ni/AC nor W<sub>2</sub>C/AC afforded the yield of monophenols higher than 20%, implying the synergistic effect between Ni and W<sub>2</sub>C in lignin conversion. Similar synergistic effect was also reported on Ni-TiN,<sup>239</sup> NiAu,<sup>240</sup> and three NiM (M = Rh, Ru, and Pd)<sup>241</sup> catalysts for organosolv lignin hydrogenolysis. Mechanistic investigation<sup>241,242</sup> indicated that the synergistic effect could be attributed to three factors: (1)



**Figure 9.** Comparison of products in the hydrogenolysis of guaiacyl glycerol- $\beta$ -guaiacyl ether (GG) over Ni/C and Pd/C. The benzene ring yield is defined as the ratio of the sum of benzene rings of the aromatic products to the added GG doubled by two (containing two benzene rings). Reprinted with permission from ref 231. Copyright 2012 Royal Society of Chemistry.

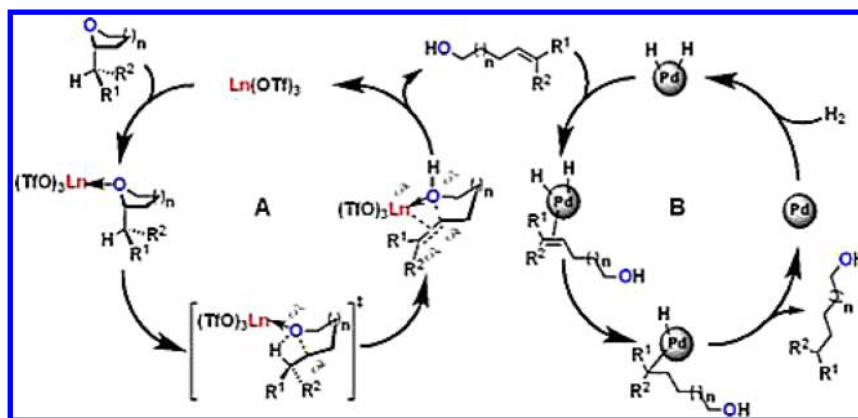
increased fraction of catalytically active surface atoms, (2) improved  $H_2$  and substrate activation capability, and (3) inhibited benzene ring hydrogenation. The latest hydrogenolysis results of lignin model compounds and real lignin over Ni catalysts are listed in Table 8.

The platinum-group metals (abbreviated as PGMs), such as Pd, Pt, Ru, Rh, and Ir, possess outstanding catalytic properties in hydrogen involved reactions. In contrast to Ni catalysts, PGMs bear higher intrinsic activity and, hence, are widely used in direct hydrogenolysis of raw and pretreated lignins. Nevertheless, milder conditions are preferred over PGM catalysts, considering that the products of hydrogenolysis (the linkage of C–C and the alcohol) are not stable in the presence of PGM under severe conditions. Under mild hydrogenolysis conditions, pinus radiata and olive tree pruning lignins are degraded into monomeric, dimeric, and oligomeric compounds over Al-SBA-15 supported Ni, Pd, Pt, Ru,<sup>243</sup> and Pd/C<sup>244</sup> via selective cleavage of the aryl-O-aliphatic and aryl-O-aryl linkages, while corn stalk lignin with different ratios of H, G, and S units are selectively hydrogenolyzed to 4-ethylphenolics (4-EP), in particular over Ru/C.<sup>245</sup> Noting that lignins from different feedstocks and extraction methods possess significantly different structures, Bouxin and co-workers<sup>246</sup> investigate the impact of the lignin structure on the hydrogenolysis products over Pt/Al<sub>2</sub>O<sub>3</sub>. It was found that the proportion of  $\beta$ -O-4 linkages in the lignin was critical for obtaining higher yields of monomeric products. Highly condensed lignin generated mainly nonalkylated phenolic products while uncondensed

lignin generated mainly phenolic products retaining the 3-carbon side chain.

Due to their high hydrogen transfer ability, PGMs generally catalyze not only the hydrogenolysis process, but also other H-related reactions. As exemplified by model compounds (Figure 9), the products over Pd/C consist mainly of dimers and cyclohexane, remarkably different from that over Ni/C, and this confirms that Pd/C hydrogenates the arenes concurrently with the hydrogenolysis of  $\beta$ -O-4 bonds.<sup>231</sup> Abu-Omar<sup>247</sup> and co-workers demonstrated that introducing Zn in Pd-based catalysts is far more effective than Pd/C alone for the cleavage of  $\beta$ -O-4 bonds in model monomeric/dimeric and artificial polymer lignin model compounds. More importantly, the hydrogenolysis is followed by a HDO of the aromatic alcohols without hydrogenating the arenes, therefore maintaining the aromaticity of the feedstock and decreasing hydrogen consumption. In regard to real lignin feedstock, addition of tiny amounts of mineral acids<sup>248</sup> or solid acid<sup>249</sup> allows the hydrogenolysis under milder conditions and accordingly enhances the depolymerization efficiency. Usually, hydrogenation is closely associated with hydrogenolysis over PGM catalysts.<sup>250</sup> Depending on reaction conditions, both processes may occur successively or simultaneously.

Besides the aromatic ethers, it should be remembered that aliphatic ethers and furans also constitute a significant component of lignin biomass; however, in the absence of allylic or benzylic junctures, the C–O bonds are typically unreactive. Marks<sup>251</sup> and co-workers used a homogeneous transition metal triflate and supported Pd nanoparticle catalyst

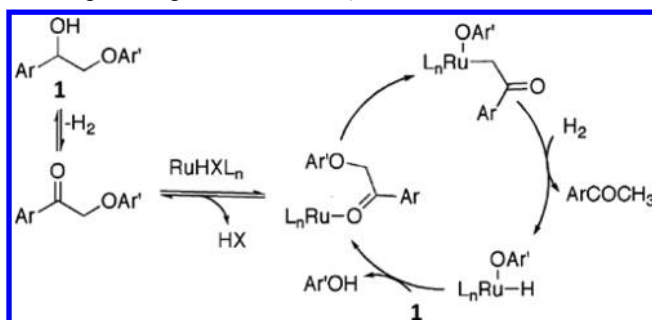


**Figure 10.** Proposed tandem pathway for lanthanide triflate/Pd nanoparticle-mediated etheric C–O bond hydrogenolysis. Ln = lanthanide; R<sup>1</sup>, R<sup>2</sup> = organic functional group. Reprinted with permission from ref 251. Copyright 2012 American Chemical Society.

system to catalyze ether hydrogenolysis in IL media with a thermodynamically based tandem strategy. The cleavage of the C–O bond is coupled via a microscopic reverse of endothermic alkene hydroalkoxylation (Cycle A in Figure 10) with exothermic C=C hydrogenation (Cycle B in Figure 10);<sup>251</sup> thus, saturated alcohols are yielded without any loss of aromaticity. If the reaction was performed with Hf(OTf)<sub>4</sub> + Pd/C in a solvent-free system, the reactant scope could be expanded to aliphatic ethers and furans.<sup>252</sup>

Homogeneous Ru catalysts also displayed high hydrogenolysis reactivity toward the cleavage of β-O-4 ethanol aryl ethers without disturbing the arene species.<sup>250,253,254</sup> In contrast to the thermal tandem strategy, homogeneous Ru, such as Ru(Cl)<sub>2</sub>(PPh<sub>3</sub>)<sub>3</sub>, RuH<sub>2</sub>(CO)(PPh<sub>3</sub>)<sub>3</sub>, and Ru-xantphos, catalyzed lignin hydrogenolysis proceeds by a redox neutral approach, i.e. a tandem dehydrogenation/C–O bond cleavage process (as shown in Scheme 12).

**Scheme 12.** Mechanism of Ru-Catalyzed C–O Bond Cleavage of Lignin-Related Polymers<sup>a</sup>



<sup>a</sup>Reprinted with permission from ref 253. Copyright 2010 American Chemical Society.

## 6.2. Hydrodeoxygenation

HDO is considered the most efficient method for bio-oil upgrading. Herein, we focus on the recent advances of HDO achieved using different types of catalysts. More fundamental knowledge on HDO of lignin model compounds has recently been reported by Gates and Rahimpour.<sup>255</sup>

**6.2.1. Monometallic catalysts.** Molybdenum oxide, sulfide, nitride, and carbide were studied as catalysts for the HDO reaction of lignin and model compounds as early as in the 1980s.<sup>256</sup> In MoO<sub>3</sub>-catalyzed HDO of lignin model

compounds, it was found that MoO<sub>3</sub> preferentially cleaved phenolic Ph-O-Me bonds over weaker aliphatic Ph-O-Me bonds.<sup>257</sup> The same phenomenon was observed in Mo<sub>2</sub>C-catalyzed HDO of anisole.<sup>258</sup> Investigation of different supports and nitridation methods showed that the supports can modify the property of active sites and hence are responsible for the products' selectivity, while the dispersion and the nitridation degree of molybdenum are crucial to the activity of the HDO reaction.<sup>223,259</sup> When MoS<sub>2</sub> supported on carbon was employed as the catalyst for lignin HDO, the properties of MoS<sub>2</sub> active sites are independent of the textural and chemical properties of different carbon supports.<sup>260</sup> Smith<sup>261</sup> and co-workers compared HDO activities of different unsupported low-surface-area Mo-based catalysts, namely, MoS<sub>2</sub>, MoO<sub>2</sub>, MoO<sub>3</sub>, and MoP, using 4-methylphenol as the substrate. The catalyst turnover frequency (TOF) based on CO uptake decreased in the order MoP > MoS<sub>2</sub> > MoO<sub>2</sub> > MoO<sub>3</sub>, while the activation energy increased in the order MoP < MoS<sub>2</sub> < MoO<sub>2</sub> < MoO<sub>3</sub>. The activity is related to the electron density of the Mo among the catalysts. The latest HDO results of lignin model compounds over Mo-based catalysts are listed in Table 9.

Transition metal phosphides Ni<sub>2</sub>P, Fe<sub>2</sub>P, Co<sub>2</sub>P, and WP<sup>265,266</sup> have been applied in the HDO of lignin-derived feedstock recently.<sup>264,267</sup> The superiority of these transition metal phosphides catalysts to noble metal catalysts is their high selectivity without compromising the substrate conversion, while their superiority to commercial hydrotreating CoMoS catalysts is their high stability in the gas-phase HDO process.<sup>264,268</sup> Considering that FeS<sub>2</sub> usually has lower activity for aromatic nucleus hydrogenation, Rinaldi<sup>269</sup> and co-workers supported FeS<sub>2</sub> on active carbon, SBA-15, SiO<sub>2</sub>, and Al<sub>2</sub>O<sub>3</sub> to catalyze the selective HDO of dibenzyl ether and toluene, with yields up to 100% realized. Meanwhile, Ni-based catalysts with different stabilizing components (SiO<sub>2</sub>, SiO<sub>2</sub>-ZrO<sub>2</sub>, CeO<sub>2</sub>-ZrO<sub>2</sub>, and δ-Al<sub>2</sub>O<sub>3</sub>) were also studied in the HDO of bio-oils.<sup>199,270</sup> Especially, the addition of Cu facilitated reduction of nickel oxide at lower temperatures<sup>271</sup> and decreased the coke formation rate.<sup>272</sup> Correspondingly, Cu promoted sol-gel Ni catalysts exhibited good performance in guaiacol HDO.<sup>270</sup> In addition, Cu mixed metal oxide catalysts tend to have weak acidity, low hydrogenation reactivity, and high hydrogenolysis activity; therefore, they are also considered promising catalysts for HDO.<sup>197,273</sup> The HDO results of different catalysts systems are listed in Table 10.



Table 9. HDO of Lignin Model Compounds over Mo-Based Catalysts

Cat.	Support	Reaction conditions			Lignin model compd	Major products	Conv. (%)	Reactor	ref
		T (°C)	P (MPa)	solvent					
MoS <sub>2</sub>	Al <sub>2</sub> O <sub>3</sub>	250–450	3.4	1-Methylnaphthalene	4-Propylguaiaicol	Propylphenols, propylbenzenes	38–99	Batch	262
MoS <sub>2</sub>		350	4	Decalin	4-Methylphenol	Toluene	60	Batch	261
MoS <sub>2</sub>	AC	300	5	Decalin	Guaiaicol	Phenol	30	Batch	260
Mo <sub>2</sub> C		150	0.1		Anisole	Benzene	100	Packed bed	258
Mo <sub>2</sub> N		300	5	Decalin	Guaiaicol	Phenol	10	Batch	263
Mo <sub>2</sub> N	Al <sub>2</sub> O <sub>3</sub>	300	5	Decalin	Guaiaicol	Catechol	66	Batch	223
Mo <sub>2</sub> N	SBA-15	300	5	Decalin	Guaiaicol	Phenol	44	Batch	223
MoN	AC	300	5	Decalin	Guaiaicol	Phenol	9.0 × 10 <sup>-6</sup> (mol/gcat.s)	Batch	259
MoP	SiO <sub>2</sub>	300	0.1		Guaiaicol	Benzene, phenol	54	Packed bed	264
MoP		350	4	Decalin	4-Methylphenol	Toluene	90	Batch	261
MoO <sub>2</sub>		350	4	Decalin	4-Methylphenol	Toluene	55	Batch	261
MoO <sub>3</sub>		350	4	Decalin	4-Methylphenol	Toluene	100	Batch	261
MoO <sub>3</sub>		320	0.1		<i>m</i> -cresol	Toluene	48.9	Packed bed	257
MoO <sub>3</sub>		320	0.1		Anisole	Benzene	78.7	Packed bed	257
MoO <sub>3</sub>		320	0.1		Guaiaicol	Phenol, benzene	74.2	Packed bed	257
MoO <sub>3</sub>		320	0.1		Diphenyl ether	Benzene, phenol	82.6	Packed bed	257

Table 10. HDO of Lignin Model Compounds over Various Metallic Catalysts<sup>a</sup>

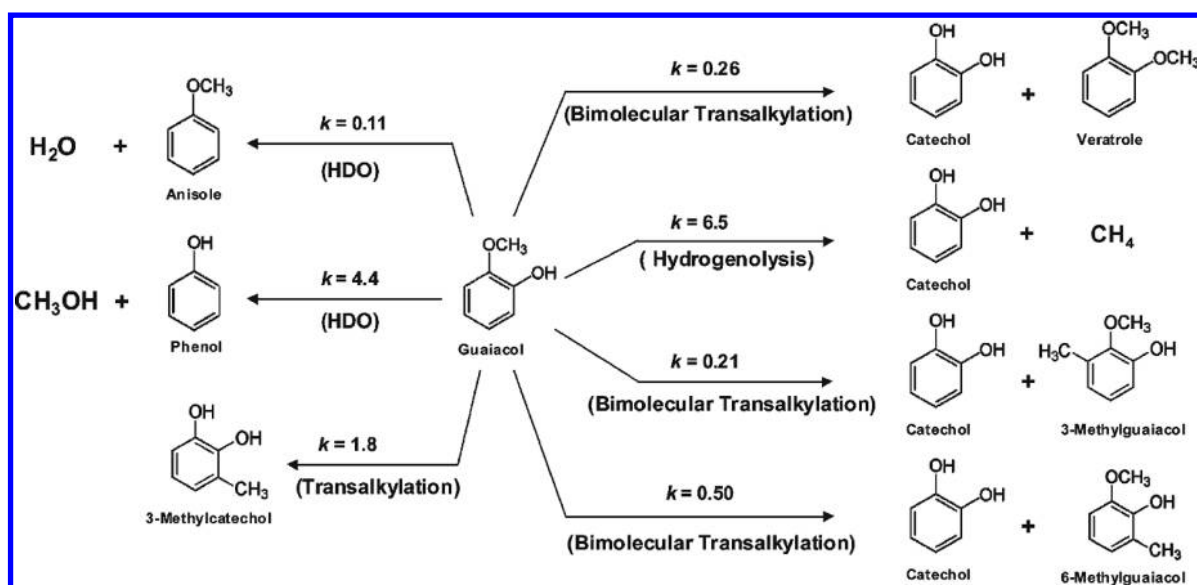
Catalyst	Support	Reaction conditions			Conv. (%)	Major products	Sele. (%)	Reactor	ref
		T (°C)	P (MPa)	Solution/Gas conc					
Ni <sub>2</sub> P	SiO <sub>2</sub>	300	0.1	0.024% GUA; 80% H <sub>2</sub> , N <sub>2</sub> rest	80	Benzene	60	Packed bed	264
Co <sub>2</sub> P	SiO <sub>2</sub>	300	0.1	0.024% GUA; 80% H <sub>2</sub> , N <sub>2</sub> rest	70	Benzene	52	Packed bed	264
Fe <sub>2</sub> P	SiO <sub>2</sub>	300	0.1	0.024% GUA; 80% H <sub>2</sub> , N <sub>2</sub> rest	64	Phenol	94	Packed bed	264
FeS <sub>2</sub>	AC	250	10	Dibenzyl ether in cyclohexane	98	Toluene	100	Packed bed	269
Ni <sub>30.3</sub> Cu <sub>10.4</sub>	CeO <sub>2</sub> –ZrO <sub>2</sub>	320	17	99% GUA	94.2	O-containing aliphatics C5–C7	92.5	Batch	270
Ni <sub>14.1</sub> Cu <sub>5.7</sub>	Al <sub>2</sub> O <sub>3</sub>	320	17	99% GUA	80.3	Aliphatics C5–C7+ benzene	49.9	Batch	270
Ni <sub>57.9</sub> Cu <sub>7.0</sub>	SiO <sub>2</sub>	320	17	99% GUA	87.1	Aliphatics C5–C7 + benzene	72.7	Batch	270
Ni <sub>36.5</sub> Cu <sub>2.3</sub>	ZrO <sub>2</sub> –SiO <sub>2</sub> –La <sub>2</sub> O <sub>3</sub>	320	17	99% GUA	85.6	Aliphatics C5–C7 + benzene	80.1	Batch	270
Ni <sub>55.4</sub>	SiO <sub>2</sub>	320	17	99% GUA	97.7	Aliphatics C5–C7 + benzene	90.9	Batch	270
Zn/Pd	AC	150	2	GG in MeOH	90	GUA and 4-propyl-GUA	85	Batch	247
Zn/Pd	AC	150	2	Vanillin in MeOH	>99	Creosol	81	Batch	247
Zn/Pd	AC	150	2	4-(Methoxymethyl)-GUA in MeOH	>99	Creosol	81	Batch	247
Zn/Pd	AC	150	2	Vanillyl alcohol in MeOH	>99	Creosol	80	Batch	247
Zn/Pd	AC	150	2	β-O-4 synthetic lignin polymer in MeOH	100	4-Propyl-GUA; dihydroconiferyl alcohol	80	Batch	247

<sup>a</sup>GUA is the abbreviation of guaiacol.

Compared to lignin model compounds, relatively limited studies have been conducted on HDO real lignin feedstocks. Water-soluble ammonium heptamolybdate (AHM) was studied in hydro-treating of five Kraft lignins and one organosolv lignin,<sup>274</sup> and the degree of HDO over AHM was as high as 98%. Recently, Li demonstrated that, over carbon supported tungsten phosphide, an appreciable yield of mixed phenols (67 mg/g lignin) could be obtained in catalytic HDO of alkaline lignin.<sup>267</sup>

It should be noted that, besides HDO reactions, Li and co-workers<sup>275</sup> recently reported that complete ethanolysis of Kraft lignin could be catalyzed over α-molybdenum carbide in an inert atmosphere at 280 °C. In their study, both the catalyst and the solvent are crucial for the liquid oil yield and product composition, whereas hydrogen plays a negative role for the formation of soluble aromatics.

As mentioned in 6.1, platinum group metal (PGMs) (Pt, Pd, Ru, Rh) catalysts alone are not a good choice for the target



**Figure 11.** Reaction network of guaiacol conversion over Pt/ $\gamma$ -Al<sub>2</sub>O<sub>3</sub> under H<sub>2</sub> pressure at 573 K. H<sub>2</sub> is omitted for simplicity. Reprinted from ref 278 with permission. Copyright 2011 American Chemical Society.

HDO process,<sup>276–278</sup> as they tend to saturate benzene rings, owing to their high hydrogenation activity. For instance, the reaction network of guaiacol HDO over Pt/ $\gamma$ -Al<sub>2</sub>O<sub>3</sub> includes intramolecular transalkylation, hydrogenolysis, and three bimolecular transalkylations (Figure 11).<sup>278</sup> To modify the catalytic activity of noble metal catalysts, Wang<sup>279</sup> and co-workers synthesized Pd nanoparticles supported on mesoporous N-doped carbon, and the resulting Pd@CN<sub>0.132</sub> catalyst showed high catalytic activity (100% conversion, 100% selectivity for 2-methoxy-4-methylphenol) in HDO vanillin at low H<sub>2</sub> pressure under mild conditions in aqueous media. In addition, synergistic catalysis of the combination of noble metal with a second metal is found in the HDO of aromatic compounds,<sup>247</sup> and will be described in the following section.

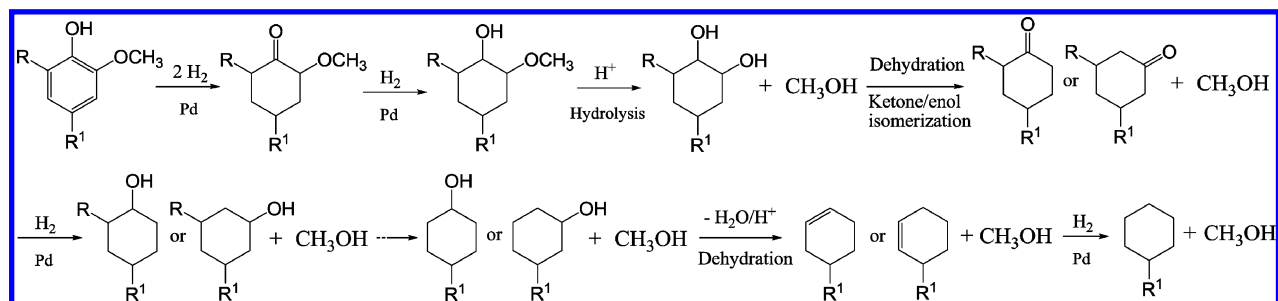
**6.2.2. Bimetallic catalysts.** In comparison with the monometallic catalyst, the use of bimetallic catalysts is an interesting strategy, as it offers the possibility to modify the catalyst property and tailor the selectivity to a particular product. Mixed sulfides of Co, Ni, Mo, and W, as well as other bimetallic catalyst systems, such as PtSn,<sup>280</sup> PtRh,<sup>277</sup> NiRe,<sup>281</sup> PtRe,<sup>282</sup> and ZnPd,<sup>247</sup> are used most frequently in lignin HDO. These bimetallic catalysts usually show a significant improvement in HDO selectivity compared to a monometal. As early as in the 1980s, CoMo catalysts have been shown to be promising for the HDO of phenol.<sup>283</sup> Later studies showed that a series of aromatic compounds exhibited significant improvement in HDO rate over Co or Ni promoted Mo catalysts compared to a sulfided Mo catalyst alone.<sup>284–286</sup>

Generally, HDO of lignin proceeds through two main routes: hydrogenation–deoxygenation or direct deoxygenation.<sup>285,287</sup> Some reports proposed that the addition of Co or Ni to Mo catalysts could strongly enhance the direct deoxygenation pathway versus the former one,<sup>285</sup> while others reported that the improvement of HDO performance was attributed to the enhancement of demethoxylation and deoxygenation pathways.<sup>284,286</sup> For sulfided CoMo catalytic systems, a clear support effect was observed in guaiacol HDO. Compared to  $\gamma$ -alumina and titania, zirconia was a preferred carrier for the CoMoS phase in the HDO reaction, as it delivered much higher catalytic activity.<sup>284</sup>

In lignin HDO reactions, CoMo catalysts are superior to Ni analogs, due to their lower hydrogenation ability to keep the aromaticity of feeds intact.<sup>286,288,289</sup> For the different substrates, Weckhuysen<sup>283</sup> and co-workers found that the  $\beta$ -O-4 and  $\beta$ -5 ether bonds have higher cleavage rates than 5–5' linkage under HDO conditions, and the major products are incompletely deoxygenated phenol or/and cresol over CoMo sulfide catalysts.

The advantages of adding a second metal can be classified in three main aspects: (i) increase catalytic activity, (ii) improve catalyst stability, and (iii) modify the selectivity. These advantages may arise from four different effects, namely, geometric (or ensemble) effects, electronic (or ligand) effects, synergistic effects, as well as bifunctional effects (which will be discussed in the next section).<sup>290</sup> Typically, the catalytic activity and selectivity are mainly affected by geometric and electronic effects, while the reaction rate is normally improved with synergistic and bifunctional effects; it should be noted that the latter two effects may also lead to the creation of new reaction pathways.

It should be pointed out that although the advantages of using bimetallic catalysts are evident, there are still several challenges to be overcome. First, the carbon deposition over (Co, Ni) and (Mo, W) catalysts<sup>291</sup> is a big problem in HDO: the coking increases with the increasing acidity of the catalysts, but the acid sites are required in the HDO mechanism.<sup>292</sup> Second, sulfide catalysts are easily deactivated via the oxidation of active sites due to the high ratio of oxygen/sulfur in the bio-oil.<sup>293</sup> Both the nature of the oxygenated compound (substrate) and the surface properties of the support are reported to be crucial to poisoning.<sup>294</sup> To solve this problem, Yan and co-workers developed a series of amorphous (Co, Ni)-(Mo, W)-B-based catalysts,<sup>293,295</sup> of which tungsten oxide or molybdenum oxide act as the Brønsted acid sites for the dehydration reaction while Ni or Co species act as the catalyst for hydrogenation.<sup>293</sup> Third, the interactions between the catalysts and impurities are yet unclear so far. This problem stands out when real feedstocks with many impurities are used. Therefore, more fundamental studies are required to establish correlations

Scheme 13. Proposed Reaction Pathway for Phenolic Aromatics HDO over Pd/C in the Presence of Acid<sup>a</sup>

<sup>a</sup>R = H, OCH<sub>3</sub>; R<sup>1</sup> = alkyl. Adapted from Lercher et al.<sup>296</sup>

Table 11. HDO of Lignin and Model Compounds over Bifunctional Catalysts

Cat.	Reaction conditions			Lignin (model) compd	Major products	Sele. (%)	Conv. (%)	ref
	T (°C)	P (MPa)	Solvent					
Pd/C + H <sub>3</sub> PO <sub>4</sub>	250	5	H <sub>2</sub> O	Cerulignol	Propylcyclohexane	66	100	296
Pd/C + H <sub>3</sub> PO <sub>4</sub>	250	5	H <sub>2</sub> O	Eugenol	Propylcyclohexane	65	99	296
Pd/C + H <sub>3</sub> PO <sub>4</sub>	250	5	H <sub>2</sub> O	4-Hydroxy-3-methoxyphenylacetone	Propylcyclohexane	71	100	296
Pd/C + H <sub>3</sub> PO <sub>4</sub>	250	5	H <sub>2</sub> O	Methoxyeugenol	Propylcyclohexane	58	92	296
Pd/C + H <sub>3</sub> PO <sub>4</sub>	250	5	H <sub>2</sub> O	Phenol	Cyclohexane	98	100	301
Pd/C + H <sub>3</sub> PO <sub>4</sub>	250	5	H <sub>2</sub> O	Catechol	Cyclohexane	87	100	301
Pd/C + H <sub>3</sub> PO <sub>4</sub>	250	5	H <sub>2</sub> O	4-Methylguaiaicol	Methylcyclohexane	78	100	301
Pd/C + H <sub>3</sub> PO <sub>4</sub>	250	5	H <sub>2</sub> O	4-Ethylguaiaicol	Ethylcyclohexane	80	100	301
Rh NPs	130	4	[Bmim][BF <sub>4</sub> ]	Phenol	Cyclohexane	67	95	302
Ru NPs	130	4	[Bmim][BF <sub>4</sub> ]	Phenol	Cyclohexane	97	77	302
Pt NPs	130	4	[Bmim][BF <sub>4</sub> ]	Phenol	Cyclohexane	98	48	302
Rh NPs	130	4	[Bmim][NTF <sub>2</sub> ]	Phenol	Cyclohexane	84	98	302
Rh NPs	130	4	[Bmim][NTF <sub>2</sub> ]	Anisole	Cyclohexane	99	73	302
Rh NPs	130	4	[Bmim][NTF <sub>2</sub> ]	<i>p</i> -Cresol	Methylcyclohexane	98	86	302
Rh NPs	130	4	[Bmim][NTF <sub>2</sub> ]	4-Ethylphenol	Ethylcyclohexane	99	84	302
Rh/Ru NPs	130	4	[Bmim][NTF <sub>2</sub> ]	4-Ethylphenol	Ethylcyclohexane	99	99	302
Pd/C + HZSM-5	200	5	H <sub>2</sub> O	Phenol	Cyclohexane	100	100	303
Pd/C + HZSM-5	200	5	H <sub>2</sub> O	4-Methylguaiaicol	Methylcyclohexane	100	88	303
Pd/C + HZSM-5	200	5	H <sub>2</sub> O	4-Ethylguaiaicol	Ethylcyclohexane	100	89	303
Pd/C + HZSM-5	200	5	H <sub>2</sub> O	Phenethoxybenzene	Cyclohexane; ethylcyclohexane	100	46/54	303
Pd/C + HZSM-5	200	5	H <sub>2</sub> O	Benzyl phenyl ether	Cyclohexane; methylcyclohexane	100	48/52	303
Pd/C + HZSM-5	200	5	H <sub>2</sub> O	Diphenyl ether	Cyclohexane	100	100	303
Pd/C + HZSM-5	200	5	H <sub>2</sub> O	2,2'-Biphenol	Bicyclohexane	100	100	303
Ru/HZSM-5	200	5	H <sub>2</sub> O	2,2'-Biphenol	Bicyclohexane	100	78	298
Ru/HZSM-5	200	5	H <sub>2</sub> O	3,3'-Oxydiphenol	Cyclohexane	100	97	298
Ru/HZSM-5	200	5	H <sub>2</sub> O	Eugenol	Propylcyclohexane	100	85	298
Ni/SiO <sub>2</sub> -ZrO <sub>2</sub>	300	5	Dodecane	Guaiaicol	Cyclohexane	100	97	304
Raney Ni + Nafion/SiO <sub>2</sub>	300	4	H <sub>2</sub> O	Phenol	Cyclohexane	100	93	305
Raney Ni + Nafion/SiO <sub>2</sub>	300	4	H <sub>2</sub> O	Guaiaicol	Cyclohexane	100	71	305
Raney Ni + Nafion/SiO <sub>2</sub>	300	4	H <sub>2</sub> O	4-Methylguaiaicol	Methylcyclohexane	100	74	305
Raney Ni + Nafion/SiO <sub>2</sub>	300	4	H <sub>2</sub> O	4-Ethylguaiaicol	Ethylcyclohexane	100	71	305
Raney Ni + Nafion/SiO <sub>2</sub>	300	4	H <sub>2</sub> O	4-Propylphenol	Propylcyclohexane	100	91	305
Raney Ni + Nafion/SiO <sub>2</sub>	300	4	H <sub>2</sub> O	Methoxyeugenol	Propylcyclohexane	89	62	301
(Ru, Rh, Pt over Al <sub>2</sub> O <sub>3</sub> ) + acidic zeolite	250	4–5	H <sub>2</sub> O	Steam explosion lignin	Toluene and alkylbenzenes	35–60	65–70	306
Ni/HZSM-5	220	0.1 (Ar)	MeOH–H <sub>2</sub> O	Kraft lignin	Alkyl substituted phenols and oligomers	97	55	307

between structure and catalytic performance on real lignin feedstock.

**6.2.3. Bifunctional catalysts.** Bifunctional catalysts, containing both metal and acid components, were developed to solve the deactivation problem caused by the conventional

sulfide-based HDO catalysts. Kou and Lercher<sup>296</sup> reported that a bifunctional combination of Pd/C, Pt/C, Ru/C, or Rh/C and phosphoric acid could selectively catalyze the HDO of phenolic components into cycloalkanes and methanol. During the reaction, metal-catalyzed hydrogenation and acid-catalyzed

hydrolysis/dehydration were supposed to couple together<sup>296–298</sup> (Scheme 13), which differs from the mechanism for sulfide catalysts.<sup>299,300</sup> A systematic kinetic study<sup>301</sup> revealed that the dual catalytic functions are indispensable and that the acid-catalyzed steps determined the overall HDO reaction; hence, high concentrations of acid sites were required in efficient HDO catalysis. Further, Kou and Dyson<sup>302</sup> substituted the Pd/C and mineral acid by metal nanoparticles and Brønsted acidic IL, providing a more efficient and less energy-demanding upgrading process. (See Table 11.)

Solid Brønsted acids were also found effective in the bifunctional catalysts combination for HDO.<sup>303,305,308–310</sup> Especially, HZSM-5 showed higher reaction rate and lower apparent activation energy compared to other tested solid acids (sulfated zirconia, Amberlyst 15, Nafion/SiO<sub>2</sub>, and Cs<sub>2.5</sub>H<sub>0.5</sub>OW<sub>12</sub>O<sub>40</sub>), due to its relatively high acid concentration in the zeolite pores.<sup>303</sup> Moreover, the combination of Pd/C and HZSM-5 was not only able to catalyze the HDO of phenolic monomers, but also the HDO of phenolic dimers. The latter one requires a cascade metal-acid-catalyzed cleavage of C–O bonds ( $\beta$ -O-4,  $\beta$ -5, etc.) and integrated hydrogenation and dehydration reactions.<sup>303</sup> This actually comprises the process of hydrogenolysis (mentioned in 6.1) and HDO and thus opens an efficient pathway for upgrading lignin-derived phenolic oils. Ni-based hydrogenation catalysts such as Raney Ni combined with Nafion (or SiO<sub>2</sub>),<sup>305</sup> Ni/HZSM-5,<sup>307,311</sup> and Ni/Al<sub>2</sub>O<sub>3</sub>–HZSM-5,<sup>309</sup> instead of precious metal catalysts, were also effective in the bifunctional HDO catalysts system.<sup>307</sup> The hydrogenation of phenol was the rate-determining step in the Ni/HZSM-5 and Ni/Al<sub>2</sub>O<sub>3</sub>–HZSM-5 system; hence, high Ni dispersions were required in efficient catalysis.<sup>309</sup>

Although widely employed as solid acids, the abundant micropores in zeolite may greatly confine the diffusion of real lignins, as well as limit the accessibility of acid sites. Therefore, efficient methods (ethanol and dilute alkali extraction) were applied to obtain reactive lignin oligomers from corn stover first, and subsequently HDO the oligomeric technical lignins with a promising conversion (35%–60%) and selectivity toward toluene (65%–70%), in the presence of PGMs catalysts and solid acid zeolites.<sup>306</sup>

### 6.3. Hydrogenation

Hydrogenation is a chemical reaction which employs a pair of hydrogen atoms to reduce or saturate organic compounds. The double or triple carbon–carbon bonds, as well as C=O bonds, are saturated during hydrogenation and increase the percentage of H in the final products. The selectivity for hydrogenation toward aromatic C=C, linear C=C, C=O, C $\equiv$ C, etc. varies drastically due to the different nature of catalysts<sup>312,313</sup> and is controllable via fine manipulation of the catalyst system and reaction conditions. Generally, hydrogenation occurs with hydrogenolysis simultaneously, or is included in the process of hydrogenolysis, HDO, and other upgrading methods.

Recently, zerovalent metals (Al, Fe, Mg, and Zn) were reported to be active for hydrogenation of the C=O groups within the bio-oil at ambient temperature and pressure to increase the chemical stability (pH value) of the obtained bio-oil.<sup>314</sup> As a pseudo precious metal catalyst, Mo<sub>2</sub>C/C prepared via a facile microwave irradiation was found to be highly active in the selective hydrogenation of naphthalene into tetralin with a 100% selectivity.<sup>315</sup> Despite this progress, precious metals are still considered more promising hydrogenation catalysts in spite of their higher costs.<sup>316,317</sup> Based on the intrinsic activities of

different precious metal catalysts and manipulation of reaction engineering, Vispute et al.<sup>215</sup> developed a tandem catalytic process that converted pyrolysis oils into industrial chemical feedstock. In this system, Ru/C and Pt/C were respectively employed for the hydrogenation of pyrolysis oil to produce polyols and alcohols. The hydrogenated products were then converted into light olefins and aromatic hydrocarbons over zeolite.

For the hydrogenation of lignin and model compounds catalyzed with supported metal, the support nature and metal dispersion, the choice of solvent, as well as the alkenyl substituent of the substrate are all crucial in determining the hydrogenation selectivity.<sup>316,318</sup> Highly polarized groups in lignin interacting with water will to some extent protect its interaction with the metal surface and result in selective hydrogenation of the aromatic ring.<sup>318,319</sup>

In comparison with conventional catalysis, electrocatalytic hydrogenation is a new technique in biomass conversion that has been reported as a way to stabilize and upgrade the biomass-derived bio-oil. Saffron, Jackson, and co-workers recently shown that Ru/C<sup>320</sup> and RANEY Nickel<sup>321</sup> were effective cathodic catalysts for electrocatalytic hydrogenation and partial hydrodeoxygenation of phenolic compounds; better results were obtained under mild conditions ( $\leq 80$  °C and ambient pressure) compared to other reduction methods.

Besides the aforementioned strategies, much research focused on different hydrogen sources and H-transfer was also widely undertaken to achieve the upgrading process under low-severity conditions,<sup>322–325</sup> as described in Laurenczy's recent review.<sup>326</sup>

### 6.4. Integrated hydrogen-processing

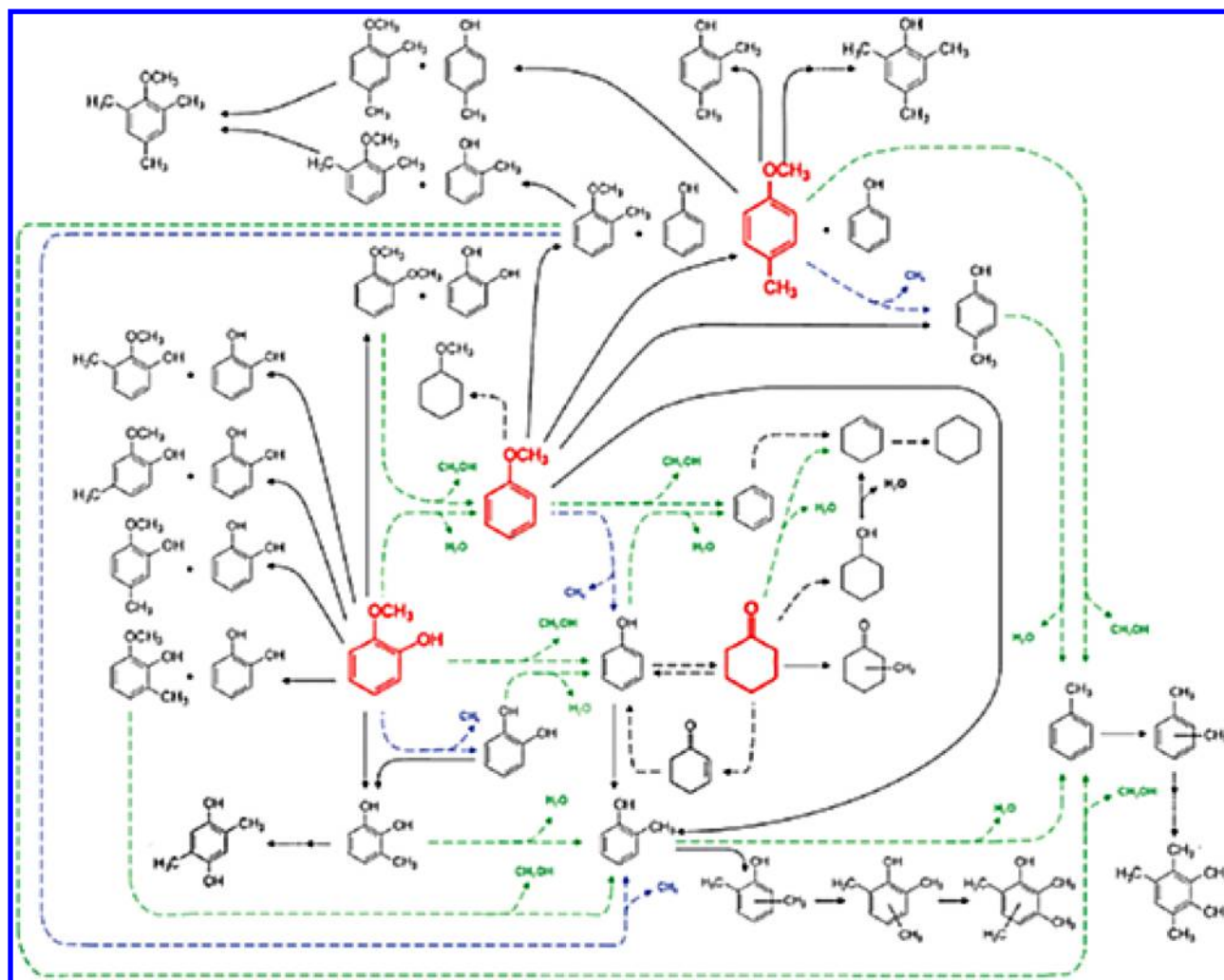
Due to the extremely complicated multifunctional groups of the lignin substrate, it is hard to obtain only one product from lignin conversion. In the aforementioned hydroprocessing reactions, they actually include various minor reactions undiscussed. Integrated hydrogen-processing that includes deconstruction of lignin and upgrading of small components to expected products is favorable. The catalyst systems which directly convert lignin to bio-oils and chemicals, or catalyze several reactions in a batch subsequently, will not only reduce the complexity of the lignin transformation and benefit the economy of the conversion process, but also increase the possibility to scale up the lignin biorefinery process.

Integrated hydrogen-processing of lignin and model compounds, including upgrading of pyrolysis oils, involves all the reactions mentioned above, such as hydrogenolysis, HDO, hydrogenation, transalkylation (hydroalkylation), etc. HDO, hydroalkylation, and dehydration reactions are favored at higher temperatures, with up to 99.9% removal of oxygen attributed to these reactions, while hydrogenolysis and hydrogenation are dominant at lower temperatures.<sup>327</sup> Almost all the hydrogenation catalysts, including bimetallic catalysts, can activate the aldehydes, ketones, phenols, and unsaturated carbon–carbon bonds of lignin.<sup>328</sup> The activity and selectivity depend mainly on the nature of the catalyst, and factors such as the solvent, hydrogen pressure, and temperature, etc. Most studies use model compounds, such as phenol, guaiacol, cresol, and anisole instead of raw lignin as substrates to identify the products and the reaction network due to the complicated structure of raw lignin.

Gates<sup>329–331</sup> and co-workers did extensive work on determining the reaction network of model compounds and



Scheme 14. Reaction Network for the Hydrotreating of Lignin-Derived Compounds (each compound shown in red was used as a reactant) with Pt/ $\gamma$ -Al<sub>2</sub>O<sub>3</sub> at 573 K and 140 kPa<sup>a</sup>



<sup>a</sup>HDO, hydrogenolysis, and hydrogenation (or dehydrogenation) reactions are represented by dashed green, blue, and black arrows, respectively. Transalkylation reactions are represented by solid black arrows. H<sub>2</sub> is omitted for simplicity. Reprinted with permission from ref 329. Copyright 2012 Royal Society of Chemistry.

real lignin catalyzed by various metallic catalysts, such as Pt/ $\gamma$ -Al<sub>2</sub>O<sub>3</sub>, in the presence of H<sub>2</sub> (Scheme 14). In their described network, the most important reaction types were hydrogenolysis, HDO, hydrogenation, and intramolecular (or bimolecular) transalkylation.<sup>329</sup> Some reactions are reversible (e.g., cyclohexanone produces phenol), while most others appeared irreversible. Transalkylation usually occurs in the presence of an acid such as  $\gamma$ -Al<sub>2</sub>O<sub>3</sub>, while the other three reactions are kinetically significant in the presence of a metal catalyst and H<sub>2</sub>.

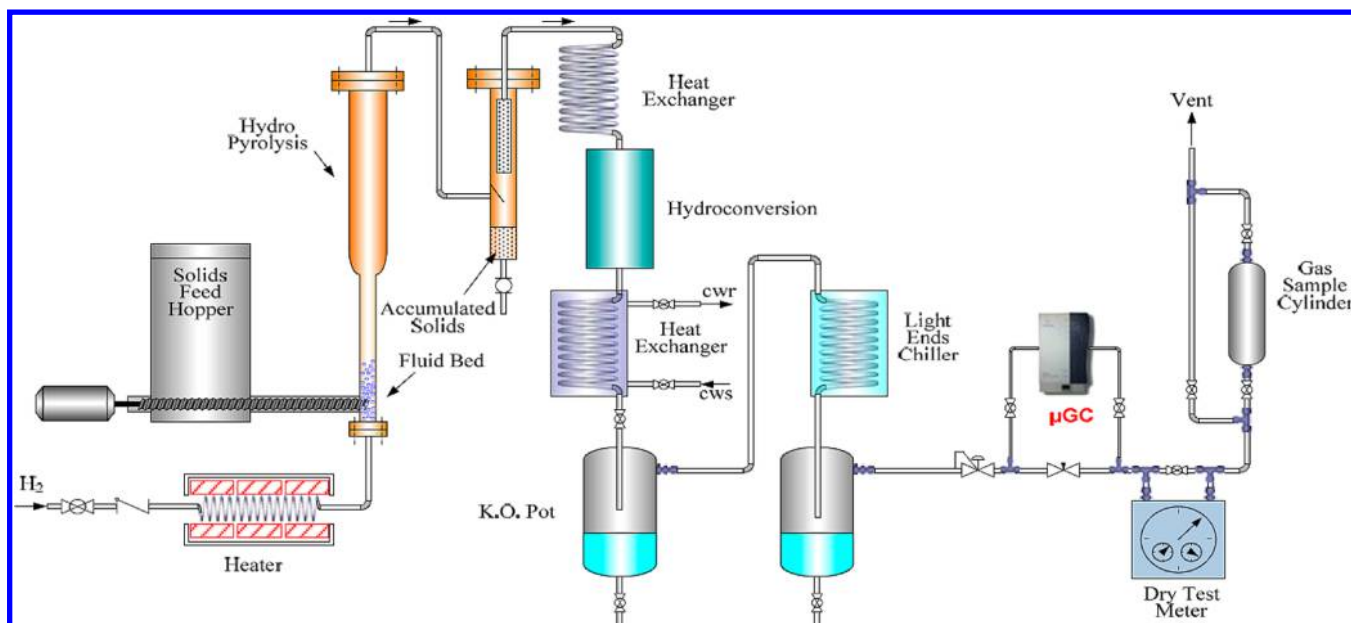
The above reaction network is probably the most comprehensive description of the hydrotreating of lignin-derived compounds. However, it is incapable of depicting the interaction between different types of hydrocarbons and oxygenated compounds during processing. To clarify the behavior of actual lignin feedstocks, one should explore the effects of linkages between the primary units, the types of lignins, and even the isolation methods.

Integrated catalytic hydrogen-processing of lignin for the production of biofuels and chemicals within the latest 5 years is summarized in Table 12. Although a large number of studies

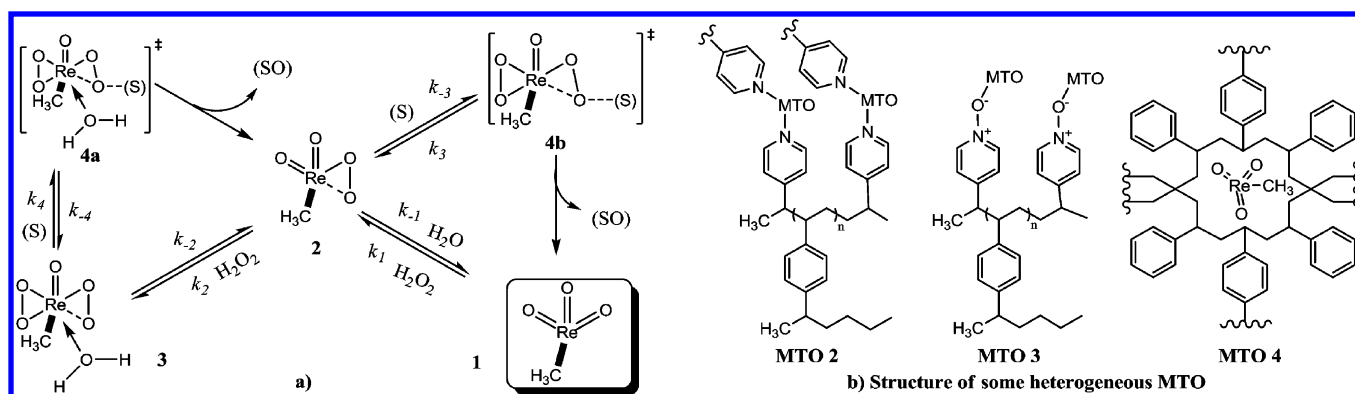
have been carried out regarding hydroprocessing of model compounds, systematic studies on real lignin, most of which have been discussed in the aforementioned section, are still very limited due to the complex structures, cross-linkages, and impurities of real lignin resources. Therefore, the reaction network of real lignin, including reaction kinetics, and the roles of the catalysts need to be more deeply understood to guide the design of the catalyst and control the product selectivity. Further research is required to address the following challenges: (1) Upgrading of pyrolysis bio-oil. This crude oil is particularly challenging for hydroprocessing; as it contains up to 50% of water and many highly oxygenated compounds, processing this feedstock may result in severe catalyst deactivation and reactor plugging because of coke formation. (2) A more efficient catalyst with multifunctional effects and long-term stability is to be developed to treat the much more complicated lignin materials. (3) Optimizing/reducing hydrogen consumption while maintaining product quality and specifications, since the cost of the hydrogen source determines to a large extent the application prospect of a conversion technology. Clarke and co-workers give an example for the deoxygenation of lignin-

Table 12. Integrated Hydroprocessing of Lignin and Model Compounds Developed in Recent Years

Feedstock	Catalyst	Conditions			Main reaction types	ref.
		T (°C)	P (MPa)	Note		
Guaiacol	Zirconia-supported mono- and bimetallic noble metal (Rh, Pd, Pt)	100–300	8	Batch reactor	Hydrogenation, HDO, hydrogenolysis, transalkylation	334
Guaiacol	PtRh/ZrO <sub>2</sub>	400	5	Batch reactor	Hydrogenation, HDO, hydrogenolysis	277
Guaiacol	PdRh/ZrO <sub>2</sub>	400	5	Batch reactor	Hydrogenation, HDO, hydrogenolysis	277
Guaiacol	CoMo/Al <sub>2</sub> O <sub>3</sub>	400	5	Batch reactor	Hydrogenation, HDO, hydrogenolysis	277
Guaiacol	NiMo/Al <sub>2</sub> O <sub>3</sub>	400	5	Batch reactor	Hydrogenation, HDO, hydrogenolysis	277
Guaiacol, cresol	Pt/ZSM-5, Pt/Al <sub>2</sub> O <sub>3</sub>	200	4	Packed-bed reactor, LHSV = 2–6 h <sup>-1</sup>	HDO, hydrogenation, isomerization	335
Phenol	Sulfide NiMo, CoMo	250	1.5	Batch reactor	HDO, hydrogenolysis, hydrogenation	336
Substituted phenols	Pd/HBEA	200–250	5	Batch reactor	Hydroalkylation, HDO	327
Aryl ethers	Ni/SiO <sub>2</sub>	120	0.6	Batch reactor	HDO, hydrogenation, hydrogenolysis	229
Aryl ethers	Ni(acac) <sub>2</sub> ligand, NaO <sup>t</sup> Bu	70	Ambient pressure	LiAl(O <sup>t</sup> Bu) <sub>3</sub> H as hydrogen source	Hydrogenolysis, hydrogenation	337
Phenol, guaiacol, and syringol	Ru/ACC	25–80	Ambient pressure	Electrocatalysis, HCl as catholyte	Hydrogenation, HDO	320
Mixture of aldehydes, ketones, acids, alcohols	Ru-based Shvo catalyst	90–145	1	Batch reactor	Hydrogenation, dehydration	338
Guaiacol, anisole, 4-methylanisole, and cyclohexanone	Pt/Al <sub>2</sub> O <sub>3</sub>	300	0.14 (30% H <sub>2</sub> + 70% N <sub>2</sub> )	Packed-bed reactor, 100 mL/min	Hydrogenation, hydrogenolysis, transalkylation	329
Lignin pyrolysis oil	Ru/C	250, 300	14	Batch reactor	Hydrogenation, hydrogenolysis, condensation.	317
Pyrolysis oils	Ru/C, Pt/C, Zeolite	Ru/C: 125, Pt/C: 250	10	Three steps: Ru/H <sub>2</sub> + Pt/H <sub>2</sub> + Zeolite	Hydrogenation, dehydration, decarbonylation, and retro-aldol condensation	215
Kraft lignin	Sulfide NiMo	395–430	9–10	Batch reactor	Hydrogenation, hydrogenolysis, HDO	274
Raw woody biomass	W <sub>2</sub> C/C	235	6	Batch reactor	Hydrogenolysis, HDO	238
Raw woody biomass	Ni–W <sub>2</sub> C/C	235	6	Batch reactor	Hydrogenolysis, HDO	238
Pine wood	Ru <sub>x</sub> Cu <sub>y</sub> @CsPW	470	4	Batch reactor	Deoxygenation, hydrogenation, isomerization, transalkylation	339
Cellulosic and woody biomass	Undisclosed	Undisclosed	Undisclosed	IH <sup>2</sup> process	Integrated hydroprocessing plus hydroconversion	333



**Figure 12.** Improved IH<sup>2</sup> pilot plant with continuous char removal. Adapted with permission from ref 333. Copyright 2012 Gas Technology Institute.



**Figure 13.** (a) Activation of hydrogen peroxide by methyltrioxo rhenium and oxygen transfer from MTO monoperoxo and diperoxo intermediates to the substrate. (S) = substrate, (SO) = oxidation product. (b) Structure of polymer-supported MTO and polystyrene-encapsulated MTO. Adapted from Herrmann<sup>341</sup> and Crestini et al.<sup>345</sup>

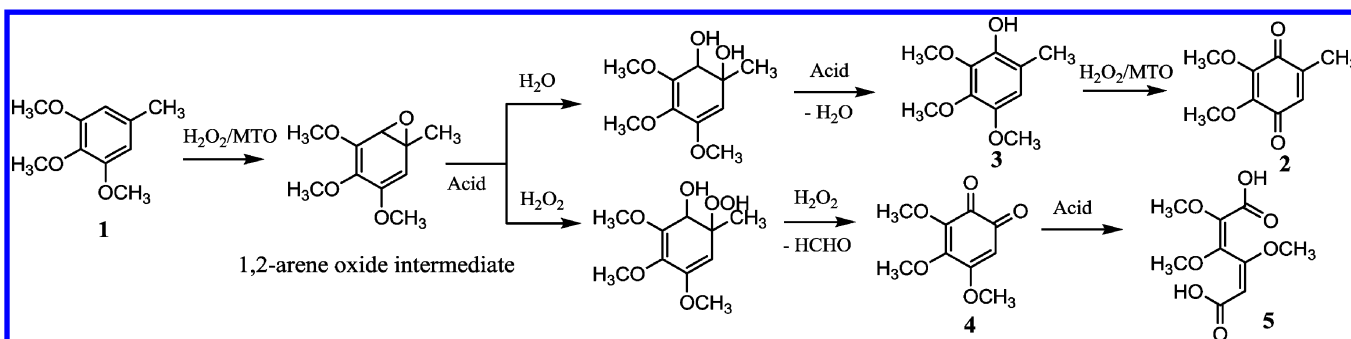
derived phenols without a hydrogen source via cross-coupling reaction to replace C–O bonds with C–C bonds.<sup>332</sup> Marker<sup>333</sup> and co-workers developed an integrated hydrolysis (pyrolysis carried out in a pressurized hydrogen atmosphere) plus hydroconversion (IH<sup>2</sup>) technology for the conversion of biomass to hydrocarbon gasoline and diesel blending components (Figure 12). The liquid products produced in this process are fully compatible with petroleum-based gasoline and diesel, contain less than 1% oxygen, and have less than 1 total acid number (TAN). Compared to the traditional fast pyrolysis plus upgrading route, IH<sup>2</sup> offers three key technical and economic advantages: (1) No external source of hydrogen or methane is required for upgrading. (2) A high quality fungible hydrocarbon product which has low TAN and low oxygen content is directly produced. (3) Capital and operating costs are lower than those of other biomass-to-fuel technologies. The DOE funding enabled rapid development of the IH<sup>2</sup> technology from initial proof-of-principle experiments through continuous testing in a 50 kg/day pilot plant. Technoeconomic work and lifecycle analysis showed that IH<sup>2</sup> technology can convert biomass to transportation fuels for less

than \$ 2.00/gallon with greater than 90% reduction in greenhouse gas emissions, rendering IH<sup>2</sup> a promising technology for large-scale application.

## 7. OXIDATION

Oxidative depolymerization of lignin is a valorization strategy that focuses on producing polyfunctional aromatic compounds. The oxidative cracking reaction includes the cleavage of the aryl ether bonds, carbon–carbon bonds, aromatic rings, or other linkages within the lignin. Nitrobenzene, metal oxides, molecular oxygen, and hydrogen peroxide are the most popular oxidants for lignin. The oxidation products of lignin are mainly polyfunctional monomeric compounds, ranging from aromatic aldehydes to carboxylic acids, such as vanillin, syringaldehyde, 4-hydroxybenzaldehyde, and muconic acid, which are alternative to fossil fuels derived chemicals. The catalytic systems that have been used for lignin oxidation can be divided into six types: organometallic catalysis, metal-free organic catalysis, acid or base catalysis, metal salts catalysis, photocatalytic oxidation, and electrocatalytic oxidative cleavage of lignin.

Scheme 15. Selective Oxidation of 1,2,3-Trimethoxy-5-methylbenzene (1) to 2,3-Dimethoxy-5-methyl-*p*-benzoquinone (2) over MTO/H<sub>2</sub>O<sub>2</sub> and HBF<sub>4</sub><sup>a</sup>



<sup>a</sup>Adapted from Adam.<sup>347</sup>

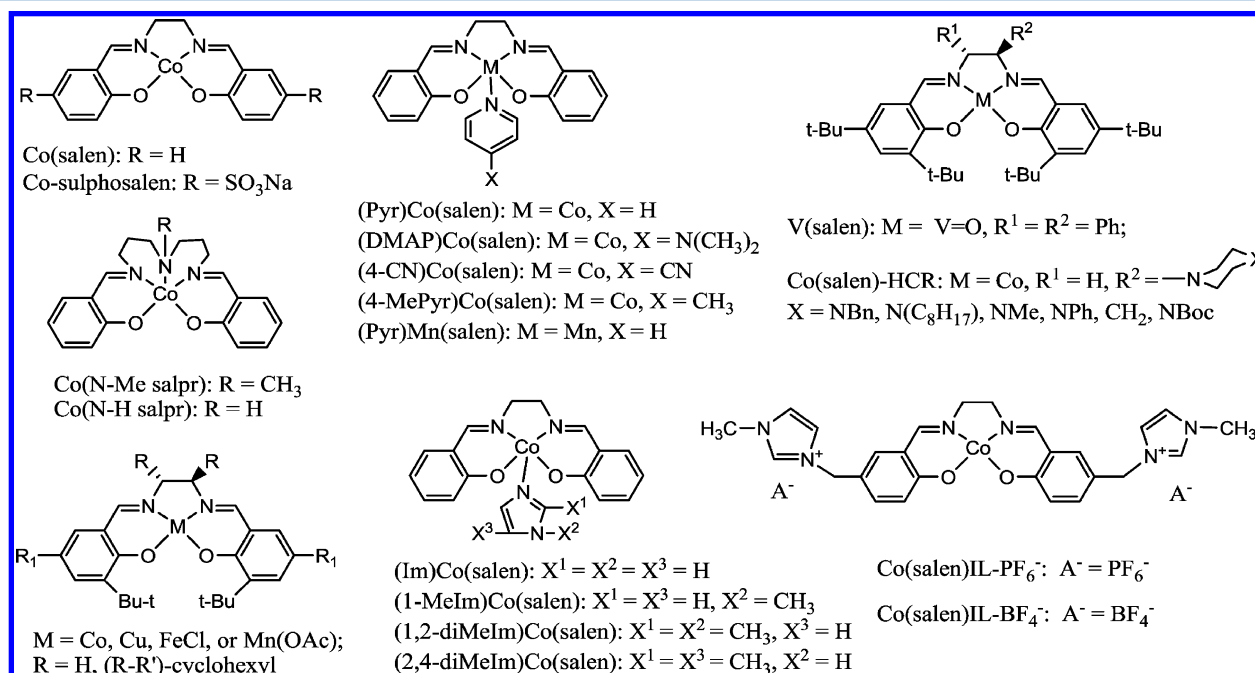


Figure 14. Salen complexes that have been applied in lignin oxidation.

### 7.1. Organometallic catalysis

Since the discovery of hydroformylation by Roelen in 1938,<sup>340</sup> catalytic applications have paved the way of organometallic compounds in industry. In recent years, several researchers have used organometallic catalysis for oxidation of lignin model compounds. Few studies have reported on the conversion of actual biomass derived lignin; thus, more research is required before this approach could be used industrially.

**7.1.1. Catalysis by methyltrioxo rhenium.** Methyltrioxo rhenium (MTO, compound 1 in Figure 13a)<sup>341</sup> is one of the simplest organometallic compounds that can be used for catalytic activation of the oxidizing species, molecular oxygen or hydrogen peroxide. In recent years, Crestini<sup>342–345</sup> and co-workers made systematic progress on MTO-catalyzed lignin oxidation reactions. The results showed that MTO in combination with H<sub>2</sub>O<sub>2</sub> was most efficient for lignin oxidative transformation.<sup>343,345</sup> In this catalytic process, activation of hydrogen peroxide happens via the formation of two peroxorhenium intermediates, a monoperoxo  $\eta^2$ -complex [MeRe(O<sub>2</sub>)<sub>2</sub>] (compound 2 in Figure 13a) and a bis-peroxo  $\eta^2$ -complex [MeRe(O<sub>2</sub>)<sub>2</sub>O] (compound 3 in Figure 13a); these

species are not only stable to peroxide, light, acid, and water, but also to high temperature in the presence of excess of H<sub>2</sub>O<sub>2</sub>.<sup>346</sup> A concerted mechanism for the oxygen transfer from MTO monoperoxo and diperoxo intermediates to the substrate by a butterfly transition state (compound 4 in Figure 13a) has been proposed.<sup>342,344</sup>

A wide range of phenolic and nonphenolic lignin model compounds, including simple phenols,<sup>343</sup> methoxybenzene species,<sup>347</sup> typical model dimers resembling the main linkages in native and technical lignins,<sup>343,345</sup> and even raw lignin samples,<sup>343</sup> have been used as feedstock for oxidative transformation over H<sub>2</sub>O<sub>2</sub>/MTO. These transformations take place at the alkyl side chain with oxidation and fragmentation reactions and at the aromatic moieties by demethylation, hydroxylation, and oxidative ring-opening cleavage reactions. Complex product mixtures are obtained, including both carboxylic acid and aldehyde derivatives that originate from oxidation of side chains, and benzoquinones and some ring oxidative cleavage products. One such example is the oxidation of a recalcitrant model compound 1,2,3-trimethoxy-5-methylbenzene (1) to 2,3-dimethoxy-5-methyl-*p*-benzoquinone (2) in



**Scheme 15.** The MTO/H<sub>2</sub>O<sub>2</sub> oxidation of **1** at room temperature in ethanol in the presence of HBF<sub>4</sub> afforded 95% conversion with the yield of **2** up to 79% within 4 h. The transformation proceeded via a rather complex cascade mechanism<sup>347–349</sup> including formation of a reactive 1,2-arene oxide intermediate, ring opening, dehydration, demethylation, and further oxidation. Side reactions of overoxidation, hydroxylation, and ring opening generated byproducts **3–5**.<sup>347</sup>

The treatment of various lignin samples<sup>343</sup> (sugar cane lignin, hardwood lignin extract, red spruce kraft lignin) in a MTO/H<sub>2</sub>O<sub>2</sub> system results in extensive oxidation on the aliphatic side chain and aromatic ring-cleavages, which generates more soluble aromatic fragments with extensive degradation, as indicated by the high amounts of carboxylic acid content and low contents in aliphatic and condensed OH groups.

With the aim to develop robust and environmentally friendly heterogeneous catalysts, polymer-supported MTO and polystyrene encapsulated MTO catalysts<sup>345</sup> (Figure 13b, MTO **2–4**) are designed in promoting oxidation of various lignin model compounds such as monomeric and dimeric, phenolic and nonphenolic lignin model compounds, and technical lignins. These heterogeneous catalysts exhibited longer lifetime and lower Lewis acidity, which guide their reactivity toward Dakin-like reactions and aliphatic C–H insertion rather than aromatic ring oxidation, thus leading to a final product with more phenolic guaiacyl groups. The mass balance measured for heterogeneous oxidations was much better than that obtained with homogeneous MTO, implying that further oxidation reactions or polymeric reactions are significantly restrained with heterogeneous oxidations.

It is important to point out that Kühn's group recently developed an efficient method for the cleavage of several  $\beta$ -O-4 over-catalytic amounts of MTO without any oxygen source.<sup>350</sup> The mechanism study showed that the reduction of Re<sup>VII</sup> to Re<sup>V</sup> by the substrate itself generated the catalytically active species, methyl dioxorhenium, which is responsible for the C–O bond activation. This work is probably the first case of nonoxidative MTO-catalyzed lignin degradation.

**7.1.2. Catalysis by salen complexes.** Salen (*N,N'*-bis(salicylidene)ethylenediamine) complexes of various transition metals ([M(salen)]) are widely used in organic reactions for a great number of substrates' oxidation or epoxidation. In comparison with other metal complex catalysts, salen complexes have several advantages, in that they are cheap, easy to synthesize, and relatively stable.<sup>351</sup> Therefore, they have been tested in the oxidation of lignin and model compounds.<sup>352</sup> The hitherto reported salen complexes for lignin oxidation are illustrated in Figure 14, and the last 10 years of oxidation results are listed in Table 13. The oxidation cases before 2005 can be referred to Zakzeski's review.<sup>28</sup>

Cobalt salen ([Co(salen)]) complexes are used most frequently in lignin oxidative degradation reaction,<sup>352–364</sup> considering that they are compatible with aqueous reaction media. Over Co salen complex, oxidation of aliphatic-OH,  $\beta$ -O-4 cleavage, ring-opening reaction, and demethoxylation may take place.<sup>354</sup> A broad variety of substrates, ranging from basic guaiacol to more complex phenolic and nonphenolic model compounds, have been tested for the oxidative production of aromatic acids, alkyl-phenyl ketones, benzoquinone derivatives, as well as densely functionalized phenoxyacrylaldehydes and benzofuran.<sup>342</sup> The reactivity of a phenolic lignin model compound is usually higher than that of the nonphenolic compound (Table 13, entries 1–2).<sup>365</sup> Varying the substitution

pattern of the aromatic ring in the salen ligand is a powerful strategy to modify the electronic and steric properties of the catalyst in terms of solubility and reactivity for oxidation.<sup>358,361</sup>

Canevali<sup>353</sup> and co-workers compared the treatments of unbleached thermomechanical pulp (TMP) fibers with molecular oxygen, in the presence of either [Co(salen)] in methanol or [Co(sulphosalen)] in water. The former catalyst exhibited better reactivity than the latter one based on the quantitative evaluation of the predominant intermonomeric units in lignin (such as  $\beta$ -O-4,  $\beta$ -5, and  $\beta$ - $\beta$  units) and the radical formation during the oxidation process, as has been characterized by 2D-HSQC-NMR, <sup>13</sup>C NMR, GPC, and EPR. In addition, the activity and stability of Co-Schiff base catalysts are strongly determined by the reaction medium, the coordination state of the complex, and pH.<sup>365</sup> For example, the catalytic activities of 5-coordinated Co-Schiff bases (Table 13, entries 12–13) are much higher than that of a 4-coordinated Co-Schiff base (Table 13, entry 14) because stronger oxygen binding occurs with 5-coordinate complexes.<sup>362</sup> In an aqueous alkaline reaction medium, both phenolic and nonphenolic model compounds' aerobic oxidation could be catalyzed by water-soluble Co-sulphosalen.<sup>365</sup> However, the catalytic activity decreases rapidly at pH higher than 10, mainly because the hydrolysis of the imine structure occurs in Co-Schiff base complexes at high pH.<sup>365–367</sup> A homogeneous vanadium complex V(salen)<sup>368</sup> was also tested for the conversion of dimeric lignin model compounds containing a  $\beta$ -O-4 linkage (Table 13, entry 15). Benzylic alcohol oxidation product was obtained as the major product in addition to small amounts of C–O bond cleavage products.

Dissolution is a critical factor for the oxidation of biomass. High oxygen and lignin solubility in IL makes it possible that the oxidation proceeds under mild conditions.<sup>369</sup> Weckhuyesen<sup>357,370</sup> and co-workers reported that model compound veratryl alcohol could be rapidly oxidized to veratraldehyde over Co(salen) in IL 1-ethyl-3-methylimidazolium diethylphosphate ([Emim]DEP) with a maximum TOF of 1300 h<sup>-1</sup> (Table 13, entries 16–19), which was almost equal to that obtained with homogeneous catalyst CoCl<sub>2</sub> (1440 h<sup>-1</sup>).<sup>370</sup> If lignin was employed, several alcohol functional groups are oxidized to the corresponding aldehyde, leaving the ether and carbon–carbon linkages intact.<sup>274e</sup>

Fadini<sup>371</sup> and co-workers demonstrated that the use of various PF<sub>6</sub><sup>-</sup> anion-based ILs in the oxidative cleavage of benzopinacol and hydrobenzoin showed a positive effect in the efficiency of the (Pyr)Mn<sup>III</sup>(salen) (OAc) catalyst (increase of the yield: 10–60%). Specifically, the above Mn-catalyst in IL *N*-octyl-3-picolinium hexafluorophosphate ([OPic][PF<sub>6</sub>]) is one of the most efficient systems for the C–C bond oxidative cleavage of benzopinacol, affording a quantitative yield (>99%) of benzophenone after 2 h at 60 °C (Table 13, entry 20). Unfortunately, this kind of ILs exhibit poor dissolubility for real lignin materials.

Badamali<sup>364</sup> and co-workers immobilized Co(salen) on SBA-15 and used it for phenolic dimer apocynol oxidation under microwave irradiation. The heterogeneous Co(salen)/SBA-15 catalyzed reaction gave a significantly superior TON and much higher yield of 2-methoxyphenol as compared to the homogeneous Co(salen). Another example is the synthesis of Salen metal complex encapsulated in Y zeolite by "impregnation" (marked as "Metal(salen)/Y-IM") and flexible ligand "ship-in-a-bottle" (marked as "Metal(salen)/Y-SB") methods. These two reusable catalysts showed almost equal activity to

Table 13. Results of Metallosalen Catalyzed Oxidation of Lignin and Model Compounds<sup>a</sup>

Entry	Catalyst	Oxidant	Solvent	Reaction condition			Substrate	Product	Result (%)		ref
				T (°C)	P (MPa)	Time (h)			Yield (%)	Conv. (%)	
1	Co-sulphosalen	O <sub>2</sub>	H <sub>2</sub> O, pH = 11	70	0.1	24	Guaiacol	2-Methoxybenzoquinone	>95	365	
2	Co-sulphosalen	O <sub>2</sub>	H <sub>2</sub> O, pH = 11	70	0.1	24	Veratryl alcohol	Veratryl aldehyde	15	365	
3	(Im)Co(salen)	O <sub>2</sub>	CH <sub>3</sub> OH	r.t.	0.4	17	Syringyl alcohol	2,6-Dimethoxybenzoquinone	5	361	
4	(1-MeIm)Co(salen)	O <sub>2</sub>	CH <sub>3</sub> OH	r.t.	0.4	17	Syringyl alcohol	2,6-Dimethoxybenzoquinone	69	361	
5	(1,2-diMeIm)Co(salen)	O <sub>2</sub>	CH <sub>3</sub> OH	r.t.	0.4	17	Syringyl alcohol	2,6-Dimethoxybenzoquinone	67	361	
6	(2,4-diMeIm)Co(salen)	O <sub>2</sub>	CH <sub>3</sub> OH	r.t.	0.4	17	Syringyl alcohol	2,6-Dimethoxybenzoquinone	72	361	
7	(Pyr)Co(salen)	O <sub>2</sub>	CH <sub>3</sub> OH	r.t.	0.4	17	Syringyl alcohol	2,6-Dimethoxybenzoquinone	82	361	
8	(DMAP)Co(salen)	O <sub>2</sub>	CH <sub>3</sub> OH	r.t.	0.4	17	Syringyl alcohol	2,6-Dimethoxybenzoquinone	50	361	
9	(4-CN)Co(salen)	O <sub>2</sub>	CH <sub>3</sub> OH	r.t.	0.4	17	Syringyl alcohol	2,6-Dimethoxybenzoquinone	64	361	
10	(4-MePyr)Co(salen)	O <sub>2</sub>	CH <sub>3</sub> OH	r.t.	0.4	17	Syringyl alcohol	2,6-Dimethoxybenzoquinone	74	361	
11	Co(N-Me salpr) with hindered base	O <sub>2</sub>	CH <sub>3</sub> OH	r.t.	0.4	24	Vanillyl alcohol	2-Methoxybenzoquinone	21–55	361	
12	(Pyr)Co(salen)	O <sub>2</sub>	CH <sub>3</sub> OH	r.t.	0.3	17	Syringyl alcohol	2,6-Dimethoxybenzoquinone	88	362	
13	Co(N-Me salpr)	O <sub>2</sub>	CH <sub>3</sub> OH	r.t.	0.3	17	Syringyl alcohol	2,6-Dimethoxybenzoquinone	71	362	
14	Co(salen)	O <sub>2</sub>	CH <sub>3</sub> OH	r.t.	0.3	17	Syringyl alcohol	2,6-Dimethoxybenzoquinone	28	362	
15	V(salen)	Air	CH <sub>3</sub> CN	80	0.1	24	3-Ethoxy-4-hydroxyphenyl-glycerol- $\beta$ -guaiacyl ether	Corresponding ketone	37	368	
16	Co salen	O <sub>2</sub>	[Emim][DEP]	80	0.5	6	Veratryl alcohol	Veratryl aldehyde	90	370	
17	Co salen	O <sub>2</sub>	[Emim][CH <sub>3</sub> SO <sub>3</sub> ]	80	0.5	6	Veratryl alcohol	Veratryl aldehyde	22	370	
18	Co salen	O <sub>2</sub>	[Bmim][PF <sub>6</sub> ]	80	0.5	6	Veratryl alcohol	Veratryl aldehyde	7	370	
19	Co salen	O <sub>2</sub>	H <sub>2</sub> O	80	0.5	6	Veratryl alcohol	Veratryl aldehyde	19	370	
20	(Pyr)Mn <sup>III</sup> (salen) (OAc)	O <sub>2</sub>	[OPic][PF <sub>6</sub> ]	60	0.1	2	Benzopinacol	Benzophenone	>99	371	
21	(Pyr)Mn <sup>III</sup> (salen) (OAc)	O <sub>2</sub>	[OPic][PF <sub>6</sub> ]	30	0.1	3	Hydrobenzoin	Benzaldehyde	41	371	
22	(Pyr)Mn <sup>III</sup> (salen) (OAc)	O <sub>2</sub>	[Bmim][PF <sub>6</sub> ]	30	0.1	3	Benzopinacol	Benzophenone	49	371	
23	(Pyr)Mn <sup>III</sup> (salen) (OAc)	O <sub>2</sub>	[Bmim][PF <sub>6</sub> ]	30	0.1	3	Hydrobenzoin	Benzaldehyde	43	371	
24	Co-sulphosalen	O <sub>2</sub>	H <sub>2</sub> O, pH = 12	90	0.8	3	2,2'-Biphenol	NS	17.1	358	
25	Co-sulphosalen	O <sub>2</sub>	H <sub>2</sub> O, pH = 12	90	0.8	3	Veratryl alcohol	Veratraldehyde	4.9	358	
26	Co(salen)	O <sub>2</sub>	NaOH, H <sub>2</sub> O	80	0.1	28	Veratryl alcohol	Veratraldehyde	43	360	
27	Co(salen)/SBA-15	H <sub>2</sub> O <sub>2</sub>	CH <sub>3</sub> CN	300 W MI	NS	0.5	Apocynol	Acetovanillone/2-methoxyquinone	11/9	364	
28	Co(salen)/SBA-15	H <sub>2</sub> O <sub>2</sub>	CH <sub>3</sub> CN	300 W MI	NS	0.66	Apocynol	Acetovanillone/2-methoxyquinone	Trance	100	364
29	Co(salen)	H <sub>2</sub> O <sub>2</sub>	CH <sub>3</sub> CN	300 W MI	NS	24	Apocynol	Acetovanillone/2-methoxyquinone	57	364	
30	Co(salen)/IL-PF <sub>6</sub> <sup>-</sup> /Pyridine	Air	NaOH/H <sub>2</sub> O	80	0.1	NS	Veratryl alcohol	Veratraldehyde	40	373	
31	Co(salen)/IL-PF <sub>6</sub> <sup>-</sup> /Pyridine	Air	K <sub>2</sub> CO <sub>3</sub> /H <sub>2</sub> O	80	0.1	NS	Veratryl alcohol	Veratraldehyde	56	373	
32	Co(salen)/IL-PF <sub>6</sub> <sup>-</sup>	Air	K <sub>2</sub> CO <sub>3</sub> /H <sub>2</sub> O	80	0.1	NS	Veratryl alcohol	Veratraldehyde	52	373	
33	Co(salen)/IL-BF <sub>4</sub> <sup>-</sup> /Pyridine	Air	K <sub>2</sub> CO <sub>3</sub> /H <sub>2</sub> O	80	0.1	NS	Veratryl alcohol	Veratraldehyde	46	373	
34	Co(salen)-HCR	O <sub>2</sub>	CH <sub>3</sub> OH	r.t.	0.34	16	Syringyl alcohol	2,6-dimethoxybenzoquinone	NS	72–92	363
35	Co(salen)-HCR	O <sub>2</sub>	CH <sub>3</sub> OH	r.t.	0.34	16	Syringyl alcohol	2-methoxybenzoquinone	NS	68–81	363
36	Co(salen)/Y-IM <sup>6</sup>	Peracetic acid	H <sub>2</sub> O + CH <sub>3</sub> OH	70	NS	3	Kraft pulp	Guaiacol	46	355	

Table 13. continued

Entry	Catalyst	Oxidant	Solvent	Reaction condition			Substrate	Product	Result (%)		ref
				T (°C)	P (MPa)	Time (h)			Yield (%)	Conv. (%)	
37	Cu(salen)/Y-SB <sup>c</sup>	Peracetic acid	H <sub>2</sub> O	70	NS	2	Kraft pulp	Oxygen delignified pulp	48 <sup>d</sup>	372	ref
38	Cu(salen)	Peracetic acid	H <sub>2</sub> O	70	NS	2	Kraft pulp	Oxygen delignified pulp	47 <sup>d</sup>	372	372

<sup>a</sup>MI is the abbreviation of "Microwave irradiation", NS is the abbreviation of "Not stated". <sup>b</sup>Cu(salen) complex was encapsulated in NaY by the "impregnation method". <sup>c</sup>Cu(salen) complex was encapsulated in NaY by the "ship-in-a-bottle method". <sup>d</sup>The result refers to "the delignification degree".

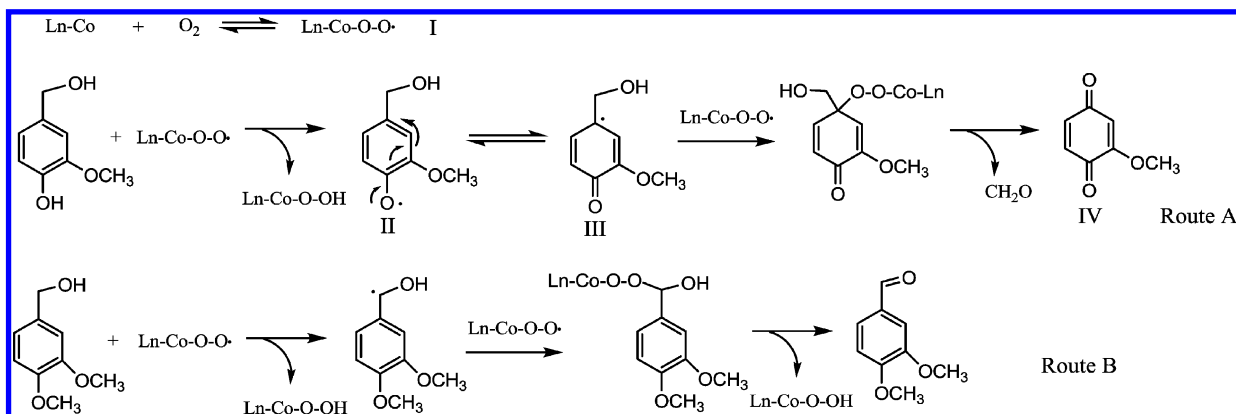
the corresponding neat complexes for the eucalyptus oxygen delignified kraft pulp using peracetic acid as an oxidant (Table 13, entries 36–38).<sup>355,372</sup>

Various mechanisms have been suggested for salen complex promoted oxidation reactions. The most accepted one<sup>354,361</sup> is described in Scheme 16. In the presence of oxygen, Co-Schiff base forms metal-O<sub>2</sub> complex oxygen-superoxocobalt I. The resulting Co(salen) superoxo adduct I abstracts a hydrogen from the phenolic substrate to produce a phenoxy radical II, which reacts with a second molecule of I via the rearrangement intermediate III and forms a *p*-quinone product IV and formaldehyde (Scheme 16, Route A). If the substrate is a nonphenolic compound such as veratryl alcohol, the abstraction of a hydrogen happens on the substitutional group to generate a benzyl radical which reacts with a second molecule of I to form the final product veratryl aldehyde (Scheme 16, Route B). The generation of hydrogen peroxide and the subsequent reactions play a key role in Co-sulphosalen catalyzed lignin oxidation.<sup>358</sup> According to Sippola's study,<sup>358</sup> the Co-sulphosalen catalyzed veratryl alcohol oxidation follows first-order kinetics.

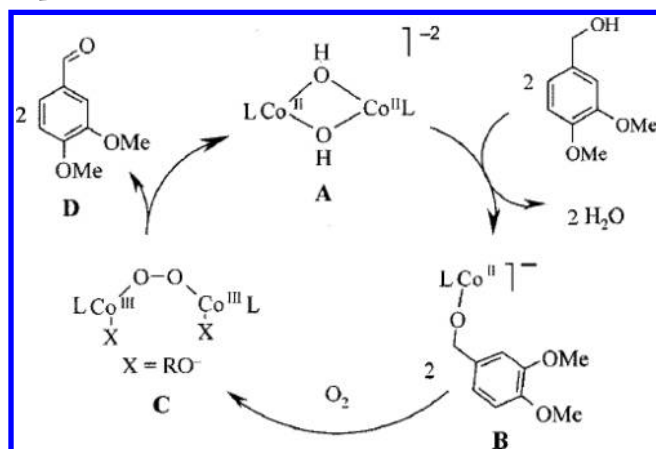
Weckhuysen<sup>360</sup> and co-workers elucidated a somewhat different mechanism of Co(salen)-catalyzed oxidation of veratryl alcohol by dioxygen in alkaline aqueous solution with *in situ* ATR-IR, Raman, and UV/vis spectroscopy (Scheme 17). In their mechanism, the reaction starts by formation of a bis- $\mu$ -hydroxo[Co(salen)]<sub>2</sub> species (A); substrate coordination to (A) releases water and an alkoxo intermediate (B); two intermediates (B) react with oxygen to form a nonplanar  $\mu$ -peroxo bridge intermediate (C), which obtains a hydrogen atom from the substrate and releases veratraldehyde (D) and the initial active species (A). In the overall cycle, two veratryl alcohol molecules are oxidized to aldehyde, and the rate-limiting step is the detachment of the product molecule.

**7.1.3. Catalysis by other metal complexes.** Barroso<sup>374</sup> and co-workers synthesized two mononuclear octahedral manganese(III) complexes (Mn-opba **1a** and **1b** in Figure 15), which are similar to the Mn(salen) complex in structure. Accordingly, these complexes exhibit activity in aerobic oxidative cleavage of aromatic *vic*-diols to produce the corresponding aldehydes or ketones in good yields under mild conditions. Complex **1b** shows lower efficiencies and selectivities than **1a** due to the stabilization effect of axial pyridine ligand coordination. Binuclear Mn(IV) complexes Mn(IV)-Me<sub>4</sub>DTNE or Mn(IV)-Me<sub>3</sub>TACN (see Figure 15) are also demonstrated to catalyze lignin model compounds oxidation.<sup>375,376</sup> These complexes are more effective for softwood pulps than hardwood pulps.

Recently, Barker, Hanson,<sup>356,377–381</sup> Toste,<sup>368</sup> and co-workers have started to use cheap vanadium(V) complexes and air for the oxidative degradation of lignin model compounds (Figure 15). The reduced vanadium species can be rapidly regenerated by air after reaction.<sup>356</sup> The solvent may play an important role in product selectivity. C–H, C–C, and C–O bond cleavages (Table 14, entry 22) occurred for the oxidation of 1,2-diphenyl-2-methoxyethanol in DMSO over vanadium **1** in Figure 15, while mostly C–C bond cleavage (Table 14, entry 23) was observed in pyridine solvent.<sup>379</sup> On the other hand, the ligand of the vanadium complex displayed different selectivities for the aerobic oxidation of lignin. Taking the phenolic model compound syringylglycerol- $\beta$ -guaiacyl ether (SG) as a substrate (Scheme 18), Salen-type catalyst (dipic)-V<sup>v</sup>(O)(O<sup>i</sup>Pr) (vanadium **2** in Figure 15) affords C–O bond

Scheme 16. Reaction Mechanism Proposed for Co(salen)-Catalyzed Lignin Model Compounds' Oxidation<sup>a</sup>

<sup>a</sup>Adapted from Sippola et al.<sup>358,365</sup> and Bozell et al.<sup>361</sup>

Scheme 17. Suggested Mechanism for Co(salen)-Catalyzed Veratryl Alcohol Oxidation with Dioxygen in Alkaline Aqueous Solution<sup>a</sup>

<sup>a</sup>Reprinted with permission from ref 360. Copyright 2005 by John Wiley & Sons, Inc.

cleavage products 1 and 2, and ketone 3 via cleavage of the benzylic C–H bond. In contrast, bis(oxyquinolate) complex (HQ)<sub>2</sub>V<sup>IV</sup>(O)(O<sup>i</sup>Pr) (vanadium 3 in Figure 15) could catalyze the C–C bond cleavage to give 2,6-dimethoxybenzoquinone 4 and acrolein derivative 5, and the benzylic C–H bond cleavage product 3.<sup>380</sup>

Other metal complexes include robust iron tetraamido macrocyclic ligand (TAML), copper-diimine complexes bis(*o*-phenanthroline)Cu, and bis(2,2'-bipyridine)Cu.<sup>382–386</sup> An inexpensive water tolerant complex Cp<sub>2</sub>Ti(BTMSA) (titanium 1 in Figure 15) was recently employed in ambient-temperature C–O bond cleavage of an  $\alpha$ -aryloxy ketone to produce acetophenone and phenol.<sup>289</sup>

**7.1.4. Biomimetic metal complex catalysts.** The motivation for using biomimetic metal complexes originates from the desire to mimic the activity of lignin peroxidase (LiP)<sup>27</sup> and manganese dependent peroxidase (MnP).<sup>387</sup> These two enzymes produced from white-rot basidiomycetes are known to oxidatively catalyze delignification of woody tissues while leaving cellulose and other polysaccharides untouched. The structures of reported biomimetic metal complexes are shown in Figure 15.<sup>28,342,388</sup>

Synthetic metalloporphyrins (Figure 16, complexes 1–3) are typical biomimetic catalysts for lignin oxidation that can yield highly oxidized metallo-oxo species similar to those generated from LiP and MnP.<sup>344</sup> These catalysts have high activity for lignin oxidation because of the structural similarity between the active site of the enzyme and metalloporphyrin complexes. These catalysts have several advantages over the enzyme-based variants: highly functionalized porphyrins bearing aryl substituents in the meso positions of the ring are resistant to oxidants, and their solubility and redox potential can be finely tuned by modification of the substituents' properties. Metallophthalocyanines<sup>389–391</sup> (Figure 16, complexes 4) are another type of biomimetic peroxidases for lignin oxidation. This kind of catalysts have the advantages that the phthalocyanines are readily available and inexpensive, and the iron(III) and manganese(III) complexes are able to catalyze the oxidation of various lignin and model compounds. However, their stability is highly dependent upon pH and the oxidant property.<sup>390</sup>

The comparative reactions between Mn(TCl<sub>8</sub>PPS<sub>4</sub>)Cl and Fe(TCl<sub>8</sub>PPS<sub>4</sub>)Cl (Figure 16, complex 1f) showed that the manganese porphyrin was more active than the iron one in extensive oxidation of 5–5' condensed and diphenylmethane lignin model compounds.<sup>392</sup> In addition, fewer condensation reactions occurred with manganese porphyrin.<sup>388,392</sup> The major disadvantage of porphyrin complexes with respect to large scale application is that they are subject to self-destruction or to forming inactive  $\mu$ -oxo complexes under catalytic oxidation conditions.<sup>393</sup> To avoid this problem, the immobilization of metalloporphyrins on solid supports such as silica gel<sup>394</sup> and naturally occurring clays<sup>393</sup> was developed for lignin oxidation. Because the catalytic center of metalloporphyrin was finely protected in this kind of heterogeneous catalysts, they are recyclable and their reactivity can be tuned by the choice of supports and immobilization characteristics.

Heterogeneous biomimetic catalysts induce a new problem of the kinetic barrier for the approach of the lignin macromolecules to the active metal site. To solve this problem, an advanced clay-porphyrin mediator system (clay-PMS) with TPYMePMn(OAc)<sub>5</sub>/clay catalyst in the presence of veratryl alcohol (VA) and 1-hydroxybenzotriazole as diffusible redox mediators was developed.<sup>395</sup> In this improved system, the redox mediator plays the role of a shuttle of the oxidation, being first oxidized by the active metal center and then diffusing to the redox potential outside the clay matrix to lignin. This novel



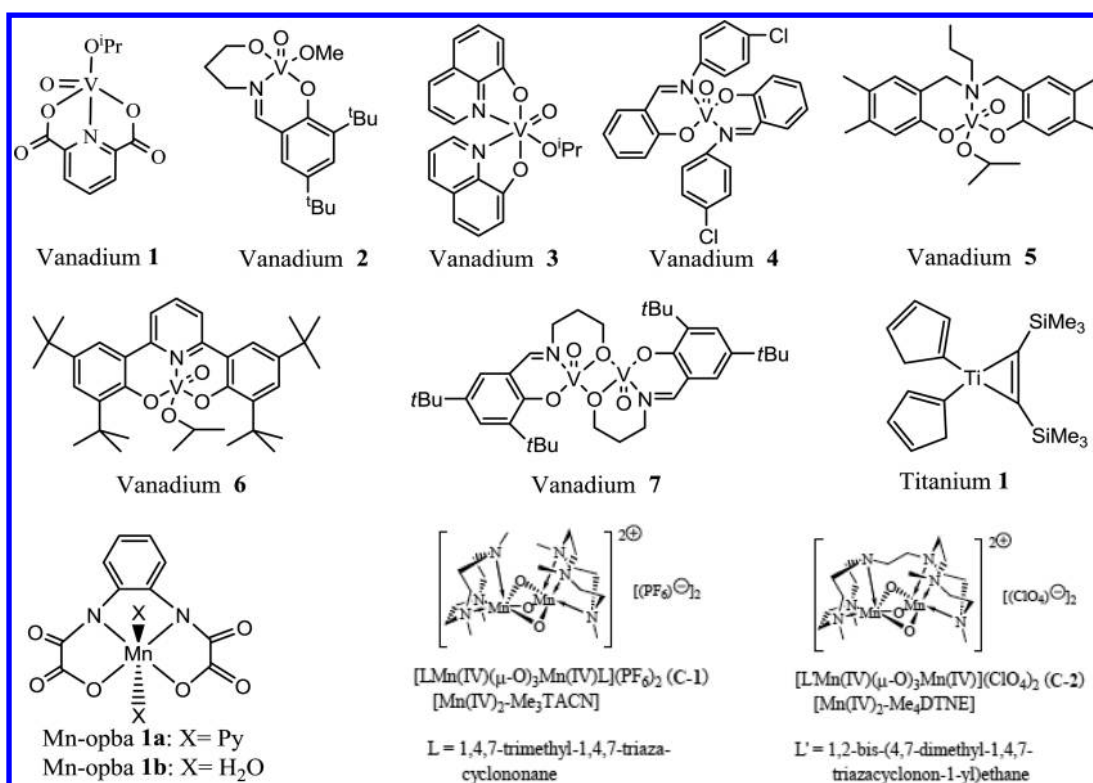


Figure 15. Vanadium, titanium, and manganese catalysts used for the aerobic oxidation of lignin and model compounds.

catalytic system had a higher reactivity than TPyMePMn(OAc) $_5$ /clay alone, and was very stable and recyclable.

Oxidation of the lignin model compounds by metalloporphyrins probably takes place via a single electron transfer (SET) mechanism.<sup>388,396,397</sup> Such a mechanism has been usually proposed for benzylic oxidation of lignin models by species including nitrobenzene and metallophthalocyanines and for redox reactions involving metallophthalocyanines. Taking the oxidation of 1,2-bis(4-methoxyphenyl)propane-1,3-diol as an example, the general reaction mechanism for both C–C and C–H bond cleavage with iron(III) porphyrin catalyst in the presence of active oxygen donor is illustrated in Scheme 19.

First, the two electron-deficient oxo-iron(IV) porphyrination radical species (X) which is formed from iron(III) porphyrin catalyst in the presence of active oxygen donor removes one electron, for example, from aromatic ring B, forming cation radical (Ya). Ya undergoes heterolytic C $_a$ -C $_\beta$  bond cleavage yielding *p*-anisaldehyde 2, and the possible hydroxymethyl radical intermediate (Z) as the cleaved products. The carbon centered radical (Z) is then attacked by molecular oxygen at a diffusion-controlled rate to form the dioxygen adduct (Za) or the related hydroperoxide intermediate. Thus, the radical intermediate (Z) is eventually converted via the common intermediate Za to the hydroxylated product 3 (Route a in Scheme 19) or to the  $\alpha$ -ketol 4 via Russer's mechanism,<sup>398</sup> involving the formation of equimolar amounts of 3 and 4. Alternatively, under anaerobic conditions, Z undergoes the second electron transfer to form the benzyl cation (Zb) and the subsequent hydroxylation to form 3 with water (Route b in Scheme 19) or the oxo-iron porphyrin complex (X) whose oxygen atom is exchanged with water.

When another type of cation radical intermediate (Yb) is formed by the one-electron transfer to the oxidizing species (X), as the fourth possibility, the same products (2–4) as

described above might be produced after the homolytic C $_a$ -C $_\beta$  bond cleavage of the intermediate Yb, accompanied by a smaller amount of  $\beta$ -ketol 5 produced by the C $_a$ -H bond cleavage.

In addition to the one-electron transfer mechanism proposed, there are other mechanisms, such as the concerted mechanism<sup>399</sup> reported for the oxidative cleavage of the C $_a$ -C $_\beta$  bond.

In the case of biomimetic oxidative degradation of aryl benzyl ether bonds, the formation of degradation products follows the process suggested by Baciocchi and co-workers.<sup>400</sup> Scheme 20 shows iron(III) porphyrin (Complex 1c in Figure 16, M = Fe) catalyzed verbutin oxidation using hydrogen peroxide as oxygen source. This process is started by the release of hydrogen from the substrate to form the corresponding radical 1, which readily reacts with the hydroxy radical attached to the central iron atom of the catalyst to form the unstable hemiacetal 2; this intermediate is then rapidly hydrolyzed to give carbonyl compound 3,4-dimethoxyphenyl-ethanone 3 and the corresponding alcohol (Route a). It is worthy of notice that ring oxygenated products quinones 6–8 are detected in this oxidation mixture. The formation of ring oxygenated products proceeds via a more complicated pathway (Route b).<sup>401,402</sup> This step involves the abstraction of the aromatic hydrogen atom at the C6-position to give the corresponding radical cation 4. The radical center of 4 combines with ferryl-oxo porphyrin to give intermediate 5. Water acting as a nucleophile reacts with the electrophilic center of 5 to afford the hemiacetal 6, which is transformed to quinone 7 by loss of methanol. The released methanol then attacks the same center of 5 to give a quinone acetal 8.

For non-phenolic lignin model compounds containing alkyl aryl ether bonds such as 2-hydroxyethyl apocynol, the final oxidative cleavage product is acetovanillone,<sup>397</sup> which is

Table 14. Organometallic Catalytic Systems for the Oxidation of Lignin Model Compounds<sup>a</sup>

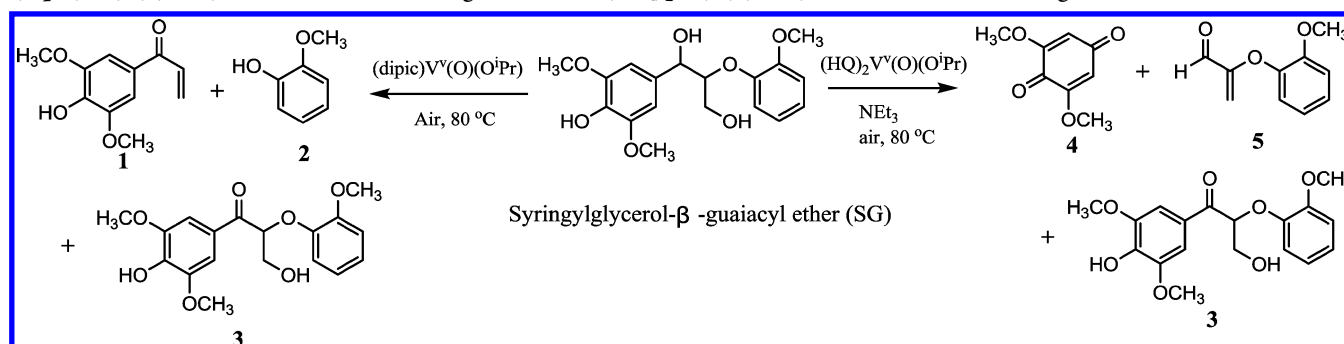
Entry	Catalyst	Oxidant	Solvent	Reaction condition			Substrate	Product	Result (%)		Ref
				T (°C)	P (MPa)	Time (h)			Yield (%) <sup>b</sup>	Conv. (%)	
1	MTO	H <sub>2</sub> O <sub>2</sub>	AcOH	rt	0.1	6			11.8	98	345
2	MTO	H <sub>2</sub> O <sub>2</sub>	AcOH	rt	0.1	6			8.5	98	345
3	MTO 3	H <sub>2</sub> O <sub>2</sub>	AcOH	rt	0.1	6			43.1	98	345
4	MTO 2	H <sub>2</sub> O <sub>2</sub>	AcOH	rt	0.1	6			75.7	98	345
5	MTO	H <sub>2</sub> O <sub>2</sub>	AcOH	rt	0.1	6			52.4	98	345
6	MTO 4	H <sub>2</sub> O <sub>2</sub>	AcOH	rt	0.1	6			62.5	97	345
7	MTO 2	H <sub>2</sub> O <sub>2</sub>	AcOH	rt	0.1	6			56.9	78	345
8	MTO 2	H <sub>2</sub> O <sub>2</sub>	AcOH	rt	0.1	6		A mixture of 6 aromatic ketone, alkene, and acids.	24	98	345
9	Vanadium 6	Air	Toluene	80	0.1	65			99	--	356
10	Vanadium 5	Air	Toluene	80	0.1	65			80	--	356
11	Vanadium 6	Air	Toluene	100	0.1	48		A mixture of 6 aromatic ketone, alkene, and acids.	--	84	356
12	Vanadium 6	Air	Toluene	100	0.1	48			19	20	356
13	Vanadium 3	Air	Dichloroethane	60	0.1	24			99	--	385
14	Vanadium 3	Air	Dichloroethane	60	0.1	24			90-98	--	385
15	Vanadium 2	Air	CH <sub>3</sub> CN	80	0.1	24			--	> 95	368
16	Vanadium 2	Air	CH <sub>3</sub> CN	80	0.1	24			50	55	368
17	Vanadium 4	Air	CH <sub>3</sub> CN	80	0.1	24			59	86	368
18	Vanadium 7	Air	CH <sub>3</sub> CN	80	0.1	24			58-80	95	368

Table 14. continued

Entry	Catalyst	Oxidant	Solvent	Reaction condition			Substrate	Product	Result (%)		Ref
				T (°C)	P (MPa)	Time (h)			Yield (%) <sup>b</sup>	Conv. (%)	
19	Vanadium <b>1</b>	Air	DMSO	100	0.1	168			--	20	379
20	Vanadium <b>1</b>	Air	DMSO	100	0.1	168			--	95	379
21	Vanadium <b>1</b>	Air	DMSO	100	0.1	20			--	94	379
22	Vanadium <b>1</b>	Air	Pyridine	100	0.1	20			--	99	379
23	bis( <i>o</i> -phenanthroline)Cu	O <sub>2</sub>	Water (pH 12)	90	0.8	0.5-3			--	--	384
24	Mn-opba <b>1a</b>	O <sub>2</sub>	Acetonitrile	40	0.1	3			10	19	374
25	Mn-opba <b>1b</b>	O <sub>2</sub>	Acetonitrile	40	0.1	3			47/18	--	374
26	Mn(IV) <sub>2</sub> -Me <sub>4</sub> DTNE	H <sub>2</sub> O <sub>2</sub>	Acetone	60	NS	0.17			Totally 60	90-95	376
27	Mn(IV) <sub>2</sub> -Me <sub>4</sub> DTNE	H <sub>2</sub> O <sub>2</sub>	Acetone	60	NS	0.17			50	50	376
28	Mn(IV) <sub>2</sub> -Me <sub>4</sub> DTNE	H <sub>2</sub> O <sub>2</sub>	Acetone	60	NS	0.17			40	40	376
29	Ru(PPh <sub>3</sub> ) <sub>3</sub> Cl <sub>2</sub> /AC	O <sub>2</sub>	PhCF <sub>3</sub>	60	0.1	15			85	92	386
30	Ru(PPh <sub>3</sub> ) <sub>3</sub> Cl <sub>2</sub> /AC	O <sub>2</sub>	PhCF <sub>3</sub>	50	0.1	15			71	96	386

<sup>a</sup>Structures of MTO catalysts are shown in Figure 12. Structures of vanadium, titanium, and manganese catalysts are shown in Figure 15. NS is the abbreviation of "Not stated". <sup>b</sup>The data refer to the total yield of all the listed products.

**Scheme 18. Oxidation of the Phenolic Lignin Model Compound Syringylglycerol- $\beta$ -guaiacyl Ether with Vanadium Catalyst (dipic)V<sup>v</sup>(O)(O<sup>i</sup>Pr) for C–O Bond Cleavage, and with (HQ)<sub>2</sub>V<sup>v</sup>(O)(O<sup>i</sup>Pr) for C–C Bond Cleavage<sup>a</sup>**



<sup>a</sup>Adapted from Hanson et al.<sup>380</sup>

obtained either via initial oxidation to the ketone 2-hydroxyethyl acetovanillone, followed by dealkylation (major route), or by dealkylation to apocynol followed by oxidation

(Scheme 21). The dealkylation reaction follows an alkali-catalyzed reaction via a neighboring group mechanism<sup>403</sup> similar to that suggested for nonphenolic  $\beta$ -ether cleavage

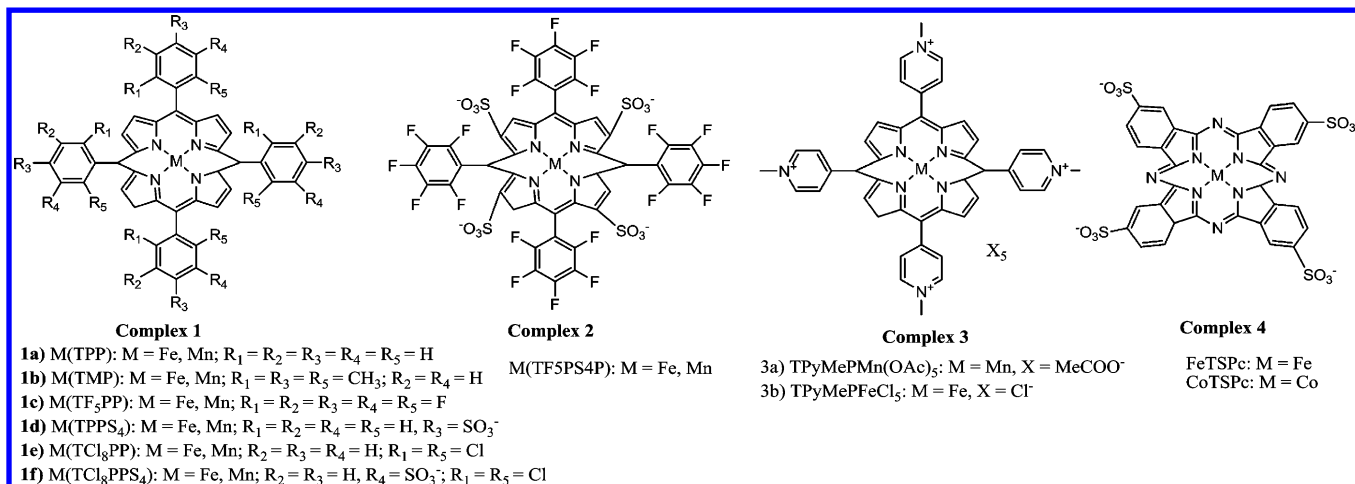
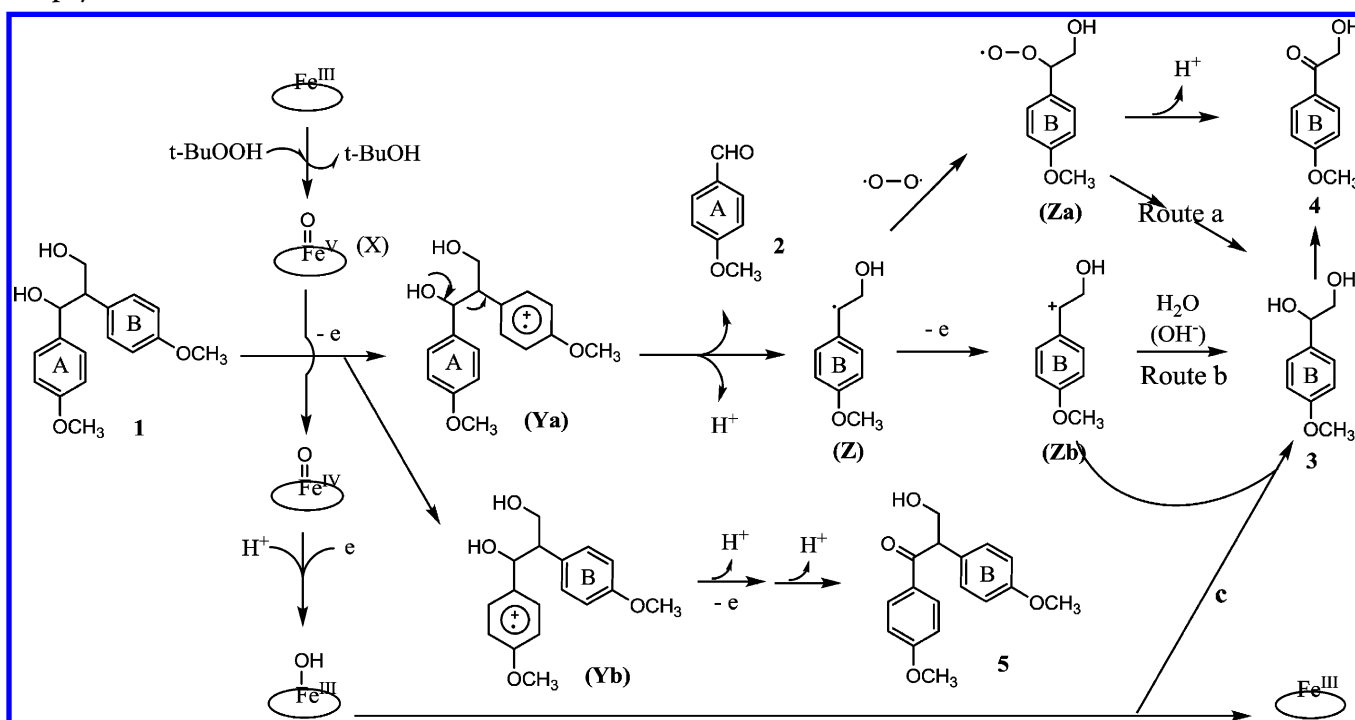


Figure 16. Structures of reported porphyrin and phthalocyanine catalysts used for lignin oxidation.

### Scheme 19. Single-Electron Transfer Mechanism for Oxidation of the Lignin Model Compound L Catalyzed by Iron(III) Porphyrin<sup>a</sup>



<sup>a</sup>Adapted from Shimada et al.<sup>388</sup>

(see Scheme 3), rather than through interaction with biomimetic catalyst.

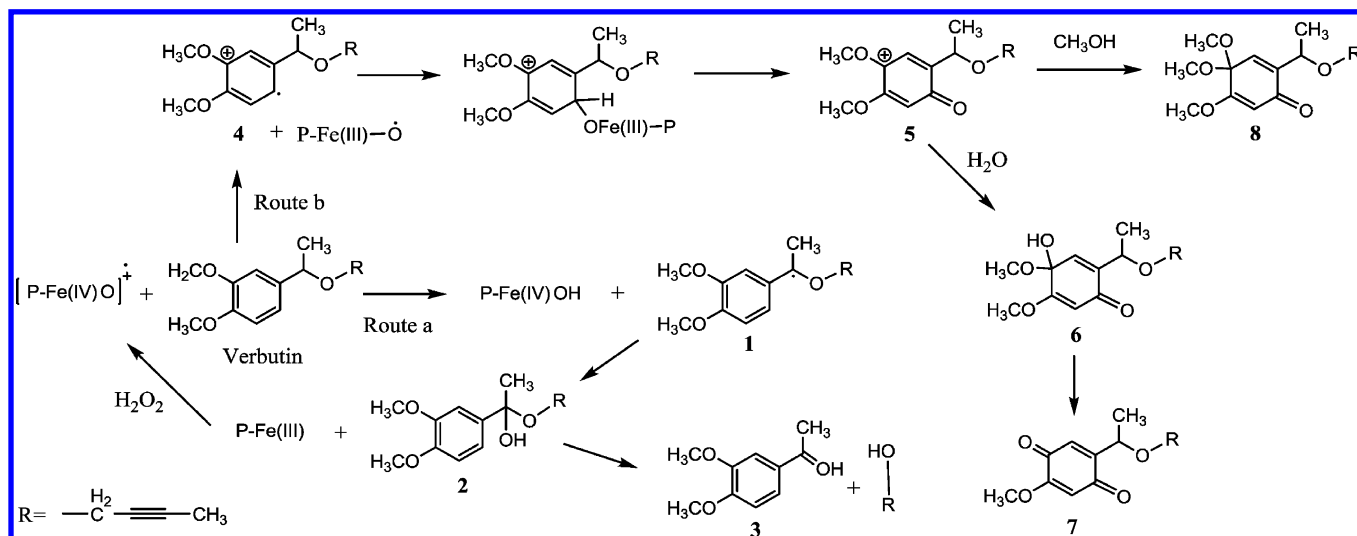
#### 7.2. Metal-free organocatalytic system

The oxidation system that is composed of 2,2,6,6-tetramethylpiperidine-1-oxyl (TEMPO), NaBr, and NaClO has been proven to be effective in the transformation of the primary hydroxyl groups of polysaccharides to carboxyl groups with high selectivity,<sup>404,405</sup> and this catalytic system has also been used for lignin oxidation recently.<sup>333,406–409</sup> A portion of lignin was converted to a water-soluble fraction when the thermomechanical pulp was treated by TEMPO-mediated oxidation.<sup>410,411</sup> Zhai<sup>333</sup> and co-workers demonstrated that, in a TEMPO-mediated oxidation system, the conversion efficiency is determined by the oxidizing agents, radical (TEMPO), and

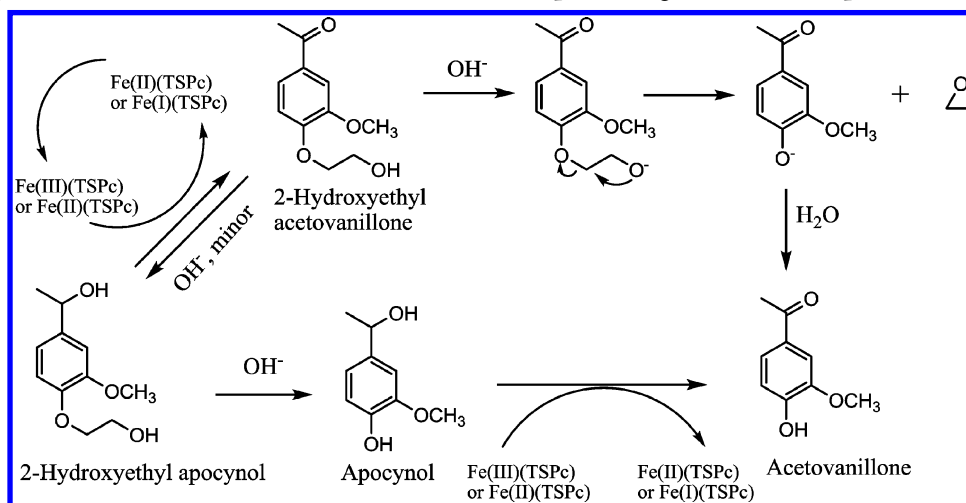
alkaline environment (pH = 10.5). According to the known TEMPO mechanism (Scheme 22, left route), two NaOCl molecules are consumed for the selective oxidation of a hydroxymethyl group to carboxyl.<sup>406</sup>

Air is possibly the cheapest and most environmentally friendly oxidant in nature. Stahl<sup>408</sup> and co-workers developed a series TEMPO-based organocatalytic system for lignin aerobic oxidative conversion. The catalyst consisting of 4-acetamido-TEMPO in combination with HNO<sub>3</sub> and HCl exhibited the best performance for chemoselective oxidation of secondary benzylic alcohols. A wide variety of lignin model compounds afforded the corresponding benzylic carbonyl compounds in 74–98% isolated yield (Scheme 23). The researchers were able to expand the substrates to natural lignin (Aspen lignin). The catalytic cycle is the same as that described with NaClO as

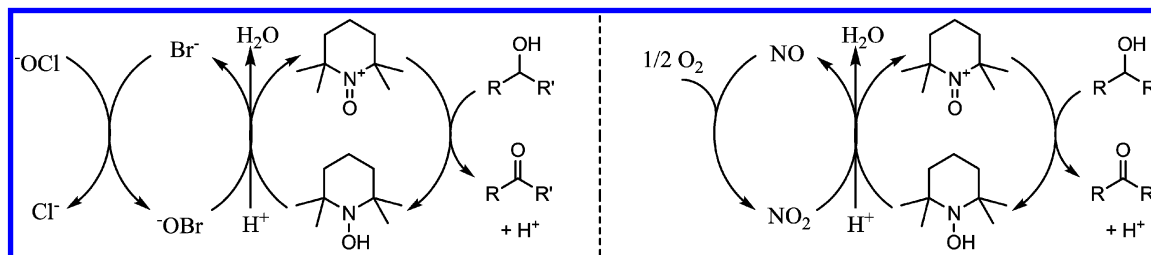


Scheme 20. Proposed Mechanism for the Biomimetic Oxidation of Verbutin<sup>a</sup>

<sup>a</sup>Adapted from Keserü et al.<sup>401</sup> and Dolphin et al.<sup>402</sup>

Scheme 21. Proposed Mechanism of Biomimetic Oxidation of Non-phenoliclignin Model Compound Verbutin<sup>a</sup>

<sup>a</sup>Adapted from Robinson et al.<sup>397</sup>

Scheme 22. Simplified TEMPO-Based Organocatalytic Cycle for the Oxidation of Alcohol<sup>a</sup>

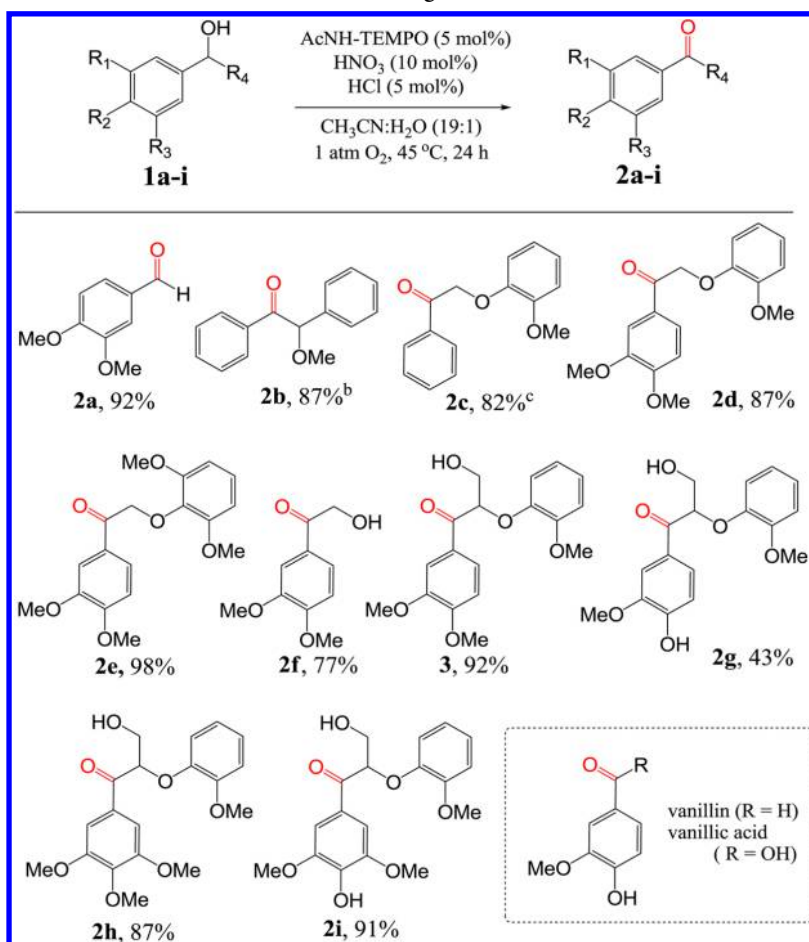
<sup>a</sup>Adapted from Kaddami,<sup>406</sup> Stahl,<sup>408</sup> and their co-workers.

oxidant (Scheme 22, right route), except that this catalytic system employs a catalytic nitroxyl species in combination with an inorganic nitrogen oxide as cocatalyst.

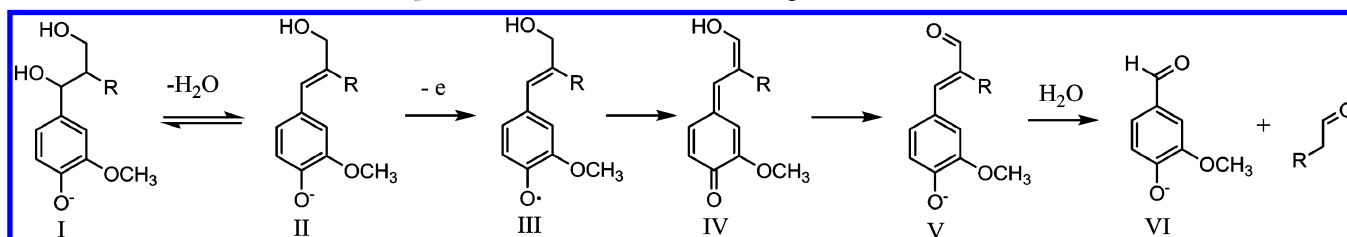
Based on the above progress, the same group further developed a two-step strategy, i.e. oxidation followed by C–O bond cleavage with formic acid, to deconstruct lignin into more than 60 wt % yields of low-molecular-weight aromatics.<sup>412</sup> It is

important to point out that the redox-neutral cleavage of C–O bonds results in no net consumption of formic acid, which is in contrast to other methods<sup>106</sup> that employ formic acid as a hydrogen source.

9-Azanoradamantane *N*-oxyl (AZADO),<sup>408</sup> with similar structure as TEMPO, and nitrogen-containing graphene material<sup>413</sup> were also reported to be efficient in oxidation of

Scheme 23. Chemoselective Metal-free Aerobic Oxidation of Lignin Models<sup>a</sup>

<sup>a</sup>Conditions: 1 mmol of alcohol **1a-j** (0.2 M in 19:1 CH<sub>3</sub>CN/H<sub>2</sub>O). <sup>b</sup>Ten mol % AA-TEMPO after 36 h. <sup>c</sup>Yield after 36 h. Adapted from Stahl<sup>408</sup> and co-workers.

Scheme 24. Reaction Mechanism Proposed for Alkaline Oxidation of Lignin To Produce Vanillin<sup>a</sup>

<sup>a</sup>Adapted from Tarabanko<sup>422</sup> and co-workers.

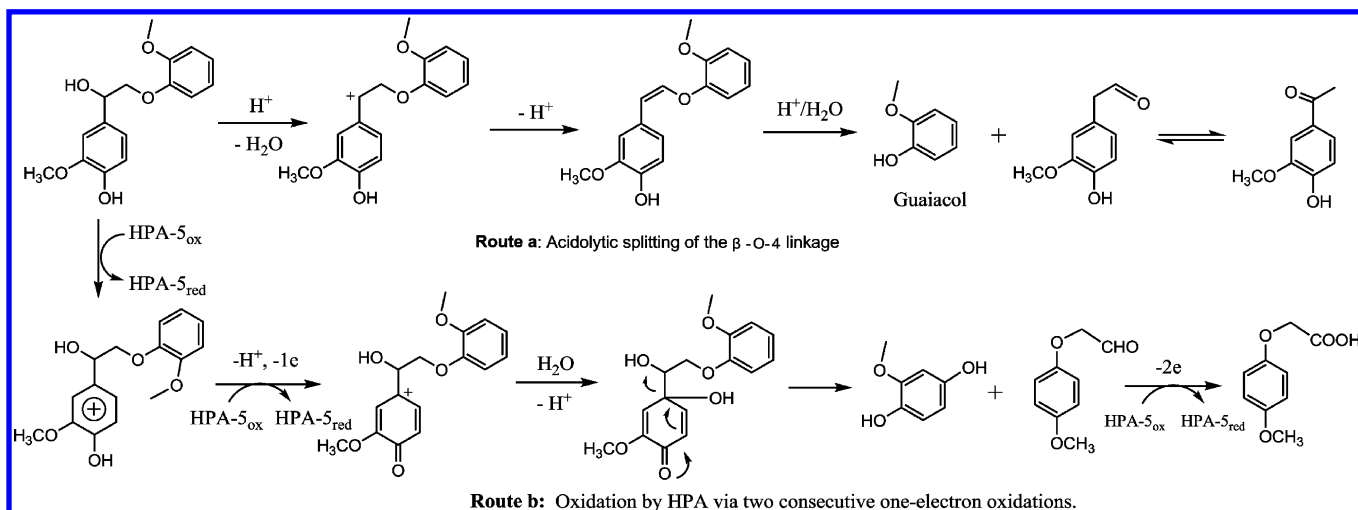
$\beta$ -O-4 and  $\alpha$ -O-4 types of lignin model compounds. Specifically, Westwood and co-workers reported for the first time that 2,3-dichloro-5,6-dicyano-1,4-benzoquinone (DDQ) could catalyze not only the oxidation of  $\beta$ -O-4 linkages,<sup>414</sup> but also the modification of the  $\beta$ - $\beta$  linkage in Kraft lignin.<sup>415</sup> Compared to many existing methods, this protocol, which can be achieved in one pot, is highly selective and gives rise to a simple product mixture that can be readily purified to give pure compounds.

### 7.3. Base and acid catalysis

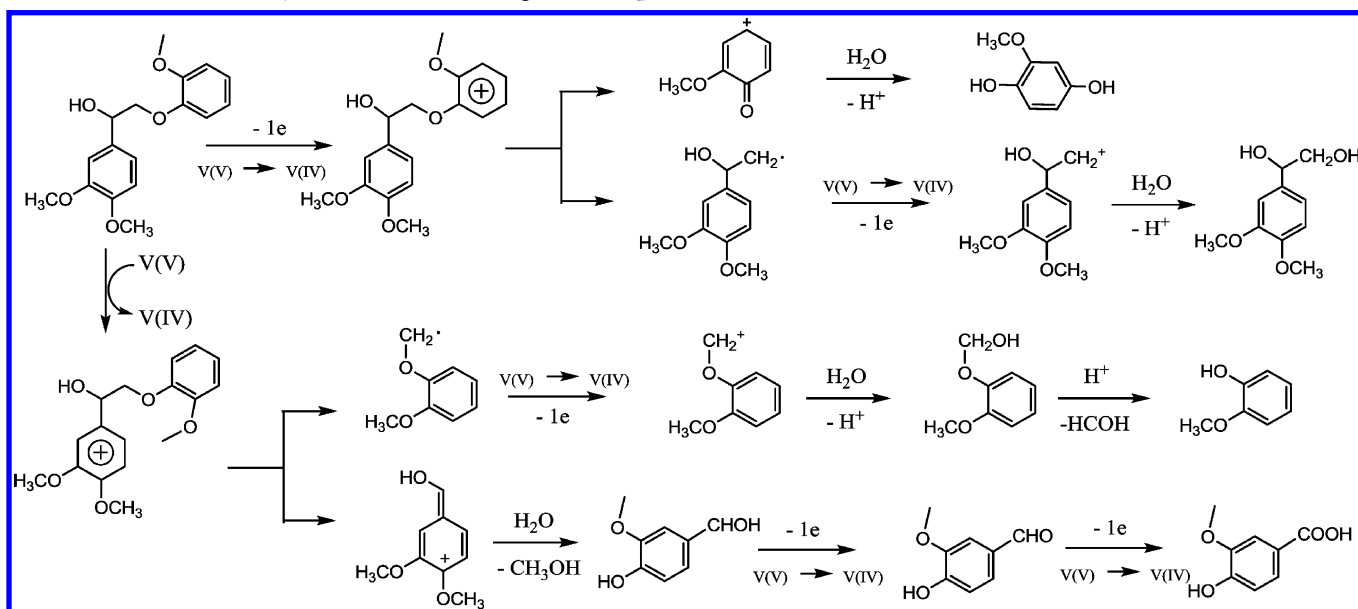
**7.3.1. Base catalysis.** Alkaline is not merely an efficient reagent for lignin hydrolysis depolymerization, it also exhibits remarkable activity in the lignin oxidation reaction. In the alkaline oxidation of lignin, NaOH, KOH, and Na<sub>2</sub>CO<sub>3</sub> are

used most frequently.<sup>416–418</sup> Nitrobenzene, metal oxides, and oxygen are mild oxidants which can preserve the lignin aromatic ring and aldehydes intact,<sup>419,420</sup> while hydrogen peroxide and permanganate may not be the preferred oxidants if the target products are aldehydes. Lignin with the native structure is easier to be cracked and oxidized than technical lignin.<sup>420</sup> The origin of the lignin, oxidant concentration, and pH value also have impacts on the conversion efficiency.<sup>41,421,422</sup>

Different mechanisms of alkaline catalyzed lignin oxidation to produce aldehyde have been proposed in the literature. The most acceptable one is the radical chain mechanism (Scheme 24) proposed by Tarabanko<sup>422</sup> and co-workers. This mechanism begins with dehydration of the lignin structure

Scheme 25. Cleavage of Phenolic  $\beta$ -O-4 Bonds in the Presence of HPA-5<sup>a</sup>

<sup>a</sup>Adapted from Evtuguin<sup>437</sup> and co-workers.

Scheme 26. HPA-5 Catalyzed Oxidative Cleavage of Non-phenolic  $\beta$ -O-4 Bonds<sup>ab</sup>

<sup>a</sup>V(V) and V(IV) are in the composition of  $\text{VO}_2^+$  and  $\text{VO}^{2+}$  ions, respectively. <sup>b</sup>Adapted from Evtuguin<sup>437</sup> and co-workers.

units (I), followed by the detachment of one electron from the phenoxyl anion II to yield the phenoxyl radical III. This radical then undergoes either disproportionation or proton detachment, followed by oxidation to form quinonemethide IV. The nucleophilic addition of the hydroxide ion to IV generates coniferaldehyde V. Finally, retro-aldol cleavage of V gives vanillin VI.<sup>423</sup>

**7.3.2. Acid catalysis.** Over 120 million tons of kraft pulp is produced from the kraft process worldwide every year, which delivers about 72 million tons of kraft lignin.<sup>424</sup> As kraft lignin only affords very low yield of vanillin (<4 wt % in most cases) by alkaline oxidation, acid is an alternative to alkaline oxidation of kraft lignin for the production of vanillin.<sup>424,425</sup> A yield of 7 wt % vanillin plus methyl vanillate can be obtained when oxidative depolymerization of kraft lignin was conducted in a batch reactor with polyoxometalate  $\text{H}_3\text{PMo}_{12}\text{O}_{40}$  as a homogeneous catalyst.<sup>398</sup> Furthermore, ca. 60 wt % of

oligomeric products that have a much lower molecular weight than kraft lignin were accumulated in this reaction.

Very recently, Rudolf von Rohr's group<sup>424–428</sup> developed a novel continuous microreactor for the acidic oxidation of kraft lignin, which overcomes the drawbacks of batch autoclaves, such as limited experimental freedom due to safety issues, challenges with running continuous reactions, and long heating/cooling times. In their entirely different reaction circumstance, the selectivity of the products might be different from those obtained with base catalysts. For instance, in  $\text{H}_2\text{O}_2$  oxidation of lignin, oxalic acid and formic acid prevailed in the alkaline environment, while formic acid and acetic acid are the dominant products in the acidic environment.<sup>429</sup>  $\text{H}_2\text{O}_2$  oxidation of guaiacol over titanium silicalite TS-1 (acidic zeolite) goes through a novel oxidative ring opening mechanism to maleic acid with the yield of ca. 20–30%.<sup>430</sup>

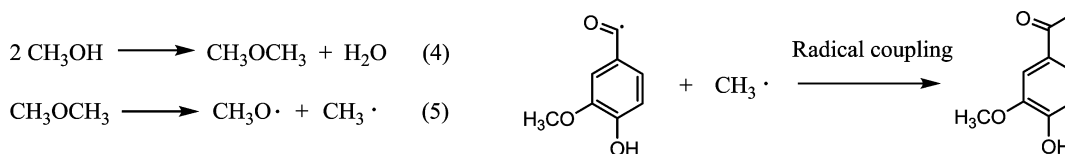
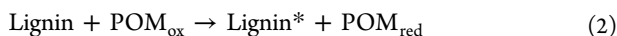


Figure 17. Formation of radical scavengers from methanol and the coupling reaction with lignin fragments. Adapted from Voitl and Rudolf von Rohr.<sup>426</sup>

## 7.4. Metal salt catalysis

**7.4.1. Polyoxometalates.** Polyoxometalates (POMs)<sup>426</sup> are a class of metal oxygen cluster anions with general formulas of  $\text{M}_x\text{O}_y^{m-}$  or  $\text{X}_z\text{M}_x\text{O}_y^{n-}$  ( $\text{M} = \text{Mo}, \text{W}, \text{V}, \text{Nb}, \text{or Ta}$ ;  $\text{X} = \text{P}, \text{Si}, \text{B}, \text{Ge}, \text{and others}$ ). They have the property of reversible oxidation and are soluble in aqueous and organic media. Several papers have been written about oxygen delignification technology using POMs. The overall stoichiometric reactions for delignification with POMs<sup>426,431,432</sup> can be summarized by eqs 2 and 3:



where  $\text{POM}_{\text{ox}}$  and  $\text{POM}_{\text{red}}$  are the oxidized and reduced forms of POMs, respectively, and  $\text{Lignin}^*$  is the oxidized form of lignin (low molecular weight or polymeric products). Under aerobic conditions, POM is an oxidative catalyst<sup>433</sup> and this redox cycle is continuously repeated, while under anaerobic conditions, POM acts as a regenerable oxidative reagent and eqs 2 and 3 take place in two separate stages.<sup>434</sup>

Weinstock<sup>435,436</sup> and co-workers reported that heteropolyanion  $[\text{SiW}_{11}\text{VO}_{40}]^{5-}$  only catalyzed anaerobic oxidation of the phenolic model compounds. Interestingly, both phenolic and nonphenolic units were reactive with a heteropolyanion  $[\text{PMo}_7\text{V}_5\text{O}_{40}]^{8-}$  (known as HPA-5) catalyst.<sup>437</sup> Phenolic  $\beta$ -aryl ether structures have a conversion, at least, five-times higher than the corresponding nonphenolic structures. Further study of the oxidation of  $\beta$ -aryl ether dimers showed that the reaction mechanisms involved are different.<sup>437</sup> The cleavage of phenolic  $\beta$ -O-4 bonds occurs predominantly through a heterolytic mechanism, which includes the hydrolytic cleavage of the alkyl-phenyl bonds in the phenolic structural units oxidized by  $[\text{PMo}_7\text{V}_5\text{O}_{40}]^{8-}$  (Scheme 25, Route a) and the typical acid-catalyzed splitting of the  $\beta$ -O-4 linkages (Scheme 25, Route b; see also Scheme 5). In contrast, the oxidative cleavage of nonphenolic  $\beta$ -aryl ether proceeds by one-electron oxidation of aromatic groups with  $\text{VO}_2^+$  released from  $[\text{PMo}_7\text{V}_5\text{O}_{40}]^{8-}$  followed by homolytic cleavage of  $\beta$ -O-4 ether and  $\text{C}_\alpha\text{-C}_\beta$  linkages (Scheme 26).<sup>437</sup>

Kadla<sup>438,439</sup> and co-workers extensively studied the oxidation of various lignin model compounds with  $\text{K}_5[\text{SiW}_{11}\text{O}_{40}]$ , in sodium acetate buffer ( $I = 0.2 \text{ M}$ ,  $\text{pH} = 5.0$ ). A dramatic increase in reactivity was observed upon addition of methoxyl groups in *ortho*-positions to the phenolic hydroxyl group. Syringyl units reacted faster than guaiacyl units. The reaction rates of *para*-substituted guaiacyl and syringyl model compounds showed a strong dependency on the nature of the substituents. The reaction rate of a 5–5' dimer lignin model compound was extremely fast. The addition of an electron-donating group in the *ortho*-phenol substituent not only increased the electron density of the aromatic ring, but also helped stabilize the intermediate phenoxy radical through resonance stabilization and delocalization. Kinetic study<sup>440</sup> of

lignin oxidation with POM anions ( $[\text{AlMn}^{\text{III}}(\text{OH}_2)\text{W}_{11}\text{O}_{39}]^{6-}$  and  $[\text{SiMn}^{\text{III}}(\text{OH}_2)\text{W}_{11}\text{O}_{39}]^{5-}$ ) showed that cation concentration and pH have a remarkable effect on the reactivity of the POMs.

As discussed above, the degradation of lignin over POMs generates various lignin radical intermediates. The coupling of these radical fragments can lead to significant repolymerization that inhibits the degradation efficiency.<sup>439</sup> Rudolf von Rohr<sup>424,426</sup> and co-workers disclosed that low molecular alcohols such as methanol could effectively prevent the repolymerization by reducing lignin–lignin condensation reactions in aqueous solvent: first, condensation of methanol catalyzed by  $\text{H}_3\text{PMo}_{12}\text{O}_{40}$  can produce dimethyl ether (eq 4 in Figure 17). Then, homolytic cleavage of the C–O bond in DME generates  $\text{CH}_3\text{O}\cdot$  and  $\text{CH}_3\cdot$  radicals (eq 5 in Figure 17), which are radical scavengers that couple with the lignin fragments before repolymerization occurs (Figure 17).

**7.4.2. Other transition metal salts.** Transition metal salts are another sort of homogeneous catalysts for lignin oxidation. Taking the advantages of IL-stabilized metal nanoparticles and the high solubility of lignin in ILs, Zhu and co-workers<sup>441</sup> reported a recyclable catalyst system, comprising nanopalladium(0) and iron bis(dicarbollide) pyridinium salt as a cocatalyst, for the oxidation of benzyl alcohol and organosolv lignin in a mixed solvent of  $[\text{Bmim}]\text{PF}_6/[\text{Bmim}][\text{MeSO}_4]$  (2:1 v/v) under oxygen atmosphere (Table 15, entries 3–7). This strategy overcomes the solubility limitation and favors the oxidative conversion of lignin model compounds. Palladium supported on  $\gamma\text{-Al}_2\text{O}_3$  was used as an efficient catalyst for catalytic wet air oxidation of lignin obtained from sugar cane bagasse with an aromatic aldehyde yield of 12%.<sup>449</sup> The reactions in the lignin degradation and aldehyde production were described as a system of complex parallel and consecutive reactions, in which pseudo-first-order steps are found.

In 2010, Weckhuysen<sup>370</sup> and co-workers reported the molecular oxygen oxidation of lignin using several transition metal catalysts, such as  $\text{CoCl}_2\cdot 6\text{H}_2\text{O}$ ,  $\text{Co}(\text{acac})_3$ ,  $\text{Co}(\text{acac})_2$ ,  $\text{Co}(\text{OAc})_2\cdot 4\text{H}_2\text{O}$ ,  $\text{Co}(\text{NO}_3)_2\cdot 6\text{H}_2\text{O}$ ,  $\text{Mn}(\text{NO}_3)_2$ ,  $\text{Mn}(\text{OAc})_2$ ,  $\text{FeC}_2\text{O}_4$ ,  $\text{FePO}_4$ ,  $\text{Cu}(\text{acac})_2$ , and  $\text{Ni}(\text{NO}_3)_2$ , etc. under mild conditions in the IL 1-ethyl-3-methylimidazolium diethylphosphate ( $[\text{Emim}]\text{DEP}$ ) medium. The activities of the catalysts were much improved compared to that in aqueous solvent (TOF:  $1440 \text{ h}^{-1}$  vs  $10\text{--}15 \text{ h}^{-1}$ ). The general activity order of the investigated transition metal cations was  $\text{Co} > \text{Cr} > \text{Fe} > \text{Ni} > \text{Mn} \gg \text{Cu}$ . Among the transition metal salts tested,  $\text{CoCl}_2\cdot 6\text{H}_2\text{O}$  in  $[\text{Emim}]\text{DEP}$  exhibited particularly high activity. The catalyst rapidly catalyzed the oxidation of benzyl and other alcohol functionalities in lignin, and left the phenolic functionality and the  $\beta$ -O-4, 5–5', and phenylcoumaran linkages intact. *In-situ* spectroscopic investigation<sup>357</sup> showed that the reaction proceeds via the coordination of alcohol-containing substrates to the Co center followed by formation of a Co-superoxo species (Scheme 27). The requisite condition for coordination of the alcohol is the presence of hydroxide.



Table 15. Lignin and Model Compounds' Oxidation Results over Different Metal Salt Catalysts

Entry	Catalyst	Oxidant	Solvent	Reaction conditions			Substrate	Product	Results		ref
				T (°C)	P (MPa)	Time (h)			Yield (%) <sup>a</sup>	Conv. (%)	
1	K <sub>2</sub> [SiW <sub>11</sub> O <sub>40</sub> ]-12 H <sub>2</sub> O	SiW <sub>11</sub> O <sub>40</sub> <sup>5-</sup>	Sodium acetate buffer, pH 5.0	25	0.1 (Ar)	1	Vanillyl alcohol	5-(1-Hydroxyethyl)-3-methoxycyclohexa-3,5-diene-1,2-dione; 4-hydroxy-3,5-dimethoxyphenylethanone; 2,6-dimethoxycyclohexa-2,5-diene-1,4-dione	46		379
2	K <sub>2</sub> [SiW <sub>11</sub> O <sub>40</sub> ]-12 H <sub>2</sub> O	SiW <sub>11</sub> O <sub>40</sub> <sup>5-</sup>	Sodium acetate buffer, pH 5.0	25	0.1 (Ar)	1	4-Hydroxy-3,5-dimethoxyphenyl-ethyl methyl ether	4-hydroxy-3,5-dimethoxyphenylethanone; 2,6-dimethoxycyclohexa-2,5-diene-1,4-dione	31		379
3	Pd NPs and pyridinium salt of iron bis(dicarbonyl)	O <sub>2</sub>	[Bmmim][PF <sub>6</sub> ]/[Bmmim][MeSO <sub>4</sub> ]	120	0.4	18	Benzyl alcohol	Benzyl aldehyde	93		441
4	Pd NPs and pyridinium salt of iron bis(dicarbonyl)	O <sub>2</sub>	[Bmmim][PF <sub>6</sub> ]/[Bmmim][MeSO <sub>4</sub> ]	120	0.4	18	4-Methoxy benzyl alcohol	4-Methoxy benzyl aldehyde	86		441
5	Pd NPs and pyridinium salt of iron bis(dicarbonyl)	O <sub>2</sub>	[Bmmim][PF <sub>6</sub> ]/[Bmmim][MeSO <sub>4</sub> ]	120	0.4	18	2-Methoxy benzyl alcohol	2-Methoxy benzyl aldehyde	77		441
6	Pd NPs and pyridinium salt of iron bis(dicarbonyl)	O <sub>2</sub>	[Bmmim][PF <sub>6</sub> ]/[Bmmim][MeSO <sub>4</sub> ]	120	0.4	18	3,4-Dimethoxy benzyl alcohol	3,4-Dimethoxy benzyl aldehyde	84		441
7	Pd NPs and pyridinium salt of iron bis(dicarbonyl)	O <sub>2</sub>	[Bmmim][PF <sub>6</sub> ]/[Bmmim][MeSO <sub>4</sub> ]	120	0.4	18	3-Phenoxy benzyl alcohol	3-Phenoxy benzyl aldehyde	80		441
8	H <sub>3</sub> PMo <sub>12</sub> O <sub>40</sub> ·xH <sub>2</sub> O	O <sub>2</sub>	80 vol % MeOH/H <sub>2</sub> O	170	0.5	0.33	Kraft spruce lignin	Monomeric oxidative products	2.92		426
9	H <sub>3</sub> PMo <sub>12</sub> O <sub>40</sub> ·xH <sub>2</sub> O	O <sub>2</sub>	80 vol % MeOH/H <sub>2</sub> O	170	0.5	0.33	Kraft poplar lignin	Monomeric oxidative products	3.25		426
10	CuSO <sub>4</sub> /FeCl <sub>3</sub>	O <sub>2</sub>	NaOH aqueous solution	170	0.5	0.33	Kraft spruce lignin	Monomeric oxidative products	1.58		426
11	CuSO <sub>4</sub> /FeCl <sub>3</sub>	O <sub>2</sub>	NaOH aqueous solution	170	0.5	0.33	Granit lignin	Monomeric oxidative products	1.38		426
12	CuSO <sub>4</sub> /FeCl <sub>3</sub>	O <sub>2</sub>	NaOH in MeOH/H <sub>2</sub> O solution	170	0.5	0.33	Granit lignin	Monomeric oxidative products	1.62		426
13	CuSO <sub>4</sub>	O <sub>2</sub>	[mnmim][Me <sub>2</sub> PO <sub>4</sub> ]	175	2.5	1.5	Hard wood organosolv lignin	<i>p</i> -Hydroxybenzaldehyde, vanillin and syringaldehyde	29.7	100	442
14	CuSO <sub>4</sub>	O <sub>2</sub>	2.0 mol/L NaOH aqueous solution	175	2.5	1.5	Hard wood organosolv lignin	<i>p</i> -Hydroxybenzaldehyde, vanillin and syringaldehyde	19.3	100	442
15	CuSO <sub>4</sub>	O <sub>2</sub>	[mPy][Me <sub>2</sub> PO <sub>4</sub> ]	175	2.5	1.5	Hard wood organosolv lignin	Vanillin, syringaldehyde and <i>p</i> -hydroxybenzaldehyde	29.1	100	442
16	FeSO <sub>4</sub>	H <sub>2</sub> O <sub>2</sub>	H <sub>2</sub> O	30–60		1	Kraft lignin from corn stalk	Decreased molecular weight and increased phenolic hydroxyl content			443
17	Cu(OH) <sub>2</sub>	O <sub>2</sub>	120 g/L NaOH	160	0.9	0.25	Pine wood	Vanillin	23.1		444
18	MnSO <sub>4</sub>	O <sub>2</sub>	120 g/L NaOH	160	0.9	0.25	Pine wood	Vanillin	12.8		444
19	MnSO <sub>4</sub>	O <sub>2</sub>	2 M NaOH solution	120	0.5	0.5	Enzymatic steam explosion lignin	Vanillin, syringaldehyde and <i>p</i> -hydroxybenzaldehyde	11.5	30	445
20	LaCl <sub>3</sub>	O <sub>2</sub>	2 M NaOH solution	120	0.5	0.5	Enzymatic steam explosion lignin	Vanillin, syringaldehyde and <i>p</i> -hydroxybenzaldehyde	8.5	13	445
21	Ammonium iron(II) sulfatehexahydrate	CuO oxidation	2 M NaOH solution	170	0.1 (N <sub>2</sub> )	2.5	Grass roots	VSC <sup>b</sup>	56.7		446

Table 15. continued

Entry	Catalyst	Oxidant	Solvent	Reaction conditions			Substrate	Product	Results		ref
				T (°C)	P (MPa)	Time (h)			Yield (%) <sup>a</sup>	Conv. (%)	
22	LaMnO <sub>3</sub>	O <sub>2</sub>	2 M NaOH solution	120	0.2	1	Kraft lignin	Oligomer (15.1) and vanillin (1.5)	16.6	46.1	447
23	LaFe <sub>0.75</sub> Mn <sub>0.25</sub> O <sub>3</sub>	O <sub>2</sub>	2 M NaOH solution	120	0.2	1	Kraft lignin	Oligomer (38.6) and vanillin (2.6)	41.2	87.2	447
24	LaFe <sub>0.5</sub> Mn <sub>0.5</sub> O <sub>3</sub>	O <sub>2</sub>	2 M NaOH solution	120	0.2	1	Kraft lignin	Oligomer (37.6) and vanillin (2.8)	40.4	87.3	447
25	LaFe <sub>0.25</sub> Mn <sub>0.75</sub> O <sub>3</sub>	O <sub>2</sub>	2 M NaOH solution	120	0.2	1	Kraft lignin	Oligomer (36.4) and vanillin (2.8)	39.2	86.0	447
26	La <sub>0.9</sub> Sr <sub>0.1</sub> MnO <sub>3</sub>	O <sub>2</sub>	2 M NaOH solution	120	0.2	1	Kraft lignin	Oligomer (34.1) and vanillin (3.0)	37.1	84.6	447
27	LaFeO <sub>3</sub>	O <sub>2</sub>	2 M NaOH solution	120	0.5	0.5	Enzymatic steam explosion lignin	Vanillinaldehyde, <i>p</i> -hydroxybenzaldehyde, syringaldehyde	15	20	448
28	LaFe <sub>0.8</sub> Cu <sub>0.2</sub> O <sub>3</sub>	O <sub>2</sub>	2 M NaOH solution	120	0.5	0.5	Enzymatic steam explosion lignin	Vanillinaldehyde, <i>p</i> -hydroxybenzaldehyde, syringaldehyde	18	34	448
29	LaMnO <sub>3</sub>	O <sub>2</sub>	2 M NaOH solution	120	0.5	0.5	Enzymatic Steam explosion lignin	Vanillinaldehyde, <i>p</i> -hydroxybenzaldehyde, syringaldehyde	14.5	20	445

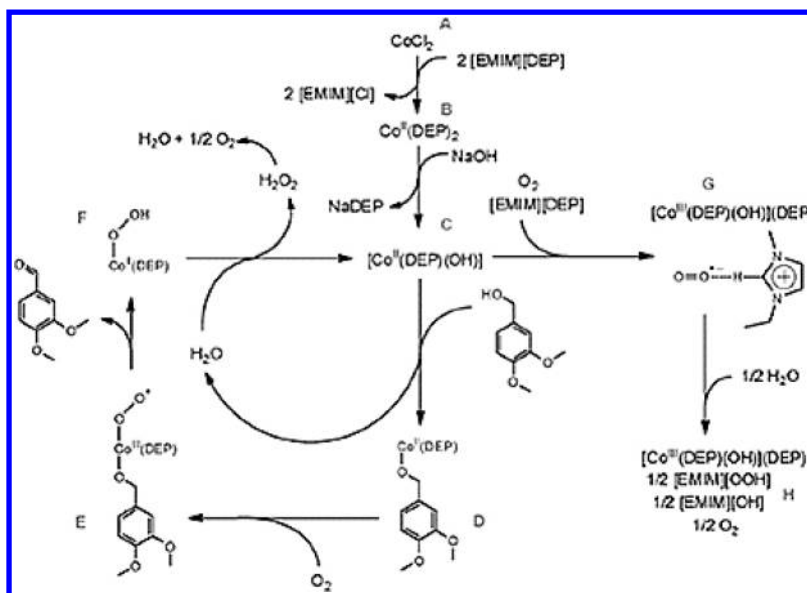
<sup>a</sup>The data refer to the total yield of all the listed products. <sup>b</sup>VSC = Sum of major 8 lignin phenols of the vanillyl V (vanillin, acetovanillone, vanillic acid), syringyl S (syringaldehyde, acetosyringone, syringic acid), and cinnamyl C (*p*-coumaric acid, ferulic acid) type.

Byproduct hydrogen peroxide underwent rapid disruption to yield water and molecular oxygen. The presence of IL greatly enhanced the catalytic activity by stabilizing reactive intermediates. This strategy represents a potential method in a biorefinery scheme to increase the oxygen functionality in intact lignin or depolymerized lignin. When an extraction solvent such as methylisobutylketone<sup>442</sup> was added to the IL system, the deep oxidation of the products could be avoided, resulting in improved yield of aromatic aldehydes (Table 15, entries 13–15).

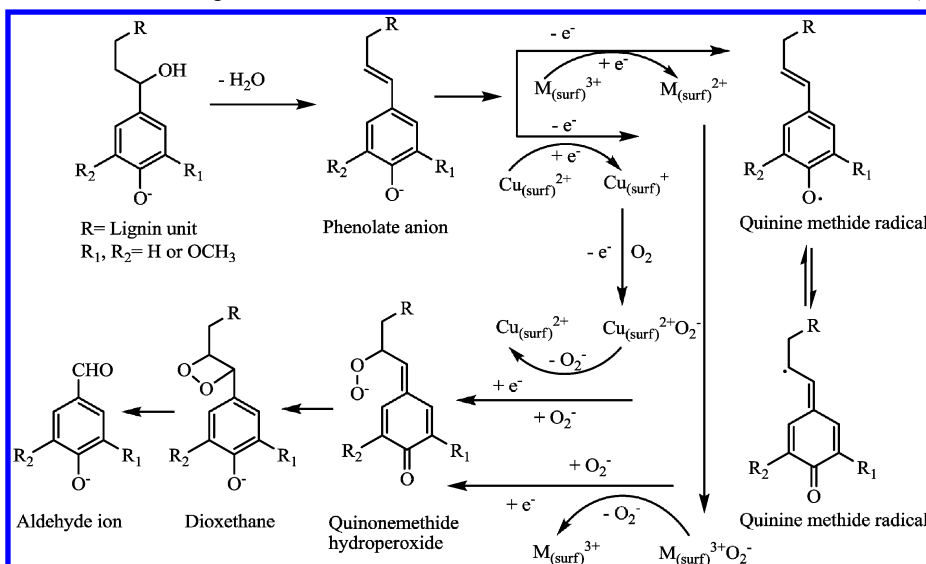
Compared with the high cost of noble metals and associated contaminations caused by transition metal ions, the affordability and stability properties of perovskite-type oxides (with the chemical formula ABO<sub>3</sub>) have placed them in a promising position as catalysts for wet air oxidation of lignin.<sup>445,450,451</sup> These perovskites include LaCoO<sub>3</sub>, LaMnO<sub>3</sub>, and LaFeO<sub>3</sub>.<sup>445,450–453</sup> They possess high activity and stability in the lignin oxidation reaction, and the catalytic activity can be increased by the partial substitution of A- or B-site cations. As an example, Wang<sup>447</sup> and co-workers found that LaFe<sub>x</sub>Mn<sub>1-x</sub>O<sub>3</sub> and La<sub>0.9</sub>Sr<sub>0.1</sub>MnO<sub>3</sub> hollow nanospheres synthesized via a urea-assisted solvothermal-calcination method showed much better catalytic performance in catalytic wet air oxidation of lignin than perovskite prepared by the traditional sol–gel method. Lin and co-workers also disclosed that Cu-doped Fe- and Co-based perovskite-type oxides LaFe<sub>1-x</sub>Cu<sub>x</sub>O<sub>3</sub><sup>448</sup> and LaCo<sub>1-x</sub>Cu<sub>x</sub>O<sub>3</sub><sup>452</sup> exhibited enhanced catalytic activity in comparison to the copper-free counterparts. These substitutions were suggested to increase the concentration of oxygen vacancies of perovskites, which promoted the amount of adsorbed oxygen surface active site [Fe(surf)<sup>3+</sup>O<sub>2</sub><sup>-</sup>] or [Co(surf)<sup>3+</sup>O<sub>2</sub><sup>-</sup>] species and improved the yield of activated species [Cu(surf)<sup>2+</sup>O<sub>2</sub><sup>-</sup>]. The proposed oxidation mechanism<sup>448,452</sup> catalyzed by Cu-doped perovskites is illustrated in Scheme 28. Substitution of the B-site is considered to be more efficient than that of the A-site.<sup>454</sup>

Wu et al.<sup>419,455</sup> obtained 14.6 wt % aromatic aldehydes (including 4.7 wt % vanillin) from steam-explosion hardwood lignin with CuSO<sub>4</sub> and FeCl<sub>3</sub> catalysts in a 13.5% NaOH solution. As an electron acceptor, Cu<sup>2+</sup> accelerates the formation of the phenoxy radical and thus speeds up the radical oxidation reaction. As for the role of Fe<sup>3+</sup> in the oxidative degradation of lignin, it acts as oxygen carrier to form an intermediate O<sub>2</sub>–Fe<sup>3+</sup>-lignin complex in the oxidation process, as illustrated in Scheme 29.<sup>456</sup> The O<sub>2</sub>–Fe<sup>3+</sup>-lignin intermediate attacks the phenolate anion in the lignin structure to form the oxidation intermediates, which are further oxidized to acids via the ionic reaction route. For more details on lignin oxidation using Fe-based catalytic systems (including bivalent and trivalent iron in the form of salts, Fenton's reagent), one can resort to a recent review<sup>457</sup> written by Ferreira and co-workers.

Aromatic aldehydes and acids in yields of 10.9% were produced by oxidation of a hardwood organosolv lignin in acetic acid/water with a Co/Mn/Zr/Br catalyst.<sup>458</sup> Since the function of the catalyst is assumed to be based on its redox potential as reported for delignification studies,<sup>459</sup> the cation redox potential below the redox potential of oxygen (O<sub>2</sub>/H<sub>2</sub>O = 1.21 V) is necessary for the reoxidation of the catalyst. The catalytic action of the transition metal salts can be ascribed to both cation and anion, rather than to the cation alone.<sup>427</sup>

Scheme 27. Proposed Oxidation Mechanism of Veratryl Alcohol to Veratraldehyde in [EMIM][DEP] Reported by Weckhuysen et al.<sup>a</sup>

<sup>a</sup>Reprinted with permission from ref 357. Copyright 2011 Royal Society of Chemistry.

Scheme 28. Proposed Mechanism of Lignin Oxidation in the Presence of Cu-Substituted Perovskite Catalysts (M = Fe or Co)<sup>a</sup>

<sup>a</sup>Adapted from Lin<sup>452</sup> and co-workers.

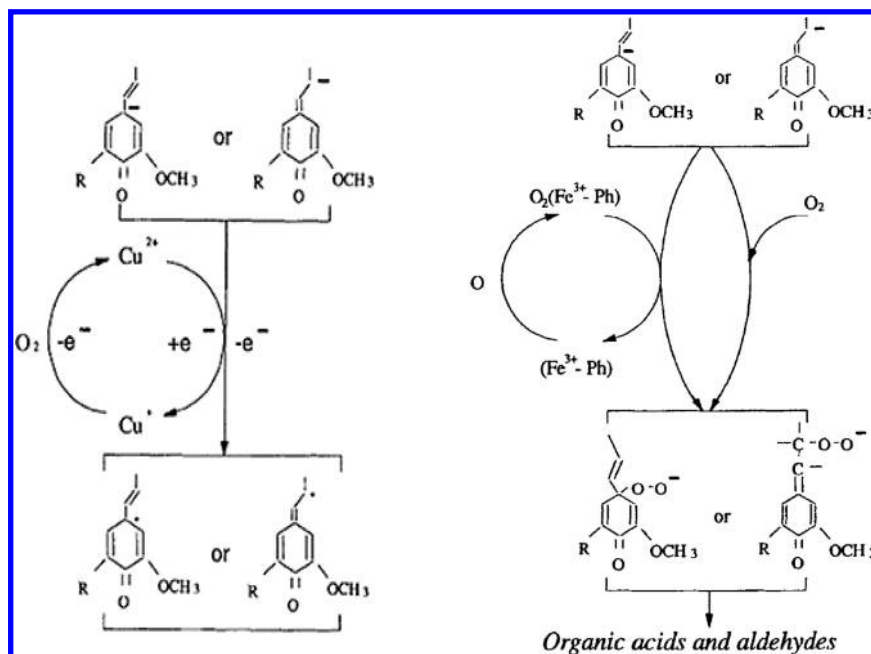
## 7.5. Photocatalytic oxidation

Heterogeneous photocatalysis for lignin degradation<sup>460,461</sup> has been studied as a way to minimize the organic pollutants in gas and liquid phases.<sup>462–467</sup> The catalyst used most frequently is TiO<sub>2</sub> due to its high activity, chemical stability, commercial availability, and low cost.<sup>468</sup> Other semiconductor materials, such as ZnO<sub>2</sub> and CdS, have also been used.<sup>469,470</sup> The photo-oxidative destruction of lignin is initiated when TiO<sub>2</sub> absorbs ultraviolet (UV) light. The short wavelength and high energy of UV light trigger reactions of two different pathways, namely, electron hole reaction and OH radical oxidation, to complete the photolysis process.<sup>471–473</sup> Both pathways have very fast reaction rates.<sup>474,475</sup>

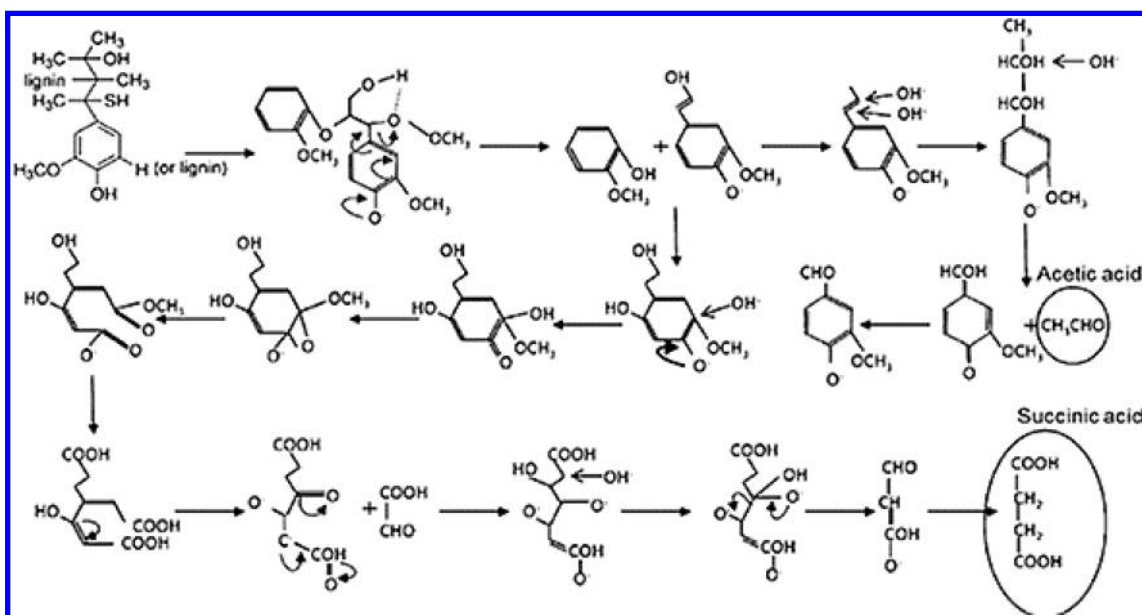
The photocatalytic ability of TiO<sub>2</sub> can be enhanced by doping TiO<sub>2</sub> with a noble-metal such as Pt.<sup>473</sup> The addition of

ferrous ions,<sup>476</sup> nanostructured CeO<sub>2</sub>, La<sub>2</sub>O<sub>3</sub>, and carbon<sup>477</sup> was also reported to enhance the catalytic activity of TiO<sub>2</sub>. Moreover, several groups<sup>472,478,479</sup> disclosed that the oxidative degradation efficiency of lignin can be significantly improved by applying a simultaneous photoelectrochemical process using a Ti/Ru<sub>0.1</sub>Sn<sub>0.6</sub>Ti<sub>0.3</sub>O<sub>2</sub> electrode, a quartz reaction device, and an artificial ultraviolet light, or by applying a hybrid process that combines photocatalytic processes (TiO<sub>2</sub> and UV light) and other catalytic strategies (such as enzyme) to degrade lignin.

Although TiO<sub>2</sub> catalyst has shown excellent performance in decomposition of lignin, it was found that lignin tended to form stable suspensions with TiO<sub>2</sub>, which made the recovery of fine TiO<sub>2</sub> powder a big challenge. This problem can be solved, in part, if TiO<sub>2</sub> is immobilized on inert supported materials such as sepiolite,<sup>468,480</sup> or activated carbon fibers.<sup>481</sup> The well

Scheme 29. Proposed Oxidation Mechanism with  $\text{Cu}^{2+}$  and  $\text{Fe}^{3+}$  as the Catalysts<sup>a</sup>

<sup>a</sup>Reprinted with permission from ref 456. Copyright 1995 Taylor & Francis.

Scheme 30. Mechanism for the Photocatalytic Oxidative Degradation of Lignin over  $\text{TiO}_2$  Proposed by Kamwilaisak and Wright<sup>a</sup>

<sup>a</sup>Reprinted from ref 472 with permission. Copyright 2012 American Chemical Society.

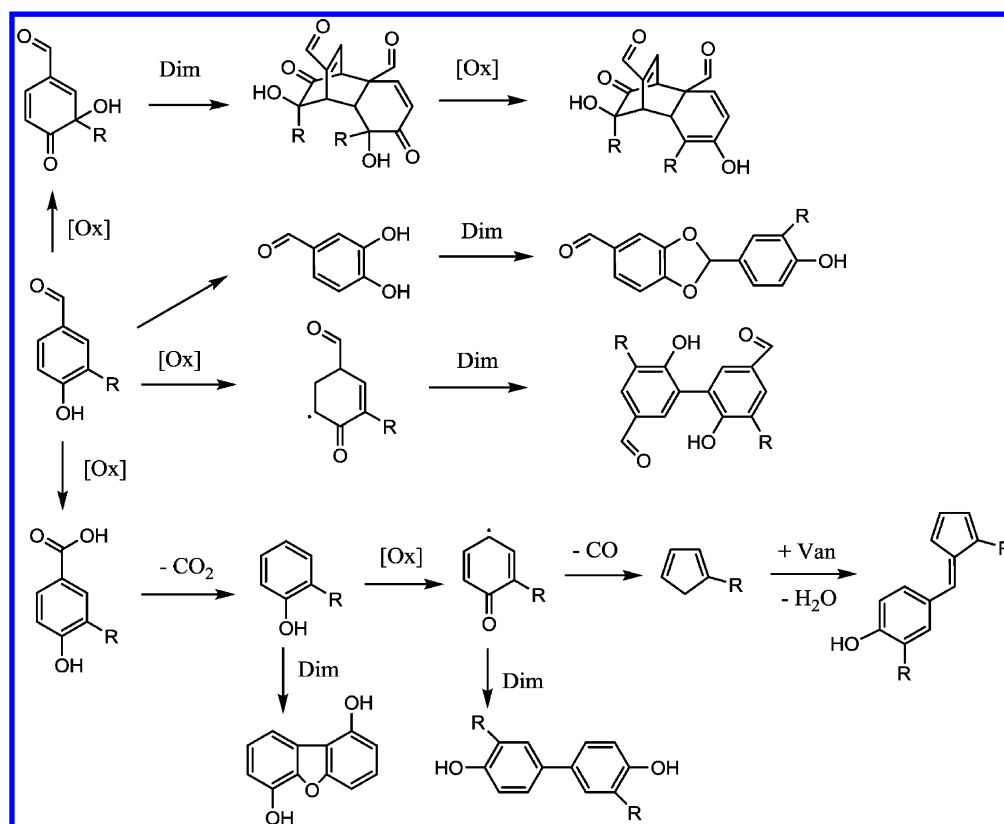
accepted lignin degradation mechanism by  $\text{TiO}_2/\text{UV}$  is illustrated in Scheme 30.<sup>472,482</sup>

### 7.6. Electrocatalytic oxidation

Electrochemical oxidation has been proposed as a potential alternative in lignin oxidative degradation.<sup>483–488</sup> The first report on this topic was made by Bailey and co-workers in 1940s.<sup>489</sup> Chen<sup>490</sup> and co-workers fabricated four different  $\text{IrO}_2$ -based electrodes ( $\text{Ti}/\text{Ta}_2\text{O}_5\text{-IrO}_2$ ,  $\text{Ti}/\text{SnO}_2\text{-IrO}_2$ ,  $\text{Ti}/\text{RuO}_2\text{-IrO}_2$ , and  $\text{Ti}/\text{TiO}_2\text{-IrO}_2$ ) and systematically studied their stability and electrochemical activity for lignin degradation to produce vanillin and vanillic acid. It was found that the

electrochemical oxidation of lignin followed pseudo-first-order kinetics, with the  $\text{Ti}/\text{RuO}_2\text{-IrO}_2$  electrode displaying the highest activity and stability. The same group further demonstrated that the  $\text{Ti}/\text{TiO}_2\text{NT}/\text{PbO}_2$  electrode was also promising for the treatment of lignin wastewater and the production of value-added chemicals.<sup>491</sup> Moodley,<sup>492</sup> Parpot,<sup>493</sup> and their co-workers investigated the electro-oxidation reactions of kraft lignin and calcium-spent liquor effluent in batch or flow cells on Ni, Au, Pt, Cu,  $\text{DSA-O}_2$ , and  $\text{PbO}_2$  anodes. Enhanced vanillin and syringaldehyde yields were



Scheme 31. Possible Vanillin Oligomerization Pathway as a Model of Side Reactions in the Lignin Oxidative Fragmentation Process<sup>a</sup>

<sup>a</sup>[Ox] stands for oxidation, [Van] for vanillin, and [Dim] for dimerization. Adapted from Di Renzo<sup>496</sup> and co-workers.

obtained through continuous extraction, which could avoid further decomposition reactions.

Almost all ILs have high conductance, and some of them can dissolve lignin effectively. Owing to these features, protic IL triethylammonium methanesulfonate<sup>494</sup> and *N*-hydroxyphthalimide (NHPI)<sup>495</sup> have been proved to be excellent mediators for selective *C*- $\alpha$ -carbonylation of nonphenolic  $\beta$ -O-4 structures in an electronic mediator system. These reactions proceed through hydrogen atom transfer in the IL-mediated electro-oxidation to afford the corresponding *C*- $\alpha$ -carbonyl products in high yields (85–97%) regardless of monomer or dimeric lignin model compounds.

Although electrochemical oxidation is a potentially promising technology for lignin oxidation or modification, the high cost and the electrode fouling caused by polymerization restrict its application.<sup>490</sup> Future work in this area should concentrate on the development of electrocatalysts with high activity, long lifetime, and low cost for lignin oxidation.

It should be noted that, in most of the strategies for lignin oxidation, the rearrangement and oligomerization of intermediate products of lignin fragmentation are inevitable side reactions. Di Renzo<sup>496</sup> and co-workers have extensively studied vanillin oligomerization as a model of side reactions in lignin fragmentation. It was found that hydrothermal treatment of vanillin under oxidative conditions can produce a wide variety of byproducts. The main oligomerization reactions involved are summarized in Scheme 31. In a water solvent, extensive demethylation and oxidative pathways occur via vanillic acid or quinonic intermediates. These reactive low molecular intermediates then underwent condensation by several mechanisms,

such as condensation of quinonic radicals,<sup>497</sup> phenolic dimerization,<sup>498</sup> or diol-aldehyde condensation to acetals.<sup>499</sup>

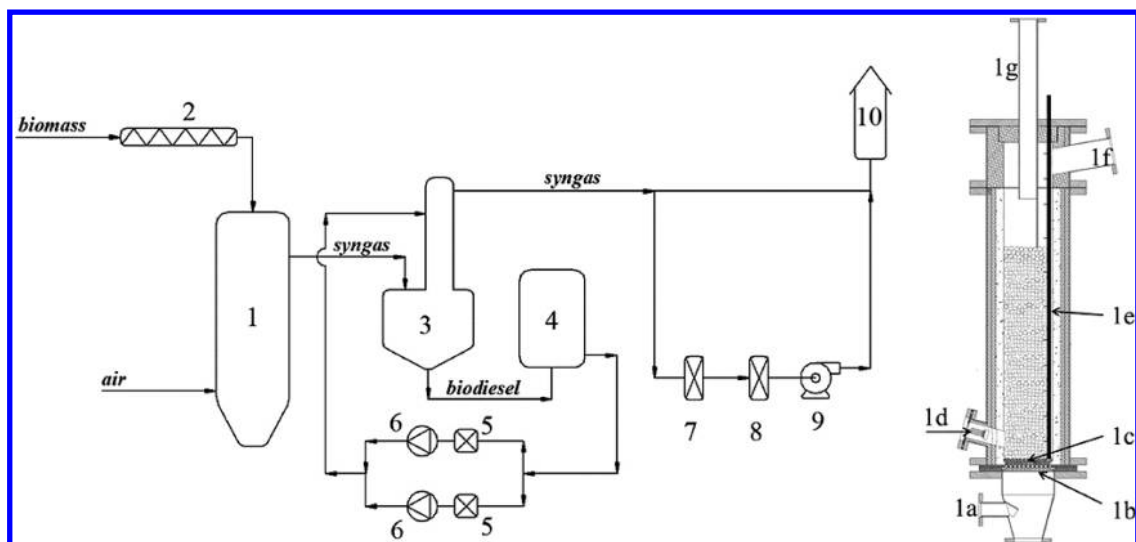
For quinonic intermediates, they can undergo ring-opening reactions to form dicarboxylic acids, or consecutive decarboxylate to cyclopentadienes. The nature of the catalyst and solvent significantly affect the products formed. For most developed lignin oxidation catalytic systems, the yields of the products, as yet, are too low to make the overall process economically viable. This is, to some extent, attributable to the complex lignin structure. Therefore, design of robust catalysts that fit with the complex structure and increase the product selectivity are promising directions for the development of lignin oxidation technology.

Oxidation of lignin and model compounds with the use of ILs represents a new opportunity for the efficient transformation of lignin to value-added chemicals. As aforementioned, there have been several good examples using ILs as solvents for the production of aromatic chemicals from lignin and model compounds. More details on lignin oxidation in ILs can be found in a critical review provided recently by Rogers and co-workers.<sup>369</sup>

## 8. OTHER DEPOLYMERIZATION PROCESS

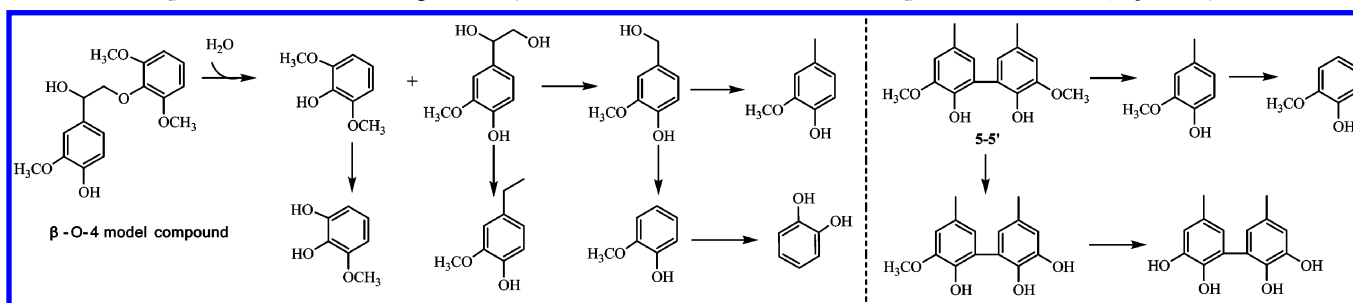
### 8.1. Gasification

Gasification of lignin produces synthesis gas (syngas) which is a mixture of hydrogen and carbon monoxide.<sup>500–502</sup> The synthesis gas can then be converted into liquid fuels by two different commercial processes: Fischer–Tropsch synthesis<sup>503</sup> or methanol/dimethyl ether synthesis.<sup>504</sup> Several reports in the



**Figure 18.** Scheme of the PRAGA (uP dRAft GASification) plant for updraft gasification and gas cleaning: (1) gasifier; (2) screw feeder; (3) scrubber; (4) biodiesel tank; (5) filter; (6) pump; (7) high-temperature coalescence filter; (8) low-temperature coalescence filter; (9) blower; (10) flare. On the right, details of the gasifier: (1a) air inlet; (1b) grate; (1c) layer of expanded clay; (1d) heating lamp; (1e) thermocouples multipoint system; (1f) gas outlet; (1g) biomass inlet.<sup>510</sup>

### Scheme 32. Aqueous-Phase Reforming Pathway of the $\beta$ -O-4 and 5-5' Model Compounds over Pt/Al<sub>2</sub>O<sub>3</sub> Catalyst<sup>a</sup>



<sup>a</sup>Reaction conditions: 0.043 g substrate, 10.98 g H<sub>2</sub>O, 0.58 g H<sub>2</sub>SO<sub>4</sub>, 0.1245 g 1% Pt/Al<sub>2</sub>O<sub>3</sub>, 29 bar He, 498 K, and 1.5 h. Adapted from Zakzeski and Weckhuysen.<sup>513</sup>

literature use supercritical water (374 °C, 218 atm) for gasification of lignin.<sup>502,505–507</sup> In terms of thermal efficiency, this process offers the advantage of eliminating the need to dry the biomass, which is especially important for lignin with high moisture content. Four main processing units are needed for the above two routes: a lignin material gasifier, a gas cleanup unit, a water–gas shift reactor in certain cases to produce hydrogen with the coformation of carbon dioxide, and finally a syngas converter. By optimization of the reaction conditions and the catalysts, numerous products, ranging from synthetic natural gas, olefins, and alcohols to various transportation fuels, such as gasoline, jet fuel, and diesel, can be fabricated through the gasification step.<sup>508</sup> Catalysts are required for several downstream processes, including (1) cracking of tars; (2) steam reforming of gas in order to increase H<sub>2</sub> content; and (3) synthesis-gas conversion.<sup>509</sup>

Although syngas routes for the production of chemicals are well established for coal and natural gas conversion, there are still huge challenges regarding lignin gasification.<sup>21</sup> One possible opportunity for future application is process intensification, which focuses on hybrid/combining processes to reduce cost.<sup>508</sup> Biomass gasifiers are still in the developmental stage with relation to producing a clean synthetic gas. Among the few reported attempts at lignin

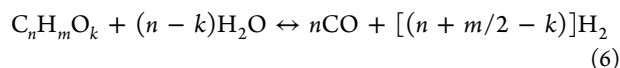
gasification at the pilot scale, Zimbardi<sup>510</sup> and co-workers carried out autothermal gasification of lignin-rich fermentation residues to evaluate the performance of a pilot plant with a feeding rate of 20–30 kg h<sup>-1</sup>. The main components of the plant are schematically shown in Figure 18. The core reactor of the plant is an autothermal fixed bed updraft gasifier, operated slightly above atmospheric conditions. The average production of raw syngas was 1.94 kg per kg of dry residue, of which H<sub>2</sub> and CO were 27.2 and 696 g, respectively. The efficiency of energy conversion from solid to cold gas was 64% and reached about 81%, including the contribution of the condensable organic fraction. It should be noted that as lignins from different plants and isolation methods represent significantly different structures and reactivity, adequate assessment of the specific lignin types in a given gasification system is needed. Jacoby<sup>511</sup> and co-workers have shown that the gasification thermodynamic state changes are functions of elemental composition, not biomass species.

### 8.2. Liquid-phase or steam reforming

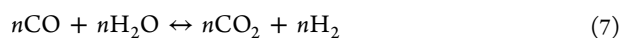
The liquid-phase reforming (LPR) of biomass refers to the conversion of biomass at temperatures lower than those required for gasification or pyrolysis (500 K for LPR vs 773 K for pyrolysis).<sup>512</sup> The preferred catalysts for these reactions are supported Group VIII transition metals, and their alloys and

mixtures, with Pt, Ru, or Rh having the highest stability and activity.<sup>512</sup> Various liquids, including water,<sup>513,514</sup> ethanol/water,<sup>515,516</sup> supercritical ethanol,<sup>517</sup> and liquid ammonia,<sup>518</sup> have been used in LPR of lignin at low/moderate pressures and temperatures. Ethanol and ammonia can readily dissolve lignin, but water is probably the preferred solvent due to its low cost and wide availability. The challenge with water as a solvent is that lignin has a low solubility in water. In the aqueous-phase reforming process, lignin was first depolymerized via cleavage of the abundant  $\beta$ -O-4 and 5-5' linkages to form aromatic monomers (Scheme 32). The alkyl chains on these monomers were then reformed to produce simple aromatics and hydrogen. Hydrolysis of the methoxy groups produced methanol, which was finally reformed to form carbon dioxide and hydrogen. It is interesting to note that the combination of an LPR reaction with a sequential HDO step over a CoMo/Al<sub>2</sub>O<sub>3</sub> or Mo<sub>2</sub>C/CNF catalyst allowed the production of BTX.<sup>519</sup>

Steam reforming of lignin to produce synthesis gas has also been reported based on a two-stage process: bio-oil is first generated by fast pyrolysis of pine sawdust, and then catalytic steam reforming of the crude oil produces hydrogen.<sup>520</sup> This two-step procedure can be summarized by eq 6:



If excess steam is used in the process, carbon monoxide can further undergo the water gas shift reaction as shown in eq 7:



Taken together, the stoichiometric maximum yield of hydrogen that can be obtained by reforming/water gas shift equals  $2 + (m - 2k)/2n$  moles per mole of carbon in the feed material.<sup>520</sup> Since the above two reactions are reversible, some carbon monoxide and methane are detected in the gas product. Therefore, hydrogen yield will always be lower than the stoichiometric maximum yield.

## 9. CONCLUDING REMARKS

Currently commercial aromatic chemicals are all derived from petrochemical feedstocks. Lignin is the only renewable feedstock in nature that comprises aromatic rings. Production of aromatic chemicals from lignin is highly atom-economic because most of the carbon, hydrogen, and oxygen atoms are well reserved in the products. Despite the renewed interest in the development of lignin valorization, no process produces liquid transportation fuels or bulk commodity chemicals (with the exception of lignosulfates) from lignin conversion due to the low overall carbon yield and separation problems. (LignoTech<sup>521</sup> is one company that has over 60 years of experience in the commercial production of lignosulfonates and lignin-based chemicals, such as dispersants, binding agents, etc. Another successful commercial process is the conversion of lignosulfonates, a byproduct of the sulfite pulping industry, to produce vanillin.<sup>416</sup>)

Design of new processes to produce value-added products and scale-up of these processes to produce lignin derived products at the commercial scale is a goal of a number of researchers working in utilization of lignin. Catalysis is a key technology for biomass conversion and for the valorization of lignin in particular. With the development of catalysis technology as well as the improvement of advanced analysis techniques, our knowledge of lignin chemistry is refined and our ability to rationally design robust catalysts has been

significantly enhanced over the past years. This review comprises the most representative examples and the recent achievements in the field of catalytic conversion of lignin for the production of valuable products through selective acid/base depolymerization, hydroprocessing degradation, oxidation, pyrolysis, gasification, or sequential processes in single reactor units. Among the above strategies, gasification and pyrolysis offer near-term solutions to the challenge presented by lignin recalcitrance, while hydroprocessing degradation of lignin into liquid biofuel requires a large amount of additional hydrogen. From a longer-term application viewpoint, production of aromatic chemicals, regardless of by acid/base depolymerization, reduction, or oxidation reaction, or integrated cascade reactions, is a promising way in terms of the use of the unique structure of lignin, and the following research fields on lignin chemistry are to be further explored.

1. The further understanding of the structure and fundamental organic chemistry of real lignin streams: Besides 2D-NMR such as HSQC, other techniques, such as GPC, SEC, <sup>31</sup>P NMR, ICP and IR, two-dimensional gas chromatography, and even 3D NMR or long-range correlation (HMBC) spectra, have been used to elucidate lignin structure. This knowledge will allow for the assessment of the reactivity of various lignins under basic, acidic, reductive, and oxidative conditions, and for the rational design of new catalysts. Currently it is hard to compare the results of different research groups, providing that each lignin resource has the inherent variability of the chemical composition and pretreating may often make it even more complex. The field needs standard protocols for the extraction of lignin, comparison of materials, catalyst, and analysis tools, so as to make the results possibly comparable.

2. Lignin model compound reactions: A lot of approaches for model compounds conversion have been tried, and certain of them have failed to realistically depolymerize real lignin because the model compounds do not represent the complexity of the lignin structure. More complex lignin model compounds should be developed. More rigorous mass balances for lignin are required, and several previous studies on lignin conversion fail to do a rigorous material balance and report artificially high yields of lignin products.

3. Thermodynamics data on lignin can provide important insight about the chemistry of lignin conversion. There is limited literature related to the thermodynamics of real lignin due to the notorious complicated reaction pathways. This could be an important area of future research.

4. Robust and recyclable catalysts which are tolerant to impurities should be developed. This approach should be combined with novel strategies (e.g., atom layer deposition technology<sup>522,523</sup>) for the preparation of highly active and stable catalysts. In-depth investigations on changes in surface chemistry, structure (phase transition), and chemical composition of the catalysts are the focal points to be studied. In the meantime, a big challenge in the design of robust catalysts in lignin processing is to develop multifunctional catalysts that are active for different functional groups, which could be used in cascade reactions allowing process intensification. While noble metal catalysts exhibited high efficiency in some depolymerization strategies, cheaper catalyst is preferable. Atomic scale control of solid catalysts<sup>524</sup> combined with the single-atom catalysis<sup>522,525</sup> should be another way to minimize the cost of the catalyst. Combination of new reaction media such as IL and novel conversion technologies such as microwave irradiation

and ultrasonic activation could also improve reaction efficiency, although there is a long way to go for practical application.

5. Development of renewable lignin-based products requires improved technologies coupled with lignin production processes. Although kraft pulping is presently the dominant process for lignin production, several pilot plants have adjusted their processes so that lignin could be used for other purposes. Researchers should work more closely with the lignin suppliers, so that the developed technologies adapt to the lignin molecular structure and the price and quality of the products are economically competitive with those obtained from fossil resources.

6. In comparison with conventional processes focusing on single reactions, combining multiple catalysts in either sequential or one-pot cascade catalysis provides distinct advantages by reducing time and yield losses associated with the isolation and purification of reaction products.<sup>25</sup> These features render multicatalysis or hybrid catalysis as a potentially cost-effective approach for lignin conversion, e.g.  $\text{IH}^2$  technology (which has been discussed in Section 6.4).

## ASSOCIATED CONTENT

### Special Issue Paper

This paper is an additional review for *Chem. Rev.* **2014**, Volume 114, Issue 3, "Chemicals from Coal, Alkynes, and Biofuels."

## AUTHOR INFORMATION

### Corresponding Author

\*(Tao Zhang) Fax: (+) 86 411 84691570; Tel: (+) 86 411 84379015; E-mail: taozhang@dicp.ac.cn.

### Notes

The authors declare no competing financial interest.

### Biographies



Changzhi Li was born in 1979. He received his Ph.D. degree in 2009 from Dalian Institute of Chemical Physics (DICP) under the supervision of Prof. Zongbao (Kent) Zhao; then he joined Prof. Tao Zhang's group, where he was promoted to an associate professor in 2012. In 2013, he won "Min Enze Energy and Chemical Engineering Award", jointly established by Chinese Academy of Engineering and Sinopec Group, for his contribution to the area of "ionic liquids mediated biomass conversion". His current research focuses on the catalytic depolymerization of lignin and the production of bulk and fine chemicals from renewable sources.



Xiaochen Zhao was born in 1984. She graduated from Dalian University of Technology in 2006 in Fine Chemical Engineering and received her Ph.D. degree in 2012 from Dalian Institute of Chemical Physics in Industrial Catalysis, during which she studied at the Inorganic Department of Fritz-Haber Institute, Max-Planck Society for one year. Her current research focuses on the selective hydrogenolysis of polyols and the application of nanocarbon materials in biomass conversion.



Ai Qin Wang joined Prof. Tao Zhang's group after she received a Ph.D. degree in 2001 from Dalian Institute of Chemical Physics (DICP) under the supervision of Profs. Dongbai Liang and Tao Zhang. In 2003, she moved to National Taiwan University as a postdoctoral fellow in Prof. Chung-Yuan Mou's group for synthesis and catalysis of gold-based alloy nanoparticles until 2005. Then, she went back to DICP and joined Prof. Tao Zhang's group, where she was promoted to a full professor in 2009. Her current research interests involve catalysis by nanogold and gold alloy particles, catalytic conversion of biomass, and design and synthesis of new catalytic materials.





George Huber is the Harvey Spangler Professor of Chemical Engineering at University of Wisconsin-Madison. His research focus is on developing new catalytic processes for the production of renewable liquid fuels and chemicals. He has done a sabbatical with Professor Tao Zhang at Dalian Institute of Chemical Physics. George did a postdoctoral stay with Avelino Corma at the Technical Chemical Institute at the Polytechnical University of Valencia, Spain (UPV-CSIC). He obtained his Ph.D. in Chemical Engineering from University of Wisconsin—Madison (2005) under the direction of James A. Dumesic. He obtained his B.S. (1999) and M.S. (2000) degrees (under the direction of Calvin Bartholomew) in Chemical Engineering from Brigham Young University.



Tao Zhang received his Ph.D. degree in 1989 from Dalian Institute of Chemical Physics (DICP), Chinese Academy of Sciences. After one year at University of Birmingham as a postdoctoral fellow, he joined DICP again in 1990, where he was promoted to a full professor in 1995. He is currently the director-general of DICP. His research interests are mainly focused on the design and synthesis of nano- and subnano-catalysts, the catalytic conversion of biomass, and environmental catalysis. He has won many important awards, such as the National Invention Prize (for three times), Distinguished Award of Chinese Academy of Sciences, Zhou Guang Zhao Foundation Award for Applied Science, and Excellent Scientist Award of Chinese Catalysis Society. Prof. Zhang is the author or coauthor of more than 300 peer-reviewed scientific publications. Over 100 patents were filed by him and co-workers. He serves as the Editor-in-Chief of *Chinese Journal of Catalysis* and as an Editorial Board Member of *Applied Catalysis B*, *ACS Sustainable Chemistry & Engineering*, *ChemPhysChem*, and *Industrial & Engineering Chemistry Research*. He was elected as an academician of Chinese Academy of Sciences in 2013.

## ACKNOWLEDGMENTS

Support from the National Natural Science Foundation of China (nos. 21473187, 21303187, and 21176235) and the CAS President's International Fellowship for Visiting Scientists (no. 2015VMA073) is gratefully acknowledged.

## REFERENCES

- (1) Huber, G. W.; Iborra, S.; Corma, A. Synthesis of transportation fuels from biomass: Chemistry, catalysts, and engineering. *Chem. Rev.* **2006**, *106*, 4044–4098.
- (2) Melero, J. A.; Iglesias, J.; Garcia, A. Biomass as renewable feedstock in standard refinery units. Feasibility, opportunities and challenges. *Energy Environ. Sci.* **2012**, *5*, 7393–7420.
- (3) Gallezot, P. Conversion of biomass to selected chemical products. *Chem. Soc. Rev.* **2012**, *41*, 1538–1558.

(4) Tuck, C. O.; Perez, E.; Horvath, I. T.; Sheldon, R. A.; Poliakov, M. Valorization of Biomass: Deriving More Value from Waste. *Science* **2012**, *337*, 695–699.

(5) Besson, M.; Gallezot, P.; Pinel, C. Conversion of Biomass into Chemicals over Metal Catalysts. *Chem. Rev.* **2014**, *114*, 1827–1870.

(6) Peng, B. X.; Yao, Y.; Zhao, C.; Lercher, J. A. Towards Quantitative Conversion of Microalgae Oil to Diesel-Range Alkanes with Bifunctional Catalysts. *Angew. Chem., Int. Ed.* **2012**, *51*, 2072–2075.

(7) Steen, E. J.; Kang, Y. S.; Bokinsky, G.; Hu, Z. H.; Schirmer, A.; McClure, A.; del Cardayre, S. B.; Keasling, J. D. Microbial production of fatty-acid-derived fuels and chemicals from plant biomass. *Nature* **2010**, *463*, 559–U182.

(8) IRENA (2014). *REmap 2030: A Renewable Energy Roadmap*, June 2014; IRENA: Abu Dhabi, <http://irena.org/remap/>.

(9) *National Twelfth Five-Year Plan on biomass energy*; Chinese National Energy Administration: Beijing, 2012.

(10) *USDA Announces Investments in Bioenergy Research and Development to Spur New Markets, Innovation, and Unlimited Opportunity in Rural America*; United States Department of Agriculture: 2013.

(11) Sawin, J. L.; Sverrisson, F. *Renewables 2014: Global status report*; REN21 secretariat: Paris, 2014.

(12) Amidon, T. E.; Liu, S. Water-based woody biorefinery. *Biotechnol. Adv.* **2009**, *27*, 542–550.

(13) Carpenter, D.; Westover, T. L.; Czernik, S.; Jablonski, W. Biomass feedstocks for renewable fuel production: a review of the impacts of feedstock and pretreatment on the yield and product distribution of fast pyrolysis bio-oils and vapors. *Green Chem.* **2014**, *16*, 384–406.

(14) Akhtari, S.; Sowlati, T.; Day, K. Economic feasibility of utilizing forest biomass in district energy systems - A review. *Renewable Sustainable Energy Rev.* **2014**, *33*, 117–127.

(15) Dutta, S.; De, S.; Saha, B.; Alam, M. I. Advances in conversion of hemicellulosic biomass to furfural and upgrading to biofuels. *Catal. Sci. Technol.* **2012**, *2*, 2025–2036.

(16) Ruppert, A. M.; Weinberg, K.; Palkovits, R. Hydrogenolysis Goes Bio: From Carbohydrates and Sugar Alcohols to Platform Chemicals. *Angew. Chem., Int. Ed.* **2012**, *51*, 2564–2601.

(17) Achyuthan, K. E.; Achyuthan, A. M.; Adams, P. D.; Dirk, S. M.; Harper, J. C.; Simmons, B. A.; Singh, A. K. Supramolecular Self-Assembled Chaos: Polyphenolic Lignin's Barrier to Cost-Effective Lignocellulosic Biofuels. *Molecules* **2010**, *15*, 8641–8688.

(18) Hu, L. H.; Pan, H.; Zhou, Y. H.; Zhang, M. Methods to Improve Lignin's Reactivity as a Phenol Substitute and as Replacement for Other Phenolic Compounds: A Brief Review. *Bioresources* **2011**, *6*, 3515–3525.

(19) Doherty, W. O. S.; Mousavioun, P.; Fellows, C. M. Value-adding to cellulosic ethanol: Lignin polymers. *Ind. Crops Prod.* **2011**, *33*, 259–276.

(20) Perlack, R. D.; Wright, L. L.; Turhollow, A. F.; Graham, R. L.; Stokes, B. J.; Erbach, D. C. *Biomass as Feedstock for a bioenergy and bioproducts industry: the technical feasibility of a billion-ton annual supply*; U. S. Department of Energy: Oak Ridge, 2005; p 5.

(21) Holladay, J. E.; White, J. F.; Bozell, J. J.; Johnson, D. *Top Value-Added Chemicals from Biomass. Vol. II: Results of Screening for Potential Candidates from Biorefinery Lignin*; U.S. Department of Commerce: VA, 2007; p 1.

(22) Biermann, C. J. *Essentials of Pulping and Papermaking*; Academic Press: San Diego, 1993.

(23) Calvo-Flores, F. G.; Dobado, J. A. Lignin as Renewable Raw Material. *ChemSusChem* **2010**, *3*, 1227–1235.

(24) Stewart, D. Lignin as a base material for materials applications: Chemistry, application and economics. *Ind. Crops Prod.* **2008**, *27*, 202–207.

(25) Gasser, C. A.; Hommes, G.; Schäffer, A.; Corvini, P. F. X. Multi-catalysis reactions: new prospects and challenges of biotechnology to valorize lignin. *Appl. Microbiol. Biotechnol.* **2012**, *95*, 1115–1134.

- (26) Ahmad, M.; Taylor, C. R.; Pink, D.; Burton, K.; Eastwood, D.; Bending, G. D.; Bugg, T. D. H. Development of novel assays for lignin degradation: comparative analysis of bacterial and fungal lignin degraders. *Mol. BioSyst.* **2010**, *6*, 815–821.
- (27) Bugg, T. D. H.; Ahmad, M.; Hardiman, E. M.; Rahmanpour, R. Pathways for degradation of lignin in bacteria and fungi. *Nat. Prod. Rep.* **2011**, *28*, 1883–1896.
- (28) Zakzeski, J.; Bruijninx, P. C. A.; Jongerius, A. L.; Weckhuysen, B. M. The Catalytic Valorization of Lignin for the Production of Renewable Chemicals. *Chem. Rev.* **2010**, *110*, 3552–3599.
- (29) Ragauskas, A. J.; Beckham, G. T.; Bidy, M. J.; Chandra, R.; Chen, F.; Davis, M. F.; Davison, B. H.; Dixon, R. A.; Gilna, P.; Keller, M.; Langan, P.; Naskar, A. K.; Saddler, J. N.; Tschaplinski, T. J.; Tuskan, G. A.; Wyman, C. E. Lignin Valorization: Improving Lignin Processing in the Biorefinery. *Science* **2014**, *344*, 709.
- (30) Xu, C. P.; Arancon, R. A. D.; Labidi, J.; Luque, R. Lignin depolymerisation strategies: towards valuable chemicals and fuels. *Chem. Soc. Rev.* **2014**, *43*, 7485–7500.
- (31) Lewin, M.; Goldstein, I. S. *Wood Structure and Composition*; CRC Press: Boca Raton, 1991; pp 183–261.
- (32) Kamm, B.; Gruber, P. R.; Kamm, M. *Biorefineries-Industrial Processes and Products*; Wiley-VCH: 2006; p 964.
- (33) Li, Z. Z. Research on renewable biomass resource-lignin. *J. Nanjing Forestry University (Nat. Sci. Ed.)* **2012**, *36*, 1–7.
- (34) Wen, J.-L.; Xue, B.-L.; Xu, F.; Sun, R.-C.; Pinkert, A. Unmasking the structural features and property of lignin from bamboo. *Ind. Crops Prod.* **2013**, *42*, 332–343.
- (35) Yue, F. X.; Lu, F. C.; Sun, R. C.; Ralph, J. Synthesis and Characterization of New 5-Linked Pinoresinol Lignin Models. *Chem. - Eur. J.* **2012**, *18*, 16402–16410.
- (36) Lu, F.; Ralph, J. *Lignin*; Elsevier: 2010; pp 169–207.
- (37) Vanholme, R.; Morreel, K.; Ralph, J.; Boerjan, W. Lignin engineering. *Curr. Opin. Plant Biol.* **2008**, *11*, 278–285.
- (38) Mansfield, S. D.; Kim, H.; Lu, F. C.; Ralph, J. Whole plant cell wall characterization using solution-state 2D NMR. *Nat. Protoc.* **2012**, *7*, 1579–1589.
- (39) Manara, P.; Zabaniotou, A.; Vanderghem, C.; Richel, A. Lignin extraction from Mediterranean agro-wastes: Impact of pretreatment conditions on lignin chemical structure and thermal degradation behavior. *Catal. Today* **2014**, *223*, 25–34.
- (40) Evtuguin, D. V.; Neto, C. P.; Silva, A. M. S.; Domingues, P. M.; Amado, F. M. L.; Robert, D.; Faix, O. Comprehensive study on the chemical structure of dioxane lignin from plantation Eucalyptus globulus wood. *J. Agric. Food Chem.* **2001**, *49*, 4252–4261.
- (41) Rodrigues Pinto, P. C.; da Silva, E. A. B.; Rodrigues, A. E. Insights into Oxidative Conversion of Lignin to High-Added-Value Phenolic Aldehydes. *Ind. Eng. Chem. Res.* **2011**, *50*, 741–748.
- (42) Zhang, A. P.; Lu, F. C.; Sun, R. C.; Ralph, J. Ferulate-coniferyl alcohol cross-coupled products formed by radical coupling reactions. *Planta* **2009**, *229*, 1099–1108.
- (43) Sannigrahi, P.; Ragauskas, A. J.; Miller, S. J. Effects of Two-Stage Dilute Acid Pretreatment on the Structure and Composition of Lignin and Cellulose in Loblolly Pine. *BioEnergy Res.* **2008**, *1*, 205–214.
- (44) Sannigrahi, P.; Ragauskas, A. J.; Miller, S. J. Lignin Structural Modifications Resulting from Ethanol Organosolv Treatment of Loblolly Pine. *Energy Fuels* **2010**, *24*, 683–689.
- (45) Guerra, A.; Filpponen, I.; Lucia, L. A.; Argyropoulos, D. S. Comparative evaluation of three lignin isolation protocols for various wood species. *J. Agric. Food Chem.* **2006**, *54*, 9696–9705.
- (46) Tohmura, S.; Argyropoulos, D. S. Determination of arylglycerol-beta-aryl ethers and other linkages in lignins using DFRC/P-31 NMR. *J. Agric. Food Chem.* **2001**, *49*, 536–542.
- (47) Wu, S.; Argyropoulos, D. S. An improved method for isolating lignin in high yield and purity. *J. Pulp. Pap. Sci.* **2003**, *29*, 235–240.
- (48) Guerra, A.; Filpponen, I.; Lucia, L. A.; Saquing, C.; Baumberger, S.; Argyropoulos, D. S. Toward a better understanding of the lignin isolation process from wood. *J. Agric. Food Chem.* **2006**, *54*, 5939–5947.
- (49) Villaverde, J. J.; Li, J. B.; Ek, M.; Ligerio, P.; de Vega, A. Native Lignin Structure of *Miscanthus x giganteus* and Its Changes during Acetic and Formic Acid Fractionation. *J. Agric. Food Chem.* **2009**, *57*, 6262–6270.
- (50) Akim, L. G.; Argyropoulos, D. S.; Jouanin, L.; Leple, J. C.; Pilate, G.; Pollet, B.; Lapierre, C. Quantitative P-31 NMR spectroscopy of lignins from transgenic poplars. *Holzforschung* **2001**, *55*, 386–390.
- (51) Xu, F.; Jiang, J. X.; Sun, R. C.; Tang, J. N.; Sun, J. X.; Su, Y. Q. Fractional isolation and structural characterization of mild ball-milled lignin in high yield and purity from *Eucommia ulmoides* Oliv. *Wood Sci. Technol.* **2008**, *42*, 211–226.
- (52) Hallac, B. B.; Sannigrahi, P.; Pu, Y.; Ray, M.; Murphy, R. J.; Ragauskas, A. J. Biomass Characterization of *Buddleja davidii*: A Potential Feedstock for Biofuel Production. *J. Agric. Food Chem.* **2009**, *57*, 1275–1281.
- (53) Hallac, B. B.; Pu, Y. Q.; Ragauskas, A. J. Chemical Transformations of *Buddleja davidii* Lignin during Ethanol Organosolv Pretreatment. *Energy Fuels* **2010**, *24*, 2723–2732.
- (54) Granata, A.; Argyropoulos, D. S. 2-Chloro-4,4,5,5-Tetramethyl-1,3,2-Dioxaphospholane, a Reagent for the Accurate Determination of the Uncondensed and Condensed Phenolic Moieties in Lignins. *J. Agric. Food Chem.* **1995**, *43*, 1538–1544.
- (55) Crestini, C.; Argyropoulos, D. S. Structural analysis of wheat straw lignin by quantitative P-31 and 2D NMR spectroscopy. The occurrence of ester bonds and alpha-O-4 substructures. *J. Agric. Food Chem.* **1997**, *45*, 1212–1219.
- (56) Monteil-Rivera, F.; Phuong, M.; Ye, M.; Halasz, A.; Hawari, J. Isolation and characterization of herbaceous lignins for applications in biomaterials. *Ind. Crops Prod.* **2013**, *41*, 356–364.
- (57) Yang, Q.; Wu, S. B.; Lou, R.; Lv, G. J. Structural characterization of lignin from wheat straw. *Wood Sci. Technol.* **2011**, *45*, 419–431.
- (58) El Hage, R.; Brosse, N.; Chrusciel, L.; Sanchez, C.; Sannigrahi, P.; Ragauskas, A. Characterization of milled wood lignin and ethanol organosolv lignin from *Miscanthus*. *Polym. Degrad. Stab.* **2009**, *94*, 1632–1638.
- (59) Samuel, R.; Pu, Y. Q.; Raman, B.; Ragauskas, A. J. Structural Characterization and Comparison of Switchgrass Ball-milled Lignin Before and After Dilute Acid Pretreatment. *Appl. Biochem. Biotechnol.* **2010**, *162*, 62–74.
- (60) Pandey, M. P.; Kim, C. S. Lignin Depolymerization and Conversion: A Review of Thermochemical Methods. *Chem. Eng. Technol.* **2011**, *34*, 29–41.
- (61) da Costa Sousa, L.; Chundawat, S. P.; Balan, V.; Dale, B. E. Cradle-to-grave assessment of existing lignocellulose pretreatment technologies. *Curr. Opin. Biotechnol.* **2009**, *20*, 339–347.
- (62) Lopez, M.; Huerta-Pujol, O.; Martinez-Farre, F. X.; Soliva, M. Approaching compost stability from Klason lignin modified method: Chemical stability degree for OM and N quality assessment. *Resour. Conserv. Recycl.* **2010**, *55*, 171–181.
- (63) Xiao, B.; Sun, X. F.; Sun, R. C. Chemical, structural, and thermal characterizations of alkali-soluble lignins and hemicelluloses, and cellulose from maize stems, rye straw, and rice straw. *Polym. Degrad. Stab.* **2001**, *74*, 307–319.
- (64) Björkman, A. Isolation of Lignin from Finely Divided Wood with Neutral Solvents. *Nature* **1954**, *174*, 1057–1058.
- (65) Baskar, C.; Baskar, S.; Dhillon, R. S. *Biomass Conversion: The Interface of Biotechnology, Chemistry and Materials Science*; Springer: 2012; p 341.
- (66) Pan, X. J.; Gilkes, N.; Kadla, J.; Pye, K.; Saka, S.; Gregg, D.; Ehara, K.; Xie, D.; Lam, D.; Saddler, J. Bioconversion of hybrid poplar to ethanol and co-products using an organosolv fractionation process: Optimization of process yields. *Biotechnol. Bioeng.* **2006**, *94*, 851–861.
- (67) Pew, J. C. Properties of powdered wood and isolation of lignin by cellulytic enzymes. *Tappi* **1957**, *40*, 553–558.
- (68) Abdulkhali, A.; Karimi, A.; Mirshokraie, A.; Hamzeh, Y.; Marlin, N.; Mortha, G. Isolation and chemical structure characterization of enzymatic lignin from *populus deltoides* wood. *J. Appl. Polym. Sci.* **2010**, *118*, 469–479.

- (69) Sun, N.; Rahman, M.; Qin, Y.; Maxim, M. L.; Rodríguez, H.; Rogers, R. D. Complete dissolution and partial delignification of wood in the ionic liquid 1-ethyl-3-methylimidazolium acetate. *Green Chem.* **2009**, *11*, 646–655.
- (70) Schuth, F.; Rinaldi, R.; Meine, N.; Kaldstrom, M.; Hilgert, J.; Rechulski, M. D. K. Mechanocatalytic depolymerization of cellulose and raw biomass and downstream processing of the products. *Catal. Today* **2014**, *234*, 24–30.
- (71) Yang, Q. L.; Shi, J. B.; Lin, L.; Peng, L. C.; Zhuang, J. P. Characterization of changes of lignin structure in the processes of cooking with solid alkali and different active oxygen. *Bioresour. Technol.* **2012**, *123*, 49–54.
- (72) Hu, Z. J.; Yeh, T. F.; Chang, H. M.; Matsumoto, Y.; Kadla, J. F. Elucidation of the structure of cellulolytic enzyme lignin. *Holzforschung* **2006**, *60*, 389–397.
- (73) Long, J.; Li, X.; Guo, B.; Wang, F.; Yu, Y.; Wang, L. Simultaneous delignification and selective catalytic transformation of agricultural lignocellulose in cooperative ionic liquid pairs. *Green Chem.* **2012**, *14*, 1935–1941.
- (74) Teramoto, Y.; Lee, S. H.; Endo, T. Pretreatment of woody and herbaceous biomass for enzymatic saccharification using sulfuric acid-free ethanol cooking. *Bioresour. Technol.* **2008**, *99*, 8856–8863.
- (75) Xu, F.; Sun, J. X.; Sun, R. C.; Fowler, P.; Baird, M. S. Comparative study of organosolv lignins from wheat straw. *Ind. Crops Prod.* **2006**, *23*, 180–193.
- (76) Holtman, K. M.; Chang, H. M.; Kadla, J. F. Solution-state nuclear magnetic resonance study of the similarities between milled wood lignin and cellulolytic enzyme lignin. *J. Agric. Food Chem.* **2004**, *52*, 720–726.
- (77) Pu, Y. Q.; Jiang, N.; Ragauskas, A. J. Ionic liquid as a green solvent for lignin. *J. Wood Chem. Technol.* **2007**, *27*, 23–33.
- (78) Yang, D.; Zhong, L.-X.; Yuan, T.-Q.; Peng, X.-W.; Sun, R.-C. Studies on the structural characterization of lignin, hemicelluloses and cellulose fractionated by ionic liquid followed by alkaline extraction from bamboo. *Ind. Crops Prod.* **2013**, *43*, 141–149.
- (79) Xin, Q.; Pfeiffer, K.; Prausnitz, J. M.; Clark, D. S.; Blanch, H. W. Extraction of lignins from aqueous-ionic liquid mixtures by organic solvents. *Biotechnol. Bioeng.* **2012**, *109*, 346–352.
- (80) Pinkert, A.; Goeke, D. F.; Marsh, K. N.; Pang, S. Extracting wood lignin without dissolving or degrading cellulose: investigations on the use of food additive-derived ionic liquids. *Green Chem.* **2011**, *13*, 3124–3136.
- (81) Muhammad, N.; Man, Z.; Bustam, M. A.; Mutalib, M. I. A.; Rafiq, S. Investigations of novel nitrile-based ionic liquids as pretreatment solvent for extraction of lignin from bamboo biomass. *J. Ind. Eng. Chem.* **2013**, *19*, 207–214.
- (82) Ji, W.; Ding, Z.; Liu, J.; Song, Q.; Xia, X.; Gao, H.; Wang, H.; Gu, W. Mechanism of Lignin Dissolution and Regeneration in Ionic Liquid. *Energy Fuels* **2012**, *26*, 6393–6403.
- (83) George, A.; Tran, K.; Morgan, T. J.; Benke, P. I.; Berruoco, C.; Lorente, E.; Wu, B. C.; Keasling, J. D.; Simmons, B. A.; Holmes, B. M. The effect of ionic liquid cation and anion combinations on the macromolecular structure of lignins. *Green Chem.* **2011**, *13*, 3375–3385.
- (84) Casas, A.; Oliet, M.; Alonso, M. V.; Rodriguez, F. Dissolution of *Pinus radiata* and *Eucalyptus globulus* woods in ionic liquids under microwave radiation: Lignin regeneration and characterization. *Sep. Purif. Technol.* **2012**, *97*, 115–122.
- (85) Achiniyu, E. C.; Howard, R. M.; Li, G. Q.; Gracz, H.; Henderson, W. A. Lignin extraction from biomass with protic ionic liquids. *Green Chem.* **2014**, *16*, 1114–1119.
- (86) Hossain, M. M.; Aldous, L. Ionic Liquids for Lignin Processing: Dissolution, Isolation, and Conversion. *Aust. J. Chem.* **2012**, *65*, 1465–1477.
- (87) Tan, S. S. Y.; MacFarlane, D. R.; Upfal, J.; Edye, L. A.; Doherty, W. O. S.; Patti, A. F.; Pringle, J. M.; Scott, J. L. Extraction of lignin from lignocellulose at atmospheric pressure using alkylbenzenesulfonate ionic liquid. *Green Chem.* **2009**, *11*, 339–345.
- (88) Ferrini, P.; Rinaldi, R. Catalytic Biorefining of Plant Biomass to Non-Pyrolytic Lignin Bio-Oil and Carbohydrates through Hydrogen Transfer Reactions. *Angew. Chem., Int. Ed.* **2014**, *53*, 8634–8639.
- (89) vom Stein, T.; Grande, P. M.; Kayser, H.; Sibilla, F.; Leitner, W.; de Maria, P. D. From biomass to feedstock: one-step fractionation of lignocellulose components by the selective organic acid-catalyzed depolymerization of hemicellulose in a biphasic system. *Green Chem.* **2011**, *13*, 1772–1777.
- (90) Bayerbach, R.; Meier, D. Characterization of the water-insoluble fraction from fast pyrolysis liquids (pyrolytic lignin). Part IV: Structure elucidation of oligomeric molecules. *J. Anal. Appl. Pyrolysis* **2009**, *85*, 98–107.
- (91) Wang, K.; Jiang, J.-X.; Xu, F.; Sun, R.-C. Effects of Incubation Time on the Fractionation and Characterization of Lignin During Steam Explosion Pretreatment. *Ind. Eng. Chem. Res.* **2012**, *51*, 2704–2713.
- (92) Zeng, J. J.; Tong, Z. H.; Wang, L. T.; Zhu, J. Y.; Ingram, L. Isolation and structural characterization of sugarcane bagasse lignin after dilute phosphoric acid plus steam explosion pretreatment and its effect on cellulose hydrolysis. *Bioresour. Technol.* **2014**, *154*, 274–281.
- (93) Wang, K.; Bauer, S.; Sun, R.-c. Structural Transformation of *Miscanthus × giganteus* Lignin Fractionated under Mild Formosolv, Basic Organosolv, and Cellulolytic Enzyme Conditions. *J. Agric. Food Chem.* **2012**, *60*, 144–152.
- (94) Zoia, L.; Orlandi, M.; Argyropoulos, D. S. Microwave-Assisted Lignin Isolation Using the Enzymatic Mild Acidolysis (EMAL) Protocol. *J. Agric. Food Chem.* **2008**, *56*, 10115–10122.
- (95) Bouxin, F. P.; Jackson, S. D.; Jarvis, M. C. Isolation of high quality lignin as a by-product from ammonia percolation pretreatment of poplar wood. *Bioresour. Technol.* **2014**, *162*, 236–242.
- (96) Roberts, V. M.; Fendt, S.; Lemonidou, A.; Li, X.; Lercher, J. A. Influence of alkali carbonates on benzyl phenyl ether cleavage pathways in superheated water. *Appl. Catal., B* **2010**, *95*, 71–77.
- (97) Yuan, Z. S.; Cheng, S. N.; Leitch, M.; Xu, C. B. Hydrolytic degradation of alkaline lignin in hot-compressed water and ethanol. *Bioresour. Technol.* **2010**, *101*, 9308–9313.
- (98) Lavoie, J.-M.; Baré, W.; Bilodeau, M. Depolymerization of steam-treated lignin for the production of green chemicals. *Bioresour. Technol.* **2011**, *102*, 4917–4920.
- (99) Roberts, V. M.; Stein, V.; Reiner, T.; Lemonidou, A.; Li, X.; Lercher, J. A. Towards Quantitative Catalytic Lignin Depolymerization. *Chem. - Eur. J.* **2011**, *17*, 5939–5948.
- (100) Mahmood, N.; Yuan, Z.; Schmidt, J.; Xu, C. C. Production of polyols via direct hydrolysis of kraft lignin: Effect of process parameters. *Bioresour. Technol.* **2013**, *139*, 13–20.
- (101) Toledano, A.; Serrano, L.; Labidi, J. Organosolv lignin depolymerization with different base catalysts. *J. Chem. Technol. Biotechnol.* **2012**, *87*, 1593–1599.
- (102) Miller, J. E.; Evans, L.; Littlewolf, A.; Trudell, D. E. Batch microreactor studies of lignin and lignin model compound depolymerization by bases in alcohol solvents. *Fuel* **1999**, *78*, 1363–1366.
- (103) Okuda, K.; Umetsu, M.; Takami, S.; Adschiri, T. Disassembly of lignin and chemical recovery - rapid depolymerization of lignin without char formation in water-phenol mixtures. *Fuel Process. Technol.* **2004**, *85*, 803–813.
- (104) Toledano, A.; Serrano, L.; Labidi, J. Improving base catalyzed lignin depolymerization by avoiding lignin repolymerization. *Fuel* **2014**, *116*, 617–624.
- (105) Li, J. B.; Henriksson, G.; Gellerstedt, G. Lignin depolymerization/repolymerization and its critical role for delignification of aspen wood by steam explosion. *Bioresour. Technol.* **2007**, *98*, 3061–3068.
- (106) Gosselink, R. J. A.; Teunissen, W.; van Dam, J. E. G.; de Jong, E.; Gellerstedt, G.; Scott, E. L.; Sanders, J. P. M. Lignin depolymerisation in supercritical carbon dioxide/acetone/water fluid for the production of aromatic chemicals. *Bioresour. Technol.* **2012**, *106*, 173–177.
- (107) Kleinert, M.; Gasson, J. R.; Barth, T. Optimizing solvolysis conditions for integrated depolymerisation and hydrodeoxygenation of



- lignin to produce liquid biofuel. *J. Anal. Appl. Pyrolysis* **2009**, *85*, 108–117.
- (108) Kleinert, M.; Barth, T. Phenols from lignin. *Chem. Eng. Technol.* **2008**, *31*, 736–745.
- (109) Wongsiriwan, U.; Noda, Y.; Song, C. S.; Prasassarakich, P.; Yeboah, Y. Lignocellulosic Biomass Conversion by Sequential Combination of Organic Acid and Base Treatments. *Energy Fuels* **2010**, *24*, 3232–3238.
- (110) Long, J. X.; Xu, Y.; Wang, T. J.; Yuan, Z. Q.; Shu, R. Y.; Zhang, Q.; Ma, L. Efficient base-catalyzed decomposition and in situ hydrogenolysis process for lignin depolymerization and char elimination. *Appl. Energy* **2015**, *141*, 70–79.
- (111) Jia, S.; Cox, B. J.; Guo, X.; Zhang, Z. C.; Ekerdt, J. G. Decomposition of a phenolic lignin model compound over organic N-bases in an ionic liquid. *Holzforchung* **2010**, *64*, 577–580.
- (112) Kleine, T.; Buendia, J.; Bolm, C. Mechanochemical degradation of lignin and wood by solvent-free grinding in a reactive medium. *Green Chem.* **2013**, *15*, 160–166.
- (113) Chakar, F. S.; Ragauskas, A. J. Review of current and future softwood kraft lignin process chemistry. *Ind. Crops Prod.* **2004**, *20*, 131–141.
- (114) Gierer, J. Chemistry of Delignification. I. General Concept and Reactions during Pulping. *Wood Sci. Technol.* **1985**, *19*, 289–312.
- (115) Gierer, J. The Chemistry of Delignification - a General Concept. *Holzforchung* **1982**, *36*, 43–51.
- (116) Gierer, J. Chemical Aspects of Kraft Pulping. *Wood Sci. Technol.* **1980**, *14*, 241–266.
- (117) Pasco, M. F.; Suckling, I. D. Lignin removal during kraft pulping an investigation by thioacidolysis. *Holzforchung* **1994**, *48*, 504–508.
- (118) Yasuda, S.; Hamaguchi, E.; Matsushita, Y.; Goto, H.; Imai, T. Ready chemical conversion of acid hydrolysis lignin into water-soluble lignosulfonate I<sub>h</sub> Hydroxymethylation and subsequent sulfonation of phenolized lignin model compounds. *J. Wood Sci.* **1998**, *44*, 116–124.
- (119) Imai, A.; Yokoyama, T.; Matsumoto, Y.; Meshitsukat, G. Significant lability of guaiacylglycerol beta-phenacyl ether under alkaline conditions. *J. Agric. Food Chem.* **2007**, *55*, 9043–9046.
- (120) Sergeev, A. G.; Hartwig, J. F. Selective, Nickel-Catalyzed Hydrogenolysis of Aryl Ethers. *Science* **2011**, *332*, 439–443.
- (121) Erdocia, X.; Prado, R.; Corcuera, M. A.; Labidi, J. Base catalyzed depolymerization of lignin: Influence of organosolv lignin nature. *Biomass Bioenergy* **2014**, *66*, 379–386.
- (122) Beauchet, R.; Monteil-Rivera, F.; Lavoie, J. M. Conversion of lignin to aromatic-based chemicals (L-chems) and biofuels (L-fuels). *Bioresour. Technol.* **2012**, *121*, 328–334.
- (123) Schultz, T. P.; Chen, C. L.; Goldstein, I. S. The attempted depolymerization of HCl lignin by catalytic hydrogenolysis. *J. Wood Chem. Technol.* **1982**, *2*, 33–46.
- (124) Zhu, Z. L.; Sun, M. M.; Su, C. G.; Zhao, H. M.; Ma, X. M.; Zhu, Z. D.; Shi, X. L.; Gu, K. F. One-pot quantitative hydrolysis of lignocelluloses mediated by black liquor. *Bioresour. Technol.* **2013**, *128*, 229–234.
- (125) Nenkova, S.; Vasileva, T.; Stanulov, K. Production of phenol compounds by alkaline treatment of technical hydrolysis lignin and wood biomass. *Chem. Nat. Compd.* **2008**, *44*, 182–185.
- (126) Deuss, P. J.; Scott, M.; Tran, F.; Westwood, N. J.; Vries, J. G. d.; Barta, K. Aromatic monomers by in situ conversion of reactive intermediates in the acid-catalyzed depolymerization of lignin. *J. Am. Chem. Soc.* **2015**, *137*, 7456–7467.
- (127) Hagglund, E.; Bjorkman, C. B. Lignin hydrochloride. *Biochem. Z.* **1924**, *147*, 74.
- (128) Papadopoulos, J.; Chen, C. L.; Goldstein, I. S. The Behavior of Lignin during Hydrolysis of Sweetgum Wood with Concentrated Hydrochloric-Acid at Moderate Temperatures. *Holzforchung* **1981**, *35*, 283–286.
- (129) Meshgini, M.; Sarkanen, K. V. Synthesis and Kinetics of Acid-Catalyzed Hydrolysis of Some Alpha-Aryl Ether Lignin Model Compounds. *Holzforchung* **1989**, *43*, 239–243.
- (130) Li, B.; Filpponen, I.; Argyropoulos, D. S. Acidolysis of Wood in Ionic Liquids. *Ind. Eng. Chem. Res.* **2010**, *49*, 3126–3136.
- (131) Kim, T. H. Sequential hydrolysis of hemicellulose and lignin in lignocellulosic biomass by two-stage percolation process using dilute sulfuric acid and ammonium hydroxide. *Korean J. Chem. Eng.* **2011**, *28*, 2156–2162.
- (132) Hepditch, M. M.; Thring, R. W. Degradation of solvolysis lignin using Lewis acid catalysts. *Can. J. Chem. Eng.* **2000**, *78*, 226–231.
- (133) Yu, H.; Hu, J.; Fan, J.; Chang, J. One-Pot Conversion of Sugars and Lignin in Ionic Liquid and Recycling of Ionic Liquid. *Ind. Eng. Chem. Res.* **2012**, *51*, 3452–3457.
- (134) Jia, S. Y.; Cox, B. J.; Guo, X. W.; Zhang, Z. C.; Ekerdt, J. G. Hydrolytic Cleavage of beta-O-4 Ether Bonds of Lignin Model Compounds in an Ionic Liquid with Metal Chlorides. *Ind. Eng. Chem. Res.* **2011**, *50*, 849–855.
- (135) Constant, S.; Basset, C.; Dumas, C.; Di Renzo, F.; Robitzer, M.; Barakat, A.; Quignard, F. Reactive organosolv lignin extraction from wheat straw: Influence of Lewis acid catalysts on structural and chemical properties of lignins. *Ind. Crops Prod.* **2015**, *65*, 180–189.
- (136) Thring, R. W.; Katikaneni, S. P. R.; Bakhshi, N. N. The production of gasoline range hydrocarbons from Alcell (R) lignin using HZSM-5 catalyst. *Fuel Process. Technol.* **2000**, *62*, 17–30.
- (137) Deepa, A. K.; Dhepe, P. L. Solid acid catalyzed depolymerization of lignin into value added aromatic monomers. *RSC Adv.* **2014**, *4*, 12625–12629.
- (138) Ben, H. X.; Ragauskas, A. J. One step thermal conversion of lignin to the gasoline range liquid products by using zeolites as additives. *RSC Adv.* **2012**, *2*, 12892–12898.
- (139) Jia, S.; Cox, B. J.; Guo, X.; Zhang, Z. C.; Ekerdt, J. G. Cleaving the beta-O-4 Bonds of Lignin Model Compounds in an Acidic Ionic Liquid, 1-H-3-Methylimidazolium Chloride: An Optional Strategy for the Degradation of Lignin. *ChemSusChem* **2010**, *3*, 1078–1084.
- (140) Cox, B. J.; Jia, S.; Zhang, Z. C.; Ekerdt, J. G. Catalytic degradation of lignin model compounds in acidic imidazolium based ionic liquids: Hammett acidity and anion effects. *Polym. Degrad. Stab.* **2011**, *96*, 426–431.
- (141) Cox, B. J.; Ekerdt, J. G. Depolymerization of oak wood lignin under mild conditions using the acidic ionic liquid 1-H-3-methylimidazolium chloride as both solvent and catalyst. *Bioresour. Technol.* **2012**, *118*, 584–588.
- (142) Roberts, V. M.; Knapp, R. T.; Li, X.; Lercher, J. A. Selective Hydrolysis of Diphenyl Ether in Supercritical Water Catalyzed by Alkaline Carbonates. *ChemCatChem* **2010**, *2*, 1407–1410.
- (143) Adler, E.; Pepper, J. M.; Eriksoo, E. Action of Mineral Acid on lignin and Model Substances of Guaiacylglycerol-beta-aryl Ether Type. *Ind. Eng. Chem.* **1957**, *49*, 1391–1392.
- (144) Johansson, B.; Miksche, G. Über die Benzyl-arylätherbindung im Lignin. II. Versuche an Modellen. *Acta Chem. Scand.* **1972**, *26*, 289–301.
- (145) Sarkanen, K. V.; Hoo, L. H. Kinetics of hydrolysis of erythro-guaiacylglycerol beta-(2-methoxyphenyl) ether and its veratryl analogue using HCl and aluminum chloride as catalysts. *J. Wood Chem. Technol.* **1981**, *1*, 11–27.
- (146) Ryabukhin, D. S.; Vasilyev, A. V.; Zarubin, M. Y. Conversions of the Bjorkman lignin from the european spruce (*Picea abies*) in trifluoromethanesulfonic acid. *Russ. J. Bioorg. Chem.* **2012**, *38*, 717–719.
- (147) Sturgeon, M. R.; Kim, S.; Lawrence, K.; Paton, R. S.; Chmely, S. C.; Nimlos, M.; Foust, T. D.; Beckham, G. T. A Mechanistic Investigation of Acid-Catalyzed Cleavage of Aryl-Ether Linkages: Implications for Lignin Depolymerization in Acidic Environments. *ACS Sustainable Chem. Eng.* **2014**, *2*, 472–485.
- (148) Lin, L.; Nakagame, S.; Yao, Y.; Yoshioka, M.; Shiraishi, N. Liquefaction Mechanism of b-O-4 Lignin Model Compound in the Presence of Phenol under Acid Catalysis: Part 2. Reaction Behavior and Pathways. *Holzforchung* **2001**, *55*, 625–630.
- (149) Lin, L. Z.; Yao, Y. G.; Yoshioka, M.; Shiraishi, N. Liquefaction mechanism of lignin in the presence of phenol at elevated temperature



without catalysts-Studies on beta-O-4 model compound. 1. Structural characterization of the reaction products. *Holzforschung* **1997**, *51*, 316–324.

(150) Varga, T. R.; Fazekas, Z.; Ikeda, Y.; Tomiyasu, H. Cleavage of diphenylether with boron trifluoride under supercritical conditions. *J. Supercrit. Fluids* **2002**, *23*, 163–167.

(151) Vuori, A.; Niemela, M. Liquefaction of Kraft Lignin 0.2. Reactions with a Homogeneous Lewis Acid Catalyst under Mild Reaction Conditions. *Holzforschung* **1988**, *42*, 327–334.

(152) Yang, L.; Li, Y.; Savage, P. E. Hydrolytic Cleavage of C-O Linkages in Lignin Model Compounds Catalyzed by Water-Tolerant Lewis Acids. *Ind. Eng. Chem. Res.* **2014**, *53*, 2633–2639.

(153) Creary, X.; Willis, E. D.; Gagnon, M. Carbocation-forming reactions in ionic liquids. *J. Am. Chem. Soc.* **2005**, *127*, 18114–18120.

(154) Zhao, D.; Wu, M.; Kou, Y.; Min, E. Ionic liquids: applications in catalysis. *Catal. Today* **2002**, *74*, 157–189.

(155) Li, C. Z.; Wang, Q.; Zhao, Z. K. Acid in ionic liquid: An efficient system for hydrolysis of lignocellulose. *Green Chem.* **2008**, *10*, 177–182.

(156) Mohan, D.; Pittman, C. U.; Steele, P. H. Pyrolysis of wood/biomass for bio-oil: A critical review. *Energy Fuels* **2006**, *20*, 848–889.

(157) Goyal, H. B.; Seal, D.; Saxena, R. C. Bio-Fuels from Thermochemical Conversion of Renewable Resources: A Review. *Renewable Sustainable Energy Rev.* **2008**, *12*, 504–517.

(158) Wright, M. M.; Daugaard, D. E.; Satrio, J. A.; Brown, R. C. Techno-Economic Analysis of Biomass Fast Pyrolysis to Transportation Fuels. *Fuel* **2010**, *89*, S2–S10.

(159) Windt, M.; Meier, D.; Marsman, J. H.; Heeres, H. J.; de Koning, S. Micro-pyrolysis of technical lignins in a new modular rig and product analysis by GC-MS/FID and GC x GC-TOFMS/FID. *J. Anal. Appl. Pyrolysis* **2009**, *85*, 38–46.

(160) Kosa, M.; Ben, H.; Theliander, H.; Ragauskas, A. J. Pyrolysis oils from CO<sub>2</sub> precipitated Kraft lignin. *Green Chem.* **2011**, *13*, 3196–3202.

(161) Mendu, V.; Harman-Ware, A. E.; Crocker, M.; Jae, J.; Stork, J.; Morton, S.; Placido, A.; Huber, G.; DeBolt, S. Identification and thermochemical analysis of high-lignin feedstocks for biofuel and biochemical production. *Biotechnol. Biofuels* **2011**, *4*, 43.

(162) Zhang, M.; Resende, F. L. P.; Moutsoglou, A.; Raynie, D. E. Pyrolysis of lignin extracted from prairie cordgrass, aspen, and Kraft lignin by Py-GC/MS and TGA/FTIR. *J. Anal. Appl. Pyrolysis* **2012**, *98*, 65–71.

(163) Gardner, D. J.; Schultz, T. P.; McGinnis, G. D. The Pyrolytic Behavior of Selected Lignin Preparations. *J. Wood Chem. Technol.* **1985**, *5*, 85.

(164) Cho, J.; Chu, S.; Dauenhauer, P. J.; Huber, G. W. Kinetics and reaction chemistry for slow pyrolysis of enzymatic hydrolysis lignin and organosolv extracted lignin derived from maplewood. *Green Chem.* **2012**, *14*, 428–439.

(165) Jiang, G.; Nowakowski, D. J.; Bridgwater, A. V. Effect of the Temperature on the Composition of Lignin Pyrolysis Products. *Energy Fuels* **2010**, *24*, 4470–4475.

(166) Klein, M. T.; Virk, P. S. Model Pathways in Lignin Thermolysis 0.1. Phenethyl Phenyl Ether. *Ind. Eng. Chem. Fundam.* **1983**, *22*, 35–45.

(167) Britt, P. F.; Buchanan, A. C.; Thomas, K. B.; Lee, S. K. Pyrolysis Mechanisms of Lignin-Surface-Immobilized Model-Compound Investigation of Acid-Catalyzed and Free-Radical Reaction Pathways. *J. Anal. Appl. Pyrolysis* **1995**, *33*, 1–19.

(168) Chu, S.; Subrahmanyam, A. V.; Huber, G. W. The pyrolysis chemistry of a beta-O-4 type oligomeric lignin model compound. *Green Chem.* **2013**, *15*, 125–136.

(169) Mullen, C. A.; Boateng, A. A. Catalytic pyrolysis-GC/MS of lignin from several sources. *Fuel Process. Technol.* **2010**, *91*, 1446–1458.

(170) Evans, R. J.; Milne, T. A.; Soltys, M. N. Direct mass-spectrometric studies of the pyrolysis of carbonaceous fuels: III. Primary pyrolysis of lignin. *J. Anal. Appl. Pyrolysis* **1986**, *9*, 207–236.

(171) Kotake, T.; Kawamoto, H.; Saka, S. Mechanisms for the formation of monomers and oligomers during the pyrolysis of a softwood lignin. *J. Anal. Appl. Pyrolysis* **2014**, *105*, 309–316.

(172) Custodis, V. B. F.; Hemberger, P.; Ma, Z. Q.; van Bokhoven, J. A. Mechanism of Fast Pyrolysis of Lignin: Studying Model Compounds. *J. Phys. Chem. B* **2014**, *118*, 8524–8531.

(173) Huang, X. Y.; Cheng, D. G.; Chen, F. Q.; Zhan, X. L. A Density Functional Theory Study on Pyrolysis Mechanism of Lignin in Hydrogen Plasma. *Ind. Eng. Chem. Res.* **2013**, *52*, 14107–14115.

(174) Beste, A.; Buchanan, A. C. Role of Carbon-Carbon Phenyl Migration in the Pyrolysis Mechanism of beta-O-4 Lignin Model Compounds: Phenethyl Phenyl Ether and alpha-Hydroxy Phenethyl Phenyl Ether. *J. Phys. Chem. A* **2012**, *116*, 12242–12248.

(175) Cai, J. M.; Wu, W. X.; Liu, R. H.; Huber, G. W. A distributed activation energy model for the pyrolysis of lignocellulosic biomass. *Green Chem.* **2013**, *15*, 1331–1340.

(176) Jiang, G.; Nowakowski, D. J.; Bridgwater, A. V. A systematic study of the kinetics of lignin pyrolysis. *Thermochim. Acta* **2010**, *498*, 61–66.

(177) Liu, Q.; Wang, S.; Zheng, Y.; Luo, Z.; Cen, K. Mechanism study of wood lignin pyrolysis by using TG–FTIR analysis. *J. Anal. Appl. Pyrolysis* **2008**, *82*, 170–177.

(178) Asmadi, M.; Kawamoto, H.; Saka, S. Thermal reactivities of catechols/pyrogallols and cresols/xlenols as lignin pyrolysis intermediates. *J. Anal. Appl. Pyrolysis* **2011**, *92*, 76–87.

(179) Ramiah, M. V. Thermogravimetric and differential thermal analysis of cellulose, hemicellulose, and lignin. *J. Appl. Polym. Sci.* **1970**, *14*, 1323–1337.

(180) Chan, R. W.; Krieger, B. B. Kinetics of dielectric-loss microwave degradation of polymers: Lignin. *J. Appl. Polym. Sci.* **1981**, *26*, 1533–1553.

(181) Nunn, T. R.; Howard, J. B.; Longwell, J. P.; Peters, W. A. Product compositions and kinetics in the rapid pyrolysis of milled wood lignin. *Ind. Eng. Chem. Process Des. Dev.* **1985**, *24*, 844–852.

(182) Ferdous, D.; Dalai, A. K.; Bej, S. K.; Thring, R. W. Pyrolysis of lignins: Experimental and kinetics studies. *Energy Fuels* **2002**, *16*, 1405–1412.

(183) Avni, E.; Coughlin, R. W. Kinetic analysis of lignin pyrolysis using non-isothermal TGA data. *Thermochim. Acta* **1985**, *90*, 157–167.

(184) Pasquali, L. C. E.; Herrera, H. Pyrolysis of lignin and IR analysis of residues. *Thermochim. Acta* **1997**, *293*, 39–46.

(185) Rao, T. R.; Sharma, A. Pyrolysis rates of biomass materials. *Energy* **1998**, *23*, 973–978.

(186) Dominguez, J. C.; Oliet, M.; Alonso, M. V.; Gilarranz, M. A.; Rodriguez, F. Thermal stability and pyrolysis kinetics of organosolv lignins obtained from Eucalyptus globulus. *Ind. Crops Prod.* **2008**, *27*, 150–156.

(187) Svenson, J.; Pettersson, J. B. C.; Davidsson, K. O. Fast pyrolysis of the main components of birch wood. *Combust. Sci. Technol.* **2004**, *176*, 977–990.

(188) Guo, Y.; Wu, S.; Wang, S.; Guo, X. Thermogravimetric Analysis of Pyrolysis Characteristics of Alkali Lignin. *Trans. China Pulp Paper* **2007**, *22*, 31–34.

(189) Murugan, P.; Mahinpey, N.; Johnson, K. E.; Wilson, M. Kinetics of the Pyrolysis of Lignin Using Thermogravimetric and Differential Scanning Calorimetry Methods. *Energy Fuels* **2008**, *22*, 2720–2724.

(190) Wang, G.; Li, W.; Li, B.; Chen, H. TG study on pyrolysis of biomass and its three components under syngas. *Fuel* **2008**, *87*, 552–558.

(191) Mani, T.; Murugan, P.; Mahinpey, N. Determination of Distributed Activation Energy Model Kinetic Parameters Using Simulated Annealing Optimization Method for Nonisothermal Pyrolysis of Lignin. *Ind. Eng. Chem. Res.* **2009**, *48*, 1464–1467.

(192) Zhou, S.; Pecha, B.; van Kuppevelt, M.; McDonald, A. G.; Garcia-Perez, M. Slow and fast pyrolysis of Douglas-fir lignin: Importance of liquid-intermediate formation on the distribution of products. *Biomass Bioenergy* **2014**, *66*, 398–409.

- (193) Kibet, J.; Khachatryan, L.; Dellinger, B. Molecular Products and Radicals from Pyrolysis of Lignin. *Environ. Sci. Technol.* **2012**, *46*, 12994–13001.
- (194) Thring, R. W.; Chornet, E.; Overend, R. P.; Heitz, M. *Lignin properties and materials*; American Chemical Society: Washington, DC, 1989; pp 228–244.
- (195) Ye, Y.; Fan, J.; Chang, J. Effect of reaction conditions on hydrothermal degradation of cornstalk lignin. *J. Anal. Appl. Pyrolysis* **2012**, *94*, 190–195.
- (196) Xu, J.; Jiang, J.; Hse, C.; Shupe, T. F. Renewable chemical feedstocks from integrated liquefaction processing of lignocellulosic materials using microwave energy. *Green Chem.* **2012**, *14*, 2821–2830.
- (197) Lu, Q.; Zhang, Y.; Tang, Z.; Li, W. Z.; Zhu, X. F. Catalytic upgrading of biomass fast pyrolysis vapors with titania and zirconia/titania based catalysts. *Fuel* **2010**, *89*, 2096–2103.
- (198) Neumann, G. T.; Hicks, J. C. Novel Hierarchical Cerium-Incorporated MFI Zeolite Catalysts for the Catalytic Fast Pyrolysis of Lignocellulosic Biomass. *ACS Catal.* **2012**, *2*, 642–646.
- (199) Pattiya, A.; Titiloye, J. O.; Bridgwater, A. V. Fast pyrolysis of cassava rhizome in the presence of catalysts. *J. Anal. Appl. Pyrolysis* **2008**, *81*, 72–79.
- (200) Li, X.; Su, L.; Wang, Y.; Yu, Y.; Wang, C.; Li, X.; Wang, Z. Catalytic fast pyrolysis of Kraft lignin with HZSM-5 zeolite for producing aromatic hydrocarbons. *Front. Environ. Sci. Eng.* **2012**, *6*, 295–303.
- (201) Ma, Z.; Troussard, E.; van Bokhoven, J. A. Controlling the selectivity to chemicals from lignin via catalytic fast pyrolysis. *Appl. Catal., A* **2012**, *423–424*, 130–136.
- (202) Ma, Z.; van Bokhoven, J. A. Deactivation and Regeneration of H-USY Zeolite during Lignin Catalytic Fast Pyrolysis. *ChemCatChem* **2012**, *4*, 2036–2044.
- (203) Ivanov, D. P.; Sobolev, V. I.; Panov, G. I. Deactivation by coking and regeneration of zeolite catalysts for benzene-to-phenol oxidation. *Appl. Catal., A* **2003**, *241*, 113–121.
- (204) Marcilla, A.; n, M. I. B.; Navarro, R. Application of TG/FTIR to the study of the regeneration process of husy and HZSM5 zeolites. *J. Therm. Anal. Calorim.* **2007**, *87*, 325–330.
- (205) Hicks, J. C. Advances in C–O Bond Transformations in Lignin-Derived Compounds for Biofuels Production. *J. Phys. Chem. Lett.* **2011**, 2280–2287.
- (206) Ravenelle, R. M.; Schussler, F.; D'Amico, A.; Danilina, N.; van Bokhoven, J. A.; Lercher, J. A.; Jones, C. W.; Sievers, C. Stability of Zeolites in Hot Liquid Water. *J. Phys. Chem. C* **2010**, *114*, 19582–19595.
- (207) Amen-Chen, C.; Pakdel, H.; Roy, C. Production of monomeric phenols by thermochemical conversion of biomass: a review. *Bioresour. Technol.* **2001**, *79*, 277–299.
- (208) Shen, D. K.; Gu, S.; Luo, K. H.; Wang, S. R.; Fang, M. X. The pyrolytic degradation of wood-derived lignin from pulping process. *Bioresour. Technol.* **2010**, *101*, 6136–6146.
- (209) Zhao, Y.; Deng, L.; Liao, B.; Fu, Y.; Guo, Q.-X. Aromatics Production via Catalytic Pyrolysis of Pyrolytic Lignins from Bio-Oil. *Energy Fuels* **2010**, *24*, 5735–5740.
- (210) Zaror, C. A.; Hutchings, C.; Leo, P.; Stiles, H. N.; Kandiyoti, R. Secondary char formation in the catalytic pyrolysis of biomass. *Fuel* **1985**, *64*, 990–994.
- (211) Patwardhan, P. R.; Brown, R. C.; Shanks, B. H. Understanding the Fast Pyrolysis of Lignin. *ChemSusChem* **2011**, *4*, 1629–1636.
- (212) Guo, D. L.; Yuan, H. Y.; Yin, X. L.; Wu, C. Z.; Wu, S. B.; Zhou, Z. Q. Effects of chemical form of sodium on the product characteristics of alkali lignin pyrolysis. *Bioresour. Technol.* **2014**, *152*, 147–153.
- (213) Jakab, E.; Faix, O.; Till, F.; Szekely, T. The effect of cations on the thermal decomposition of lignins. *J. Anal. Appl. Pyrolysis* **1993**, *25*, 185–194.
- (214) Jones, S.; Zhu, Y. *Preliminary economics for the production of pyrolysis oil from lignin in a cellulosic ethanol biorefinery*; Pacific Northwest National Laboratory: Richland, 2009; pp 1–32.
- (215) Vispute, T. P.; Zhang, H.; Sanna, A.; Xiao, R.; Huber, G. W. Renewable Chemical Commodity Feedstocks from Integrated Catalytic Processing of Pyrolysis Oils. *Science* **2010**, *330*, 1222–1227.
- (216) Pollard, A. S.; Rover, M. R.; Brown, R. C. Characterization of bio-oil recovered as stage fractions with unique chemical and physical properties. *J. Anal. Appl. Pyrolysis* **2012**, *93*, 129–138.
- (217) Meier, D.; van de Beld, B.; Bridgwater, A. V.; Elliott, D. C.; Oasmaa, A.; Preto, F. State-of-the-art of fast pyrolysis in IEA bioenergy member countries. *Renewable Sustainable Energy Rev.* **2013**, *20*, 619–641.
- (218) Greenhalf, C. E.; Nowakowski, D. J.; Harms, A. B.; Titiloye, J. O.; Bridgwater, A. V. A comparative study of straw, perennial grasses and hardwoods in terms of fast pyrolysis products. *Fuel* **2013**, *108*, 216–230.
- (219) KiOR website: <http://www.kior.com/>.
- (220) Mukkamala, S.; Wheeler, M. C.; van Heiningen, A. R. P.; DeSisto, W. J. Formate-Assisted Fast Pyrolysis of Lignin. *Energy Fuels* **2012**, *26*, 1380–1384.
- (221) Kleinert, M.; Barth, T. Towards a lignocellulosic biorefinery: Direct one-step conversion of lignin to hydrogen-enriched biofuel. *Energy Fuels* **2008**, *22*, 1371–1379.
- (222) Kleinert, M.; Gasson, J. R.; Eide, I.; Hilmen, A. M.; Barth, T. Developing solvolytic conversion of lignin-to-liquid (LtL) fuel components: Optimization of quality and process factors. *Cellul. Chem. Technol.* **2011**, *45*, 3–12.
- (223) Tyrone Ghampson, I.; Sepúlveda, C.; Garcia, R.; García Fierro, J. L.; Escalona, N.; DeSisto, W. J. Comparison of alumina- and SBA-15-supported molybdenum nitride catalysts for hydrodeoxygenation of guaiacol. *Appl. Catal., A* **2012**, *435–436*, 51–60.
- (224) Barta, K.; Warner, G. R.; Beach, E. S.; Anastas, P. T. Depolymerization of organosolv lignin to aromatic compounds over Cu-doped porous metal oxides. *Green Chem.* **2014**, *16*, 191–196.
- (225) Warner, G.; Hansen, T. S.; Riisager, A.; Beach, E. S.; Barta, K.; Anastas, P. T. Depolymerization of organosolv lignin using doped porous metal oxides in supercritical methanol. *Bioresour. Technol.* **2014**, *161*, 78–83.
- (226) Pepper, J. M.; Hibbert, H. Studies on Lignin and Related Compounds. LXXXVII. High Pressure Hydrogenation of Maple Wood. *J. Am. Chem. Soc.* **1948**, *70*, 67–71.
- (227) Wenkert, E.; Michelotti, E. L.; Swindell, C. S. Nickel-induced conversion of carbon-oxygen into carbon-carbon bonds. One-step transformations of enol ethers into olefins and aryl ethers into biaryls. *J. Am. Chem. Soc.* **1979**, *101*, 2246–2247.
- (228) Sergeev, A. G.; Webb, J. D.; Hartwig, J. F. A Heterogeneous Nickel Catalyst for the Hydrogenolysis of Aryl Ethers without Arene Hydrogenation. *J. Am. Chem. Soc.* **2012**, *134*, 20226–20229.
- (229) He, J.; Zhao, C.; Lercher, J. A. Ni-Catalyzed Cleavage of Aryl Ethers in the Aqueous Phase. *J. Am. Chem. Soc.* **2012**, *134*, 20768–20775.
- (230) Song, Q.; Cai, J. Y.; Zhang, J. J.; Yu, W. Q.; Wang, F.; Xu, J. Hydrogenation and cleavage of the C–O bonds in the lignin model compound phenethyl phenyl ether over a nickel-based catalyst. *Chin. J. Catal.* **2013**, *34*, 651–658.
- (231) Song, Q.; Wang, F.; Xu, J. Hydrogenolysis of lignosulfonate into phenols over heterogeneous nickel catalysts. *Chem. Commun.* **2012**, *48*, 7019–7021.
- (232) Kelley, P.; Lin, S.; Edouard, G.; Day, M. W.; Agapie, T. Nickel-Mediated Hydrogenolysis of C–O Bonds of Aryl Ethers: What Is the Source of the Hydrogen? *J. Am. Chem. Soc.* **2012**, *134*, 5480–5483.
- (233) Song, Q.; Wang, F.; Xu, J.; Cai, J.; Zhang, J.; Wang, Y.; Yu, W. Lignin depolymerization (LDP) in alcohol over nickel-based catalysts via a fragmentation-hydrogenolysis process. *Energy Environ. Sci.* **2013**, *6*, 994–1007.
- (234) Tilly, D.; Chevallier, F.; Mongin, F.; Gros, P. C. Bimetallic Combinations for Dehalogenative Metalation Involving Organic Compounds. *Chem. Rev.* **2014**, *114*, 1207–1257.
- (235) Ji, N.; Zhang, T.; Zheng, M. Y.; Wang, A. Q.; Wang, H.; Wang, X. D.; Chen, J. G. G. Direct Catalytic Conversion of Cellulose into



Ethylene Glycol Using Nickel-Promoted Tungsten Carbide Catalysts. *Angew. Chem., Int. Ed.* **2008**, *47*, 8510–8513.

(236) Wang, A. Q.; Zhang, T. One-Pot Conversion of Cellulose to Ethylene Glycol with Multifunctional Tungsten-Based Catalysts. *Acc. Chem. Res.* **2013**, *46*, 1377–1386.

(237) Zheng, M. Y.; Pang, J. F.; Wang, A. Q.; Zhang, T. One-pot catalytic conversion of cellulose to ethylene glycol and other chemicals: From fundamental discovery to potential commercialization. *Chin. J. Catal.* **2014**, *35*, 602–613.

(238) Li, C. Z.; Zheng, M. Y.; Wang, A. Q.; Zhang, T. One-pot catalytic hydrocracking of raw woody biomass into chemicals over supported carbide catalysts: simultaneous conversion of cellulose, hemicellulose and lignin. *Energy Environ. Sci.* **2012**, *5*, 6383–6390.

(239) Molinari, V.; Giordano, C.; Antonietti, M.; Esposito, D. Titanium Nitride-Nickel Nanocomposite as Heterogeneous Catalyst for the Hydrogenolysis of Aryl Ethers. *J. Am. Chem. Soc.* **2014**, *136*, 1758–1761.

(240) Zhang, J. G.; Asakura, H.; van Rijn, J.; Yang, J.; Duchesne, P.; Zhang, B.; Chen, X.; Zhang, P.; Saeys, M.; Yan, N. Highly efficient, NiAu-catalyzed hydrogenolysis of lignin into phenolic chemicals. *Green Chem.* **2014**, *16*, 2432–2437.

(241) Zhang, J. G.; Teo, J.; Chen, X.; Asakura, H.; Tanaka, T.; Teramura, K.; Yan, N. A Series of NiM (M = Ru, Rh, and Pd) Bimetallic Catalysts for Effective Lignin Hydrogenolysis in Water. *ACS Catal.* **2014**, *4*, 1574–1583.

(242) Wang, X.; Rinaldi, R. Solvent Effects on the Hydrogenolysis of Diphenyl Ether with Raney Nickel and their Implications for the Conversion of Lignin. *ChemSusChem* **2012**, *5*, 1455–1466.

(243) Toledano, A.; Serrano, L.; Pineda, A.; Romero, A. A.; Luque, R.; Labidi, J. Microwave-assisted depolymerisation of organosolv lignin via mild hydrogen-free hydrogenolysis: Catalyst screening. *Appl. Catal., B* **2014**, *145*, 43–55.

(244) Torr, K. M.; van de Pas, D. J.; Cazeils, E.; Suckling, I. D. Mild hydrogenolysis of in-situ and isolated *Pinus radiata* lignins. *Bioresour. Technol.* **2011**, *102*, 7608–7611.

(245) Ye, Y.; Zhang, Y.; Fan, J.; Chang, J. Selective production of 4-ethylphenolics from lignin via mild hydrogenolysis. *Bioresour. Technol.* **2012**, *118*, 648–651.

(246) Bouxin, F. P.; McVeigh, A.; Tran, F.; Westwood, N. J.; Jarvis, M. C.; Jackson, S. D. Catalytic depolymerisation of isolated lignins to fine chemicals using a Pt/alumina catalyst: part 1-impact of the lignin structure. *Green Chem.* **2015**, *17*, 1235–1242.

(247) Parsell, T. H.; Owen, B. C.; Klein, L.; Jarrell, T. M.; Marcum, C. L.; Hauptert, L. J.; Amundson, L. M.; Kenttamaa, H. I.; Ribeiro, F.; Miller, J. T.; Abu-Omar, M. M. Cleavage and hydrodeoxygenation (HDO) of C-O bonds relevant to lignin conversion using Pd/Zn synergistic catalysis. *Chem. Sci.* **2013**, *4*, 806–813.

(248) Yan, N.; Zhao, C.; Dyson, P. J.; Wang, C.; Liu, L. t.; Kou, Y. Selective Degradation of Wood Lignin over Noble-Metal Catalysts in a Two-Step Process. *ChemSusChem* **2008**, *1*, 626–629.

(249) Liguori, L.; Barth, T. Palladium-Nafion SAC-13 catalyzed depolymerisation of lignin to phenols in formic acid and water. *J. Anal. Appl. Pyrolysis* **2011**, *92*, 477–484.

(250) Nagy, M.; David, K.; Britovsek, G. J. P.; Ragauskas, A. J. Catalytic hydrogenolysis of ethanol organosolv lignin. *Holzforschung* **2009**, *63*, 513–520.

(251) Atesin, A. C.; Ray, N. A.; Stair, P. C.; Marks, T. J. Etheric C-O Bond Hydrogenolysis Using a Tandem Lanthanide Triflate/Supported Palladium Nanoparticle Catalyst System. *J. Am. Chem. Soc.* **2012**, *134*, 14682–14685.

(252) Li, Z.; Assary, R. S.; Atesin, A. C.; Curtiss, L. A.; Marks, T. J. Rapid Ether and Alcohol C-O Bond Hydrogenolysis Catalyzed by Tandem High-Valent Metal Triflate plus Supported Pd Catalysts. *J. Am. Chem. Soc.* **2014**, *136*, 104–107.

(253) Nichols, J. M.; Bishop, L. M.; Bergman, R. G.; Ellman, J. A. Catalytic C-O Bond Cleavage of 2-Aryloxy-1-arylethanol and Its Application to the Depolymerization of Lignin-Related Polymers. *J. Am. Chem. Soc.* **2010**, *132*, 12554–12555.

(254) Wu, A.; Patrick, B. O.; Chung, E.; James, B. R. Hydrogenolysis of beta-O-4 lignin model dimers by a ruthenium-xantphos catalyst. *Dalton Trans.* **2012**, *41*, 11093–11106.

(255) Saidi, M.; Samimi, F.; Karimipourfard, D.; Nimmanwudipong, T.; Gates, B. C.; Rahimpour, M. R. Upgrading of lignin-derived bio-oils by catalytic hydrodeoxygenation. *Energy Environ. Sci.* **2014**, *7*, 103–129.

(256) Chum, H. L.; Johnson, D. K. *Liquid fuels from lignins: Annual Report*; National Renewable Energy Laboratory (NREL): Golden, CO, 1986.

(257) Prasomsri, T.; Shetty, M.; Murugappan, K.; Roman-Leshkov, Y. Insights into the catalytic activity and surface modification of MoO<sub>3</sub> during the hydrodeoxygenation of lignin-derived model compounds into aromatic hydrocarbons under low hydrogen pressures. *Energy Environ. Sci.* **2014**, *7*, 2660–2669.

(258) Lee, W. S.; Wang, Z. S.; Wu, R. J.; Bhan, A. Selective vapor-phase hydrodeoxygenation of anisole to benzene on molybdenum carbide catalysts. *J. Catal.* **2014**, *319*, 44–53.

(259) Ghampson, I. T.; Sepúlveda, C.; Garcia, R.; Radovic, L. R.; Fierro, J. L. G.; DeSisto, W. J.; Escalona, N. Hydrodeoxygenation of guaiacol over carbon-supported molybdenum nitride catalysts: Effects of nitriding methods and support properties. *Appl. Catal., A* **2012**, *439–440*, 111–124.

(260) Ruiz, P. E.; Frederick, B. G.; De Sisto, W. J.; Austin, R. N.; Radovic, L. R.; Leiva, K.; García, R.; Escalona, N.; Wheeler, M. C. Guaiacol hydrodeoxygenation on MoS<sub>2</sub> catalysts: Influence of activated carbon supports. *Catal. Commun.* **2012**, *27*, 44–48.

(261) Whiffen, V. M. L.; Smith, K. J. Hydrodeoxygenation of 4-Methylphenol over Unsupported MoP, MoS<sub>2</sub>, and MoO<sub>x</sub> Catalysts. *Energy Fuels* **2010**, *24*, 4728–4737.

(262) Ratcliff, M.; Posey, F.; Chum, H. L. Catalytic hydrodeoxygenation and dealkylation of a lignin model Compound. *Prepr. Pap., Am. Chem. Soc., Div. Fuel Chem.* **1987**, *32*, 249–256.

(263) Ghampson, I. T.; Sepúlveda, C.; Garcia, R.; Frederick, B. G.; Wheeler, M. C.; Escalona, N.; DeSisto, W. J. Guaiacol transformation over unsupported molybdenum-based nitride catalysts. *Appl. Catal., A* **2012**, *413–414*, 78–84.

(264) Zhao, H. Y.; Li, D.; Bui, P.; Oyama, S. T. Hydrodeoxygenation of guaiacol as model compound for pyrolysis oil on transition metal phosphide hydroprocessing catalysts. *Appl. Catal., A* **2011**, *391*, 305–310.

(265) Ding, L. N.; Wang, A. Q.; Zheng, M. Y.; Zhang, T. Selective Transformation of Cellulose into Sorbitol by Using a Bifunctional Nickel Phosphide Catalyst. *ChemSusChem* **2010**, *3*, 818–821.

(266) Zhao, G. H.; Zheng, M. Y.; Wang, A. Q.; Zhang, T. Catalytic Conversion of Cellulose to Ethylene Glycol over Tungsten Phosphide Catalysts. *Chin. J. Catal.* **2010**, *31*, 928–932.

(267) Ma, X. L.; Tian, Y.; Hao, W. Y.; Ma, R.; Li, Y. D. Production of phenols from catalytic conversion of lignin over a tungsten phosphide catalyst. *Appl. Catal., A* **2014**, *481*, 64–70.

(268) Bui, P.; Cecilia, J. A.; Oyama, S. T.; Takagaki, A.; Infantes-Molina, A.; Zhao, H.; Li, D.; Rodríguez-Castellón, E.; Jiménez López, A. Studies of the synthesis of transition metal phosphides and their activity in the hydrodeoxygenation of a biofuel model compound. *J. Catal.* **2012**, *294*, 184–198.

(269) Ji, N.; Wang, X.; Weidenthaler, C.; Spliethoff, B.; Rinaldi, R. Iron(II) Disulfides as Precursors of Highly Selective Catalysts for Hydrodeoxygenation of Dibenzyl Ether into Toluene. *ChemCatChem* **2015**, *7*, 960–966.

(270) Bykova, M. V.; Ermakov, D. Y.; Kaichev, V. V.; Bulavchenko, O. A.; Saraev, A. A.; Lebedev, M. Y.; Yakovlev, V. A. Ni-based sol-gel catalysts as promising systems for crude bio-oil upgrading: Guaiacol hydrodeoxygenation study. *Appl. Catal., B* **2012**, *113–114*, 296–307.

(271) De Rogatis, L.; Montini, T.; Cognigni, A.; Olivieri, L.; Fornasiero, P. Methane partial oxidation on NiCu-based catalysts. *Catal. Today* **2009**, *145*, 176–185.

(272) Lee, J.-H.; Lee, E.-G.; Joo, O.-S.; Jung, K.-D. Stabilization of Ni/Al<sub>2</sub>O<sub>3</sub> catalyst by Cu addition for CO<sub>2</sub> reforming of methane. *Appl. Catal., A* **2004**, *269*, 1–6.

- (273) Deutsch, K. L.; Shanks, B. H. Hydrodeoxygenation of lignin model compounds over a copper chromite catalyst. *Appl. Catal., A* **2012**, *447–448*, 144–150.
- (274) Oasmaa, A.; Alen, R.; Meier, D. Catalytic Hydrotreatment of Some Technical Lignins. *Bioresour. Technol.* **1993**, *45*, 189–194.
- (275) Ma, R.; Hao, W. Y.; Ma, X. L.; Tian, Y.; Li, Y. D. Catalytic Ethanolysis of Kraft Lignin into High-Value Small-Molecular Chemicals over a Nanostructured alpha-Molybdenum Carbide Catalyst. *Angew. Chem., Int. Ed.* **2014**, *53*, 7310–7315.
- (276) Ardiyanti, A. R.; Gutierrez, A.; Honkela, M. L.; Krause, A. O. I.; Heeres, H. J. Hydrotreatment of wood-based pyrolysis oil using zirconia-supported mono- and bimetallic (Pt, Pd, Rh) catalysts. *Appl. Catal., A* **2011**, *407*, 56–66.
- (277) Lin, Y.-C.; Li, C.-L.; Wan, H.-P.; Lee, H.-T.; Liu, C.-F. Catalytic Hydrodeoxygenation of Guaiacol on Rh-Based and Sulfided CoMo and NiMo Catalysts. *Energy Fuels* **2011**, *25*, 890–896.
- (278) Nimmanwudipong, T.; Runnebaum, R. C.; Block, D. E.; Gates, B. C. Catalytic Conversion of Guaiacol Catalyzed by Platinum Supported on Alumina: Reaction Network Including Hydrodeoxygenation Reactions. *Energy Fuels* **2011**, *25*, 3417–3427.
- (279) Xu, X.; Li, Y.; Gong, Y.; Zhang, P.; Li, H.; Wang, Y. Synthesis of Palladium Nanoparticles Supported on Mesoporous N-Doped Carbon and Their Catalytic Ability for Biofuel Upgrade. *J. Am. Chem. Soc.* **2012**, *134*, 16987–16990.
- (280) Gonzalez-Borja, M. A.; Resasco, D. E. Anisole and Guaiacol Hydrodeoxygenation over Monolithic Pt-Sn Catalysts. *Energy Fuels* **2011**, *25*, 4155–4162.
- (281) Feng, B.; Kobayashi, H.; Ohta, H.; Fukuoka, A. Aqueous-phase hydrodeoxygenation of 4-propylphenol as a lignin model to n-propylbenzene over Re-Ni/ZrO<sub>2</sub> catalysts. *J. Mol. Catal. A: Chem.* **2014**, *388*, 41–46.
- (282) Ohta, H.; Feng, B.; Kobayashi, H.; Hara, K.; Fukuoka, A. Selective hydrodeoxygenation of lignin-related 4-propylphenol into n-propylbenzene in water by Pt-Re/ZrO<sub>2</sub> catalysts. *Catal. Today* **2014**, *234*, 139–144.
- (283) Jongerius, A. L.; Jastrzebski, R.; Bruijninx, P. C. A.; Weckhuysen, B. M. CoMo sulfide-catalyzed hydrodeoxygenation of lignin model compounds: An extended reaction network for the conversion of monomeric and dimeric substrates. *J. Catal.* **2012**, *285*, 315–323.
- (284) Bui, V. N.; Laurenti, D.; Delichere, P.; Geantet, C. Hydrodeoxygenation of guaiacol Part II: Support effect for CoMo catalysts on HDO activity and selectivity. *Appl. Catal., B* **2011**, *101*, 246–255.
- (285) Romero, Y.; Richard, F.; Brunet, S. Hydrodeoxygenation of 2-ethylphenol as a model compound of bio-crude over sulfided Mo-based catalysts: Promoting effect and reaction mechanism. *Appl. Catal., B* **2010**, *98*, 213–223.
- (286) Bui, V. N.; Laurenti, D.; Afanasiev, P.; Geantet, C. Hydrodeoxygenation of guaiacol with CoMo catalysts. Part I: Promoting effect of cobalt on HDO selectivity and activity. *Appl. Catal., B* **2011**, *101*, 239–245.
- (287) Romero, Y.; Richard, F.; Renème, Y.; Brunet, S. Hydrodeoxygenation of benzofuran and its oxygenated derivatives (2,3-dihydrobenzofuran and 2-ethylphenol) over NiMoP/Al<sub>2</sub>O<sub>3</sub> catalyst. *Appl. Catal., A* **2009**, *353*, 46–53.
- (288) Popov, A.; Kondratieva, E.; Gilson, J. P.; Mariey, L.; Travert, A.; Mauge, F. IR study of the interaction of phenol with oxides and sulfided CoMo catalysts for bio-fuel hydrodeoxygenation. *Catal. Today* **2011**, *172*, 132–135.
- (289) Desnoyer, A. N.; Fartel, B.; MacLeod, K. C.; Patrick, B. O.; Smith, K. M. Ambient-Temperature Carbon–Oxygen Bond Cleavage of an  $\alpha$ -Aryloxy Ketone with Cp<sub>2</sub>Ti(BTMSA) and Selective Protonolysis of the Resulting Ti–OR Bonds. *Organometallics* **2012**, *31*, 7625–7628.
- (290) Alonso, D. M.; Wettstein, S. G.; Dumesic, J. A. Bimetallic catalysts for upgrading of biomass to fuels and chemicals. *Chem. Soc. Rev.* **2012**, *41*, 8075–8098.
- (291) Furimsky, E.; Massoth, F. E. Deactivation of hydroprocessing catalysts. *Catal. Today* **1999**, *52*, 381–495.
- (292) Mortensen, P. M.; Grunwaldt, J. D.; Jensen, P. A.; Knudsen, K. G.; Jensen, A. D. A review of catalytic upgrading of bio-oil to engine fuels. *Appl. Catal., A* **2011**, *407*, 1–19.
- (293) Wang, W.; Yang, Y.; Luo, H.; Peng, H.; He, B.; Liu, W. Preparation of Ni(Co)–W–B amorphous catalysts for cyclopentanone hydrodeoxygenation. *Catal. Commun.* **2011**, *12*, 1275–1279.
- (294) Popov, A.; Kondratieva, E.; Mariey, L.; Goupil, J. M.; El Fallah, J.; Gilson, J. P.; Travert, A.; Mauge, F. Bio-oil hydrodeoxygenation: Adsorption of phenolic compounds on sulfided (Co)Mo catalysts. *J. Catal.* **2013**, *297*, 176–186.
- (295) Wang, W.; Yang, Y.; Luo, H.; Liu, W. Effect of additive (Co, La) for Ni–Mo–B amorphous catalyst and its hydrodeoxygenation properties. *Catal. Commun.* **2010**, *11*, 803–807.
- (296) Zhao, C.; Kou, Y.; Lemonidou, A. A.; Li, X. B.; Lercher, J. A. Highly Selective Catalytic Conversion of Phenolic Bio-Oil to Alkanes. *Angew. Chem., Int. Ed.* **2009**, *48*, 3987–3990.
- (297) Guvenatam, B.; Kursun, O.; Heeres, E. H. J.; Pidko, E. A.; Hensen, E. J. M. Hydrodeoxygenation of mono- and dimeric lignin model compounds on noble metal catalysts. *Catal. Today* **2014**, *233*, 83–91.
- (298) Zhang, W.; Chen, J. Z.; Liu, R. L.; Wang, S. P.; Chen, L. M.; Li, K. G. Hydrodeoxygenation of Lignin-Derived Phenolic Monomers and Dimers to Alkane Fuels over Bifunctional Zeolite-Supported Metal Catalysts. *ACS Sustainable Chem. Eng.* **2014**, *2*, 683–691.
- (299) Furimsky, E. Catalytic hydrodeoxygenation. *Appl. Catal., A* **2000**, *199*, 147–190.
- (300) Girgis, M. J.; Gates, B. C. Reactivities, reaction networks, and kinetics in high-pressure catalytic hydroprocessing. *Ind. Eng. Chem. Res.* **1991**, *30*, 2021–2058.
- (301) Zhao, C.; He, J. Y.; Lemonidou, A. A.; Li, X. B.; Lercher, J. A. Aqueous-phase hydrodeoxygenation of bio-derived phenols to cycloalkanes. *J. Catal.* **2011**, *280*, 8–16.
- (302) Yan, N.; Yuan, Y.; Dykeman, R.; Kou, Y.; Dyson, P. J. Hydroxylation of Lignin-Derived Phenols into Alkanes by Using Nanoparticle Catalysts Combined with Brønsted Acidic Ionic Liquids. *Angew. Chem., Int. Ed.* **2010**, *49*, 5549–5553.
- (303) Zhao, C.; Lercher, J. A. Selective Hydrodeoxygenation of Lignin-Derived Phenolic Monomers and Dimers to Cycloalkanes on Pd/C and HZSM-5 Catalysts. *ChemCatChem* **2012**, *4*, 64–68.
- (304) Zhang, X. H.; Zhang, Q.; Chen, L. A.; Xu, Y.; Wang, T. J.; Ma, L. L. Effect of calcination temperature of Ni/SiO<sub>2</sub>-ZrO<sub>2</sub> catalyst on its hydrodeoxygenation of guaiacol. *Chin. J. Catal.* **2014**, *35*, 302–309.
- (305) Zhao, C.; Kou, Y.; Lemonidou, A. A.; Li, X. B.; Lercher, J. A. Hydrodeoxygenation of bio-derived phenols to hydrocarbons using RANEY (R) Ni and Nafion/SiO<sub>2</sub> catalysts. *Chem. Commun.* **2010**, *46*, 412–414.
- (306) Laskar, D. D.; Tucker, M. P.; Chen, X. W.; Helms, G. L.; Yang, B. Noble-metal catalyzed hydrodeoxygenation of biomass-derived lignin to aromatic hydrocarbons. *Green Chem.* **2014**, *16*, 897–910.
- (307) Singh, S. K.; Ekhe, J. D. Towards effective lignin conversion: HZSM-5 catalyzed one-pot solvolytic depolymerization/hydrodeoxygenation of lignin into value added compounds. *RSC Adv.* **2014**, *4*, 27971–27978.
- (308) Li, N.; Huber, G. W. Aqueous-phase hydrodeoxygenation of sorbitol with Pt/SiO<sub>2</sub>-Al<sub>2</sub>O<sub>3</sub>: Identification of reaction intermediates. *J. Catal.* **2010**, *270*, 48–59.
- (309) Zhao, C.; Kasakov, S.; He, J.; Lercher, J. A. Comparison of kinetics, activity and stability of Ni/HZSM-5 and Ni/Al<sub>2</sub>O<sub>3</sub>-HZSM-5 for phenol hydrodeoxygenation. *J. Catal.* **2012**, *296*, 12–23.
- (310) Zhu, X.; Lobban, L. L.; Mallinson, R. G.; Resasco, D. E. Bifunctional transalkylation and hydrodeoxygenation of anisole over a Pt/HBeta catalyst. *J. Catal.* **2011**, *281*, 21–29.
- (311) Song, W. J.; Liu, Y. S.; Barath, E.; Zhao, C.; Lercher, J. A. Synergistic effects of Ni and acid sites for hydrogenation and C–O bond cleavage of substituted phenols. *Green Chem.* **2015**, *17*, 1204–1218.



- (312) Gallezot, P.; Richard, D. Selective hydrogenation of  $\alpha,\beta$ -unsaturated aldehydes. *Catal. Rev.: Sci. Eng.* **1998**, *40*, 81–126.
- (313) Cai, H.; Li, C.; Wang, A.; Zhang, T. Biomass into chemicals: One-pot production of furan-based diols from carbohydrates via tandem reactions. *Catal. Today* **2014**, *234*, 59–65.
- (314) Liu, W.-J.; Zhang, X.-S.; Qy, Y.-C.; Jiang, H.; Yu, H.-Q. Bio-oil upgrading at ambient pressure and temperature using zero valent metals. *Green Chem.* **2012**, *14*, 2226–2233.
- (315) Pang, M.; Liu, C.; Xia, W.; Muhler, M.; Liang, C. Activated carbon supported molybdenum carbides as cheap and highly efficient catalyst in the selective hydrogenation of naphthalene to tetralin. *Green Chem.* **2012**, *14*, 1272–1276.
- (316) Nimmanwudipong, T.; Runnebaum, R. C.; Ebeler, S. E.; Block, D. E.; Gates, B. C. Upgrading of Lignin-Derived Compounds: Reactions of Eugenol Catalyzed by HY Zeolite and by Pt/ $\gamma$ -Al<sub>2</sub>O<sub>3</sub>. *Catal. Lett.* **2012**, *142*, 151–160.
- (317) Ben, H.; Mu, W.; Deng, Y.; Ragauskas, A. J. Production of renewable gasoline from aqueous phase hydrogenation of lignin pyrolysis oil. *Fuel* **2013**, *103*, 1148–1153.
- (318) Anderson, J. A.; Athawale, A.; Imrie, F. E.; McKenna, F. M.; McCue, A.; Molyneux, D.; Power, K.; Shand, M.; Wells, R. P. K. Aqueous phase hydrogenation of substituted phenyls over carbon nanofibre and activated carbon supported Pd. *J. Catal.* **2010**, *270*, 9–15.
- (319) Pérez, Y.; Fajardo, M.; Corma, A. Highly selective palladium supported catalyst for hydrogenation of phenol in aqueous phase. *Catal. Commun.* **2011**, *12*, 1071–1074.
- (320) Li, Z.; Garedew, M.; Lam, C. H.; Jackson, J. E.; Miller, D. J.; Saffron, C. M. Mild electrocatalytic hydrogenation and hydrodeoxygenation of bio-oil derived phenolic compounds using ruthenium supported on activated carbon cloth. *Green Chem.* **2012**, *14*, 2540–2549.
- (321) Lam, C. H.; Lowe, C. B.; Li, Z.; Longe, K. N.; Rayburn, J. T.; Caldwell, M. A.; Houdek, C. E.; Maguire, J. B.; Saffron, C. M.; Miller, D. J.; Jackson, J. E. Electrocatalytic upgrading of model lignin monomers with earth abundant metal electrodes. *Green Chem.* **2015**, *17*, 601–609.
- (322) Xu, W.; Miller, S. J.; Agrawal, P. K.; Jones, C. W. Depolymerization and Hydrodeoxygenation of Switchgrass Lignin with Formic Acid. *ChemSusChem* **2012**, *5*, 667–675.
- (323) Wang, X.; Rinaldi, R. Exploiting H-transfer reactions with RANEY® Ni for upgrade of phenolic and aromatic biorefinery feeds under unusual, low-severity conditions. *Energy Environ. Sci.* **2012**, *5*, 8244–8260.
- (324) Holmelid, B.; Kleinert, M.; Barth, T. Reactivity and reaction pathways in thermochemical treatment of selected lignin-like model compounds under hydrogen rich conditions. *J. Anal. Appl. Pyrolysis* **2012**, *98*, 37–44.
- (325) Wang, X. Y.; Rinaldi, R. A Route for Lignin and Bio-Oil Conversion: Dehydroxylation of Phenols into Arenes by Catalytic Tandem Reactions. *Angew. Chem., Int. Ed.* **2013**, *52*, 11499–11503.
- (326) Grasmann, M.; Laurenczy, G. Formic acid as a hydrogen source - recent developments and future trends. *Energy Environ. Sci.* **2012**, *5*, 8171–8181.
- (327) Zhao, C.; Camaioni, D. M.; Lercher, J. A. Selective catalytic hydroalkylation and deoxygenation of substituted phenols to bicycloalkanes. *J. Catal.* **2012**, *288*, 92–103.
- (328) Al-Sabawi, M.; Chen, J. Hydroprocessing of Biomass-Derived Oils and Their Blends with Petroleum Feedstocks: A Review. *Energy Fuels* **2012**, *26*, 5373–5399.
- (329) Runnebaum, R. C.; Nimmanwudipong, T.; Block, D. E.; Gates, B. C. Pt/ $\gamma$ -Al<sub>2</sub>O<sub>3</sub> Catalytic conversion of compounds representative of lignin-derived bio-oils: a reaction network for guaiacol, anisole, 4-methylanisole, and cyclohexanone conversion catalysed by Pt/ $\gamma$ -Al<sub>2</sub>O<sub>3</sub>. *Catal. Sci. Technol.* **2012**, *2*, 113–118.
- (330) Runnebaum, R. C.; Nimmanwudipong, T.; Limbo, R. R.; Block, D. E.; Gates, B. C. Conversion of 4-Methylanisole Catalyzed by Pt/ $\gamma$ -Al<sub>2</sub>O<sub>3</sub> and by Pt/SiO<sub>2</sub>-Al<sub>2</sub>O<sub>3</sub>: Reaction Networks and Evidence of Oxygen Removal. *Catal. Lett.* **2012**, *142*, 7–15.
- (331) Runnebaum, R. C.; Lobo-Lapidus, R. J.; Nimmanwudipong, T.; Block, D. E.; Gates, B. C. Conversion of Anisole Catalyzed by Platinum Supported on Alumina: The Reaction Network. *Energy Fuels* **2011**, *25*, 4776–4785.
- (332) Leckie, S. M.; Harkness, G. J.; Clarke, M. L. Catalytic constructive deoxygenation of lignin-derived phenols: new C-C bond formation processes from imidazole-sulfonates and ether cleavage reactions. *Chem. Commun.* **2014**, *50*, 11511–11513.
- (333) Marker, T.; Roberts, M.; Linck, M.; Felix, L.; Ortiz-Toral, P.; Wangerow, J.; Tan, E.; Gephart, J.; Shonnard, V. *Biomass to Gasoline and Diesel Using Integrated Hydrolysis and Hydroconversion*; Gas Technology Institute: 2012.
- (334) Gutierrez, A.; Kaila, R. K.; Honkela, M. L.; Slioor, R.; Krause, A. O. I. Hydrodeoxygenation of guaiacol on noble metal catalysts. *Catal. Today* **2009**, *147*, 239–246.
- (335) Wang, Y. X.; He, T.; Liu, K. T.; Wu, J. H.; Fang, Y. M. From biomass to advanced bio-fuel by catalytic pyrolysis/hydro-processing: Hydrodeoxygenation of bio-oil derived from biomass catalytic pyrolysis. *Bioresour. Technol.* **2012**, *108*, 280–284.
- (336) Senol, O. I.; Ryymin, E. M.; Viljava, T. R.; Krause, A. O. I. Effect of hydrogen sulphide on the hydrodeoxygenation of aromatic and aliphatic oxygenates on sulphided catalysts. *J. Mol. Catal. A: Chem.* **2007**, *277*, 107–112.
- (337) Samant, B. S.; Kabalka, G. W. Hydrogenolysis–hydrogenation of aryl ethers: selectivity pattern. *Chem. Commun.* **2012**, *48*, 8658–8660.
- (338) Busetto, L.; Fabbri, D.; Mazzoni, R.; Salmi, M.; Torri, C.; Zanotti, V. Application of the Shvo catalyst in homogeneous hydrogenation of bio-oil obtained from pyrolysis of white poplar: New mild upgrading conditions. *Fuel* **2011**, *90*, 1197–1207.
- (339) Al Maksoud, W.; Larabi, C.; Garron, A.; Szeto, K. C.; Walter, J. J.; Santini, C. C. Direct thermocatalytic transformation of pine wood into low oxygenated biofuel. *Green Chem.* **2014**, *16*, 3031–3038.
- (340) Roelen, O., Chemische Verwertungsgesellschaft, mbH Oberhausen. German Patent DE 849,548, 1938.
- (341) Herrmann, W. A.; Fischer, R. W. Multiple Bonds between Main-Group Elements and Transition Metals. 136. "Polymerization" of an Organometal Oxide: The Unusual Behavior of Methyltrioxorhenium(VII) in Water. *J. Am. Chem. Soc.* **1995**, *117*, 3223–3230.
- (342) Lange, H.; Decina, S.; Crestini, C. Oxidative upgrade of lignin—Recent routes reviewed. *Eur. Polym. J.* **2013**, *49*, 1151–1173.
- (343) Crestini, C.; Pro, P.; Neri, V.; Saladino, R. Methyltrioxorhenium: a new catalyst for the activation of hydrogen peroxide to the oxidation of lignin and lignin model compounds. *Bioorg. Med. Chem.* **2005**, *13*, 2569–2578.
- (344) Crestini, C.; Crucianelli, M.; Orlandi, M.; Saladino, R. Oxidative strategies in lignin chemistry: A new environmental friendly approach for the functionalisation of lignin and lignocellulosic fibers. *Catal. Today* **2010**, *156*, 8–22.
- (345) Crestini, C.; Caponi, M. C.; Argyropoulos, D. S.; Saladino, R. Immobilized methyltrioxo rhenium (MTO)/H<sub>2</sub>O<sub>2</sub> systems for the oxidation of lignin and lignin model compounds. *Bioorg. Med. Chem.* **2006**, *14*, 5292–5302.
- (346) Herrmann, W. A.; Fischer, R. W.; Scherer, W.; Rauch, M. U. Methyltrioxorhenium(VII) as catalyst for epoxidations: structure of the active species and mechanism of catalysis. *Angew. Chem., Int. Ed. Engl.* **1993**, *32*, 1157–1160.
- (347) Adam, W.; Herrmann, W. A.; Saha-Möller, C. R.; Shimizu, M. Oxidation of methoxybenzenes to p-benzoquinones catalyzed by methyltrioxorhenium(VII). *J. Mol. Catal. A: Chem.* **1995**, *97*, 15–20.
- (348) Saladino, R.; Neri, V.; Wincione, E.; Marini, S.; Colleta, M.; Fiorucci, C.; Filippone, P. A new and efficient synthesis of ortho- and para-benzoquinones of cardanol derivatives by the catalytic system MeReO<sub>3</sub>–H<sub>2</sub>O<sub>2</sub>. *J. Chem. Soc., Perkin Trans. 1* **2000**, *1*, 581–586.
- (349) Adam, W.; Herrmann, W. A.; Lin, J.; Saha-Möller, C. R. Catalytic Oxidation of Phenols to p-Quinones with the Hydrogen Peroxide and Methyltrioxorhenium(VII) System. *J. Org. Chem.* **1994**, *59*, 8281–8283.

- (350) Harms, R. G.; Markovits, I. I. E.; Drees, M.; Herrmann, W. A.; Cokoja, M.; Kuhn, F. E. Cleavage of C-O Bonds in Lignin Model Compounds Catalyzed by Methylidioxorhenium in Homogeneous Phase. *ChemSusChem* **2014**, *7*, 429–434.
- (351) Haikarainen, A.; Sipila, J.; Pietikainen, P.; Pajunen, A.; Mutikainen, I. Synthesis and characterization of bulky salen-type complexes of Co, Cu, Fe, Mn and Ni with amphiphilic solubility properties. *J. Chem. Soc., Dalton Trans.* **2001**, 991–995.
- (352) Zhou, X. F.; Qin, J. X.; Wang, S. R. Oxidation of a Lignin Model Compound of Benzyl-Ether Type Linkage in Water with H<sub>2</sub>O<sub>2</sub> under an Oxygen Atmosphere Catalyzed by Co(Salen). *Drewno* **2011**, *54*, 15–25.
- (353) Zoia, L.; Canevali, C.; Orlandi, M.; Tolppa, E.-L.; Sipila, J.; Morazzoni, F. Radical formation on TMP fibers and related lignin chemical changes. *Bioresources* **2008**, *3*, 21–33.
- (354) Zhou, X. F.; Liu, J. Co(salen)-catalysed oxidation of synthetic lignin-like polymer: Co(salen) effects. *Hem. Ind.* **2012**, *66*, 685–692.
- (355) Zhou, X. F. Selective Oxidation of Kraft Lignin over Zeolite-Encapsulated Co(II) [H<sub>4</sub>]salen and [H<sub>2</sub>]salen Complexes. *J. Appl. Polym. Sci.* **2014**, *131*, 40809.
- (356) Zhang, G.; Scott, B. L.; Wu, R.; Silks, L. A. P.; Hanson, S. K. Aerobic Oxidation Reactions Catalyzed by Vanadium Complexes of Bis(Phenolate) Ligands. *Inorg. Chem.* **2012**, *51*, 7354–7361.
- (357) Zakzeski, J.; Bruijninx, P. C. A.; Weckhuysen, B. M. In situ spectroscopic investigation of the cobalt-catalyzed oxidation of lignin model compounds in ionic liquids. *Green Chem.* **2011**, *13*, 671–680.
- (358) Sippola, V.; Krause, O.; Vuorinen, T. Oxidation of lignin model compounds with cobalt-sulphosalen catalyst in the presence and absence of carbohydrate model compound. *J. Wood Chem. Technol.* **2004**, *24*, 323–340.
- (359) Lu, X. J.; Zhou, X. F. Co(Salen)-Catalysed Oxidation of Synthetic Lignin-Like Polymer: H<sub>2</sub>O<sub>2</sub> Effects. *Oxid. Commun.* **2014**, *37*, 572–582.
- (360) Kervinen, K.; Korpi, H.; Mesu, J. G.; Soulimani, F.; Repo, T.; R, B.; Leskela, M.; Weckhuysen, B. M. Mechanistic Insights into the Oxidation of Veratryl Alcohol with Co(salen) and Oxygen in Aqueous Media: An in-situ Spectroscopic Study. *Eur. J. Inorg. Chem.* **2005**, *2005*, 2591–2599.
- (361) Cedeno, D.; Bozell, J. J. Catalytic oxidation of para-substituted phenols with cobalt-Schiff base complexes/O<sub>2</sub>-selective conversion of syringyl and guaiacyl lignin models to benzoquinones. *Tetrahedron Lett.* **2012**, *53*, 2380–2383.
- (362) Bozell, J. J.; Hames, B. R.; Dimmel, D. R. Cobalt-Schiff Base Complex Catalyzed Oxidation of Para-Substituted Phenolics. Preparation of Benzoquinones. *J. Org. Chem.* **1995**, *60*, 2398–2404.
- (363) Biannic, B.; Bozell, J. J.; Elder, T. Steric effects in the design of Co-Schiff base complexes for the catalytic oxidation of lignin models to para-benzoquinones. *Green Chem.* **2014**, *16*, 3635–3642.
- (364) Badamali, S. K.; Luque, R.; Clark, J. H.; Breedon, S. W. Microwave assisted oxidation of a lignin model phenolic monomer using Co(salen)/SBA-15. *Catal. Commun.* **2009**, *10*, 1010–1013.
- (365) Sippola, V. O.; Krause, A. O. I. Oxidation activity and stability of homogeneous cobalt-sulphosalen catalyst - Studies with a phenolic and a non-phenolic lignin model compound in aqueous alkaline medium. *J. Mol. Catal. A: Chem.* **2003**, *194*, 89–97.
- (366) Fullerton, T. J.; Ahern, S. P. Salcomine as a catalyst for oxygen delignification. *Tappi* **1978**, *61*, 37–39.
- (367) Fullerton, T. J.; Ahern, S. P. Catalytic oxidation of 2,6-di-*t*-butylphenol by salcomine-type complexes in the presence of water. *Tetrahedron Lett.* **1976**, *17*, 139–142.
- (368) Son, S.; Toste, F. D. Non-Oxidative Vanadium-Catalyzed C-O Bond Cleavage: Application to Degradation of Lignin Model Compounds. *Angew. Chem., Int. Ed.* **2010**, *49*, 3791–3794.
- (369) Chatel, G.; Rogers, R. D. Review: Oxidation of Lignin Using Ionic Liquids-An Innovative Strategy To Produce Renewable Chemicals. *ACS Sustainable Chem. Eng.* **2014**, *2*, 322–339.
- (370) Zakzeski, J.; Jongorius, A. L.; Weckhuysen, B. M. Transition metal catalyzed oxidation of Alcell lignin, soda lignin, and lignin model compounds in ionic liquids. *Green Chem.* **2010**, *12*, 1225–1236.
- (371) Riano, S.; Fernandez, D.; Fadini, L. Oxidative cleavage of vic-diols catalyzed by manganese(III) complexes in ionic liquids. *Catal. Commun.* **2008**, *9*, 1282–1285.
- (372) Zhang, N.; Zhou, X. F. Salen copper (II) complex encapsulated in Y zeolite: An effective heterogeneous catalyst for TCF pulp bleaching using peracetic acid. *J. Mol. Catal. A: Chem.* **2012**, *365*, 66–72.
- (373) Sonar, S.; Ambrose, K.; Hendsbee, A. D.; Masuda, J. D.; Singer, R. D. Synthesis and application of Co(salen) complexes containing proximal imidazolium ionic liquid cores. *Can. J. Chem.* **2012**, *90*, 60–70.
- (374) Barroso, S.; Blay, G.; Fernandez, I.; Pedro, J. R.; Ruiz-Garcia, R.; Pardo, E.; Lloret, F.; Munoz, M. C. Chemistry and reactivity of mononuclear manganese oxamate complexes: Oxidative carbon-carbon bond cleavage of vic-diols by dioxygen and aldehydes catalyzed by a trans-dipyridine manganese(III) complex with a tetradentate o-phenylenedioxamate ligand. *J. Mol. Catal. A: Chem.* **2006**, *243*, 214–220.
- (375) Alves, V.; Capanema, E.; Chen, C. L.; Gratzl, J. Comparative studies on oxidation of lignin model compounds with hydrogen peroxide using Mn(IV)-Me(3)TACN and Mn(IV)-Me4DTNE as catalyst. *J. Mol. Catal. A: Chem.* **2003**, *206*, 37–51.
- (376) Cui, Y.; Chen, C. L.; Gratzl, J. S.; Patt, R. A. Mn(IV)-Me4DTNE complex catalyzed oxidation of lignin model compounds with hydrogen peroxide. *J. Mol. Catal. A: Chem.* **1999**, *144*, 411–417.
- (377) Hanson, S. K.; Baker, R. T.; Gordon, J. C.; Scott, B. L.; Silks, L. A. P.; Thorn, D. L. Mechanism of Alcohol Oxidation by Dipicolinate Vanadium(V): Unexpected Role of Pyridine. *J. Am. Chem. Soc.* **2010**, *132*, 17804–17816.
- (378) Hanson, S. K.; Baker, R. T.; Gordon, J. C.; Scott, B. L.; Sutton, A. D.; Thorn, D. L. Aerobic Oxidation of Pinacol by Vanadium(V) Dipicolinate Complexes: Evidence for Reduction to Vanadium(III). *J. Am. Chem. Soc.* **2009**, *131*, 428–429.
- (379) Hanson, S. K.; Baker, R. T.; Gordon, J. C.; Scott, B. L.; Thorn, D. L. Aerobic Oxidation of Lignin Models Using a Base Metal Vanadium Catalyst. *Inorg. Chem.* **2010**, *49*, 5611–5618.
- (380) Hanson, S. K.; Wu, R.; Silks, L. A. P. C-C or C-O Bond Cleavage in a Phenolic Lignin Model Compound: Selectivity Depends on Vanadium Catalyst. *Angew. Chem., Int. Ed.* **2012**, *51*, 3410–3413.
- (381) Wigington, B. N.; Drummond, M. L.; Cundari, T. R.; Thorn, D. L.; Hanson, S. K.; Scott, S. L. A Biomimetic Pathway for Vanadium-Catalyzed Aerobic Oxidation of Alcohols: Evidence for a Base-Assisted Dehydrogenation Mechanism. *Chem. - Eur. J.* **2012**, *18*, 14981–14988.
- (382) Argyropoulos, D. S.; Suchy, M.; Akim, L. Nitrogen-Centered Activators of Peroxide-Reinforced Oxygen Delignification. *Ind. Eng. Chem. Res.* **2004**, *43*, 1200–1205.
- (383) Korpi, H.; Lahtinen, P.; Sippola, V.; Krause, O.; Leskela, M.; Repo, T. An efficient method to investigate metal-ligand combinations for oxygen bleaching. *Appl. Catal., A* **2004**, *268*, 199–206.
- (384) Sippola, V. O.; Krause, A. O. I. Bis(o-phenanthroline)copper-catalysed oxidation of lignin model compounds for oxygen bleaching of pulp. *Catal. Today* **2005**, *100*, 237–242.
- (385) Hanson, S. K.; Wu, R.; Silks, L. A. P. Mild and Selective Vanadium-Catalyzed Oxidation of Benzylic, Allylic, and Propargylic Alcohols Using Air. *Org. Lett.* **2011**, *13*, 1908–1911.
- (386) Takezawa, E.; Sakaguchi, S.; Ishii, Y. Oxidative cleavage of vic-diols to aldehydes with dioxygen catalyzed by Ru(PPh<sub>3</sub>)(3)Cl<sub>2</sub> on active carbon. *Org. Lett.* **1999**, *1*, 713–715.
- (387) Hofrichter, M. Review: lignin conversion by manganese peroxidase (MnP). *Enzyme Microb. Technol.* **2002**, *30*, 454–466.
- (388) Shimada, M.; Habe, T.; Higuchi, T.; Okamoto, T.; Panijpan, B. Biomimetic Approach to Lignin Degradation 0.2. The Mechanism of Oxidative C-C Bond-Cleavage Reactions of Lignin Model Compounds with Natural Iron(III) Porphyrin Chloride as a Heme-Enzyme Model System. *Holzforschung* **1987**, *41*, 277–285.
- (389) Zhu, W.; Ford, W. T. Oxidation of Lignin Model Compounds in Water with Dioxygen and Hydrogen-Peroxide Catalyzed by Metallophthalocyanines. *J. Mol. Catal.* **1993**, *78*, 367–378.



- (390) Cui, F.; Dolphin, D. Metallophthalocyanines as possible lignin peroxidase models. *Bioorg. Med. Chem.* **1995**, *3*, 471–477.
- (391) Barbat, A.; Gloaguen, V.; Sol, V.; Krausz, P. Aqueous extraction of glucuronoxylans from chestnut wood: New strategy for lignin oxidation using phthalocyanine or porphyrin/H<sub>2</sub>O<sub>2</sub> system. *Bioresour. Technol.* **2010**, *101*, 6538–6544.
- (392) Crestini, C.; Saladino, R.; Tagliatestaa, P.; Boschia, T. Biomimetic degradation of lignin and lignin model compounds by synthetic anionic and cationic water soluble manganese and iron porphyrins. *Bioorg. Med. Chem.* **1999**, *7*, 1897–1905.
- (393) Crestini, C.; Pastorini, A.; Tagliatesta, P. Metalloporphyrins immobilized on montmorillonite as biomimetic catalysts in the oxidation of lignin model compounds. *J. Mol. Catal. A: Chem.* **2004**, *208*, 195–202.
- (394) Ghiaci, M.; Molaie, F.; Sedaghat, M. E.; Dorostkar, N. Metalloporphyrin covalently bound to silica: preparation, characterization and catalytic activity in oxidation of ethyl benzene. *Catal. Commun.* **2010**, *11*, 694–699.
- (395) Crestini, C.; Pastorini, A.; Tagliatesta, P. The immobilized porphyrin-mediator system Mn(TMePyP)/clay/HBT (clay-PMS): A lignin peroxidase biomimetic catalyst in the oxidation of lignin and lignin model compounds. *Eur. J. Inorg. Chem.* **2004**, *2004*, 4477–4483.
- (396) Cho, D. W.; Latham, J. A.; Park, H. J.; Yoon, U. C.; Langan, P.; Dunaway-Mariano, D.; Mariano, P. S. Regioselectivity of Enzymatic and Photochemical Single Electron Transfer Promoted Carbon-Carbon Bond Fragmentation Reactions of Tetrameric Lignin Model Compounds. *J. Org. Chem.* **2011**, *76*, 2840–2852.
- (397) Robinson, M. J.; Wright, L. J.; Suckling, I. D. Fe(TSPc)-catalysed benzylic oxidation and subsequent dealkylation of a non-phenolic lignin model. *J. Wood Chem. Technol.* **2000**, *20*, 357–373.
- (398) Russell, G. A. Deuterium isotope effects in the autoxidation of aralkylhydrocarbons. Mechanism of the interaction of peroxy radicals. *J. Am. Chem. Soc.* **1957**, *79*, 3871–3877.
- (399) Kirk, T. K.; Nakatsubo, F. Chemical mechanism of an important cleavage reaction in the fungal degradation of lignin. *Biochim. Biophys. Acta, Gen. Subj.* **1983**, *756*, 376–384.
- (400) Baciocchi, E.; Belvedere, S.; Bietti, M. Oxidation of  $\alpha$ -alkylbenzyl alcohols catalysed by 5,10,15,20-tetrakis-(pentafluorophenyl)porphyrin iron(III) chloride. Competition between C-H and C-C bond cleavage. *Tetrahedron Lett.* **1998**, *39*, 4711–4714.
- (401) Keseru, G. M.; Balogh, G. T.; Bokotey, S.; Arvai, G.; Bertok, B. Metalloporphyrin catalysed biomimetic oxidation of aryl benzyl ethers. Implications for lignin peroxidase catalysis. *Tetrahedron* **1999**, *55*, 4457–4466.
- (402) Cui, F.; Dolphin, D. Iron porphyrin catalyzed oxidation of lignin model compounds: Oxidation of phenylpropane and phenylpropene model compounds. *Can. J. Chem.* **1995**, *73*, 2153–2157.
- (403) Gierer, J.; Ljunggren, S. Alkaline Treatment of Lignin. *Svensk. Papperstidn.* **1979**, *82*, 71.
- (404) Mishra, S. P.; Thirree, J.; Manent, A. S.; Chabot, B.; Daneault, C. Ultrasound-Catalyzed Tempo-Mediated Oxidation of Native Cellulose for the Production of Nanocellulose: Effect of Process Variables. *Bioresources* **2011**, *6*, 121–143.
- (405) Shibata, I.; Isogai, A. Depolymerization of cellouronic acid during TEMPO-mediated oxidation. *Cellulose* **2003**, *10*, 151–158.
- (406) Sbiai, A.; Kaddami, H.; Sautereau, H.; Maazouz, A.; Fleury, E. TEMPO-mediated oxidation of lignocellulosic fibers from date palm leaves. *Carbohydr. Polym.* **2011**, *86*, 1445–1450.
- (407) Ma, P.; Zhai, H. Selective TEMPO-mediated oxidation of thermomechanical pulp. *BioResources* **2013**, *8*, 4396–4405.
- (408) Rahimi, A.; Azarpira, A.; Kim, H.; Ralph, J.; Stahl, S. S. Chemoselective Metal-Free Aerobic Alcohol Oxidation in Lignin. *J. Am. Chem. Soc.* **2013**, *135*, 6415–6418.
- (409) Nguyen, J. D.; Matsuura, B. S.; Stephenson, C. R. J. A Photochemical Strategy for Lignin Degradation at Room Temperature. *J. Am. Chem. Soc.* **2014**, *136*, 1218–1221.
- (410) Ma, P.; Law, K. N.; Daneault, C. Influence of Oxidation on Intrinsic Fiber Strength. *Cellul. Chem. Technol.* **2009**, *43*, 387–392.
- (411) Okita, Y.; Saito, T.; Isogai, A. TEMPO-mediated oxidation of softwood thermomechanical pulp. *Holzforschung* **2009**, *63*, 529–535.
- (412) Rahimi, A.; Ulbrich, A.; Coon, J. J.; Stahl, S. S. Formic-acid-induced depolymerization of oxidized lignin to aromatics. *Nature* **2014**, *515*, 249–252.
- (413) Gao, Y. J.; Zhang, J. G.; Chen, X.; Ma, D.; Yan, N. A Metal-Free, Carbon-Based Catalytic System for the Oxidation of Lignin Model Compounds and Lignin. *ChemPlusChem* **2014**, *79*, 825–834.
- (414) Lancefield, C. S.; Ojo, O. S.; Tran, F.; Westwood, N. J. Isolation of Functionalized Phenolic Monomers through Selective Oxidation and C O Bond Cleavage of the b-O-4 Linkages in Lignin. *Angew. Chem., Int. Ed.* **2015**, *54*, 258–262.
- (415) Tran, F.; Lancefield, C. S.; Kamer, P. C. J.; Lebl, T.; Westwood, N. J. Selective modification of the beta-beta linkage in DDQ-treated Kraft lignin analysed by 2D NMR spectroscopy. *Green Chem.* **2015**, *17*, 244–249.
- (416) Araujo, J. D. P.; Grande, C. A.; Rodrigues, A. E. Vanillin production from lignin oxidation in a batch reactor. *Chem. Eng. Res. Des.* **2010**, *88*, 1024–1032.
- (417) Azarpira, A.; Ralph, J.; Lu, F. C. Catalytic Alkaline Oxidation of Lignin and its Model Compounds: a Pathway to Aromatic Biochemicals. *BioEnergy Res.* **2014**, *7*, 78–86.
- (418) Wu, A.; Lauzon, J. M.; Andriani, I.; James, B. R. Breakdown of lignins, lignin model compounds, and hydroxy-aromatics, to C1 and C2 chemicals via metal-free oxidation with peroxide or persulfate under mild conditions. *RSC Adv.* **2014**, *4*, 17931–17934.
- (419) Villar, J. C.; Caperos, A.; Garcia-Ochoa, F. Oxidation of hardwood kraft-lignin to phenolic derivatives with oxygen as oxidant. *Wood Sci. Technol.* **2001**, *35*, 245–255.
- (420) Villar, J. C.; Caperos, A.; GarciaOchoa, F. Oxidation of hardwood kraft-lignin to phenolic derivatives. Nitrobenzene and copper oxide as oxidants. *J. Wood Chem. Technol.* **1997**, *17*, 259–285.
- (421) Maziero, P.; Neto, M. D.; Machado, D.; Batista, T.; Cavalheiro, C. C. S.; Neumann, M. G.; Craievich, A. F.; Rocha, G. J. D.; Polikarpov, I.; Goncalves, A. R. Structural features of lignin obtained at different alkaline oxidation conditions from sugarcane bagasse. *Ind. Crops Prod.* **2012**, *35*, 61–69.
- (422) Tarabanko, V. E.; Hendogina, Y. V.; Petuhov, D. V.; Pervishina, E. P. On the role of retroaldol reaction in the process of lignin oxidation into vanillin. Kinetics of the vanillideneacetone cleavage in alkaline media. *React. Kinet. Catal. Lett.* **2000**, *69*, 361–368.
- (423) Tarabanko, V. E.; Petukhov, D. V.; Selyutin, G. E. New mechanism for the catalytic oxidation of lignin to vanillin. *Kinet. Catal.* **2004**, *45*, 569–577.
- (424) Voitl, T.; Rudolf von Rohr, P. Demonstration of a Process for the Conversion of Kraft Lignin into Vanillin and Methyl Vanillate by Acidic Oxidation in Aqueous Methanol. *Ind. Eng. Chem. Res.* **2010**, *49*, 520–525.
- (425) Werhan, H.; Assmann, N.; Rudolf von Rohr, P. Lignin oxidation studies in a continuous two-phase flow microreactor. *Chem. Eng. Process.* **2013**, *73*, 29–37.
- (426) Voitl, T.; Rudolf von Rohr, P. Oxidation of Lignin Using Aqueous Polyoxometalates in the Presence of Alcohols. *ChemSusChem* **2008**, *1*, 763–769.
- (427) Werhan, H.; Mir, J. M.; Voitl, T.; Rudolf von Rohr, P. Acidic oxidation of kraft lignin into aromatic monomers catalyzed by transition metal salts. *Holzforschung* **2011**, *65*, 703–709.
- (428) Werhan, H.; Farshori, A.; Rudolf von Rohr, P. Separation of lignin oxidation products by organic solvent nanofiltration. *J. Membr. Sci.* **2012**, *423*, 404–412.
- (429) Xiang, Q.; Lee, Y. Y. Oxidative cracking of precipitated hardwood lignin by hydrogen peroxide. *Appl. Biochem. Biotechnol.* **2000**, *84*, 153–162.
- (430) Su, J.; Yang, L. S.; Liu, R. N.; Lin, H. F. Low-temperature oxidation of guaiacol to maleic acid over TS-1 catalyst in alkaline aqueous H<sub>2</sub>O<sub>2</sub> solutions. *Chin. J. Catal.* **2014**, *35*, 622–630.
- (431) Evtuguin, D. V.; Neto, C. P.; Rocha, J.; de Jesus, J. D. P. Oxidative delignification in the presence of molybdovanadophosphate

heteropolyanions: mechanism and kinetic studies. *Appl. Catal., A* **1998**, *167*, 123–139.

(432) Khenkin, A. M.; Neumann, R. Oxidative C-C Bond Cleavage of Primary Alcohols and Vicinal Diols Catalyzed by HSPV2Mo10O40 by an Electron Transfer and Oxygen Transfer Reaction Mechanism. *J. Am. Chem. Soc.* **2008**, *130*, 14474–14476.

(433) Evtuguin, D. V.; Neto, C. P. New Polyoxometalate Promoted Method of Oxygen Delignification. *Holzforschung* **1997**, *51*, 338–342.

(434) Weinstock, I. A.; Attala, R. H.; Reiner, R. S.; Moen, M. A.; Hammel, H. E.; Houtman, C. J.; Hill, C. L. A new environmentally benign technology and approach to bleaching kraft pulp. Polyoxometalates for selective delignification and waste mineralization. *New J. Chem.* **1996**, *20*, 269–275.

(435) Weinstock, I. A.; Attala, R. H.; Reiner, R. S.; Moen, M. A.; Hammel, K. E.; Houtman, C. J.; Hill, C. L.; Harrup, M. K. A new environmentally benign technology for transforming wood pulp into paper. Engineering polyoxometalates as catalysts for multiple processes. *J. Mol. Catal. A: Chem.* **1997**, *116*, 59–84.

(436) Weinstock, I. A.; Hammel, K. E.; Moen, M. A.; Landucci, L. L.; Ralph, S.; Sullivan, C. E.; Reiner, R. S. Selective transition-metal catalysis of oxygen delignification using water-soluble salts of polyoxometalate (POM) anions. Part II. Reactions of alpha-[SiVW11O40](5-) with phenolic lignin-model compounds. *Holzforschung* **1998**, *52*, 311–318.

(437) Evtuguin, D. V.; Daniel, A. I. D.; Silvestre, A. J. D.; Amado, F. M. L.; Neto, C. P. Lignin aerobic oxidation promoted by molybdovanadophosphate polyanion [PMo7V5O40](8-). Study on the oxidative cleavage of beta-O-4 aryl ether structures using model compounds. *J. Mol. Catal. A: Chem.* **2000**, *154*, 217–224.

(438) Kim, Y. S.; Chang, H. M.; Kadla, J. F. Polyoxometalate (POM) oxidation of lignin model compounds. *Holzforschung* **2008**, *62*, 38–49.

(439) Kim, Y. S.; Chang, H. M.; Kadla, J. F. Polyoxometalate (POM) oxidation of milled wood lignin (MWL). *J. Wood Chem. Technol.* **2007**, *27*, 225–241.

(440) Ruuttunen, K.; Vuorinen, T. Developing catalytic oxygen delignification for kraft pulp: Kinetic study of lignin oxidation with polyoxometalate anions. *Ind. Eng. Chem. Res.* **2005**, *44*, 4284–4291.

(441) Zhu, Y.; Chuanchao, L.; Sudarmadji, M.; Hui Min, N.; Biying, A. O.; Maguire, J. A.; Hosmane, N. S. An Efficient and Recyclable Catalytic System Comprising Nanopalladium(0) and a Pyridinium Salt of Iron Bis(dicarbollide) for Oxidation of Substituted Benzyl Alcohol and Lignin. *ChemistryOpen* **2012**, *1*, 67–70.

(442) Liu, S. W.; Shi, Z. L.; Li, L.; Yu, S. T.; Xie, C. X.; Song, Z. Q. Process of lignin oxidation in an ionic liquid coupled with separation. *RSC Adv.* **2013**, *3*, 5789–5793.

(443) Wu, H. R.; Chen, F. G.; Feng, Q. G.; Yue, X. P. Oxidation and Sulfomethylation of Alkali-Extracted Lignin from Corn Stalk. *Bioresources* **2012**, *7*, 2742–2751.

(444) Taraban'ko, V. E.; Koropatchinskaya, N. V.; Kudryashev, A. V.; Kuznetsov, B. N. Influence of Lignin Origin on the Efficiency of the Catalytic-Oxidation of Lignin into Vanillin and Syringaldehyde. *Russ. Chem. Bull.* **1995**, *44*, 367–371.

(445) Deng, H. B.; Lin, L.; Sun, Y.; Pang, C. S.; Zhuang, J. P.; Ouyang, P. K.; Li, Z. J.; Liu, S. J. Perovskite-type Oxide LaMnO<sub>3</sub>: An Efficient and Recyclable Heterogeneous Catalyst for the Wet Aerobic Oxidation of Lignin to Aromatic Aldehydes. *Catal. Lett.* **2008**, *126*, 106–111.

(446) Otto, A.; Simpson, M. J. Evaluation of CuO oxidation parameters for determining the source and stage of lignin degradation in soil. *Biogeochemistry* **2006**, *80*, 121–142.

(447) Gao, P.; Li, C.; Wang, H.; Wang, X.; Wang, A. Perovskite hollow nanospheres for the catalytic wet air oxidation of lignin. *Chin. J. Catal.* **2013**, *34*, 1811–1815.

(448) Zhang, J. H.; Deng, H. B.; Lin, L. Wet Aerobic Oxidation of Lignin into Aromatic Aldehydes Catalysed by a Perovskite-type Oxide: LaFe(1-x)Cu(x)O(3) (x = 0, 0.1, 0.2). *Molecules* **2009**, *14*, 2747–2757.

(449) Sales, F. G.; Maranhao, L. C. A.; Lima, N. M.; Abreu, C. A. M. Kinetic evaluation and modeling of lignin catalytic wet oxidation to

selective production of aromatic aldehydes. *Ind. Eng. Chem. Res.* **2006**, *45*, 6627–6631.

(450) Deng, H. B.; Lin, L.; Sun, Y.; Pang, C. S.; Zhuang, J. P.; Ouyang, P. K.; Li, J. J. Activity and stability of LaFeO<sub>3</sub> catalyst in lignin catalytic wet oxidation to aromatic aldehydes. *Chin. J. Catal.* **2008**, *29*, 753–757.

(451) Deng, H. B.; Lin, L.; Sun, Y.; Pang, C. S.; Zhuang, J. P.; Ouyang, P. K.; Li, J. J.; Liu, S. J. Activity and Stability of Perovskite-Type Oxide LaCoO<sub>3</sub> Catalyst in Lignin Catalytic Wet Oxidation to Aromatic Aldehydes Process. *Energy Fuels* **2009**, *23*, 19–24.

(452) Deng, H. B.; Lin, L.; Liu, S. J. Catalysis of Cu-Doped Co-Based Perovskite-Type Oxide in Wet Oxidation of Lignin To Produce Aromatic Aldehydes. *Energy Fuels* **2010**, *24*, 4797–4802.

(453) Gao, P.; Li, N.; Wang, X.; Zhang, T. Perovskite LaMnO<sub>3</sub> hollow nanospheres: The synthesis and the application in catalytic wet air oxidation of phenol. *Mater. Lett.* **2013**, *92*, 173–176.

(454) Royer, S.; Levasseur, B.; Alamdari, H.; Barbier, J.; Duprez, D.; Kaliaguine, S. Mechanism of stearic acid oxidation over nanocrystalline La<sub>1-x</sub>A<sub>x</sub>BO<sub>3</sub> (A' = Sr, Ce; B = Co, Mn): The role of oxygen mobility. *Appl. Catal., B* **2008**, *80*, 51–61.

(455) Wu, G. X.; Heitz, M.; Chornet, E. Improved Alkaline Oxidation Process for the Production of Aldehydes (Vanillin and Syringaldehyde) from Steam-Explosion Hardwood Lignin. *Ind. Eng. Chem. Res.* **1994**, *33*, 718–723.

(456) Wu, G. X.; Heitz, M. Catalytic Mechanism of Cu<sup>2+</sup> and Fe<sup>3+</sup> in Alkaline O-2 Oxidation of Lignin. *J. Wood Chem. Technol.* **1995**, *15*, 189–202.

(457) Magario, I.; Einschlag, F. S. G.; Rueda, E. H.; Zygadlo, J.; Ferreira, M. L. Mechanisms of radical generation in the removal of phenol derivatives and pigments using different Fe-based catalytic systems. *J. Mol. Catal. A: Chem.* **2012**, *352*, 1–20.

(458) Partenheimer, W. The aerobic oxidative cleavage of lignin to produce hydroxyaromatic benzaldehydes and carboxylic acids via metal/bromide catalysts in acetic acid/water mixtures. *Adv. Synth. Catal.* **2009**, *351*, 456–466.

(459) Gaspar, A. R.; Gamelas, J. A. F.; Evtuguin, D. V.; Neto, C. P. Alternatives for lignocellulosic pulp delignification using polyoxometalates and oxygen: a review. *Green Chem.* **2007**, *9*, 717–730.

(460) Linsebigler, A. L.; Guanguan, L.; Yates, J. T. Photocatalysis on TiO<sub>2</sub> Surfaces: Principles, Mechanisms, and Selected Results. *Chem. Rev.* **1995**, *95*, 735–758.

(461) Walsh, K.; Sneddon, H. F.; Moody, C. J. Solar Photochemical Oxidations of Benzylic and Allylic Alcohols Using Catalytic Organooxidation with DDQ: Application to Lignin Models. *Org. Lett.* **2014**, *16*, 5224–5227.

(462) Cortes, J. A.; Alarcon-Herrera, M. T.; Villicana-Mendez, M.; Gonzalez-Hernandez, J.; Perez-Robles, J. F. Impact of the Kind of Ultraviolet Light on the Photocatalytic Degradation Kinetics of the TiO<sub>2</sub>/UV Process. *Environ. Prog. Sustainable Energy* **2011**, *30*, 318–325.

(463) Karaoglu, M. H.; Dogan, M.; Alkan, M.; Ugurlu, M. Photooxidative Degradation of Cationic Dyes Using Uv/H<sub>2</sub>O<sub>2</sub> and Uv/H<sub>2</sub>O<sub>2</sub>/TiO<sub>2</sub> Process. *Fresenius Environ. Bull.* **2012**, *21*, 1758–1763.

(464) Ksibi, M.; Ben Amor, S.; Cherif, S.; Elaloui, E.; Houas, A.; Elaloui, M. Photodegradation of lignin from black liquor using a UV/TiO<sub>2</sub> system. *J. Photochem. Photobiol., A* **2003**, *154*, 211–218.

(465) Pu, Y. Q.; Anderson, S.; Lucia, L.; Ragauskas, A. J. Investigation of the photo-oxidative chemistry of acetylated softwood lignin. *J. Photochem. Photobiol., A* **2004**, *163*, 215–221.

(466) Ugurlu, M.; Karaoglu, M. H. Removal of AOX, total nitrogen and chlorinated lignin from bleached Kraft mill effluents by UV oxidation in the presence of hydrogen peroxide utilizing TiO<sub>2</sub> as photocatalyst. *Environ. Sci. Pollut. Res.* **2009**, *16*, 265–273.

(467) Ugurlu, M.; Karaoglu, M. H.; Vaizogullar, A. I. Decolourization and Removal of Phenol Compounds from Olive Mill Wastewater by O-2/Uv/Nabo2h2o2 Center Dot 3h(2)O. *Fresenius Environ. Bull.* **2013**, *22*, 754–765.

(468) Ugurlu, M.; Karaoglu, M. H. TiO<sub>2</sub> supported on sepiolite: Preparation, structural and thermal characterization and catalytic



behaviour in photocatalytic treatment of phenol and lignin from olive mill wastewater. *Chem. Eng. J.* **2011**, *166*, 859–867.

(469) Kansal, S. K.; Singh, M.; Sud, D. Studies on TiO<sub>2</sub>/ZnO photocatalysed degradation of lignin. *J. Hazard. Mater.* **2008**, *153*, 412–417.

(470) Yeber, M. C.; Rodriguez, J.; Freer, J. Photocatalytic degradation of cellulose bleaching effluent by supported TiO<sub>2</sub> and ZnO. *Chemosphere* **2000**, *41*, 1193–1197.

(471) Felicio, C. M.; Machado, A. E. D.; Castellan, A.; Nourmamode, A.; Perez, D. D.; Ruggiero, R. Routes of degradation of beta-O-4 syringyl and guaiacyl lignin model compounds during photobleaching processes. *J. Photochem. Photobiol., A* **2003**, *156*, 253–265.

(472) Kamwilaisak, K.; Wright, P. C. Investigating Laccase and Titanium Dioxide for Lignin Degradation. *Energy Fuels* **2012**, *26*, 2400–2406.

(473) Ma, Y. S.; Chang, C. N.; Chiang, Y. P.; Sung, H. F.; Chao, A. C. Photocatalytic degradation of lignin using Pt/TiO<sub>2</sub> as the catalyst. *Chemosphere* **2008**, *71*, 998–1004.

(474) Lanzalunga, O.; Bietti, M. Photo-radiation chemical induces degradation of lignin model compounds. *J. Photochem. Photobiol., B* **2000**, *56*, 85–108.

(475) Tanaka, K.; Calanag, C. R.; Hisanaga, T. Photo catalyzed degradation of lignin on TiO<sub>2</sub>. *J. Mol. Catal. A: Chem.* **1999**, *138*, 287–294.

(476) Portjanskaja, E.; Preis, S. Aqueous photocatalytic oxidation of lignin: The influence of mineral admixtures. *Int. J. Photoenergy* **2007**, *2007*, 1–7.

(477) Rangel, R.; Mercado, G. J. L.; Bartolo-Perez, P.; Garcia, R. Nanostructured-[CeO<sub>2</sub>, La<sub>2</sub>O<sub>3</sub>, C]/TiO<sub>2</sub> Catalysts for Lignin Photodegradation. *Sci. Adv. Mater.* **2012**, *4*, 573–578.

(478) Kaneko, M.; Nemoto, J.; Ueno, H.; Gokan, N.; Ohnuki, K.; Horikawa, M.; Saito, R.; Shibata, T. Photoelectrochemical reaction of biomass and bio-related compounds with nanoporous TiO<sub>2</sub> film photoanode and O<sub>2</sub>-reducing cathode. *Electrochem. Commun.* **2006**, *8*, 336–340.

(479) Pelegrini, R.; Reyes, J.; Duran, N.; Zamora, P. P.; de Andrade, A. R. Photoelectrochemical degradation of lignin. *J. Appl. Electrochem.* **2000**, *30*, 953–958.

(480) Ugurlu, M.; Karaoglu, M. H. Photocatalytic Removal of Olive Mill Waste Water by TiO<sub>2</sub> Loaded on Sepiolite and Under Natural Solar Irradiation. *Environ. Prog. Sustainable Energy* **2011**, *30*, 326–336.

(481) Yuan, R. S.; Guan, R. B.; Liu, P.; Zheng, J. T. Photocatalytic treatment of wastewater from paper mill by TiO<sub>2</sub> loaded on activated carbon fibers. *Colloids Surf., A* **2007**, *293*, 80–86.

(482) Hasegawa, I.; Inoue, Y.; Muranaka, Y.; Yasukawa, T.; Mae, K. Selective Production of Organic Acids and Depolymerization of Lignin by Hydrothermal Oxidation with Diluted Hydrogen Peroxide. *Energy Fuels* **2011**, *25*, 791–796.

(483) Rafiee, M.; Nematollahi, D. Electrochemical oxidation of catechols in the presence of cyanoacetone and methyl cyanoacetate. *J. Electroanal. Chem.* **2009**, *626*, 36–41.

(484) Salazar, R.; Encina, P. A. N.; Camargo, C.; Squella, J. A.; Vergara, L. J. N. Electrochemical oxidation of C<sub>4</sub>-vanillin- and C<sub>4</sub>-isovanillin-1,4-dihydropyridines in aprotic medium: Reactivity towards free radicals. *J. Electroanal. Chem.* **2008**, *622*, 29–36.

(485) Shao, D.; Liang, J. D.; Cui, X. M.; Xu, H.; Yan, W. Electrochemical oxidation of lignin by two typical electrodes: Ti/Sb-SnO<sub>2</sub> and Ti/PbO<sub>2</sub>. *Chem. Eng. J.* **2014**, *244*, 288–295.

(486) Tian, M.; Bakovic, L.; Chen, A. Kinetics of the electrochemical oxidation of 2-nitrophenol and 4-nitrophenol studied by in situ UV spectroscopy and chemometrics. *Electrochim. Acta* **2007**, *52*, 6517–6524.

(487) Zhu, H. B.; Chen, Y. M.; Qin, T. F.; Wang, L.; Tang, Y.; Sun, Y. Z.; Wan, P. Y. Lignin depolymerization via an integrated approach of anode oxidation and electro-generated H<sub>2</sub>O<sub>2</sub> oxidation. *RSC Adv.* **2014**, *4*, 6232–6238.

(488) Rochefort, D.; Bourbonnais, R.; Leech, D.; Paice, M. G. Oxidation of lignin model compounds by organic and transition metal-based electron transfer mediators. *Chem. Commun.* **2002**, 1182–1183.

(489) Bailey, A.; Brooks, H. M. Electrolytic Oxidation of Lignin. *J. Am. Chem. Soc.* **1946**, *68*, 445–446.

(490) Tolba, R.; Tian, M.; Wen, J. L.; Jiang, Z. H.; Chen, A. C. Electrochemical oxidation of lignin at IrO<sub>2</sub>-based oxide electrodes. *J. Electroanal. Chem.* **2010**, *649*, 9–15.

(491) Pan, K.; Tian, M.; Jiang, Z. H.; Kjartanson, B.; Chen, A. C. Electrochemical oxidation of lignin at lead dioxide nanoparticles photoelectrodeposited on TiO<sub>2</sub> nanotube arrays. *Electrochim. Acta* **2012**, *60*, 147–153.

(492) Moodley, B.; Mulholland, D. A.; Brookes, H. C. The electro-oxidation of lignin in Sappi Saiccor dissolving pulp mill effluent. *Water SA* **2011**, *37*, 33–40.

(493) Parpot, P.; Bettencourt, A. P.; Carvalho, A. M.; Belgsir, E. M. Biomass conversion: attempted electrooxidation of lignin for vanillin production. *J. Appl. Electrochem.* **2000**, *30*, 727–731.

(494) Reichert, E.; Wintringer, R.; Volmer, D. A.; Hempelmann, R. Electro-catalytic oxidative cleavage of lignin in a protic ionic liquid. *Phys. Chem. Chem. Phys.* **2012**, *14*, 5214–5221.

(495) Shiraishi, T.; Takano, T.; Kamitakahara, H.; Nakatsubo, F. Studies on electro-oxidation of lignin and lignin model compounds. Part 2: N-Hydroxyphthalimide (NHPI)-mediated indirect electro-oxidation of non-phenolic lignin model compounds. *Holzforschung* **2012**, *66*, 311–315.

(496) Constant, S.; Robitzer, M.; Quignard, F.; Di Renzo, F. Vanillin oligomerization as a model of side reactions in lignin fragmentation. *Catal. Today* **2012**, *189*, 123–128.

(497) Nishimura, R. T.; Giammanco, C. H.; Vosburg, D. A. Green, Enzymatic Syntheses of Divanillin and Diapocynin for the Organic, Biochemistry, or Advanced General Chemistry Laboratory. *J. Chem. Educ.* **2010**, *87*, 526–527.

(498) Cypres, R.; Bettens, B. Pyrolytic Fragmentation Mechanisms of Phenol and Cresols. *Tetrahedron* **1974**, *30*, 1253–1260.

(499) Pingali, S. R. K.; Jursic, B. S. Microwave-assisted synthesis of 1,3-benzodioxole derivatives from catechol and ketones or aldehydes. *Tetrahedron Lett.* **2011**, *52*, 4371–4374.

(500) Farzaneh, A.; Richards, T.; Sklavounos, E.; van Heiningen, A. A Kinetic Study of CO<sub>2</sub> and Steam Gasification of Char from Lignin Produced in the SEW Process. *BioResources* **2014**, *9*, 3052–3063.

(501) Isha, R.; Williams, P. T. Pyrolysis-gasification of agriculture biomass wastes for hydrogen production. *J. Energy Inst.* **2011**, *84*, 80–87.

(502) Yamaguchi, A.; Hiyoshi, N.; Sato, O.; Shirai, M. Gasification of Organosolv-lignin Over Charcoal Supported Noble Metal Salt Catalysts in Supercritical Water. *Top. Catal.* **2012**, *55*, 889–896.

(503) van der Laan, G. P.; Beenackers, A. Kinetics and Selectivity of the Fischer–Tropsch Synthesis: A Literature Review. *Catal. Rev.: Sci. Eng.* **1999**, *41*, 255–318.

(504) Tijn, P. J. A.; Waller, F. J.; Brown, D. M. Methanol technology developments for the new millennium. *Appl. Catal., A* **2001**, *221*, 275–282.

(505) Resende, F. L. P.; Fraley, S. A.; Berger, M. J.; Savage, P. E. Noncatalytic gasification of lignin in supercritical water. *Energy Fuels* **2008**, *22*, 1328–1334.

(506) Yamaguchi, A.; Hiyoshi, N.; Sato, O.; Osada, M.; Shirai, M. Lignin gasification over supported ruthenium trivalent salts in supercritical water. *Energy Fuels* **2008**, *22*, 1485–1492.

(507) Yamaguchi, A.; Hiyoshi, N.; Sato, O.; Osada, M.; Shirai, M. Lignin Gasification over Charcoal-supported Palladium and Nickel Bimetal Catalysts in Supercritical Water. *Chem. Lett.* **2010**, *39*, 1251–1253.

(508) Lin, Y. C.; Huber, G. W. The critical role of heterogeneous catalysis in lignocellulosic biomass conversion. *Energy Environ. Sci.* **2009**, *2*, 68–80.

(509) Ferdous, D.; Dalai, A. K.; Bej, S. K.; Thring, R. W. Production of H<sub>2</sub> and medium heating value gas via steam gasification of lignins in fixed-bed reactors. *Can. J. Chem. Eng.* **2001**, *79*, 913–922.

(510) Cerone, N.; Zimbardi, F.; Contuzzi, L.; Alvino, E.; Carnevale, M. O.; Valerio, V. Updraft Gasification at Pilot Scale of Hydrolytic Lignin Residue. *Energy Fuels* **2014**, *28*, 3948–3956.

(511) Venkitasamy, C.; Hendry, D.; Wilkinson, N.; Fernando, L.; Jacoby, W. A. Investigation of thermochemical conversion of biomass in supercritical water using a batch reactor. *Fuel* **2011**, *90*, 2662–2670.

(512) Cortright, R. D.; Davda, R. R.; Dumesic, J. A. Hydrogen from catalytic reforming of biomass-derived hydrocarbons in liquid water. *Nature* **2002**, *418*, 964–967.

(513) Zakzeski, J.; Weckhuysen, B. M. Lignin Solubilization and Aqueous Phase Reforming for the Production of Aromatic Chemicals and Hydrogen. *ChemSusChem* **2011**, *4*, 369–378.

(514) Kudo, S.; Hachiyama, Y.; Takashima, Y.; Tahara, J.; Idesh, S.; Norinaga, K.; Hayashi, J. Catalytic Hydrothermal Reforming of Lignin in Aqueous Alkaline Medium. *Energy Fuels* **2014**, *28*, 76–85.

(515) Zakzeski, J.; Jongerius, A. L.; Bruijninx, P. C. A.; Weckhuysen, B. M. Catalytic Lignin Valorization Process for the Production of Aromatic Chemicals and Hydrogen. *ChemSusChem* **2012**, *5*, 1602–1609.

(516) Jongerius, A. L.; Copeland, J. R.; Foo, G. S.; Hofmann, J. P.; Bruijninx, P. C. A.; Sievers, C.; Weckhuysen, B. M. Stability of Pt/ $\gamma$ -Al<sub>2</sub>O<sub>3</sub> Catalysts in Lignin and Lignin Model Compound Solutions under Liquid Phase Reforming Reaction Conditions. *ACS Catal.* **2013**, *3*, 464–473.

(517) Huang, X. M.; Koranyi, T. I.; Boot, M. D.; Hensen, E. J. M. Catalytic Depolymerization of Lignin in Supercritical Ethanol. *ChemSusChem* **2014**, *7*, 2276–2288.

(518) Strassberger, Z.; Prinsen, P.; van der Klis, F.; van Es, D. S.; Tanase, S.; Rothenberg, G. Lignin solubilisation and gentle fractionation in liquid ammonia. *Green Chem.* **2015**, *17*, 325–334.

(519) Jongerius, A. L.; Bruijninx, P. C. A.; Weckhuysen, B. M. Liquid-phase reforming and hydrodeoxygenation as a two-step route to aromatics from lignin. *Green Chem.* **2013**, *15*, 3049–3056.

(520) Czernik, S.; French, R.; Feik, C.; Chornet, E. Hydrogen by catalytic steam reforming of liquid byproducts from biomass thermoconversion processes. *Ind. Eng. Chem. Res.* **2002**, *41*, 4209–4215.

(521) Borregaard LignoTech website: <http://www.lignotech.com/>.

(522) Sun, S. H.; Zhang, G. X.; Gauquelin, N.; Chen, N.; Zhou, J. G.; Yang, S. L.; Chen, W. F.; Meng, X. B.; Geng, D. S.; Banis, M. N.; Li, R. Y.; Ye, S. Y.; Knights, S.; Botton, G. A.; Sham, T. K.; Sun, X. L. Single-atom Catalysis Using Pt/Graphene Achieved through Atomic Layer Deposition. *Sci. Rep.* **2013**, *3*, 1775.

(523) Lee, J. C.; Jackson, D. H. K.; Li, T.; Winans, R. E.; Dumesic, J. A.; Kuech, T. F.; Huber, G. W. Enhanced stability of cobalt catalysts by atomic layer deposition for aqueous-phase reactions. *Energy Environ. Sci.* **2014**, *7*, 1657–1660.

(524) Schuth, F. Control of Solid Catalysts Down to the Atomic Scale: Where is the Limit? *Angew. Chem., Int. Ed.* **2014**, *53*, 8599–8604.

(525) Yang, X. F.; Wang, A. Q.; Qiao, B. T.; Li, J.; Liu, J. Y.; Zhang, T. Single-Atom Catalysts: A New Frontier in Heterogeneous Catalysis. *Acc. Chem. Res.* **2013**, *46*, 1740–1748.